The Pharmaceutical Potential of Compounds from Tasmanian *Clematis* species

by
Fangming Jin

Bachelor in Pharmacology of Chinese Medicine (from Nanjing University of Traditional Chinese Medicine, China)

Master of Pharmaceutical Science (from University of Tasmania, Australia)

Submitted in fulfilment of the requirement for the Degree of Doctor of Philosophy

School of Pharmacy
University of Tasmania
May 2012

DEDICATION

To

My loving parents and husband,

and

My beloved supervisors, Dr. Christian Narkowicz and Dr. Glenn A Jacobson,

For their on-going support and sacrifices,

I dedicate my research to you.

DECLARATION OF ORIGINALITY

This thesis contains no material that has been accepted for the award of any other degree or diploma in any other tertiary institution.

To the best of my knowledge and belief, this thesis contains no material previously published or written by any other person except where due reference is made in the text of the thesis.

Fangming Jin

May 7, 2012

AUTHORITY OF ACCESS

This thesis may be available for loan and limited copying in accordance with the Copyright Act 1968.

Fangming Jin

May 7, 2012

ABSTRACT

Aims

The aim of the study was to investigate the antitumour, antibacterial and anti-inflammatory activities of some Tasmanian native *Clematis* spp. and to isolate and identify the potential pharmaceutical constituents.

Methods

The antitumour activities, antibacterial activities and anti-inflammatory effects of leaf material of *Clematis* spp. were screened by P388 cytotoxic assay, minimum inhibition concentrations (MICs) and inhibitory NO production by lipopolysaccharides (LPS) stimulated Raw 264.7 cells, respectively. The bioactive-guided fractionation methodologies, including cartridge fractionation, HPLC columns fractionation and Sephadex LH-20 column purification, were employed to isolate active constituents. The chemical profiles of active constituents were determined by ELSD, UV, LC-MS and GC-MS.

Scanning electron microscopy (SEM), Gram stain, antibiotic interaction with chequerboard, deoxycholate-induced lysis and the antibiotic resistant mechanism study of *P. aeruginosa* were employed to study the antibacterial mechanism of the active constituent. The anti-inflammatory activity was also investigated by basal (unstimulated) and LPS- and phytohaemagglutinin A (PHA)-stimulated cytokine release from peripheral blood mononuclear cells (PBMC).

Some novel compounds in Tasmanian native *Clematis* spp. were determined by HPLC, LC-MS and LTQ-Orbitrap-MS.

Results and discussion

Ten out of eleven investigated *Clematis* spp. showed cytotoxic activities against P388 cells with different IC_{50} values (0.084-3.106 mg/ml). Ranunculin and its isomer were determined as the antitumour constituents. These compounds could be hydrolysed by the cell medium to produce protoanemonin. The antitumour study determined that ranunculin was a pro-cytotoxin with the antitumour activity derived from protoanemonin.

Eight investigated *Clematis* spp. showed different antibacterial effects against *E. coli* (MIC=0.39-3.13 mg/ml) and *P. aeruginosa* (MIC=0.31-6.25 mg/ml). Ranunculin, the antibacterial constituent in *Clematis* spp., was selective against Gram negative bacteria. In particular, it had a stronger antibacterial effect than gentamicin against clinically isolated multi-drug resistant *P. aeruginosa*. The change in ranunculin treated sensitive *P. aeruginosa* was elongation and cell lysis in multi-drug resistant *P. aeruginosa* observed by SEM and obtained by deoxycholate-induced lysis study. These results imply that the antibacterial mechanism of ranunculin against sensitive and multi-drug resistance *P. aeruginosa* may be different. The antibacterial effect of ranunculin might be still contributed to by protoanemonin.

Eleven investigated *Clematis* spp. showed varied inhibition of NO production. Ranunculin and its isomers were determined as one of the anti-inflammatory constituents in Tasmanian *Clematis* spp. For the cytokine study, in the presence of LPS and PHA, *C. aristata*-L leaf at 10 μg/ml significantly decreased the release of IL-1β ($P<0.01$) and TNF-α ($P<0.05$) compared with LPS and PHA alone. These results provide experimental data of the anti-inflammatory activities of Tasmanian *Clematis* spp.

Flavonoids and hydroxycinnamate esters were obtained in these investigated *Clematis* spp. The amounts of nine hydroxycinnamate esters were varied in each *Clematis* leaf material. This would be the first time to discover these hydroxycinnamte esters in Tasmanian *Clematis* spp.

Conclusion

The study demonstrated the antitumour, antibacterial and anti-inflammatory activities of Tasmanian native *Clematis* spp. Ranunculin was discovered to be a pro-cytotoxin of protoanemonin, which was one of the active constituents. This study was the first to investigate the therapeutic value of Tasmanian native *Clematis* spp. and discover the antibacterial value of protoanemonin in multi-drug resistant *P. aeruginosa* and its complicated antibacterial mechanism against sensitive and multidrug resistant *P. aeruginosa*. The anti-inflammatory activities may be the most distinguishing therapeutic value of Tasmanian *Clematis* spp. Furthermore, study of the chemical constituents suggested that Tasmanian *Clematis* spp. contained

phenolic compounds. Although this study only provided the basic and preliminary experimental data on the biological, potential pharmaceutical constituents and some novel compounds of Tasmanian *Clematis* spp., further investigation into usage and identification of effective pharmaceutical constituents would be worthy.

ACKNOWLEDGEMENTS

First and above all I would like to thank the School of Pharmacy, University of Tasmania (UTAS) who provided scholarship to fund my PhD candidature.

I express my sincere gratitude, and heartfelt thanks to my beloved supervisor Dr. Christian Narkowicz and Glenn A. Jacobson for finding this interesting research project for me. Their knowledge, support and guidance, timely words of encouragement have helped this project to reach full bloom. I am always obliged to them.

I would also like to extend my sincere gratitude to School of Pharmacy technical staff: Dr. Peter Traill (Laboratory Manager), Mr Tony Whitty and Mrs Heather Galloway for their invaluable services. To Mr David Loveridge, thank you for your support on installing useful software in my computer and your friendly help when my laptop collapsed.

I convey my heart felt gratefulness to the people in the Central Science Laboratory, UTAS: Associate Professor Noel Davies for sparing me his valuable time and knowledge in analysing compounds. I would like to extend my sincere thanks to Dr Karsten Goemann for carrying out scanning electron microscopy and Mr Edwin Lowe and Mr Richard Wilson for LTQ-Oribitrap-MS analysis.

I would like to express my upmost gratitude to Dr. Silvana Bettiol and Dr Richard Bradbury (School of Medicine, UTAS). Thank you for providing bacteria for my study, your patience in teaching me knowledge and laboratory techniques in microbiology. Thank you for providing valuable discussion and supporting information with regard to the questions I encountered in the study. To Miss Karla Mettrick (School of Medicine, UTAS), thank you for your help in the bacterial membrane permeability study and confocal microscopy. To Mr Roger Latham (Menzies Research Institute, UTAS), thank you for sharing your excellent experience with me on the laboratory techniques of microbiology.

I would like to express my thanks to Associate Professor Gregory Woods (Immunology Member, Menzies Research Institute, UTAS) who provided P388 cells and Raw 264.7 cells and thank you for your teaching me the cell techniques and providing advice. To Miss Gabby Brown, thank you for your assistance in my laboratory work performed at Menzies. Thank you to Associate Professor Dominic Geraghty (School of Human Life Science, UTAS) for the cytokine study of my sample.

Within the of School of Pharmacy, I would like to express my greatful thanks to Professor Stuart McLean, Mr. Adam Pirie and Dr. Kwang Choon Yee for suggestions regarding my study.

I would also like to acknowledge the following people: Mr Tom Wright (School of Management, UTAS) for providing plant species and for setting up facilities for growing my investigated plants in the courtyard of the School of Pharmacy; Dr. Yuji Mortia (Department of Microbiology, School of Pharmacy, Aichi Gakuin University, Japan) for studying the antibiotic resistant mechanism of *Pseudomonas aeruginosa*.

And finally, I am grateful to the individuals over the years in School of Pharmacy for being a warm group to study amongst.

TABLE OF CONTENT

LIST OF FIGURES

Chapter 1

Chapter 2

Chapter 3

Chapter 4

Chapter 5

LIST OF TABLES

Chapter 1

Chapter 2

Chapter 3

Chapter 4

Chapter 5

LIST OF SCHEME

LIST OF ABBREVIATIONS

5-FU	5-fluorouracil
5-LOX	5-lipoxygenase
AA	adjuvant arthritis
ACN	acetonitrile
ALPS	autoimmune lymphoproliferative syndrome
APC	antigen-presenting cell
APCI	atmospheric pressure chemical ionization
ATCC	American type culture collection
AUC	area under curve
BP	blood pressure
CA	chemical abstract
cAMP	cyclic adenosine monophosphate
CF	converting factor
CI	cytotoxic index
ConA	concanavalin A
COX-1	cyclooxygenase-1
COX-2	cyclooxygenase-2
DCM	dichloromethane
DMARDs	disease-modifying anti-rheumatic drugs
DMEM	dulbecco's modified eagle medium
DMSO	dimethyl sulfoxide
DNA	deoxyribonucleic acid
DTH	delayed type hypersensitivity
ELSD	evaporative light scattering detector
eNOS	endothelial NO synthase
ESI	electrospray ioization
FBS	fetal bovin serum

FIC	fractional inhibitory concentration
G-	Gram negative
G+	Gram positive
GC-MS	gas chromatography-mass spectrometry
GM-CSF	granulocyte-macrophage colony-stimulating factor
HCA	hydroxycinnamic acid
HCl	hydrochloride
HIV	human immunodeficiency virus
HPLC	high performance liquid chromatography
IC_{50}	half maximal inhibitory concentration
IFN	interferon
IL-10	interleukin-10
IL-1β	interleukin-1 beta
IL-1α	interleukin-1 alpha
IL-4	interleukin-4
IL-6	interleukin-6
IL-8	interleukin-8
iNOS	inducible NO synthase
LC-MS	high performance liquid chromatography-mass spectrometry
LD	lethal dose
LPS	lipopolysaccharides
LTQ-Orbitrap-MS	linear ion trap quadrupole-Orbitrap-mass spectrometry
MBC	minimum bactericidal concentration
MCP-1	monocyte chemotactic protein 1
MeOH	methanol
MHB	muller hinton broth
MIA	minimum inhibition amount
MIC	minimum inhibitory concentration

MIP-1	macrophage inflammatory protein-1
MMPs	matrix metalloproteinases
mRNA	messenger ribonucleic acid
MTT	3-4,5-dimethylthiazol-2-yl-2,5-diphenyl tetrazolium bromide
MW	molecular weight
NCI	National Cancer Instituent
NED	1-N-napthylethylenediamine dihydrochloride
NO	nitric oxide
NS	normal saline
NSU	neurosugical unit
OA	osteoarthritis
OD	optical density
PA	*Pseudomonas aeruginosa*
PARP	poly (ADP-ribose) polymerase
PBMC	peripheral blood mononuclear cells
PBS	phosphate buffered saline
PDA	photodiode array detector
PDMS	polydimethylsiloxane
PGE2	prostaglandin E2
PHA	phytohaemagglutinin A
PPARα	peroxisome proliferator-activated receptor alpha
PPARϒ	peroxisome proliferator-activated receptor gamma
RA	rheumatoid arthritis
RAN	ranunculin
RPMI	Rosewell Park Memorial Institute
SC_{50}	50% scavenging concentration
SD	standard deviation
SEM	scanning electron microscopy

SLE	systemic lupus erythermatosus
SPME	solid phase microextraction
TCM	Traditional Chinese Medicine
TH1	T helper 1
TNF-α	tumour necrosis factor-alpha
TYR	tyrosinase
TYRP-1	tyrosinase-related protein 1
TYRP-2	tyrosinase-related protein 2
UPLC-MS	ultraperformance liquid chromatography-mass spectromertry
SAN	sulfanilamide
-SH	thiol group
SPE	solid-phase extract

HUMANS TALK WITH NATURE

LIKE

A DEAF TALKS WITH A MUTE.

Chapter 1 Introduction to the medicinal properties of *Clematis* species.

1.1 Background

Clematis is a member of the Ranunculaceae family, which includes anemones, peonies, buttercups and aquilegias as well. More than 250 species and at least 5000 cultivars exist in the world distributed from cool temperate to tropical regions in China, Europe, Australia, New Zealand, India, North America, northern Africa, the Himalayas, Europe and Japan.

Clematis are charming climbers, bearing flowers in profusely generally in spring or summer in a variety of colours. They are often referred to as the queen of the flowering vines. Some species can grow 7 to 10 metres in a single season; others reach a height of only 1.5 to 3.5 metres. Sepals make up the colourful portion of the flower. These may be thin, wide, pointed, rounded, crinkled, twisted, or even crimped. They may be marked with centre bars, stripes, or vivid shadings. The flower form varies from nodding, pitcher-shaped, bell-shaped, or star-shaped, to the familiar large, flat, erectly held blossoms. Flowers may have contrasting coloured stamens or no stamens at all. Small-flowered varieties offer a range of fragrances lacking in the large-flowered varieties. [(1)]

For the growing conditions, *Clematis* needs fertile soil, excellent drainage and a cool root-run. Analysis of cultural soil showed that most *Clematis* can grow very well in slightly acid soil.[(2)] Roots can be kept cool by mulching heavily, shading with shrubs, or planting where they can spread under paving. They need plenty of summer watering, especially in their first two years until they are well established. *Clematis* are heavy feeders, so need fertiliser like blood and bone and compost

applied preferably before flowering, in late spring and early summer. The climbers need support such as a post or trellis, and look wonderful climbing through trees that they will not damage.

1.2 Traditional medicinal uses

1.2.1 The usage in China

In Traditional Chinese Medicine (TCM), around 68 *Clematis* spp., fresh or sundried, are used in 34 Chinese herbal preparations that are used mainly to treat inflammatory conditions and infections. The properties (as referred to in TCM) are acrid, salty, warm, slightly bitter and mildly toxic. The active agents are said to enter the bladder and liver meridians. The actions are dispelling wind and removing damp, and promoting blood circulation to relieve pain. Indications for use include rheumatoid arthritis (RA), gout, pain in the lower back and limbs, stroke, headache and tonsillitis. Furthermore, *Clematis* is used for treatment of deeply lodged fish bones in the throat. *Clematis* is also used to remove phlegm, promote urination, help menses, tetanus, and beriberi, for acute hepatitis with jaundice, calculus in the urinary tract, calculus in the gall bladder, inflammation of the mammary glands, the inflammation of the glans of children, bone spurs and hemorrhoids. A summary of TCM herbs using *Clematis* spp. their plant resource, and indications are listed in Table 1.1.[3]

Table 1.1 The therapeutic indications for *Clematis* spp. herbal preparations and the various plant tissues used to prepare them, including leaf, stem, root, leaf and stem, leaf and root, stem and root and whole plant as described in 'Chinese Materia Medica'.[3]

TCM Herb	Plant resource	Indication
xi ye tie xian lian	*C. aethusifolia Turczb* (leaf, stem)	RA, indigestion，vomit， echinococcosis，scrotum eczema，carbuncle
nv wei	*C. apiifolia DC.* (leaf, stem or root)	RA, lack of breast milk, toothache, lacquer dermatitis, suppurative keratitis
mian hua teng	*C. apiifolia DC. Var. obtusidentata Rehd. et Wils* (stem)	amenorrhea, indigestion, lack of breast milk, dysentery
da mu tong	*C. argentilucida (Levl. et Vant.) W.T Wang* (stem)	urination, gonorrhea, lack of breast milk, carbuncle, rheumatism
	C. grata Wall var. grandidentata Rehd et Wils	
hong ding pa teng	*C. brevicaduata DC.* (stem or root)	urinary tract infection, RA, lack of breast milk
mao mu tong	C. buchananiana DC. (stem)	pharyngitis, tonsillitis, urinary tract infection, bruises
	C. buchananiana DC. Var. rugosa Hook. F. et Thoms	
	C. chinensis Osbeck (stem & root)	
	C. chinensis Retz; C. sinensis Lour.	
	C. hexapetala Pall. ; C. angustofolia Jacq	
wei ling xian	*C. terniflora DC. var. mandshurica (Rupr) Ohwi*	RA, numbness, meridian spasm, kip adverse, beriberi, malaria
	C. mandshurica Rupr.	
	C. meyeniana Walp	
	C. uncinata Champ. Ex Benth	
	C. uncinata Champ. Ex Benth var. biternata W. T. Wang	
wei ling xian ye	*C. chinensis Osbeck* (leaf)	sore throat, RA, stye, conjunctivitis, bruises
jin si mu tong	*C. chrysocoma Franch*(stem & root)	urination, edema, urinary tract infection, amenorrhea, carbuncle, RA, bruises, purulent conjunctivitis, suppurative keratitis,
lan lu hu	*C. clarkeana Levl.et Vant* (stem and root)	carbuncle, sore throat, edema of beriberi, urinary tract infection, amenorrhea, lack of breast milk
da hua wei ling xian	*C. courtoisii Hand. Mazz*. (stem & root)	urination, constipation, toothache, suppurative keratitis, insect and snake bite

Table 1.1 (continued)

TCM Herb	Plant resource	Indication
xiao nian yao	*C. fasciculiflora Franch* (root, leaf & out layer of stem)	RA, bruise, mastitis, carbuncle
	C. montana Buch. -Ham. var. fasciculiflora (franch.) Bruhl	
gan mu tong	*C. filamentaos Dunn* (leaf & root)	hypertension, Insomnia, headache, numbness, purulent conjunctivitis,suppurative keratitis, toothache
shan mu tong	*C. finetiana Levl. et Vant.* (leaf& stem)	joint swelling and pain, bruises, urination, lack of breast milk
	C. pavoliniana Pamp	
shan mu tong gen	*C. clarkeana Levl.et Vant*	RA, bruise, suppurative keratitis
tie xian lian	*C. florida Thunb*. (whole or root)	RA, urination, amenorrhea, constipation, suppurative keratitis,
	C. florida Thunb var plena D. Don (whole or root)	insect and snake bite, jaundice, toothache
ran ran cao	*C. glauca Wild* (whole plant)	rheumatic arthralgia， enteritis, dysentery, carbuncle, pruritus,
	C. orientalis L. var. glauca Maxim	insect and snake bite
xue li kai	*C. henryi Oliv.* (root or leaf)	sore throat, headache, bruise, stomach, carbuncle, mumps
da ye tie xian lian	*C. heracleifolia DC.* (whole plant or root)	rheumatic arthralgia, deep abscess, lymph node tuberculosis
	C. heracleifolia DC. var. ichangensis Rehd. Et Wils	
tie xian tou gu cao	*C. intricata Bunge* (whole plant)	RA, limbs numbness, spasm pain, psoriasis,
	C. orientalis I. var. intricata (Bge) Maxim	scabies skin disease
xiao mu tong	*C. lasiandra Maxim* (stem& root)	rheumatic arthralgia, bruises, oedema, urinary tract infection,
	C. loureiriana DC. (whole plant)	urination, carbuncle
zi mu tong	*C. loureiriana DC. Var. subpeltata Hand. Mazz* (stem)	RA, back and leg pain, oedema,
	C. smilacifolia Wall	urinary tract infection, cold
sha ye tie xian lian	*C. meyeniana Walp. var. granulata Finet et Gagnep*	oedema, urination, rheumatism, lack of breast milk, carbuncle
	C. granulata (Finet et Gagnep.) Ohwi	
chuan mu tong	*C. montana Buch. -Ham. ex DC.* (stem)	urinary tract infection, urinary tract tumours, amenorrhea,
	C. armandii Franch	edema, urinary tract infection,tongue sores,
	C. armandii Franch var. biondiana (Pavol) Rehd	lack of breast milk, joint swelling and pain
	C. biondiana Pavol	

Table 1.1 (continued)

TCM Herb	Plant resource	Indication
feng teng cao	*C. peterae Hand. -Hazz* (leaf&stem) *C. gouriana Roxb var. finetii Rehd.et Wils*	rheumatic arthralgia, rubella itching, carbuncle, urination, purulent conjunctivitis,suppurative keratitis, headache
feng teng cao gen	*C. peterae Hand.-Hazz*	RA, urination, oedema, urinary tract infection/tumour，amenorrhea, bruises
hua mu tong	*C. pseudopogonandra Finet et Gagnep*	oedema, urination, urinary tract infection, dysentery, tongue sores, lack of breast milk
liu ye jian xue fei	*C. quinquefoliolata Hutch* (whole plant, or root)	RA, numbness, stomach, acute gastroenteritis, stomach, amenorrhea, migraine, neuralgia, facial paralysis
xiao jiu tou shi zi cao	*C. ranunculoides Franch.*(whole plant, or root) *C. pterantha Dunn var. grossedentata Rehd. et Wils*	carbuncle, mastitis, oedema, urination, bruises
xi mu tong	*C. rubifolia C.H. Wright* (whole plant) *C. splendens Levl. et Van*	rheumatic arthralgia, bruises, urethritis, irregular menstruation, lack of breast milk, cystitis
xin jiang mu tong	*C. sibirica (L.) Mill* (stem) *C. alpina (L.) Mill.subsp.sibirica Kuntze*	urinary tract infection, tongue sores, lack of breast milk
gan qing tie xian lian	*C. tangutica (Maxim.) Korsh* (whole plant, or stem & leaf) *C. orientalis L. var. tangutica Maxim* *C. tangutica (Maxim.) Korsh. var. obtusiuscula Rejd. Et Wils*	indigestion, carbuncle sore, eczema
tong jiao wei ling xian	*C. terniflora DC*. *C. paniculata Thunb*	RA, carbuncle, insect, snake bite, tonsillitis, pharyngitis
la mu tong	*C. yunnanensis Franch* (stem, or whole plant)	RA, lumbago, urination

According to the record in the Chinese Materia Medica,[3] in all above preparations, "Wei Ling Xian" is the most commonly used in TCM with anti-inflammatory and anti-rheumatoid activities. The name of "Wei Ling Xian" means panacea and the discovery of its therapeutic value is told in a story. In the year of 785-805 AD, Zhou Juncao wrote "Biography of Wei Ling Xian", in which the name of "Wei Ling Xian" was recorded. A person suffered a serious disease that made his leg too painful to walk on for ten years. All doctors had no idea of the treatment for that disease. One day, this patient came across a Korean monk. This monk spoke to him: 'Only one herb is enough to treat your disease, but I don't know if that herb grows here." Then the patient's family and the monk were looking for that herb in the surrounding mountains. Finally, they found this herb. The patient was able to walk after using this herb for several days. This herb was named as "Wei Ling Xian". According to the record, "Wei Ling Xian" used in Korea was a plant belonging to *Clematis* species. However, the earliest record of "Wei Ling Xian" in TCM was in the book of "Ji Yan Fang", written by Yao Zengheng, stretching back to the Liang Dynasty (502-557AD), which is far earlier than the story of Zhou Juncao.

The dosage of herbal preparation is 3-9 g for oral medications, but for deeply lodged fish bone, the dosage can be up to 30 g.[3] For external use, a decoction is used for washing the affected part. Furthermore, there are some pharmaceutical products, such as "Feng Shi Gu Tong Yao Jiu", "Wei Ling Xian Die Da Tablet", and "Huo Luo Xiao Tong Tablet", and "Wei Ling Xian Injection" that are used for the treatment of arthritis.[3] Furthermore, the total saponins of Radix Clematidis (the root extract of *C.*

chinensis, C. hepapetala or *C. mashurica*) are used in preparation of pharmaceuticals for treatment of RA.[4] There are some prescriptions that include *Clematis* and other herbs used together to treat some diseases. Some of the herbal medicines that include *Clematis* spp. are described in Table 1.2

Table 1.2 Clinical usage of *Clematis* spp. in TCM.

No.	Condition	Source	Ref.
1	gynecological diseases and dermatoses	*C. armandii* and/or *C. montana* 1-10g	(5)
2	cardiovascular and cerebrovascular diseases	*C. chinensis* 30-400g	(6)
3	rheumatosis and rheumatoid arthritis	*C. chinensis* 27-33g *C. chinensis* 10-20g *C. chinensis* 250g	(7) (8) (9)
4	urinogenital system disease	*C. armandii*	(10)
5	ischemic necrosis of bone	*C. chinensis* 90g	(11)
6	osteo-hyperplasia and protrusion of intervertebral disc	*C. chinensis* 100-300g	(12)
7	anti-inflammatory, analgesic and antibacterial effects	Radix Clematidis 5-10g	(13),(14)
8	traumatic injuries	*C. huchouensis* 1-12g *C. loureiriana* 1-16g *C. lasiandra* 1-10g *C. intricata* 1-16g	(15) (16) (17),(18) (19)
9	fracture and hyperosteogeny (Plaster)	*C. chinensis* 400 g	(20)
10	lithangiuria	Radix Clematidis 100 g	(21)
11	rhinitis	*Clematis* spp.	(22)
12	bone disease and fracture	*C. chinensis* 200 g	(23)
13	senile acute urine retention	Caulis Clematidis Armandii (*C. armandii* and/or *C. montana*) 3-20g	(24)
14	hepatoma,hepatitisB, hepatocirrhosis, and hepatic fibrosis	*C. armandii* 2-10%	(25)

Table 1.2 (continued)

No.	Condition	Source	Ref.
15	primary hepatic carcinoma	Caulis Clematidis Armandii (*C. armandii* and/or *C. montana*) 2-7%	(26)
16	osteoarthritis	*C. chinensis* 7-39 g	(27)
17	vasculitis	Caulis Clematidis Armandii (*C. armandii* and/or *C. montana*) 5-15 g	(28)
18	cholelithiasis	*Clematis* spp.	(29)
19	fungal dermatosis or bromhidrosis	*C. montana* 3-10 g	(30)
20	improving erectile dysfunction and blood circulation	*C. apiifolia*	(31)
21	repressing withdrawal symptom	3-6 wt.% of *C. mandshurica*	(32)
22	nervous paralysis	*C. maudshurica Rupr*	(33)

1.2.2 Usage in other countries

Clematis spp. are not only used in Chinese medicine, but also used as folk remedies worldwide for the treatment of various inflammatory ailments.

In Australia, *C. glycinoides* DC. was used as a medicinal plant in the treatment of headaches and colds by the inhalation of the vapors emitted from freshly crushed leaves.[34] *C. pickeringii* stems have been used in aboriginal medicine in Australia for the treatment of various diseases that are considered as inflammatory in nature, eg. asthma, arthritis, rheumatism, fever, oedema, infections, snakebite and related inflammatory diseases.[35]

C. brachiata is used in Kenya for the management of headaches, malaria and other febrile illnesses, abdominal disorders, yaws, and skin disorders. Old stems and leaves are chewed for the management of toothache and sore throat.[36] Whole *C. dioica* is used in Guatemala for the treatment of gonorrhoea.[37] *C. flammna* flowering herbs were used in Turkish folk medicine for the treatment of diseases that are thought to be inflammatory in nature, such as rheumatism and to reduce fever.[38]

C. mandshurica Rupr roots are used in traditional Korean medicine to treat inflammation-related diseases.[39] In recent years, SKI360X**,** an extract purified from a mixture of three Oriental herbal medicines (*C. mandshurica, Trichosanthes kirilowii* and *Prunella vulgaris*), was studied for anti-inflammatory and analgesic efficacy in Korea.

SKI306X has been widely used for the treatment of inflammatory diseases such as lymphadenitis and arthritis in Far East Asia. The result of a double-blind, placebo controlled study performed to evaluate the efficacy and safety of SKI306X in 96 patients with classical osteoarthritis (OA) of the knee demonstrated that SKI306X provided clinical efficacy in patients with OA.[40] The pharmacological efficacy of SKI306X in treating OA in part may result from the inhibition of apoptosis in chondrocytes by *C. mandshurica*.[41] The efficacy and safety of SKI306X was compared with that of diclofenac sodium for the treatment of OA of the knee. In a randomised, double-blind, active comparator-controlled trial, a total of 249 patients were randomly assigned to receive either 200 mg of SKI306X three times daily or

100 mg of diclofenac sustained release once daily. SKI306X demonstrated efficacy statistically comparable to that of diclofenac. Both treatments were well tolerated, however, the SKI306X treatment group experienced less heartburn.[42]

Furthermore, SKI306X can delay the destruction of cartilage in RA. The result of a 6-week, multicentre, randomized, double-blind, double-dummy, Phase III, noninferiority clinical study performed by Song suggested that SKI306X was generally well tolerated and not inferior to celecoxib in regard to pain relief in these Korean patients with RA.[43]

1.3 Chemical constituents

The chemical compounds detected in *Clematis* spp. are mainly saponins, flavonoids, lignans, anemonin, protoanemonin, and essential oils.

1.3.1 Anemonin and Protoanemonin

Anemonin and protoanemonin were isolated from several *Clematis* species.[44-48] Protoanemonin is unstable and can conjugate to form anemonin. Anemonin has *cis* and *trans* forms. Ranunculin, the glycoside of protoanemonin, was isolated from some plants. Figure 1.1 shows the chemical structure of protoanemonin, anemonin (*cis*- and *trans*-) and ranunculin.

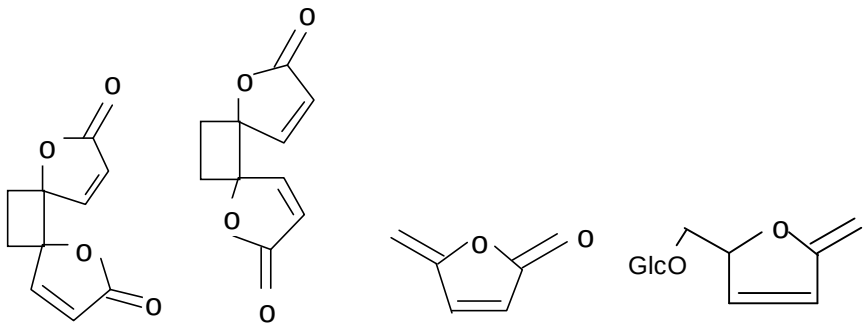

cis-anemonin *trans*-anemonin protoanemonin ranunculin

Figure 1.1 The chemical structures of protoanemonin, anemonin and the parent glycoside, ranunculin.

Anemonin and protoanemonin were thought to be responsible for the antimicrobial activity of extracts of *Clematis* spp.[(49)] Furthermore, protoanemonin had been isolated from the Australian 'headache vine' *C. glycinoides* and other Australian *Clematis* spp. Quantitative examination of this and the other six Australian *Clematis* taxa has shown protoanemonin concentrations of 2.19, 0.31, 1.96, 0.17, 0.87, 1.31 and 1.21% (dry weight) for *C. aristata*, *C. fawcettii*, *C. gentianoides*, *C. glycinoides*, *C. microphylla*, *C. microphylla* var. *leptophylla* and *C. pubescens*, respectively.[(50)]

A high performance liquid chromatography (HPLC) study of the distribution and quantitation of protoanemonin was carried out on several Italian *Ranunculaceae* species. The results indicated that protoanemonin may be a useful chemical marker in elucidating systematic relationships within this family.[(51)]

The results of a GC-MS analysis of one Asian and several Tasmanian *Clematis* spp. performed in this laboratory[(52)] showed that ranunculin with a retention time of 1.66 min and protoanemonin with a retention time of 6.80 minutes were obtained from

each sample (Table 1.3). The mass of protoanemonin in leaf was higher than in stem and root ($P<0.05$).

Table 1.3 Percentage of protoanemonin in *Clematis* spp. fresh material (mean±SD; n=3).

	Protoanemonin in fresh material (%) w/w			
	Leaf	Stem	Root	Flower
C. gentianoides	0.716±0.078	0.588±0.073	0.168±0.041	0.172
C. aristata (N)	0.188±0.029	0.240±0.072	0.216±0.025	
C. aristata (W)	0.708±0.080	0.312±0.071	0.288±0.049	
C. 'garden surprise'	0.500±0.094	0.524±0.095	0.236±0.037	
C. montana alba	0.312±0.050	0.064±0.017	0.076±0.016	

1.3.2. Saponins

The saponins in *Clematis* spp. are mostly triterpene saponins. The aglycones are typically oleanolic acid and hederagenin. They are illustrated in Figure 1.2. The sugar substituents are mainly glucose, rhamnose, arabinose, xylose and ribose.

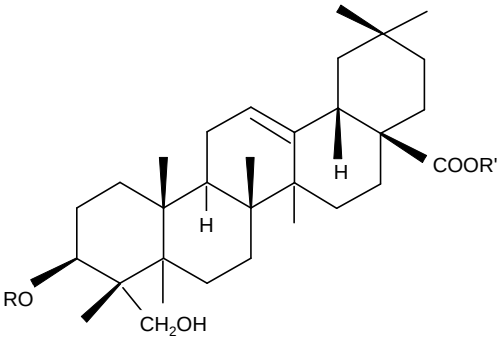

A. hederagenin

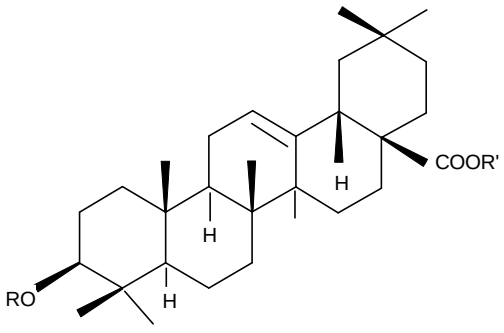

B. oleanolic acid

Figure1.2 Structures of the aglycones of saponins from *Clematis* spp.

Table 1.4 Saponins isolated from various *Clematis* spp.

No.	Name	Aglycone	Source	Ref.
1	Vitalboside A	B[1]	*C. vitalba*	(53)
2	Clemontanoside F	B	*C. montana*	(54)
3	Clematichinenoside A	B	*C. chinensis* roots	(55)
4	Clematichinenoside C	B	*C. chinensis* roots	(56)
5	Clemastanoside A	B	*C. stans* roots	(57)
6	Clemastanoside B	B	*C. stans* roots	(57)
7	Clemastanoside C	B	*C. stans* roots	(57)
8	Huzhangoside B	B	*C. stans* roots	(57)
9	Huzhangoside C	B	*C. stans* roots	(57)
10	Huzhangoside D	B	*C. stans* roots	(57)
11	Clemontanoside-E	B	*C. montana* roots	(58)
12	Clemontanoside B	B	*C. montana* defatted leaves	(59)
13	Vitalboside B	A[2]	*C. vitalba*	(53)
	Vitalboside B	A	*C. tangutica*	(60)
14	Tanguticoside A	A	*C. tangutica*	(60)
15	Tanguticoside B	A	*C. tangutica*	(60)
16	Clematichinenoside B	A	*C. chinensis*	(55)
17	Clematibetoside A	A	*C. tibetana* aerial part	(61)
18	Clematibetoside C	A	*C. tibetana* aerial part	(61)
19	Clematernosides C	A	*C. terniflora* roots	(62)
20	Clemastanoside D	A	*C. terniflora* roots	(62)
21	Clemastanoside E	A	*C. terniflora* roots	(62)
22	Clemastanoside F	A	*C. terniflora* roots	(62)
23	Clemastanoside G	A	*C. terniflora* roots	(62)
24	Clemontanoside-C	A	*C. montana* stems	(63)
25	Saponins A'	A	*C. songarica* MeOH ext	(64)
26	Saponins B'	A	*C. songarica* MeOH ext	(64)
27	Songaroside A'	A	*C. songarica* leave	(66), (67)
28	Songaroside B'	A	*C. songarica* leaves	(65), (66)
29	Songaroside A	A	*C. songarica* leaves	(65), (66)
30	Songaroside B	A	*C. songarica* leaves	(65), (66)
31	Clematernosides A	B	*C. terniflora* roots	(62)
32	Clematernosides B	B	*C. terniflora* roots	(62)
33	Clematernosides E	B	*C. terniflora* roots	(62)
34	Clematernosides F	B	*C. terniflora* roots	(62)
35	Clematernosides G	B	*C. terniflora* roots	(62)
36	Clematernosides H	B	*C. terniflora* roots	(62)
37	Clematernosides I	B	*C. terniflora* roots	(62)
38	Clematernosides J	B	*C. terniflora* roots	(62)
39	Clematernosides K	B	*C. terniflora* roots	(62)
40	Clematoside-S	A	*C. grata* roots	(67)
41	Clematomandshurica saponins E	B	*C. mandshurica* roots & rhizomes	(68)
42	Montanosides 1	B	*C. montana*	(69)
43	Montanosides 2	B	*C. montana*	(69)
44	Clematiganoside A	B	*C. ganpiniana*	(70)

[1] Oleanolic acid [2] Hederagenin

Table 1.4 suggests that *Clematis* spp. were rich in saponins. It was reported that saponins are the active constituents for some biological activities. A saponin-enriched fraction prepared from the methanol extract of the roots of *C. chinensis* showed cytotoxic activity against HL-60 promyelocytic leukemia cells, from which five new triterpene saponins based on oleanolic acid, along with three known saponins, were isolated. Among the isolated saponins, monodesmosidic saponins exhibited cytotoxic activities against cultured tumour cells.[71] Clematomandshurica saponins A and B, isolated from the roots and rhizomes of *C. mandshurica* showed significant inhibitory activity on cyclooxygenase-2 (IC_{50}=2.66 and 2.58 μM, respectively).[72] Clematochinenosides A, C, D, E and F isolated from *C. chinensis* could inhibit COX-1 and COX-2 enzymes.[73] Furthermore, saponins extracted from *C. ganpiniana* could inhibit cell proliferation and induce cell apoptosis of gastric carcinoma cell line SGC-7901, which might be partly related to the inhibition of the NF-κB expression.[74]

1.3.3 Flavonoids

The flavonoids isolated from *Clematis* species include isoquercitin, rutin,[57, 75] quercetin[57, 76-78] and kaempferol[79, 80] Some of the flavonoids isolated from *Clematis* spp. are summarized in Table 1.5.

Table 1.5 Flavonoids isolated from *Clematis* spp.

No.	Compound	Source	Ref.
1	4,7-dimethoxykeampferol	*C. purpurea* var. *hybrida*	(77)
2	kaempferol-3-neohesperidin	*C. purpurea* var. *hybrida*	(77)
3	kaempferol-7-O-glucoside	*C. purpurea* var. *hybrida*	(77)
4	kaempferol-3-O- glucoside	*C. trichotoma,*	(75)
		C. purpurea var. *hybrida*	(77)
5	rutin	*C. stans Sieb. Et Zucc*	(57)
	rutin	*C. trichotoma*	(75)
6	isoquercitrin	*C. stans Sieb. Et Zucc*	(57)
		& *C. rehderiana*	(81)
7	quercetin-3,7-biglucoside	*C. purpurea* var. *hybrida*	(77)
8	quercetin3-O-beta-D-glucuronopyranoside	*C. stans Sieb. Et Zucc*	(57)
		& *C. rehderiana*	(81)
9	terniflonoside A	*C. terniflora*	(82)
10	isovitexinn6”-O-E-p-coumarate	*C. rehderiana*	(81)
11	3,5,7,3’-tetrahydroxyflavone	*C. terniflora*	(83)
12	5,7,3’,5’-tetrahydroxy-dihydroflavone	*C. terniflora*	(83)

Besides flavonoids listed in Table 1.5, *C. hexapetala* are rich in flavonoids. Twelve flavonoids were isolated from this plant by Dong *et al*.[(84)] They are 3,5,6,7,8,3',4'-heptamethoxyflavone, nobiletin, liquiritigenin, hesperetin, naringenin, liquiritigen-7-O-β-D-glucopyranoside,µ5,7,4'-trihydroxy-3'-methoxyflavanone-7-O-α-L-rhamnopyranosyl (1->6)-β-D-glucopyranoside, 6-hydroxybiochain A, formononetin, daidzein, genistein, and tectoridin. Chen [(85)] detected a kind of dihydroxy flavone glycoside from *Clematis armandiiµ*(muutong),uthatuisu5,4’-dihydroxy-3'-methoxyflavaone-7-(6''-O-β-L-rhamonpyranosyl)-β-glucopyranoside.uApigeninu7-(*p*-coumaroyl)-D-glucosideuwasoisolated in *C. terniflora* var. *robusta* flowers.[(86)] From the ethyl acetate and *n*-butanol fractions of *C. purpurea* var. *hybrida* flowers cultivated in Egypt, kaempferol-3-O-glucoside, kaempferol-7-O-glucoside and quercetin-3,7-O-diglucoside were isolated.[(77)]

Du *et al.*[81] obtained a new flavone C-glycoside (isovitexin 6"-O-E-p-coumarate) and two known flavonoid glycosides (isoquercitrin and quercetin 3-O-β-D-glucuronopyranoside) from an ethanol extract of aerial parts of *C. rehderiana*, and isoquercitrin scavenged DPPH radical strongly with an IC_{50} of 13.5 μM. Study from Gulibahaer *et al.*[87] showed that all parts of *C. sibirica* (L.) Mill were rich in flavonoids, and the contents of flavonoids followed the sequence of leaf > fruit > stem. The LC-MS results from a previous study in this laboratory,[52] as referred to in Table 1.6, showed that the five samples each contained four of the same high molecular weight (MW) flavonoids that have not previously been reported from the leaf of *Clematis* species. The molecular weights were 722, 788, 950 and 1096, respectively. The aglycone analysis by LC-MS showed that the aglycones were consistent with quercetin and kaempferol, which are the usual ones found in *Clematis* spp.

Table 1.6 Chemical constituents of *Clematis* species leaves determined by LC-MS.

Retention time (min)	MW	Aglycone	Glycoside	Molecularbformula (proposed)
10.90	722	kaempferol	3xC_6 sugars	$C_{33}H_{40}O_{21}$
9.88	788	quercetin	3xC_6 sugars	$C_{33}H_{40}O_{22}$
10.64	950	quercetin	4xC_6 sugars	$C_{39}H_{50}O_{27}$
9.52	1096	kaempferol	5xC_6 sugars	$C_{45}H_{60}O_{31}$

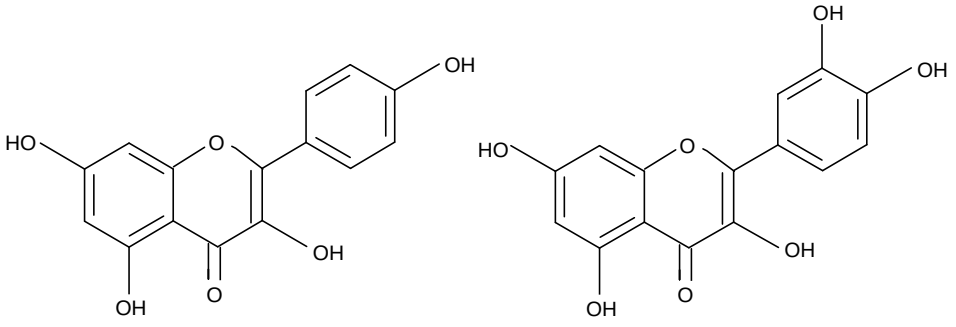

Kaempferol Quercetin

Figure1.3 Molecular structure of kaempferol and quercetin.

1.3.4 Lignans

In 1995, Kizu [57] isolated 5 lignan consistuents from the root of *C. stans Sieb. et Zucc*. They were clemastanin A, clemastanin B (Figure 1.3), (+)-lariciresinol 4-O-D-glucopyranoside, (+)-lariciresinol4'-O-D-glucopyranoside and (+)-pinoresinol 4,4'-O-bis-D-glucopyranoside, in which clemastanin A and clemastanin B were the first detected compounds. Huang isolated (+)-pinoresinol 4,4'-O-bis-D-glucopyranoside, (+)-pinoresinol4'-O-D-glucopyranoside,a(+)-syringaresinol4'-O-D-glucopyranoside, (+)-lariciresinol-4,4'-O-bis-D-glucopyranoside,a(+)-lariciresinol4-O-D-glucopyranoside, (+)-lariciresinol 4'-O-D-glucopyranoside from *C. armandii*.[88]

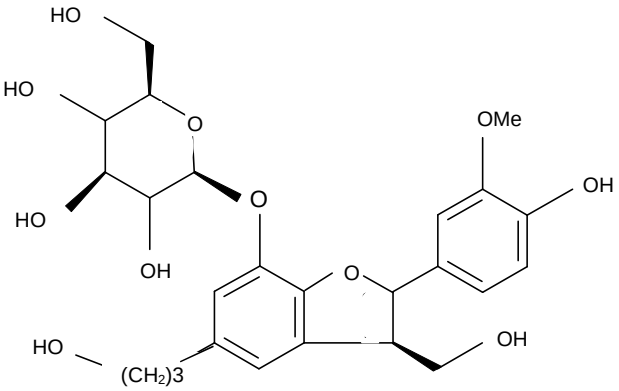

Clemastanin A

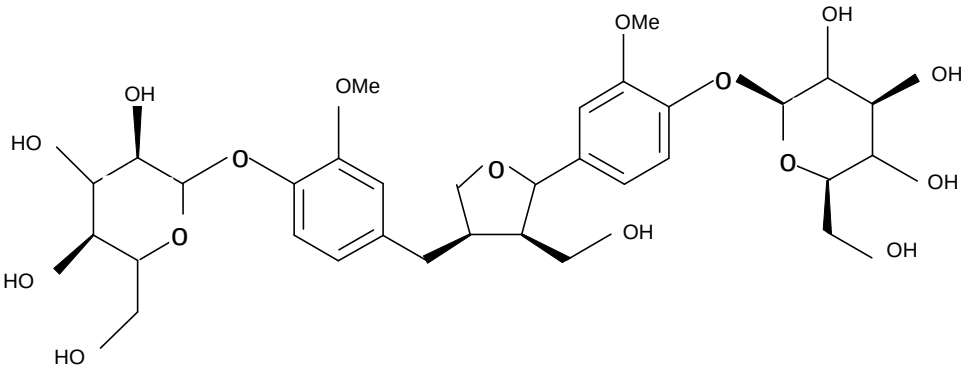

Clemastanin B

Figure1.4 Molecular structures of clemastanin A and clemastanin B

Some lignan constituents were obtained from *C. parviloba*. They are (+)pinoresinol, (+)pinoresinol-4'-O-β-D-glucopyranoside,a(-)syringaresinol,a(+)syringaresino-4'-O-β-D-glucopyranoside,a(-)episyringaresinol,a(+)medioresinol-4'-O-beta-D-glucopyranoside,a(+)lariciresinol-4-O-beta-D-glucopyrano-side,a(+)lariciresinol-4'-O-beta-D glucopyranosideaanda(+)lariciresinol-4,4'-O-bis-β-D-glucopyranoside.[89] Two new lignans, clemomanshurinane A and B were isolated from the roots and rhizomes of *C. manshurica*.aClemomanshurinaneAaandaB,a(+)dihydrodehydrodiconiferylaalcoholaanda(+)-lariciresinola4,4'-O-bis-β-D-glucopyranoside had inhibitory effects on COX-2 at a final concentration of 10^{-5} mol/l, with the inhibition rates 65.8%, 71.8%, 53.3%aanda60.3%,arespectively.[90]aFurthermore,astigmasterol-3-O-β-D-glucopyranoside was obtained in *C. terniflora*[83] and *C. armandii*.[91]

1.3.5 Other constituents

Beside the saponins, flavonoids and lignans, other constituents were also obtained from *Clematis* spp.

Two new macrocyclic glycosides, clemahexapetoside A and B were isolated from the roots and rhizomes of *C. hexapetala*.[92] Shi analysed the roots and rhizomes of *C. mandshurica Rupr.* and *C. hexapetala Pall* and two macrocyclic glucosides, clemochinenoside A from *C. hexapetala* and clemochinenoside B from *C. mandshurica*, were isolated.[93] Phytochemical investigation of *C. armandii* has resulted in the isolation of two new macrocyclic compounds named

clemoarmanosidesaAaandaB,aalongawithatwoaknownamacrocyclicacompoundsabercchemolideaandaclemochinenosideaB.[94]aPolysaccharides were obtained from stem, leaves and flowers of *C. songarica* Bge [95] and roots of *C. chinenesis* osbeck. [96]

A new phenolic glycoside, 2,6-dimethoxy-4-(3-hydroxy-propen-1-yl)phenyl-4-O-alpha-L-rhamnopyranosyl-(1->6)-beta-D-glucopyranoside and a new D-ribono-gamma-lactone derivative, 3-O-beta-D-glucopyranosyl-2-hydroxymethyl-D-ribono-gamma-lactone have been isolated from the roots and rhizomes of *C. hexapetala Pall* by Dong.[97] Three new phenolic glycosides, clemomandshuricosides A-C and two new D-ribono-gamma-lactone derivatives were isolated from the roots and rhizomes of *C. mandshurica*.[98]

Jiang[99] analysed the chemical components of the essential oils from *C. hexapetala* by using gas chromatography-mass spectrometry (GC-MS). The result showed that the major components of the essential oil from *C. hexapetala* were palmitic acid and 3-hydroxy-4-methoxyl benzaldehyde. The volatile components between stems and roots of five *Clematis* species from China were studied and analyzed by GC-MS combined with alternative moving window factor analysis. The major volatile components were n-hexadecanoic acid and (ZZ)-9,12-octadecadienoic acid.[100]

Furthermore, three new alkaloids, methyl 7-ethoxy-3-indolecarbonate, methyl 7-O-α-l-rhamnopyranosyl-(1->6)-β-D-glucopyranosyla3-indolecarbonateaandaα-lrhamnopy-ranosyl-(1->6)-β-d-glucopyranosyl 3-indolecarbonate have been isolated from the

roots of *C. mandshurica*.[101] Two aporphine alkaloid, β-magnoflorine and α–magnoflorine were obtained from *C. parviloba*.[102] Five compounds, scopoletin, caffeic acid, inositol, 1-tria-contanol and β-sitosterol were isolated from the aerial part of *C. intricata* for the first time.[103] Nine compounds, friedelin, anemonin, β-sitosterol, palmitic acid, vanillic acid, isolariciresinol, 5-hydroxymethyl-5H-furan-2-one, n-nonane, daucosterol, were isolated from the roots and rhizomes of *C. hexapetala*.[104] Clemaphenol A and dihydro-4-hydroxy-5-hyroxymethy-2(3H)-furanone were separated from the root of *C. chinensis*.[105] Sucrose octaacetate, which rarely exists in plants, was isolated from *C. japonica* root [106]. Analysis of the reaction product of [1-^{14}C] linolenic acid incubated with a homogenate of leaves of *C. vitalba* by reversed-phase high-performance liquid radio chromatography demonstrated the presence of the 12-oxo-10,15(Z)-phytodienoic acid, 9(S)-hydroxy-10(E),12(Z),15(Z)-octaclecatrienoic acid, omega5(Z)-etherolenic acid, and 9-[1 '(E), 3'(Z),6'(Z)-nonatrienyloxy]-8(Z)-nonenoic acid [8(Z)-colnelenic acid].[107]

Furthermore, other constituents like anthocyanin, stigmasterol, coumarin, organic acid, steroid, phenolic glycoside and volatile constituents have been isolated from *Clematis* species. [76, 91, 108-118]

A literature study of the chemical constituents of *Clematis* spp. worldwide revealed that *Clematis* spp. are rich in different kinds of chemical constituents, including flavonoids, saponins, phenolic glycosides, alkaloids, etc. The large variety of

chemical constituents suggests that *Clematis* spp. might provide natural resources for the discovery of biologically active constituents of therapeutic value in the future.

1.4 Biological Activity

Clematis spp. do not only have a large variety of chemical constituents, reports on the biological activity of *Clematis* spp. are also numerous, and some species are already formulated as medicines and used clinically.

1.4.1 Antimicrobial activity

Clematis spp. were reported to have antibacterial activity in many papers and in a previous study conducted in this laboratory.

C. cirrhosa was active against *Trichophyton violaceum*.[119] *C. hirsuta* (leaves) showed a pronounced antifungal activity against *Candida albicans* and the dermatophytes *Trichophyton rubrum*, *Epidermophyton floccosum*, and *Microsporum canis*.[120] Two new triterpene saponins isolated from the ethanol extract of the aerial parts of *C. tangutica* showed evident antifungal activity (MIA(minimum inhibition amount) approximately 2.5 μg/disc) against *Saccharomyces cerevisiae*, similar to the positive control amphotericin B and ordinary activities (MIA approximately 10 μg/disc) against *Penicillium avellaneum* UC-4376, *Candida glabrata*, *Trichosporon*

beigelii and *Pyricularia oryzae*.[121] A decoction of *C. chinensis* had antibacterial activity against *Staphylococcus aureus* and *Shigella shigae*. [122]

A broad activity against pathogenic yeast and yeast-like microorganisms was shown in crude extracts of young shoots of *C. vitalba*. MICs ranging from 1.4 to 12.3 μg/ml were observed. After fractionating with petroleum ether, ethyl acetate and methanol, antimycotic activity was observed only in methanol fractions.[123] Comparison of the antibacterial activity of *Clematis* spp. showed that the antibacterial activity in lipid-soluble constituents isolated from the leaves of *C. flammula* and *C. tecta* was strongest, followed by *C. fremonti*, and *C. integrifolia* and *C. vitalba* was the least effective.[124] β-magnoflorine and α–magnoflorine, aporphine alkaloids isolated from *C. parviloba*, had potent antifungal activities against *Penicillium avellaneum* UC-4376.[102]. Moreover, antimicrobial activity was obtained from a fruit extract of *C. apiifolia* DC. It exhibited MICs in the vicinity of 0.1% against various yeasts and of less than or equal to 0.4% for the non-lactic bacteria. MICs against lactic acid bacteria were about 0.2%. Its principal antimicrobial compound was protoanemonin.[125]

The antimicrobial activity of Australian native and Tasmania native *Clematis* spp. were studied previously in this laboratory by Jin.[52] Polar fractions had the highest antibacterial activities. *C. gentianoides* stem had the highest activity against *Escherichia coli* and *C.* 'garden surprise' stem had the highest activity against *Bacillus subtilis*. These effects did not seem to be due to protoanemonin only. The

non-polar fraction of *C.* 'garden surprise' extract had the highest activity against *Candida albicans* (inhibition radius was 14 mm) and *C. gentianoides* flowers had the strongest activity against *T. mentagrophytes* (inhibition radius was 8.5 mm). Compared with the study by Herz[46], who considered the protoanemonin (Figure 1.3) to be the active antibacterial constituent in *C. disoscoreifolia*, the antimicrobial effects of *Clematis* spp. in Jin's study was not correlated solely to the protoanemonin content.[52] Therefore, there might be other compounds present in some of the extracts that contributed to the above results.

1.4.2 Anticancer

A saponin-enriched fraction prepared from the MeOH extract of the roots of *C. chinensis* showed cytotoxic activity against HL-60 promyelocytic leukemia cells. Among the isolated saponins, monodesmosidic saponins exhibited cytotoxic activities against cultured tumour cells [126]. The total saponin of *C. chisensis Osbeck* had cytocidal effects on experimental tumour EAC cells, S180A cells and HepA cells *in vitro*. The IC_{50} values were 242aμg/ml, 193aμg/ml and 130aμg/ml respectively. *In vivo* the growth of transplanted mouse tumour (S180) was inhibited by the *C. chisensis Osbeck* with inhibitory rates 40.3% (0.25 g/kg), 55.1% (0.5 g/kg), 53.0% (1 g/kg), but *C. chisensis Osbeck* (0.2 g/kg, 0.4g/kg, 0.5 g/kg) has no effect on survival time of tumour-implanted mice (S180A).[127]

A study from Ding *et al.*[128] showed that triterpenoid derivatives from *C. ganpiniana* could significantly inhibitory activities against MCF-7 and MDA-MB-231with IC_{50}

values of 0.7-16.5 μg/ml. Clematosides S and α-hederin, two saponins isolated from stems of *C. parviloba*, had moderate cytotoxic activities against four human tumour cell lines (HCT-8, Bel-7402, BGC-823 and A-2780) with IC_{50} values in the range of 1.44-6.86 μg/ml.[(129)]

Table 1.7 Antitumour activities of *Clematis* spp.

		% P388 cell control growth……									
Fraction from C18 cartridge		[a]1	1	[b]2	2	[c]3	3	[d]4	4	[e]5	5
~extract mass assayed (μg)		[f]5	[g]0.5	5	0.5	5	0.5	5	0.5	5	0.5
C. gentianoides	leaf	0	81	0	65	25	99	29	69	22	93
	stem	0	60	0	42	33	109	12	99	19	98
	root	0	78	0	57	10	85	11	87	42	110
	flower	0	86	2	67	9	115	10	85	32	104
C. 'garden surprise'	leaf	0	72	1	47	20	100	28	100	27	109
	stem	0	41	3	46	9	104	7	107	14	97
	root	0	86	0	55	16	105	6	106	9	93
C. aristata (W)	.leaf	0	45	**3**	**13**	6	89	8	101	9	100
	.stem	0	51	0	40	3	94	4	97	9	107
	.root	0	78	0	37	4	108	13	84	85	107
C. aristata (N)	.leaf	14	83	6	92	47	106	22	104	8	99
	.stem	0	75	0	41	79	102	107	102	88	113
	.root	3	91	0	89	56	109	38	110	54	95
C. montana alba	leaf	0	90	2	80	10	104	9	102	9	90
	stem	0	99	0	88	107	104	49	111	15	106
	root	0	81	0	51	0	94	30	92	75	110

[a]1 is the first fraction from C18 cartridge [b]2 is the second fraction from C18 cartridge
[c]3 is the third fraction from C18 cartridge [d]4 is the fourth fraction from C18 cartridge
[e]5 is the fifth fraction from C18 cartridge [f]5 is 5μg extract assayed
[g]0.5 is 0.5 μg extract assayed

Two triterpene glycosides, montanosides 1 and 2 which were isolated from methanolic extract of *C. montana*, had cytotoxic activities against various squamous carcinoma cells and human gingival fibroblast cells.[(69)] The *C. mandshurica* saponins showed significant anticancer activities on Sarcoma-180, HepA and P338 tumours implanted in mice.[(130)] The above literature study revealed that saponins are the major antitumour constituents in *Clematis* spp. Furthermore, ranunculin had cytotoxic

activity against tumour cells *in vitro*, and it proved that this cytotoxic activity related to inhibition of DNA polymerase.[131]

The results of antitumour activity studied in this laboratory by Jin showed that SPE fractions 1 and 2 of investigated Tasmanian native *Clematis* spp. had antitumour activities (Table 1.7) and there was a significant antitumour activity at 2 µg/ml of *C. aristata* (W) solvent extract (13.2% P338 cell control growth).[52]

1.4.3 Anti-inflammation and analgesic effects

The pharmaceuticals of "Wei Ling Xian" are used to treat parotitis, cholecystits, periodontitis, rheumatoid arthritis, faucitis, acute tonsillitis, acute icterohepatitis and conjunctivitis clinically.[49] Furthermore, *Clematis* spp. may offer some protection against OA. Six petal *Clematis* root parenteral solution ("Wei Ling Xian") significantly decreased the interlukin-1β level in the joint fluid in an animal mode of OA and in the supernatant from *in vitro* cultured chondrocytes. Presumably the therapeutic effect of "Wei Ling Xian" on OA can be due to these activities.[132]

Li *et al.*[133] found the ethanol extracts of three *Clematis* species, *C. pickeringii*, *C. glycinoides* and *C. microphylla*, inhibited the activities of cyclooxygenase-1 (COX-1), cyclooxygenase-2 (COX-2) and 5-lipoxygense (5-LOX) to different extents. The stem extract of *C. pickeringii* showed the highest inhibitory activities among the three species against COX-1, COX-2 and 5-LOX with IC_{50} values of 73.5, 101.2 and 29.3 µg/ml. One of its fractions also significantly elevated peroxisome proliferator-

activated receptor alpha (PPARα) expression by 173, 280 and 435% and gamma (PPARϒ) expression by 140, 228 and 296% at 4, 8 and 16 μg/ml, respectively.

Compound Radix Clematidis mixture markedly decreased the frequency of body distortion induced by acetic acid in mice and significantly prolonged the latent period of pain reaction induced by a hot board in mice. This mixture also inhibited tumefaction in feet induced by albumn injection, and reduced the degree of tumefaction in the auricle induced by dimethylbenzene. These results show that the compound Radix Clematis mixture has a significant role in anti-inflammation and analgesia.[134],[135] *C. intricata*, one of the species of "Tou Gu Cao", exhibited analgesic effects and the ability to inhibit the increase of abdominal capillary permeability induced by acetic acid.[136]

Extracts of dried *C. vitalba L.* aerial parts were shown to have a potent effect on carrageenan-induced hind paw oedema and acetic acid-induced increased vascular permeability models. In addition, a new C-glycosylflavone, 4'-O-coumaroyl-isovitexine (vitalboside) was isolated as the main active ingredient of the aerial parts. Vitalboside showed a potent and dose-dependent (in 75 and 150 mg/kg dose) *in vivo* anti-inflammatory activity against acute (carrageenan-, serotonin- and PGE (2)-induced hind paw oedema model, castor oil-induced diarrhea), subacute (subcutaneous air-pouch) and chronic (Freund's complete adjuvant-induced arthritis) models of inflammation. This compound was the main antinociceptive principle, which was assessed by using the models based on the inhibition of *p*-benzoquinone-

induced writhings, as well as antipyretic activity against Freund's complete adjuvant-induced increased body temperature.[137] *C. herryi*[49] had sedative activity. Mostafa *et al.*[138] reported that the aqueous extract of *C. brachiate* leaf could significantly ($P<0.05$) reduce rat paw oedema induced by carrageenan and histamine.

The anti-inflammatory and analgesic effects of *C. chinensis* total saponins were obtained.[139] They could markedly inhibit dimethylbenzene-induced ear swelling in mice and relieve pain of mice, and also significantly inhibit the swelling of paw induced by egg white and the granuloma induced by cotton in the rat. Furthermore, the total saponins of *C. chinensis*[140] were effective on adjuvant arthritis (AA) in rats and decreased the levels of IL-1, IL-6, IL-8, TNF-α and PGE2. Study from Sun *et al.*[141] reported the potential anti-inflammatory therapeutic value of AR-6, a triterpene saponin isolated from *C. chinensis* osbeck, in RA. It significantly decreased the symptoms of adjuvant-induced arthritis in rats and decreased the proliferation of synoviocyte. Anti-arthritic effects of AR-6 correlated with significant decrease of NO and TNF-α produced by peritoneal macrophages, *ex vivo* and *in vitro*. Clematichinenosides AR and AR2[142] also isolated from the root of *C. chinensis* osbeck, decreased the secretion of TNF-α in murine peritoneal macrophages induced by lipopolysaccharides (LPS). Saponins from *C. chinensis* Osbeck roots were effective on the OA model in rats.[143] It dose-dependently reduced cartilage injury and proteoglycan degradation in rats, and also prevented sodium nitroprusside- and monosodium iodoacetate-induced rabbit chondrocyte impairment.

SKI306X, an extract purified from a mixture of three Oriental herbal medicines (*C. mandshurica, Trichosanthes kirilowii* and *Prunella vulgaris*), was studied in Korea for anti-inflammatory and analgesic efficacy. SKI306X[144] inhibited the expression of COX-2 enzyme without affecting COX-1 and COX-2 activity. Leukotriene B4 production and TNF-α release (IC_{50}=97.6 ± 17.8 μg/ml) and NO production (IC_{50}=280 ± 17.8 μg/ml) was also inhibited by SKI306X (IC_{50}=98.7 ± 4.26 μg/ml). But interleukin-1 alpha (IL-1α) release was not attenuated by SKI306X. This result suggested that inhibition of these mediators by SKI306X may be one of the mechanisms responsible for its anti-inflammatory effects. Furthermore, SKI306X[145] did not cause significant gastric irritation, erosion, or ulceration up to the orally administered dose of 2 g/kg and the intraperitoneal dose of 125 mg/kg, because SKI306X could spare the gastric mucosa through significantly suppressing gastric leukotriene synthesis.

SKI306X inhibited *in vitro* cartilage degradation and the production of inflammatory mediator.[146] It had a therapeutic effect on OA as well. It could inhibit proteoglycan degradation in cartilage explant culture, and its prophylactic administration significantly protected the knee joint of rabbit from OA-like change in a collagenase-induced experimental OA model.[147] The results of the study performed by Lee showed that the pharmacological efficacy of SKI306X in protecting OA in part may result from the inhibition of staurosporin-induced apoptosis in chondrocytes by *C. mandshurica*. The level of Bcl-2 expression was decreased after staurosporin treatment, but it was sustained after the combination treatment with *C. mandshurica*.

Whereas staurosporin induced the degradation of 32 kDa caspase-3 precursor and the production of 85-kDa cleavage products of poly (ADP-ribose) polymerase (PARP) in aatime-dependentafashion,a*C.amandshurica*atreatmentaprevented those manifestations.[41]

C. mandshurica could ameliorate inflammatory disease by exerting an anti-inflammatory effect in cases of pro-inflammatory and cell-mediated inflammation.[39] The ethanolic extract of *C. mandshurica* at 100 μg/ml was found to significantly block the production of the pro-inflammatory mediators, nitric oxide (NO) and PGE2, in LPS/interferon (IFN)-γ-stimulated mouse peritoneal macrophages, by up to 77% and 59%, respectively. In addition, it significantly inhibited cell proliferation and cytokine production (IL-2 and IFN-γ) in splenocytes stimulated with concanavalin A (5 μg/ml). Furthermore, the extract reduced *in vivo* inflammation in oxazolone-induced delayed type hypersensitivity model mice.

Lee[148] showed that *C. mandshurica* could prevent staurosporin-induced down-regulation of several antiapoptotic bcl-2 family proteins Bcl-xL and Bcl-2, and staurosporin-induced up-regulation of an apoptotic bcl-2 family protein Bax. *C. mandshurica* also prevented staurosporin-induced down-regulation of a premitochondrial antiapoptotic protein 14-3-3. The siRNA to 14-3-3 abolished the prevention of caspase-3 activation by *C. mandshurica*. A viability assay corroborated that silencing of the 14-3-3 gene abolished this apoptosis protection efficacy by *C. mandshurica*. These results suggest *C. mandshurica* could prevent staurosporin-induced apoptosis in articular chondrocytes. Their following study[149] demonstrated

C. mandshurica could prevent TNF-related apoptosis inducing ligand-induced apoptosis in primary cultured articular chondrocytes.

Immunoprecipitation assay elucidated that *C. mandshurica* prevented the staurosporin-induced reduction of the interactions between 14-3-3 with phospho-ser112-Bad and Bcl-xL to phospho-ser155-Bad.[148] *C. mandshurica* Maxim. water extract had a beneficial effect on rats AA. The administration of the extract (2, 5 and 10 mg/kg, subcutaneously) inhibited the inflammatory response and restored the weight of body and immune organs of AA rats. It reduced the increased synoviocyte proliferation and levels of TNF-α and IL-1 in supernatants of synoviocytes in AA rats significantly, and markedly increased IL-10 in synoviocytes at protein and transcription level.[150]

1.4.4 Effects on cardiovascular system

C. heapetalis was protective in experimental acute myocardial ischemia in rats. Its decoction and infusion had the effect of inhibition, then excitation of toad heart [49]. The appropriations decreased the blood pressure in dogs, and the infusion had more efficacy than the decoction[49]. Karpovich[151] found that *C. hexapetala* can decrease the blood pressure (BP) in narcotized cats after intravenous administration of 0.1 mg/kg 70% alcohol extract. The degree of depression of BP was 41.7%.

Ho *et al*. studied the cardiovascular pharmacology of aqueous of *C. chinensis* extracts in rats both *in vivo* and *in vitro*. *C. chinensis* extracts produced a hypotensive

response that was mediated through histaminergic activity. Furthermore, *C. chinensis* extracts relaxed isolated methoxamine preconstricted helical tail artery strips and produced both negative chronotropic and inotropic effects on isolated atria.[152]

1.4.5 Antimalarial activity

C. brachiata is used in Kenya for the management of headaches, malaria and other febrile illnesses, abdominal disorders, yaws, and skin disorders. Old stems and leaves are chewed for the management of toothache and sore throat. The stem and leaf extracts had insignificant antimalarial activity. The root extract of *C. brachiata* gave the highest *in vitro* antimalarial activity against the multidrug-resistant strain, *Plasmodium falciparum* VI/S (MIC_{50}=39.24 mg/ml). The toxicity of the extracts was assessed using the brine shrimp lethality bioassay. The LD_{50} values of the stem and leaf methanol extracts against the brine shrimp larvae was 365.60 and 66.5 mg/ml, respectively.[36]

Radix Clematidis has been used to remedy malaria among Fujian people. Attempts were made to extract the effective anti-malaria ingredient from Radix Clematidis. The inhibition rates of *P. berghei* mouse malaria protozoon were compared by testing different extracts from Radix Clematidis.[153]

1.4.6 Effects on the urinary system

C. hexapetala showed anti-diuretic activity in animal trials. The efficacy of 2 ml of a 50% water decoction was the same as 0.1 unit of posterior pituitary hormone. The

decoction can contract the kidney as well. However, *C. montana* and *C. armandii* had obvious diuretic activity and enhanced the excretion of electrolytes.[49] The infusions of the root and aerial part of *C. montevidensis Spreng* showed a moderate diuretic activity. This effect could be due, at least in part, to the presence of oleanolic acid isolated from this plant.[154]

1.4.7 Effects on the biliary tract and hepatic protective activity

Song[49] reviewed the water decoction and alcohol extract of *C. chinensis* for their effect on the biliary tract in animals. The results showed that both extracts increased bile secretion in rats. The alcohol extraction also enhanced dog bile secretion and dilated choledochus sphincter. The isolated guinea pig ileum smooth muscle was dilated, against the ileum contraction due to acetylcholine and histamine. The decoction of *C. hexapetala* root had obvious stimulatory action in the isolated mouse, rat and rabbit intestinal tube.[49]

Chui[155] studied the hepatic protective effect of *C. chinensis* extract on carbon tetrachloride-induced hepatotoxicity in rats. The results of amine transferase, aspartate aminotransferase and alanine aminotransferase, have shown a significant hepatic protective effect after treatment with *C. chinensis* ($P<0.005$). In addition, the fatty degeneration around the central vein area and necrosis of the central lobule was moderately changed.

1.4.8 Androgen target organs

The effect of *C. fusca Turcz.* preparations on the prostate and seminal vesicles was studied in castrated rats. There was seen an intensification of the functional activity of these organs, similar to the result of methyltestosterone action.(156)

1.4.9 Other activities

Clematis spp. were reported to have other biological activities. The whole plant of *C. heracleifolia* was appreciably active against recombinant HIV-1 protease at a concentration of 100 mg/ml.(157) The antioxidant activity was obtained from *C. glauca* Willd. The leaves were superior to flowers, fruits and stems in the hydroxyl and superoxide anion free radical scavenging capacities.(158) *C. chinensis* osbeck polysaccharide had significant antioxidant activity *in vitro* and *in vivo*. It could eliminate the hydroxyl free radical and the superoxide anion free radical, reduce red blood cell autoxidation haemolysis induced by H_2O_2, and raise the activities of superoxide dismutase and glutathione peroxidase in hepatic injury mice serum and liver.(159)

Pawar studied the cytotoxic effect of the extracts of *C. ligustifolia* on the porcine renal cell line LLC-PK1. Using bioactivity-directed fractionation, the cytotoxic constituents, quinatic acid, arjunolic acid, and 30-norarjunolic acid along with six glycosides of hederagenin and one glycoside of oleanolic acid were isolated. Out of all the cytotoxic constituents tested only collinsonidine, quinatic acid and 30-norarjunolic acid induced apoptosis as determined in the caspase 3/7 assay. The

findings suggested that structural features of the oleanane skeleton and the nature and type of saccharide linkages play an important role in the cytotoxic and apoptosis-inducing properties of these compounds.[160]

Anemonin, isolated from *C. crassifolia* Benth showed both time- and dose-dependent inhibition (IC_{50}=43.5 μM) of tyrosinase, which participates in the synthesis of melanin. Western blot analysis and immunocytochemical staining revealed that expression of TYR, tyrosinase-related protein 1 (TYRP1) and tyrosinase-related protein 2 (TYRP2) was decreased in anemonin-treated melanocytes. Additionally, reverse transcription and quantitative real-time polymerase chain reaction analyses revealed that expression of mRNAs for microphthalmia-associated transcription factor, TYR, TYRP1, and TYRP2 was also suppressed by anemonin.[161]

An extract of an American original plant, *C. dioica*, showed evident inhibition zones (>9 mm) against *Neisseria gonorrhoeae* isolated from symptomatic patients.[37] Reports from Mostafa *et al*[138] suggested the aqueous extract of *C. brachiate* leaf had antinociceptive and antipyretic properties. The extract reduced the writhing caused by acetic acid in rats and a significant ($P<0.05$) lowering of Brewer's yeast-provoked elevated body temperature was observed.

In the worldwide study of biological activity of *Clematis* spp., although different species demonstrated their potential therapeutic value, the most well-studied species are *C. chinensis* and *C. mandshurica*, especially the anticancer and anti-inflammatory

effects of both species. The saponins isolated from both species might play important roles in their antitumour activities. Furthermore, *C. chinensis* also showed other biological activities, including antimicrobial activity, effects on cardiovascular system, hepatic protective activity. Its polysaccharide had antioxidant activities. However, to our knowledge, other *Clematis* spp. including the Australian native species, have not been studied as well as *C. chinensis* and *C. mandshurica*. Therefore, it might be valuable to make further investigation on other species of *Clematis*.

1.5 Tasmanian *Clematis* species

There are some Australian native species of *Clematis*, such as *C. aristata, C. gentianoides, C. glycinoides, C. microphylla, C. fawcettii, C. microphylla var. leptophylla* and *C. pubescens*, from which, *C. gentianoides* and *C. aristata* (including wide leaf form and narrow leaf form) are Tasmanian native species as well. *C. microphylla* is also found on Flinders Island, which is a part of Tasmania. A recent Australian hybrid of *C. gentianoides* and *C. aristata* developed by Will Fletcher is *C.* "garden surprise". It has a prostrate, mound-forming habit, large white flowers and no climbing tendrils.

Southwell[(50)] has investigated the protoanemonin concentration in Australian *Clematis* species, including *C. aristata, C. fawcettii, C. gentianoides, C. microphylla, C. microphylla* var. *leptophylla* and *C. pubescens*. Research by Li[(131)] exerted that Australian *Clematis* spp. had inhibited COX1, COX2 and 5-LOX and activated

PPARs. However, there appears to be no published research of other biological activities from Tasmanian *Clematis* spp. Therefore, in a previous study in this laboratory,[52] four Tasmaina *Clematis* spp. (*C. gentianoides*, *C. aristata* [wide leaf form (W)], *C. aristata* [narrow leaf form (N)] and *C.* 'garden surprise') and one Chinese *Clematis* (*C. montana alba*) were chosen for investigation of chemical constituents and biological activities (antioxidant, antitumour and antimicrobial assays).

Protoanemonin was determined in the leaf, stem and root of each species by GC-MS. The mass of protoanemonin in leaf was higher than in stem and root ($P<0.05$). On LC-MS of flavonoids in the five species of *Clematis,* four high molecular weight flavonoids were found, that have never been reported in *Clematis* spp. before.

The leaf of *C.* 'garden surprise' (Tasmanian species) and *C. montana alba* (Chinese species) had the highest antioxidant activity, but the antioxidant activities were relatively poor with gallic acid equivalent values of 22.3 μg/mg and 15.3 μg/mg, respectively. A polar fraction of leaf, stem and root extracts of *C. aristata* (W) had antitumour activity with the highest activity in leaf (13.2% P388 control cell growth at 2 μg/ml). Using tea tree oil as positive control, the water soluble fraction of *Clematis* spp. solvent extracts had obvious antibacterial activity. *C. montana alba* root had the highest antibacterial activity against *E. coli* and *C.* 'garden surprise' stem had the highest activity against *B. subtilis*. The non-polar fraction of *C.* 'garden surprise' extract had the highest activity against *C. albicans* (inhibition radius was 14

mm) and *C. gentianoides* flowers had the strongest activity against *T. mentagrophytes* (inhibition radius was 8.5 mm). Comparing the results of biological activity with chemical constituent data, it seems that protoanemonin was not the only compound that contributed to antioxidant, antitumour and antimicrobial activities.

The Australian *Clematis* spp. contained considerably more protoanemonin than *C. montana alba* and had higher biological activities in antitumour and antimicrobial assays. The results of these studies justify the further investigations of biologically active chemical constituents from Australian *Clematis* spp.

1.6 Scope of Research

Based on the literature above, *Clematis* spp. in worldwide showed a broad range of biological activities. Compounds existing in *Clematis* spp. include ranunculin, anemonin, protoanemonin, saponins, flavonoids, lignans, phenolic glycosides. Australia and Tasmania have native *Clematis* species. Southwell[50] and Li *et.al*[133] reported the protoanemonin concentration and anti-inflammatory activities respectively of Australian native *Clematis* spp., however, to date, there have been no studies on the chemical constituents and biological activities of Tasmanian native *Clematis* spp. Based on the previous study results performed in this laboratory (described in 1.5), the rationale of this study was to investigate the biological effects and pharmaceutical potential of constituents from Tasmanian native *Clematis* spp.

In this study, the antibacterial, antitumour and anti-inflammatory activities were

investigated as Tasmanian *Clematis* spp. have previously indicated potential antibacterial and antitumour effects in pilot work in this laboratory. The purported anti-inflammatory property is a traditional use of *Clematis* spp. plants in worldwide folk medicines. At the same time, identifying antibacterial, antitumour and anti-inflammatory constituents in the investigated Tasmanian native *Clematis* spp. was characterised.

All available *Clematis* spp in Tasmania, both native and exotic species and different cultivars, were obtained from nurseries, gardens and from the wild. These plants were extracted and the extracts were screened for biological activities and analysed by HPLC and LC-MS where necessary to determine their chemical profile.

The most promising extracts were selected for further investigation. They were subjected to bioactity-guided fractionation methodologies including cartridge fractionation, HPLC column (C18 analytical and semi-preparative columns, carbohydrate column) fractionation, and LH-20 Sephadex column purification resulting in the isolation and purification of novel compounds.

The antitumour effects of IC_{50} of active *Clematis* spp. extracts and active constituents were determined by a colourimetric [3-(4,5-dimethylthiazol-2,5-diphenyltetrazolium bromide (MTT)] assay. The antibacterial activities of crude extracts, active fractions and effective constituents were investigated by determination their minimum inhibition concentration (MIC). Antibacterial testing against a broad range of

microorganisms was commenced. The antibacterial mechanisms of isolated active constituents were studied in a series of experiments. Anti-inflammatory activities were investigated with assays developed in-house, including the Griess assay, and cytokine assay. The novel compounds[52] previously detected were chemically characterised by LC-MS and LTQ-Orbitrap-MS.

Chapter 2 Antitumour activity of Tasmanian *Clematis* species extracts and their cytotoxic chemical constituents

Abstract- The medicinal plants *Clematis* species (*Ranunculaceae*) are used in folk medicine in China as analgesic, diuretic and anti-inflammatory agents. The purpose of this study was to assess the anticancer activity of Tasmanian *Clematis* species for their potential as new chemotherapy drug sources. In this study, extracts of eleven Tasmanian *Clematis* plants from four species were evaluated for dose-dependent cytotoxic effects against the P388 cell line using a colourimetric MTT assay. The effective extracts were fractionated by C18 HPLC analytical and semi-preparative columns, HPLC carbohydrate analytical column and Sephadex LH-20 column to determine cytotoxic constituents.

Ten out of eleven investigated *Clematis* spp. had cytotoxic effects on P388 cells. The antitumour activities from high to low were *C. microphylla*- TN > *C. aristata*-L > *C. aristata*-TN1 > *C. aristata*-TN > *C. aristata*-W2 > *C. gentianoides*-UTAS > *C. aristata*-EN > *C. aristata*-W3 > *C. aristata*-W1 > *C. vitalba*-RS. The IC_{50} of the most effective two plants (*C.* aristata-L and *C. microphylla*-TN) were 0.164 mg/ml and 0.084 mg/ml, respectively. As a result of this investigation, ranunculin and its isomers were determined as the antitumour constituents in Tasmanian *Clematis* spp. These compounds could be hydrolysed by the cell medium to protoanemonin. The antitumour study exerted that ranunculin was a pro-cytotoxin, and the real antitumour constituent of *Clematis* spp. was protoanemonin. No other cytotoxic constituents were present in concentrations high enough to demonstrate P388 toxicity.

2.1 Introduction

Cancer: it is difficult to imagine anyone who has not heard of this illness. It is a term used for diseases in which abnormal cells divide without control and are able to invade other tissues. Throughout medical history, plant products have been shown to be valuable sources of novel anti-cancer drugs. Examples are taxol which was isolated from the bark of the Pacific Yew tree by Wall and Wani in 1967, the vinca alkaloids derived from the Madagscan periwinkle plant *Catharanthus roseus* and the camptothecins isolated from Chinese tree *Camptotherca acuminate.* Dennis *et al.*[162] summarized some cytotoxic drugs developed from plant resources, which are presented in Table 2.1.

Table 2.1 Some cytotoxic drugs developed from plant sources, adopted from Dennis *et al.*[162]

Drug	Mechanism of action	Plant source
Vinblastin, vincristine	Inhibition of tubulin polymerization	*Catharanthus roseus* (Apocynaceae)
Etoposide, teniposide	Inhibition of topoisomerase II	*Podophyllum peltatum* *P. emodi* (Berberidaceae)
Paclitaxel, docetaxel	Promotion of tubulin stabilization	*Taxus brevifolia* (Taxaceae)
Irinotencan, topotencan 9-Aminocampothecin 9-Nitrocamptothecin	Inhibtion of topoisomerase I	*Camptotheca acuminata* (Nyssacead)
Homoharringtonine	Inhibtion of DNA, polymerase α	*Harringtonia cephalotaxus* (Cephalotaxaceae)
4-Ipomeanol	Cytochrome P-450-mediated conversion into DNA-binding metabolites	*Ipomoeca batatas* (Convolvulaceae)
Elliptinium	Inhibtion of topoisomerase II	*Bleekeria vitensis* (Apocynaceae)
Flavopiridol	Inhibition of cyclin-dependent kinases	*Amoora rohituka, Dysoxylum binectariferum* (Maliaceae)

There are some studies indicating that *Clematis* spp. also have potential antitumour activities (section 1.4.2). Saponins, which mainly exist in roots and stems, are reported to be major antitumour constituents in *Clematis* spp. Ranunculin was reported to have cytotoxic activity related to inhibition of DNA polymerase.[131] However, there is no published studies reporting the antitumour effects of *Clematis* leaf material. Previous studies performed in this laboratory have indicated that Tasmanian native *Clematis* spp. leaf extracts fractions also show cytotoxic activities against P388 cells (Table 1.7). Therefore, the antitumour activities of Tasmanian leaf fractions will be screened and compared, and their active constituents will be investigated in this chapter.

In this study, the *in vitro* microculture assay of P388 cell viability by the MTT method was used to screen the *in vitro* antitumour activity of leaf extracts of Tasmanian *Clematis* species. The P388 cells cytotoxicity assay is the primary screening model at the National Cancer Instituent (NCI), with a critical role as the "funnel" or "gate" through which all compounds must first pass.[163] MTT assay is one of three alternative assays for cellular growth and viability for possible use in primary screening of new drugs. It is a metabolic assay. Living cells are able to cleave the yellow-coloured MTT into a blue-coloured insoluble product (formazan) by the mitochondrial enzyme succinate-dehydrogenase.[164] The formation of formazan is proportional to viable cell numbers and can be measured conveniently in an automated colourimeter. The potential antitumour constituents in the investigated

Clematis spp. were isolated, following initial screening by bioassy-guided fractionation.

Headspace-GC/MS-SPME is employed in this study. SPME is a sample enrichment technique, used to transfer analytes to the GC. This technique was invented by Pawliszyn in 1989.[165] The basic principle of SPME sampling is the partitioning of analyte between the fibre coating and the sample matrix. In this experiment, the SPME-Headspace technique was employed, which a SPME fibre is inserted into the headspace without contacting the sample. The fibre coating absorbs vapours of analytes from the headspace.

2.2 Experimental

2.2.1 Reagents used

2.2.1.1 Extraction and isolation of plant material

The solvents used for extraction of plant material were laboratory reagent grade dichloromethane (DCM) (Polytreat, Australia) and methanol (MeOH) (>98%) (BDH, Australia). Solvents were freshly redistilled before use. Cartridge isolation was performed on Strata-X33 µm polymeric sorbent 200 mg/3 ml solid-phase extract (SPE) cartridges (Phenomenex, Australia) by MeOH (HPLC grade, Optigen, Australia). Gel permeation chromatography was performed on Sephadex LH-20

(Sigma, Australia) using 100% MeOH. HPLC column chromatography was carried out by distilled water and acetonitrile (ACN) (HPLC grade, Optigen, Australia).

2.2.1.2 Antitumour assay (P388 murine leukaemia cell line)

Pipettes and pipette tips of various sizes and a 200 µl multichannel pipette were from Eppendorf, Australia; MTT, gentamicin, L-glutamine, trypan blue solution (0.4%) and phosphate buffered saline (PBS) tablets were purchased from Sigma-Aldrich, Australia. Rosewell park memorial instituent 1640 (RPMI-1640) medium, Dulbecco's modified eagle medium (DMEM) and foetal bovine serum (FBS) were purchased from Invitrogen, Australia. Sterile tissue culture flasks, sterile 96-well/flat bottom microplates, sterile centrifuge tubes with triple seal cap (15 ml and 50 ml) were purchased from Iwaki, Japan. Sterile disposable plastic pipettes (10 ml) were purchased from Sterilin, UK. Autoclavable V-shape reagent reservoirs (70 ml) were purchased from Socorex, Switzerland.

2.2.2 Instruments

2.2.2.1 Sonicator

Sonicator (Sanophon Ultrasonic cleaner, Australia) was used for improving extraction speed.

2.2.2.2 High Pressure Liquid Chromatography (Analytical and Semi-preparative)

All HPLC analyses were performed using Varian equipment that included a Model 230 solvent delivery system equipped with a Model 410 autosampler, a Model 335 photo-diode array detector (PDA) (Varian, Australia) and a Model 2000ES evaporative light scattering detector (ELSD) (Alltech, Australia). Analytical analysis columns used were an Apollo C18 5 µm, 250 mm x 4.6 mm (GRACE, USA) connected with a C18 guard cartridge, 4 x 3 mm (Phenomenex, Australia), and Alltech Prevail® carbohydrate column 5 µm, 250 mm x 4.6 mm (Alltech, Australia) connected with a 4 x 3 mm NH_2 guard cartridge (Phenomenex, Australia). The semi-preparative HPLC column was an Apollo C18 5 µm, 250 mm x 10 mm (GRACE, USA).

2.2.2.3 High Performance Liquid Chromatography-Mass Spectrometry (LC-MS)

LC-MS was performed using a Waters Alliance 2690 high performance liquid chromatograph (HPLC) and Waters 996 PDA detector (Waters, USA) coupled to a Finningan LCQ ion trap mass spectrometer (Finningan Coorporation, USA). The analytical column was the same as used for HPLC.

2.2.2.4 Ultra Performance Liquid Chromatography-Mass Spectrometry (UPLC-MS)

A Water Acquity H-Class UPLC system connected to a Xevo triple quadrupole mass spectrometer was used for UPLC-MS analysis (Waters, Australia). The column was a BEH amide column, 1.7 µm, 50 mm x 2.1 mm diameter (Waters, Australia).

2.2.2.5 Gas Chromatography-Mass Spectrometry (GC-MS)

GC-MS was performed using a Varian 3800 GC connected to a Varian 1200 triple quadrupole mass spectrometer. The column was a 30 m x 0.25 mm diameter, 0.25 micron film VF5-ms. A Varian 1177 injector was used in split mode. All equipment was from Varian, Australia.

2.2.2.6 Microplate reader

A model 680 microplate reader (Bio-Rad Laboratories, USA) was used in the MTT assay for reading the absorbance of formazan. The absorbate wavelength was 490 nm.

2.2.2.7 Biosafety II cabinet

A Top Safe model 1.2 ABC Class II Biological Safety Cabinet (Euroclone, Italy) was used for personal, environment and product protection.

2.2.2.8 CO_2 incubator

A Mitre 4000 Series CO_2 cell culture incubator (Cotherm Scientific, New Zealand) was used to incubate P388 cells.

2.2.2.9 Microscopy and Hemacytometer

Model 225 Microscope (Gillet & Sibert, England) and B.S. 748 Hemacytometer (Hawksley, England) were used to observe and count P388 cells in cell culture.

2.2.2.10 Rotary Evaporator

A rotary evaporator (Heidolph Laboratory Products, Germany) was used for removing the excess solvents from the solutions.

2.2.2.11 Solid phase microextraction (SPME) fibre with holder

Fused silica fibres (75µm) coated with polydimethylsiloxane (PDMS), and Supelco manual SPME syringe were obtained from Supelco, Australia.

2.2.2.12 Fraction collector

Waters Fraction Collector III (Waters, USA) was used for performing HPLC fractionation.

2.2.2.13 Centrifuge

Model 7111 (Surgical & Medical Products, Australia) was used for centrifuging cell suspension.

2.2.2.14 Stirrer hotplate

Stirrer hotplate (Scientific equipment manufacturer, Australia) was used for stirring and maintaining temperature (35°C) of cell culture media.

2.2.3 Plant material

Two *C. aristata* cultivars and a *C. microphylla* were purchased from Plants of Tasmania Nursery, Ridgeway and a *C. aristata* was purchased from Lindisfarne Village Garden Centre, Lindisfarne in January 2008. Two cultivars of *C. aristata* were collected in Weilangta Forest and Eaglehawk Neck, respectively, in March 2008. *C. vitalba* was collected from a private garden in Regent Street, Sandy Bay, and *C. gentianoides* was collected from the University of Tasmania Hobart Campus in March 2008. Two cultivars of *C. aristata* were collected in Weilangta Forest, Tasmanian in March 2009. *C. microphylla* was collected from a private garden in Bellerive in February, 2009. All collected plants were identified by the Tasmanian Herbarium. Leaves were picked from fresh plants and cleaned with tap water, then were dried with paper towel. The leaves were weighed prior to extraction. These tested plants and their collecting location and dates are summarised in Table 2.2.

Table 2.2 Resource of plant material.

Species	Location	Date	Sample code
C. aristata	Tasmanian Nursery	11/01/08	CA-TN1
C. aristata	Tasmanian Nursery	11/01/08	CA-TN
C. aristata	Lindisfarne	11/01/08	CA-L
C. aristata	Eaglehawk Neck	14/02/08	CA-EN
C. aristata	Weilangta Forest	2/03/08	CA-W1
C. aristata	Weilangta Forest	1/03/09	CA-W2
C. aristata	Weilangta Forest	1/03/09	CA-W3
C. microphylla	Tasmanian Nursery	11/01/08	CM-TN
C. microphylla	Bellerive	15/02/09	CM-B
C. gentianoides	UTAS	7/03/08	CG-UTAS
C. vitalba	Regent Street	11/04/08	CV-RS

2.2.4 Extraction and Isolation techniques

2.2.4.1 Methanol, Methanol-DCM and DCM Extraction

Weighed plant material was extracted sequentially, once with MeOH, once with a mixture of MeOH and DCM (1:1) and once with DCM alone. The solvent was removed from combined extracts by rotary evaporation. The dry extract (solvent extract) was weighed and prepared as 100 mg/ml solutions with MeOH in a vial.

2.2.4.2 SPE cartridge fractionation

A SPE cartridge was prepared by washing with 2 ml of MeOH, then 2 ml of 10% MeOH/H_2O solution. Water (1.8 ml) was mixed with *Clematis* spp. solvent 0.2 ml extract containing 20 mg of extract in MeOH, and applied to the cartridge. The eluent was collected (fraction 1). Then 2 ml of 40%, 70%, 90% and 100% MeOH/H_2O were applied to the cartridge sequentially and fractions 2, 3, 4 and 5 were collected, respectively, for each *Clematis* spp. solvent extract.

2.2.4.3 C18 column fractionation

A C18 column was prepared using silica gel C18-coated to a height of 5.4 cm in a glass column of 1.9 cm diameter. This was designed to fractionate more polar partitions of *Clematis* spp. solvent extracts. The procedure of fractionation was the same as for the SPE cartridge. The C18 column was prepared by washing with 50 ml MeOH, then 50 ml of 10% MeOH/H_2O solution. Water (54 ml) was mixed with *Clematis* spp. solvent extract (6 ml) containing 600 mg of extract in methanol, and

applied to the cartridge. The eluent was collected (fraction 1). Then 60 ml of 40%, 70%, 90% and 100% MeOH/H_2O were applied to the cartridge sequentially and fractions 2, 3, 4 and 5 were collected, respectively, for *Clematis* spp. solvent extracts with best antitumour activity.

2.2.4.4 C18 HPLC analytical column fractionation

The fractionation method was time-based with 22 seconds per fraction. The lag time of the fraction collector was 7 seconds. Fractions were collected in 96-well microplates. HPLC was performed by gradient elution. The flow rate was 0.8 ml/minute. Partial loop injection (20 µl) was used. The solvent A was ACN and solvent B was 2% acetic acid in water for HPLC. The elution gradient was from 5% A and 95% B to 25% A and 75% B at 15 minutes, then to 40% A and 60% B at 25 minutes, then to 100% A at 35 minutes and held until 40 minutes. The UV detection wavelength was between 200 nm and 400 nm.

2.2.4.5 Sephadex LH-20 fractionation

Method A: Gel permeation chromatography was performed using Sephadex LH-20 using 100% MeOH as the eluent. The size of the column was 32 cm x 1 cm (length x diameter). Fractions were 5 ml each in 15 ml vials.

Method B: The C18 coated column fraction 1 (10% MeOH/H_2O fraction) was fractionated by a Sephadex LH-20 column which was 51 cm long and the diameter

was 2.4 cm. Two-bed volumes (460 ml) methanol were applied to the column and 20 ml fractions were collected in Erlenmeyer flasks.

2.2.4.6 Recrystallization of Sephadex LH-20 fractions

The solvent in Sephadex LH-20 fractions was removed by rotary evaporation. Fractions were weighed and dissolved in 0.5 ml of MeOH, and then left in a fume hood to evaporate solvent slowly.

2.2.4.7 HPLC Carbohydrate column fractionation

The method of fractionation was time-based. The first seven fractions were 0.8 minute per fraction and the last two fractions were 1 minute per fraction. The lag time of the fraction collector was 7 seconds. Fractions were collected in 1 ml Eppendorf tubes. HPLC was performed by isocratic elution using 17% A and 83% B. The flow rate was 0.98 ml/minute. Solvent A was ACN and solvent B was 0.04% ammonium hydroxide in water. Partial loop injection of 20 µl was used.

2.2.4.8 C18 semi-preparative HPLC column fractionation

The fractionation method was volume-based with 2 ml per fraction. The lag time of the fraction collector was 2 seconds. Fractions were collected in glass tubes. HPLC was performed by gradient elution. The flow rate was 3.8 ml/minutes. The injection volume, mobile phases, elution gradient and the UV dection wavelength were the same as the HPLC conditions for C18 analytical column fractionation (2.2.4.4). ACN

in each fraction was removed by evaporation in a fume hood for 24 hours. Then water was removed by freeze drying. Each fraction was redissolved in 1.5 ml of MeOH.

2.2.4.9 Investigation of chemical constituents by HPLC-UV and -ELSD

HPLC analysis with detection by UV or ELSD was employed to investigate the chemical constituents of *Clematis* spp. The flow rate, mobile phase, elution gradient and the UV detection wavelength were the same as the HPLC conditions for C18 analytical column fractionation (2.2.4.4).

ELSD was operated with the tube temperature 93°C, nitrogen flow 2.4 ml/minutes, gain of 2 with impactor off. Fixed loop injection (10 µl) was used. The mobile phases consisted of ACN (A) and 0.04 % ammonium hydroxide in water (B) with isocratic elution of 17% A and 83% B. The flow rate was 0.98 ml/minutes and running time was 15 min.

Analytical C18 and carbohydrate columns were employed in this investigation.

2.2.4.10 Determination of chemical constituents by HPLC-MS

The column, flow rate, injection volume, mobile phase and elution gradient applied for the LC-MS analyses were the same as for HPLC as described in 2.2.4.4. The detection wavelength was 220-400 nm.

Negative ion electrospray ionization (ESI) and both positive and negative atmospheric pressure chemical ionization (APCI) were applied to the samples. Conditions for negative ESI were as follows; needle voltage 4 KV, capillary voltage -15 V, capillary temperature 220°C, sheath gas (nitrogen) 65 psi, auxiliary gas (nitrogen) 20 psi. The full scan range from *m/z* 200 to 1200, and data dependent MS^2 and MS^3 scans were acquired from the most intense ion with 30% collision energy. $[M-H]^-$ and $[M+CH_3COO]^-$ ions were typically observed in this mode.

Negative ion APCI conditions were as follows; capillary temperature 150°C, APCI vapourizer temperature 450°C, needle voltage 6 KV, sheath gas 35 psi and capillary voltage -8 V. Ions from *m/z* 140 to 800 were acquired, and data dependent MS^2 scans were acquired from the most intense ion with collision energy of 25%. A post-column addition of 5% formic acid (20 µl/minute) was applied.

2.2.4.11 Determination of chemical constituent by UPLC-MS

Solvent A was 1% acetic acid in water and solvent B was ACN. The elution gradient was from 10% A and 90% B for 1.0 minute, then to 80% A and 20% B at 5 minutes, then re-equilibrated for 2 minutes. The flow rate was 0.35 ml/minute. The injection volume was 1 µl. Positive ion electrospray MS data were collected over the range *m/z* 50 to 400 in 0.4 second, followed by negative ions from *m/z* 50 to 1000 in 0.4 seconds. Cone voltage was 35 V, needle voltage was 2.45 KV, source temperature was 150°C, desolvation temperature was 400°C, desolvation gas was nitrogen at 1000 l/hour.

2.2.4.12 Headspace-GCMS-SPME

A Varian 1177 injector was used in split mode. The flow rate of carrier gas (helium) was 1.2 ml/minute in constant flow mode; the injection temperature was 280°C. Samples were injected split (8:1). The ion source temperature was 220°C and the transfer line was held at 290°C. The range from *m/z* 35 to 140 was scanned every 0.3 second. The GC oven temperature was held at 35°C for 4 minutes then ramped from to 230°C at 25°C per minute.

Method A: *C. aristata*-L leaf was placed and crushed into a 10 ml screw top vial with PTFE/silicon cap. The blank SPME fibre was run before exposure to the leaf-containing vial to eliminate carryover from previous exposures. Then the fibre was exposed to the headspace of the vial for 10 minutes. The fibre was then desorbed in the injection port for 3 minutes.

Method B: The solution of recrystallized Sephadex LH-20 fraction (0.1ml) with 1.9 ml of RPMI-1640 and DMEM were separately placed into two 10 ml screw top vials with PTFE/silicon caps. They were placed in a 35°C CO_2 incubator for 3 hours. Before and after incubation, both vials were placed into a 35°C stirrer hotplate and the liquid in vials were stirred by a magnetic stir, then the fibre was exposed to the headspace of the vial for 10 minutes. The fiber was then desorbed in the injection port for 3 minutes.

2.2.5 Antitumour Assay (P388 Murine Leukaemia Cell Line)

The method to determine the cytotoxic activity followed the method from Choo *et al*. and Manosroi *et al*.[166, 167] with slight modification.

For the screening study, a volume of 10 µl of a two-fold dilution series of the crude extracts dissolved in 7% DMSO/PBS was incubated for 48 hours with 100 µl of P388 cell culture in 96-well microplates (1 x 10^5 cells/well) without renewal of the medium. The negative controls were 7% DMSO/PBS and blank.

For the determination of the antitumour effect of fractions, 100 µl of original or diluted fractions were added into each well. Solvent was evaporated in a biosafety hood. P388 cell culture (100 µl) (1 x 10^5 cells/well) was added into each well of 96-well microplates and incubated 48 hours without renewal of the medium. Three negative controls were used in this assay. The first was the mobile phase, which was prepared at the same time as the fractions, i.e. mobile phase of 50% A + 50% B. The second negative control was MeOH, i.e. 100 µl of MeOH was added into the same 96-well microplate, then evaporated in the biosafety II cabinet. The third negative control was blank (nothing added to the well).

After 48 hours of incubation, 20 µl of MTT solution (5 mg/ml) was added into each well of culture medium. After a further 4 hours of incubation, 100 µl of 0.04 N HCl in anhydrous isopropanol solution (MTT solvent) was added to each well and the formazan crystals in each well were dissolved by stirring with a pipette. The optical

density measurements were made by using a microplate reader at 490 nm. The P388 cell growth (comparative to control cells) was determined using the absorbance values obtained when the yellow dye MTT tetrazolum is reduced by healthy cells to the purple coloured MTT formazan and was expressed as the percent cytotoxicity (cytotoxicity%). The calculation of cytotoxicity% follows the equation:

Cytotoxicity% = $[1-(OD_{490\ treated}/OD_{490\ control})] \times 100$.

Each extract or fraction was analysed in triplicate. The results were expressed as mean of triplicate.

2.3 Results and Discussion

2.3.1 Cytotoxic IC_{50} of *Clematis* spp. extracts

MTT assay, a simple and reliable technique, which measures cell viability, can be used for screening of anti-tumour agents. Figure 2.1 presented the dose-response curve by plotting of cytotoxicity% versus the concentration (mg/ml) of SPE cartridge fractions 2 of tested *Clematis* materials. Each fraction was analysed in triplicate. The results were expressed as mean. The IC_{50} of each *Clematis* SPE cartridge fraction 2 was calculated from the equation which was set up by the linear trendline using the cytotoxicity% data on dose-response curves where the 50% cytotoxicity% was included in the trendline. The results are summarized in Figure 2.2.

Results in Figures 2.1 and 2.2 showed that ten out of eleven *Clematis* spp. had cytotoxicity against P388 cells and their antitumour activities were different. CM-TN had the strongest cytotoxic activity, with an IC_{50} of 0.084 mg/ml. In a previous study undertaken in this laboratory,[52] the cytotoxic activity of five SPE cartridge fractions of five *Clematis* spp. was determined against P388 cells by MTT assay. Results demonstrated that the antitumour activity varied in different species. Fractions 2 eluting with 40% MeOH/H_2O showed stronger cytotoxic effects than the other fractions. *C. aristata* wide leaf form (the same as CA-L in this study) had the strongest effects of all the other fractions, only *C. aristata* wide leaf form fraction 1 showed antitumour activity. There were no antitumour activities detected in the fractions 3 to 5 of any tested *Clematis* spp. extract (Table 1.7). Based on previous

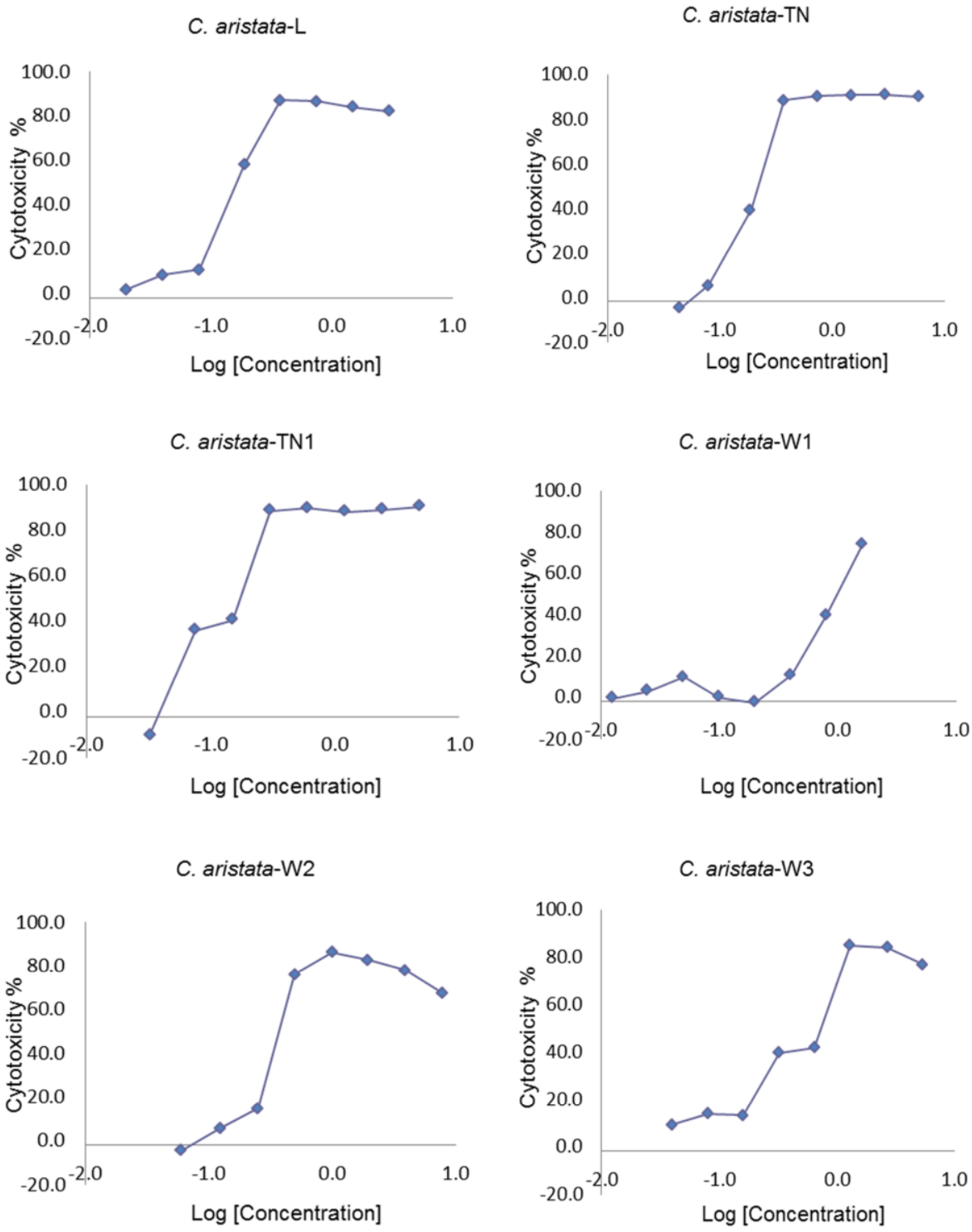

Figure 2.1 Dose-resopnse curves of the antitumour activities of *Clematis* spp. SPE cartridge fraction 2 against P388 cells by ploting cytotoxic index (cytotoxicity %) verse the log concentration of fractions (Log [Concentrations]).

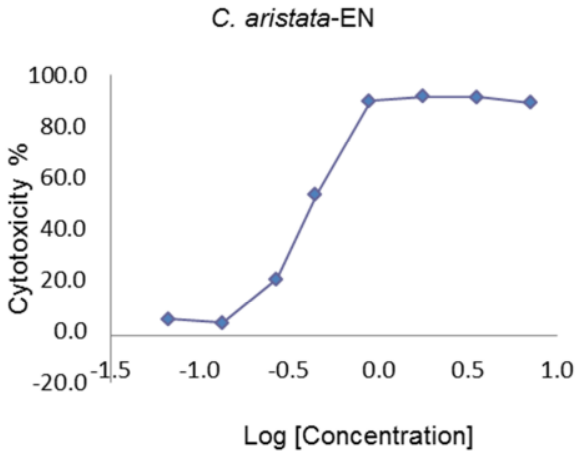

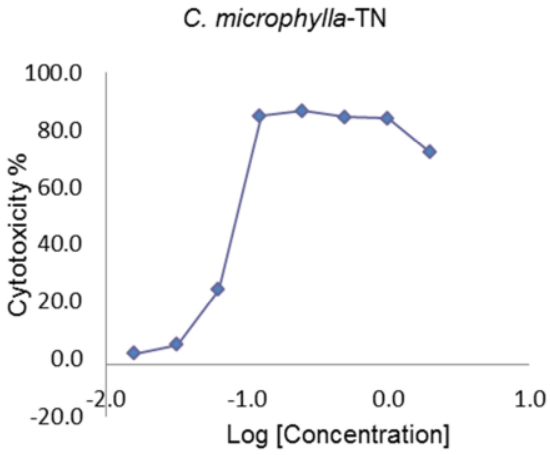

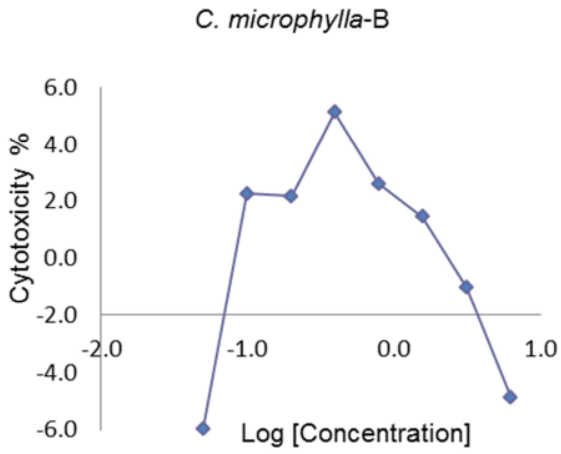

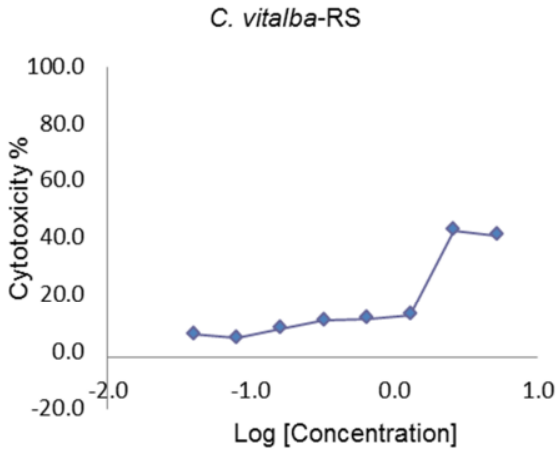

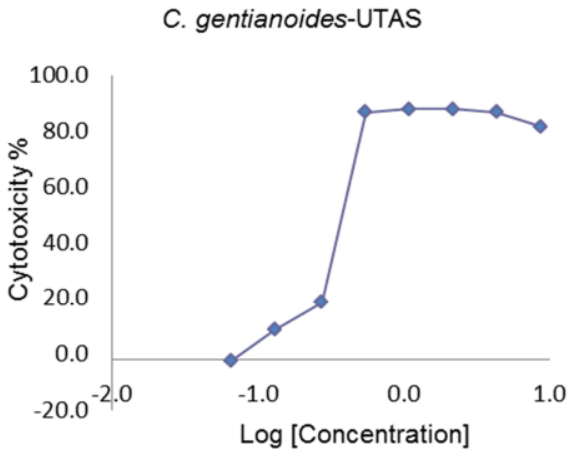

Figure 2.1 (continued)

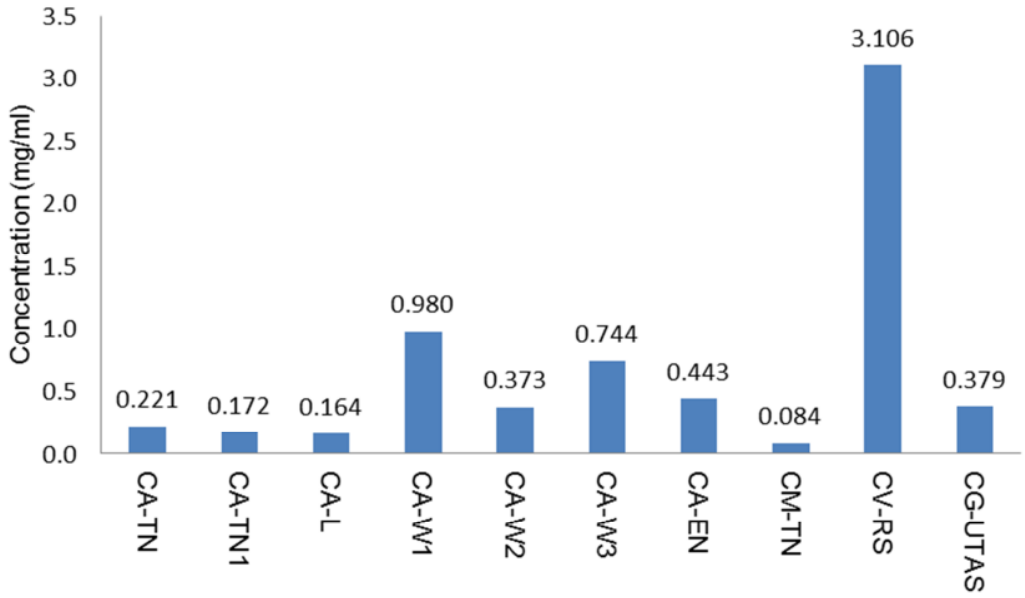

Figure 2.2 Antitumour IC_{50} of SPE cartridge fraction 2 of ten *Clematis* spp. against P388 cells. The labels of each plants used are the code which were presented in Table 2.1.

Screening results, SPE cartridge fraction 2 of each *Clematis* spp. were employed in this study to investigate their antitumour effects. This choice negtated the determination of possible antitumour constituents in *C. aristata* wide form leaf SPE cartridge fraction 1.

Of the eight C. aristat plants, two cultivars were collected from Plants of Tasmanian Nurery (CA-TN and CA-TN1) and one cultivar was collected from Lindisfare (CA-L). All three had similar IC_{50} values: 0.221 mg/ml, 0.172 mg/ml and 0.164 mg/ml, respectively. Three *C. aristata* cultivars from Weilangta forest (CA-W1, -W2 and -W3) and a cultivar from Eaglehawk Neck (CA-EN) showed similar cytotoxicity against P388 cells. Their IC_{50} values were 0.980 mg/ml, 0.373 mg/ml, 0.744 mg/ml and 0.443 mg/ml, respectively. In all *C. aristata* cultivars, the biggest difference in

IC_{50} values was observed between CA-L (0.172 mg/ml) and CA-W1 (0.980 mg/ml). This difference (about 5-fold) might be contributed to by seasons (Janrary versus March), the environmental condition (eg. sunshine, nutrients), or genotypic differences.

It was observed that the antitumour activities of *C. aristata* cultivars might show a relationship with seasons. Although form variation was presented between CA-L (wide leaf form) and CA-TN and –TN1 (both are narrow leaf form), their antitumour activities were the same and they were all collected in January. CA-W1, -W2, -W3 and -EN had the same antitumour effects and they were collected between the middle of Feburary and early March.

The most significant variation cytotoxic effect within species was observed in *C. microphylla. C. microphylla* collected from Plants of Tasmanian Nursery (CM-TN) showed the strongest antitumour activities of all the investigated *Clematis* spp., however, *C. microphylla* collected form Bellerive (CM-B) did not show any antitumour activity. There was not any form variation observed between both cultivars and the collection dates, differed by only about one month, similar to the difference in collection date for CA-TN and CA-EN.

Variation of the antitumour activities between species was observed. *C. vitabla* showed lower antitumour effects than *C. aristata, C. gentianoides* and *C. microphylla*

in the effective plants. *C. vitalba* was collected in April, which was later than the other tested *Clematis* plants.

Factors that caused the difference in antitumour activities have not been investigated in this study. The difference is possibly related to several factors: species differences, plant development (for example, leaf age), environmental conditions (like nutrient, water, sunshine), plant stresses such as browsing, or genotypic differences. However, as the aim of this study was to determine the potential antitumour constituents in Tasmanian native *Clematis* spp., the investigation of environmental conditions and their influence on biological activity was not performed.

Although cytotoxic activities of *Clematis* spp. against P388 cells were obtained in this experiment, their antitumour effects were not especially potent (84-3100 μg/ml). Compared with other antitumour herbal medicines, the values of IC_{50} for *Clematis* spp. were high. For example, the IC_{50} of chloroform leaf and stem extract of *Typhonium flagelliforme* against P388 cells was only 8 μg/ml,[166] which was more than ten times more potent than *C. aristata*-TN. Furthermore, the IC_{50} of $CHCl_3$/MeOH extract of *Taiwanofungus camphoratus* against P388 cells was 4.1 μg,[168] much more potent than *Clematis* spp. extract fraction 2.

2.3.2 Antitumour activities of HPLC fractions of *C. aristata*-L and *C. microphylla*-TN

Based on the screening results, the two fractions with the highest antitumour activities (CM–TNii and CA-Lii) were fractionated by analytical C18 HPLC column

to determine active constituents following the method described in 2.2.4.4. The cytotoxic activity of HPLC fractions of CM-TNii and CA-Lii against P388 cells were determined by the MTT assay. Results are shown in Figure 2.3.

Three different amounts of CA-Lii, 72 µg, 36 µg and 18 µg, were fractionated by C18 analytical HPLC column, each mass in triplicate. Data shown in Figure 2.3 is mean data of triplicate determination. Results shown in Figure 2.3 (A) showed that there were two zones with cytotoxicity% of more than 50% at 72 µg. The first zone was from fraction 3 to fraction 15. The second zone started from fraction 21 and ended at fraction 23. In all these fractions, fraction 6, 7, 11, 12, 13, 14 and 15 demonstrated cytotoxicity% of more than 90%. When the concentration of CA-Lii decreased, the cytotoxic activity against P388 cells was mainly exerted in the first zone. At 36 µg, the fractions within cytotoxicity% more than 50% are fractions 10 to 14. In these fractions, fractions 10, 11, 12 and 14 had a cytotoxicity% more than 90%. However, when the concentration of CA-Lii decreased to 18 µg, the cytotoxic activities were only observed in fractions 10, 11 and 14, whose cytotoxicity % was 98.8%, 99% and 99.1%, respectively.

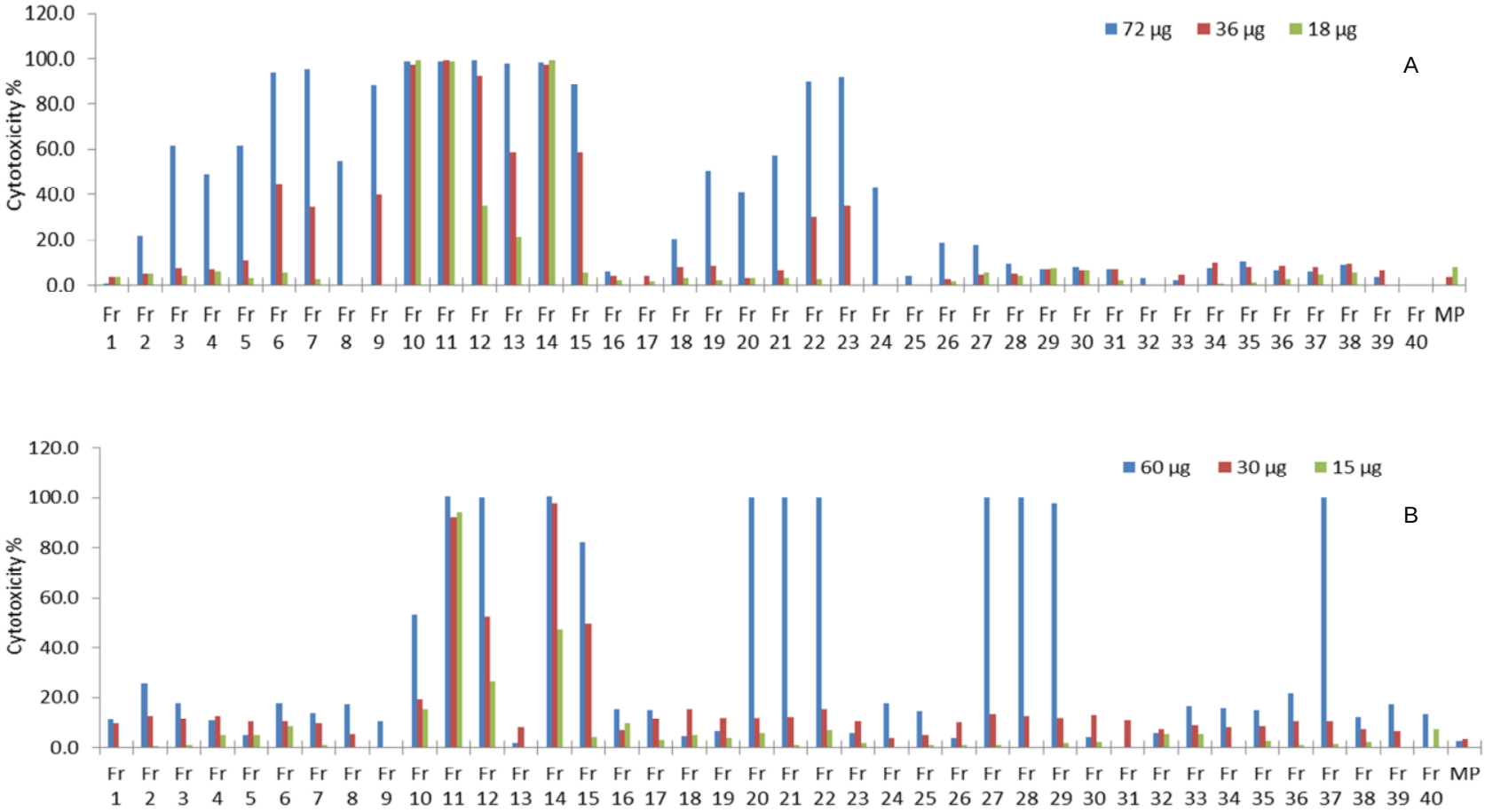

Figure 2.3 Antitumour activities (cytotoxicity%) of analytical C18 HPLC column fractions against P388 cells. A is the P388 cyototxicity of HPLC fractions of CA-Lii at 72 µg (blue), 36 µg (red) and 18 µg (green). B is the P388 cyototxicity of HPLC fractions of CM-TNii at 60 µg (blue), 30 µg (red) and 15 µg (green). Values are the mean of triplicate determinations.

Three different amounts of CM-TNii, 60 µg, 30 µg and 15 µg, were fractionated by C18 analytical HPLC column, each mass in triplicate. Data shown in Figure 2.3 is mean data of triplicate determination. Results in Figure 2.3 (B) showed that there were five inhibition zones at the amount of 60 µg. The first zone included fractions 10 and 11. The second zone included fractions 14 and 15. The third zone was from fraction 20 to fraction 22, the fourth zone included fraction 27 and 28 and the last zone was only fraction 37. All fractions in five zones had cytotoxicity% more than 90% except fraction 15. When the amount of CM-TNii decreased to 30 µg, the cytotoxic activity against P388 cells was mainly exerted in fraction 11 and 14, giving a cytotoxicity% of 92.2% and 97.6%, respectively. When the amount of CM-TNii decreased to 15 µg, only fraction 11 exerted the cytotoxicity against P388 cells, giving the cytotoxicity % of 94.1%.

HPLC-UV and –ELSD chromatograms of CA-Lii are shown in Figure 2.4. ELSD was employed in this study because it can detect compounds without a UV chromophore. The signal from ELSD is approximately proportional to the mass of compound. Two cytotoxic active zones and the most effective fractions, fractions 10, 11 and 14 are labelled in this figure.

There were 6 peaks in zone 1 of the ELSD chromatogram (Figure 2.4 B), labelled as 1, 2, 3, 4, 5 and 6, with retention times of 1.61, 2.75, 3.10, 3.43, 3.99 and 5.21 minutes, respectively. By comparing with the chromatograms of a blank (Appendix I), the first three peaks were injection artefacts. The relative total area of peaks 4, 5

and 6 were 10.4%, 45.4% and 20.1%, respectively. At the lowest amount of18 µg, fractions 10, 11

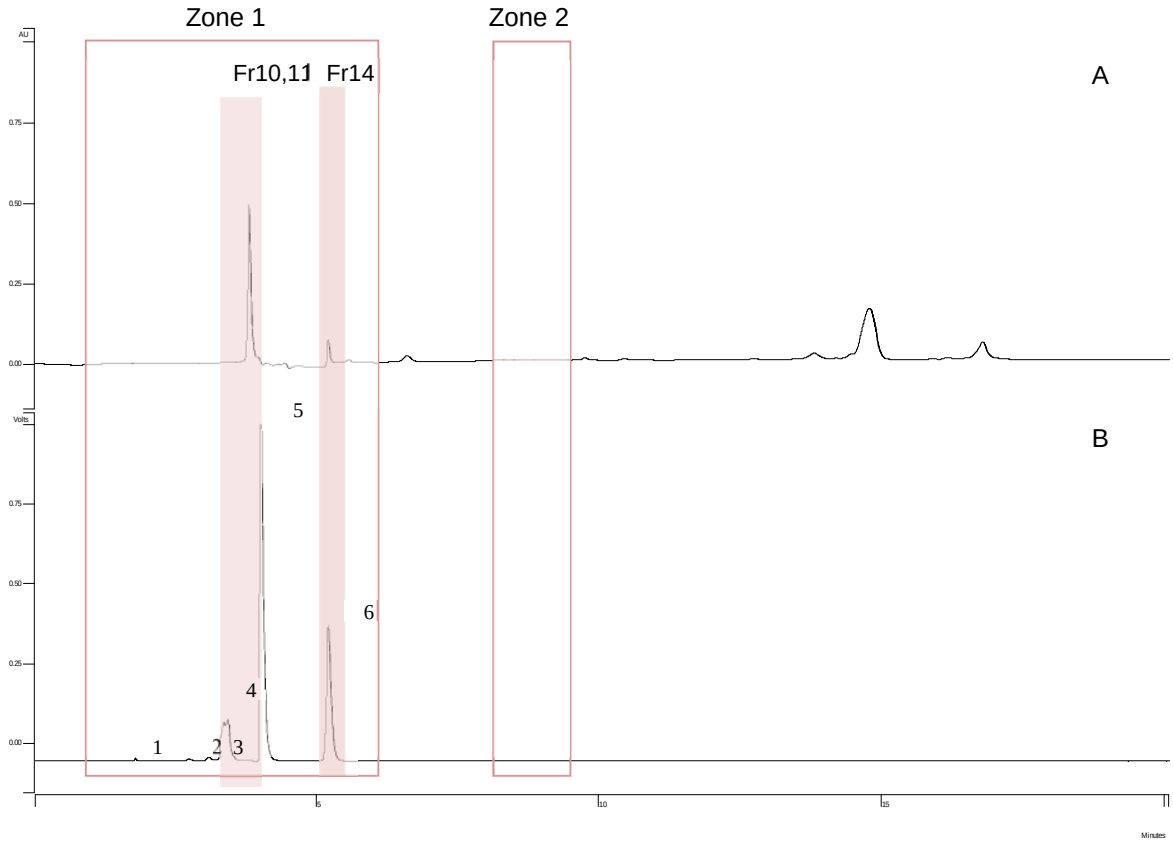

Figure 2.4 HPLC chromatograms of CA-Lii. A is the HPLC-UV chromatogram at 254 nm. B is the HPLC-ELSD chromatogram. Two red frames labelled the P388 cytotoxic chromatographic Zones 1 and 2. Purple areas highlight the chromatogram of P388 cytotoxic HPLC fractions 10, 11 and 14.

and 14 exerted cytotoxicity% more than 90%. Figure 2.4 A showed that one peak was in fraction 10 and 11 and a peak in fraction 14. But Figure 2.4 B showed that peak 4 was included in fraction 10, three quarters of peak 5 were included in fraction 11 and peak 6 was included in fraction 14. As the amount of CA-Lii was 18 µg, the quantity of compound corresponding to peak 4 was 2.5 µg, the amount of compound corresponding to peak 5 in fraction 11 was 6.1 µg, and the amount of compound

corresponding to peak 6 in fraction 14 was 3.6 µg. This result suggested that chromatographic peaks 4, 5 and 6 had the antitumour activity. In the MTT assay, each well had a final volume of 200 µl. This study did not determine the mass of each fraction, the antitumour concentration of each active chromatographic active peak was not evaluated.

Compared with significant peaks observed in zone 1, there seemed to be no peaks observable in zone 2 by either UV or ELSD. The relative peak area of zone 2 was only 0.039%. At their cytotoxic active amount 36 µg, the mass of the peaks in fraction 21, 22 and 23 was 0.014 µg. These results also suggested that if cytotoxic active compounds existed in zone 2, their efficacy was much higher than compounds obtained in fraction 10 and 11 and fraction 14. As explained in the previous section, this study did not determine the mass of each fraction, the antitumour concentration of each active compound was not evaluated. Results in this experiment revealed the correlation between the active fractions and the chromatographic effective peaks. The HPLC peaks of three most effective HPLC fractions of CA-Lii were peaks 4, 5 and 6 (Figure 2.4 B).

HPLC-UV and –ELSD chromatograms of CM-TNii are shown in Figure 2.5. Five cytotoxic active zones and the most effective fraction, fraction 10, are labelled in this figure.

As shown in Figure 2.5 B, peak 4 in zone 1 with retention time of 3.95 minutes and the peak 5 in zone 2 with retention time of 5.05 minutes of CM-TNii, giving the relative total area of 33.6% and 12.9%, had the same retention time as peak 5 and 6 (Figure 2.4 B) of CA-Lii. At 15 µg of CM-TNii, HPLC fraction 11 had cytotoxicity% more than 90%. Five-sixths of chromatographic peak 4 was included in fraction 11, so the mass of peak 4

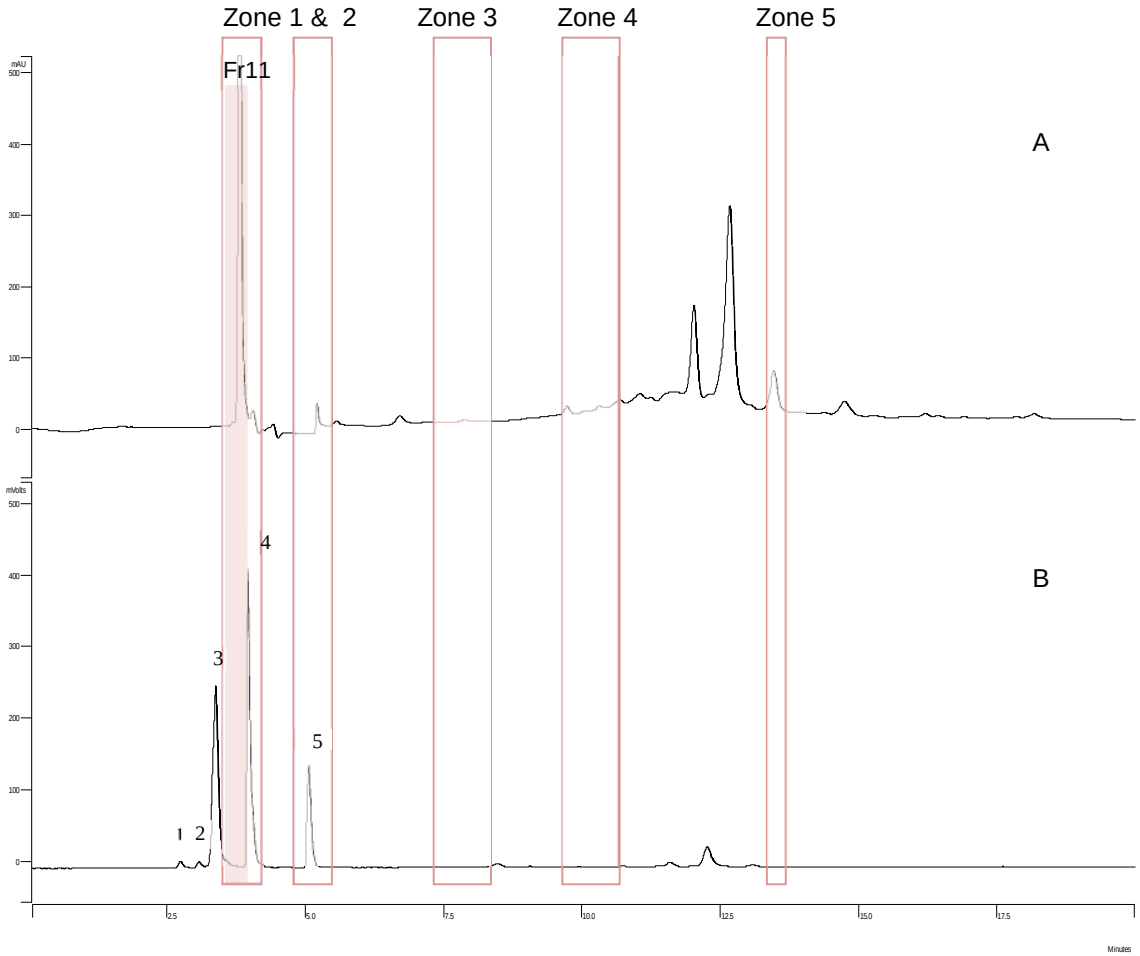

Figure 2.5 HPLC chromatogram at of CM-TNii. A is the HPLC-UV chromatogram at 254 nm. B is the HPLC-ELSD chromatogram. The five red frames indicate the P388 cytotoxic zones 1, 2, 3, 4 and 5. Purple areas highlights the chromatograme of P388 cytotoxic HPLC fraction 11.

in fraction 11 was approximately 4.2 μg. Peak 5, obtained in fraction 14 in zone 2, had cytotoxicity% of 47.2% when CM-TNii was 15 μg, therefore, the quantity of the peak 5 was 1.9 μg. This result suggests that peak 4 and 5 are the two of the cytotoxic constituents in CM-TNii.

In the ELSD chromatograms of CM-TNii (Figure 2.5 B), the 3 peaks with retention time of 2.73, 3.07 and 3.36 minutes before zone 1 would be the same as peaks 2-4 in zone 1 of CA-Lii (Figure 2.4 B), but they did not show any cytotoxic effects. Peaks 1 and 2 were artefact peaks. The yield of peak 3 in the ELSD chromatogram of CM-TNii was 34.5%. At the highest amount of CM-TNii (60 μg), the quantity of the compound corresponding to peak 3 was 20.7 μg. Although the amount of compound corresponding to the peak 3 obtained in CM-TNii was higher than that obtained in CA-Lii, its cytotoxic in CM-TNii (20.7 μg giving cytotoxicity% of 53.4%) was lower than that obtained in CA-Lii (2.5 μg giving cytotoxicity% of 100%). We could not explain this phenomenon at this stage of this study. Peak 5 (included in fraction 14) of CM-TNii at 3.9 μg had cytotoxicity% of 97.7%, which was the same level of P388 cytotoxicity as CA-Lii chromatographic peak 6 (3.6 μg giving cytotoxicity% of 99.3%).

There was no significant peak obtained in zones 3 and 4. The total content of compounds in zones 3 and 4 was 1.11% and 0.39%, respectively, based on peak integration. Following the injection of 60 μg, the quantity of compounds in zones 3 and 4 was estimated to be respectively 0.66 μg and 0.23 μg based on peak integration.

There was a peak obtained in zone 5 shown in Figrue 2.5 A, but this peak was not observed in Figure 2.5 B. The total content of compounds in zone 5 was 0.045% based on peak integration. Following the injection of 60 μg, the quantity of compounds in zone 5 was estimated to be 0.028 μg. These results suggested that cytotoxic active compounds existed in zones 3, 4 and 5, their efficacy was much higher than compounds obtained in active zone 1 and 2 of CM-TNii.

Results in this study showed that CA-L and CM-TN had antitumour activity in different chromatographic zones. Although chromatographic peaks 5 and 6 of CA-Lii (Figure 2.4 B) and chromatographic peaks 4 and 5 of CM-TNii (Figure 2.5 B) showed the antitumour effects at the lowest amounts of both fractions, compared with zone 2 of CA-Lii and zone 3-5 of CM-TNii, the amount of these compounds were much higher than the potent antitumour constituents in the other zones with antitumour activities.

2.3.3 Antitumour activity of Sephadex LH-20 column fractions

Based on the results in 2.3.2, the determination of chemical constituents of active chromatographic peaks of CA-Lii (peaks 5 and 6 shown in Figure 2.4 B) and CM-TNii (peaks 4 and 5 shown in Figure 2.5 B) were undertaken. As they corresponded to HPLC fraction 11 and fraction 14 (Figure 2.3), respectively, both fractions were fractionated by Sephadex LH-20 column following method A described in 2.2.4.5. For the HPLC fractions 11of CA-Lii (CA-Lii11) and CM-TNii (CM-TNii11), three amounts of HPLC fractions were applied to a Sephadex LH-20 column. For the

HPLC fractions 14 of CA-Lii (CA-Lii14) and CM-TNii (CM-TNii14), only a single amount of fraction was applied to the Sephadex LH-20 column. The amount of fractions applied to the Sephadex LH-20 column was estimated by the amount of CA-Lii and CM-TNii applied to HPLC column multiplied by the relative total area (%) of peaks in CA-Lii11, CA-Lii14, CM-TNii11 and CM-TNii14. The determination of antitumour activity of each fraction was undertaken in duplicate and results were expressed as the mean of duplicate results (Table 2.3). Mobile phase was MeOH.

Sephadex LH-20 is size exclusion chromatography. As the retention time of CA-Lii peaks 5 and 6 (and CM-TNii peak 4 and 5) were close to each other in the C18 HPLC column analysis. Also, these compounds are very polar, so it was possible that there were some unresolved compounds present. The Sephadex LH-20 column chromatography was employed in this study with a objective of giving a better separation of polar compounds than the separation by C18 HPLC.

Data in Table 2.3 showed that when the amounts of CA-Lii11was 80 μg and 60 μg, Sephadex LH-20 fractions 7, 8 and 9 had cytotoxic activities against the P388 cell line. All these three fractions had cytotoxicity% of more than 90%. When the amount of HPLC fraction 11 decreased to 40 μg, the antitumour activities were obtained in Sephadex LH-20 fraction 8 and 9, and their cytotoxicity% were 98.8% and 77.9%, respectively. For the 30 μg of CA-Lii14, only fraction 8 had antitumour activity, with a cytotoxicity% of 97.6%.

When the amount of CM-TNii11was 40 μg, Sephadex LH-20 fractions 7, 8 and 9 showed cytotoxic activities against the P388 cell line. These three fractions had cytotoxicity% more than 90%. When the concentration of HPLC fraction 11 decreased to 30 μg, the antitumour activity was observed in Sephadex LH-20 fraction 8, whose cytotoxicity% was 92.4%. A cytotoxicity% of only 23.4% was obtained in 20 μg of CM-TNii11 and no cytotoxic effect was obtained in the Sephadex LH-20 fractions of CM-TNii14 at the amount of 14 μg.

Results from this experiment revealed a dose dependent antitumour activity of active Sephadex LH-20 column fractions of CA-Lii11 and CM-TNii11. Sephadex LH-20 fractions 7, 8 and 9 of CA-Lii11 and CM-TNii11 had cytotoxic activity. When the amount was decreased, the antitumour activity was only obtained in fraction 8. For both CA-Lii14 and CM-TNii14, the antitumour activity was only obtained in Sephadex LH-20 fraction 8 of CA-Lii14. As the separation mechanism of Sephadex LH-20 is dependent primarily on the molecular size of compounds, it is likely that the same cytotoxic active compounds were present in Sephadex LH-20 fractions 7, 8 and 9, and most of this compound was in fraction 8. As the active Sephadex LH-20 fraction of CA-Lii14 was still fraction 8, it was suggested that the active antitumour constituent of CA-Lii14 was the same as CA-Lii11.

Table 2.3 P388 antitumour activity (cytotoxicity%) of Sephadex LH-20 fractions of CA-Lii11, CA-Lii14, CM-TNii11 and CM-TNii14 (n=2). Three amounts of CA-Lii11 were fractionated, 80, 60 and 40 µg. The amount of CA-Lii14 was 30 µg. Three amounts of CM-TNii11 fractionated were 40, 30 and 20 µg; and the amount of CM-TNii14 was 14 µg. Mobile phase was methanol.

Sample	*C. aristata* -L (cytotoxicity%)				*C. microphylla* -TN (cytotoxicity%)			
	Fraction 11			Fraction 14	Fraction 11			Fraction 14
	80 µg	60 µg	40 µg	30 µg	40 µg	30 µg	20 µg	14 µg
Fraction 1	0	0	0	0	0	0	0	0
Fraction 2	0	0	0	0	0	0	0	0
Fraction 3	10.9	7.8	0	0	0	0	5.3	0
Fraction 4	0	0	0	0	0	0	0	0
Fraction 5	0	0	0	0	9.9	4.7	0	0
Fraction 6	0	0	0	4.2	0	0	0	0
Fraction 7	99.9	99.5	32.2	0	100	23.1	0	0
Fraction 8	100	99.2	98.8	97.6	100	92.4	23.4	0
Fraction 9	99.8	95.9	77.9	0	98.3	0	0	0
Fraction 10	0	0.3	0	0	0	0.4	0	0.7
Fraction 11	1.4	0	0	0	0	0	0.7	0
Fraction 12	0	7.2	0	0	8.5	0	0	0.1
Fraction 13	2.4	0	0	0	4.4	0.8	0	0
Fraction 14	0	0	0	0	6.2	1.8	0	3.9
Fraction 15	0	0	0	0	0	0	0	0
Fraction 16	0	0	0	0	0	0	0	0
Fraction 17	0	0	0	0	0	0	0	0
Fraction 18	0	1.0	0	0	0	0	4.7	0
Fraction 19	0	3.9	0	0	0	5.7	0	0
Fraction 20	0	0	0	0	0	0	0	0
Mobile-phase	2.1	0	0.8	0.3	4.5	0	0	0

2.3.4 Antitumour activity of Carbohydrate HPLC column fractions and the effective constituents determined by LC-MS

Based on the results in 2.3.3, both Sephadex LH-20 fraction 8 of CA-Lii11 (CA-Lii11-8) and CA-Lii14 (CA-Lii14-8) were fractionated on an analytical carbohydrate HPLC column, connected to a fraction collector. As the C18 column is a reverse-phase, the constituents in fraction 11 and 14 would be expected to be a relatively polar compounds. The carbohydrate column was employed in this procedure of fractionation as it has greater retention time of polar glycosides and thus can more successfully fractionate polar compounds. The antitumour activities of each carbohydrate HPLC column fraction are listed in Figure 2.6.

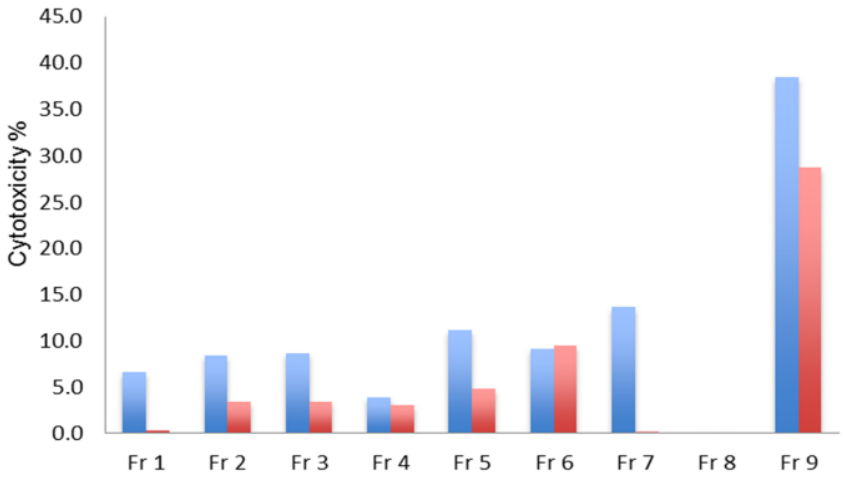

Figure 2.6 Antitumour activities of carbohydrate HPLC column fractions of CA-Lii11-8 (blue) and CA-Lii14-8 (red).

Results in Figure 2.6 revealed that the carbohydrate fraction 9 of both CA-Lii11-8 and CA-Lii14-8 had cytotoxicity against P388 cells. Their cytotoxicity% was 38.39%

and 28.78%, respectively. The HPLC-ELSD chromatograms and activity zones of both fractions 9 corresponded are shown in Figure 2.7 with a common peak.

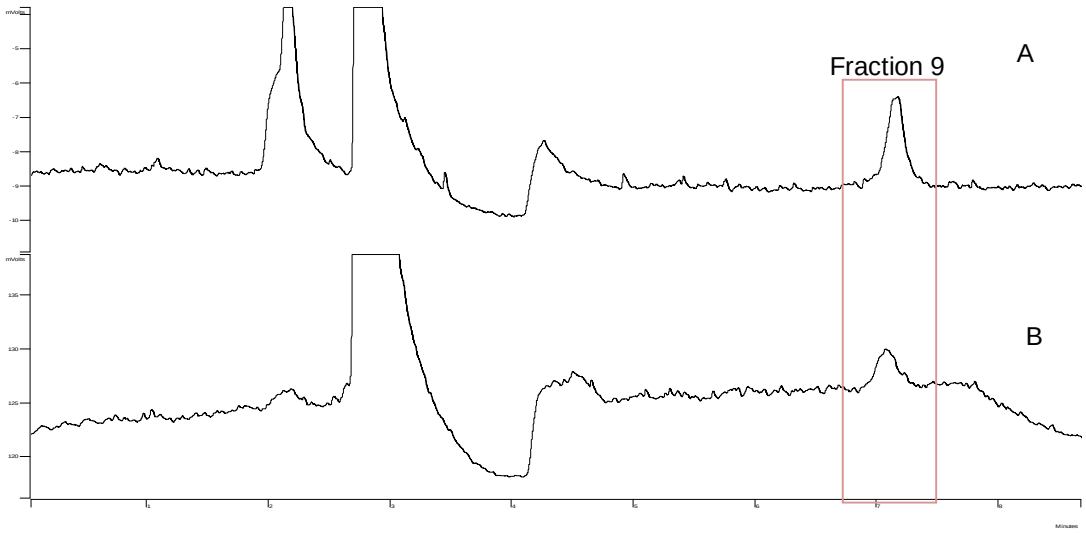

Figure 2.7 Carbohydrate column HPLC-ELSD chromatograms of CA-Lii11-8 (A) and CA-Lii14-8 (B). The red frame shows the active carbohydrate fractions in both Sephadex LH-20 fractions.

A chromatographic peak was obtained in fraction 9 (CA-Lii11-8-9 and CA-Lii14-8-9). As the retention time of this peak (7.10 minutes) in two fractions was the same, it is suggested that the cytotoxic active constituent of both fractions were the same. The AUC of CA-Lii11-8-9 and CA-Lii14-8-9 was 41125 and 27428, respectively, which showed the antitumour activity was related to the amount of this compound, as the AUC of the compound was proportional to the cytotoxicity. There were no other P388 active compounds detected. Therefore, this active constituent was determined by LC-MS negative ion APCI. The LC chromatogram and MS and MS^2 spectrum are shown in Figure 2.8. CA-Lii11-8-9 and CA-Lii14-8-9 had the same spectra (Figure 2.8).

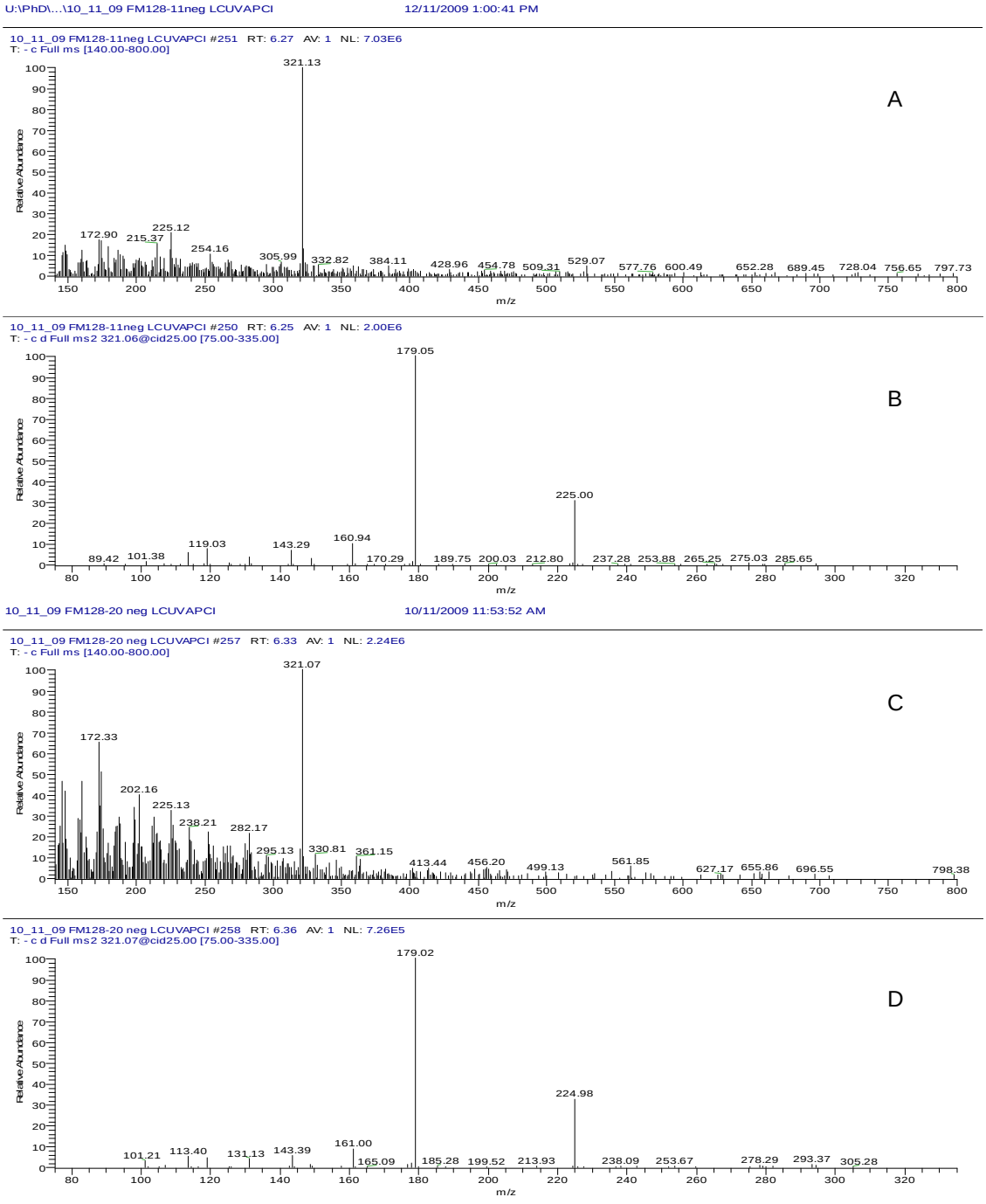

Figure 2.8 LC-MS chromatogram of active HPLC carbohydrate column chromatographic peak of *C. aristata*-L. A and B are the MS spectrum and MS^2 spectrum of CA-Lii11-8-9. C and D are the MS spectrum and MS^2 spectrum of CA-Lii14-8-9.

In Figure 2.8 A and C, MS spectra showed *m/z* at 321 corresponding to $[M + COO]^-$ as the LC-MS system contained formic acid; therefore, the MW of M is 276. In Figure 2.8 B and D, the MS^2 spectrum showed a daughter ion at *m/z* at 179 corresponding to a hexose (MW 180). The difference between 276 and 180 is 96, which is consistent with the MW of protoanemonin. The mass spectrum of this peak is consistent with a sugar attached to protoanemonin, and is therefore consistent with ranunculin. But in the LC-MS analysis of CA-Lii on a C18 HPLC column, it is likely that two compounds are consistent with ranunculin, one is in C18 HPLC column fraction 11 (as shown in Figure 2.7 A), and the other was in C18 HPLC column fraction 14 (as shown in Figure 2.7 B).

In order to confirm this hypothesis, CA-Lii was analysed by LC-MS using negative ion esi. Two peaks with retention times of 3.80 minutes (peak 1) and 4.69 minutes (peak 2) had the same MS data. The MS and MS^2 spectrum of both chromatographic peaks were shown in Figure 2.9. The peak with retention time of 3.80 minutes was in CA-Lii11 and the peak with retention time of 4.69 minutes was in CA-Lii14.

As shown in LC chromatogram of Figure 2.9, the MS and MS^2 spectra of both peaks (retention times of 3.80 minutes and 4.69 minutes) were shown to be the same. Acetate was employed in the negative ion mode. The MS spectrum showed *m/z* at 275, 551, 335, 661 and 311 peaks that corresponding to $[M-H]^-$, $[2M-H]^-$, $[M+CH_3COO]^-$, $[2M + CH_3COO]^-$ and $[M + Cl]^-$. Their MS^2 spectra were the same as the MS^2 spectra of HPLC carbohydrate fraction 9 (Figure 2.8 B and D). Therefore, this

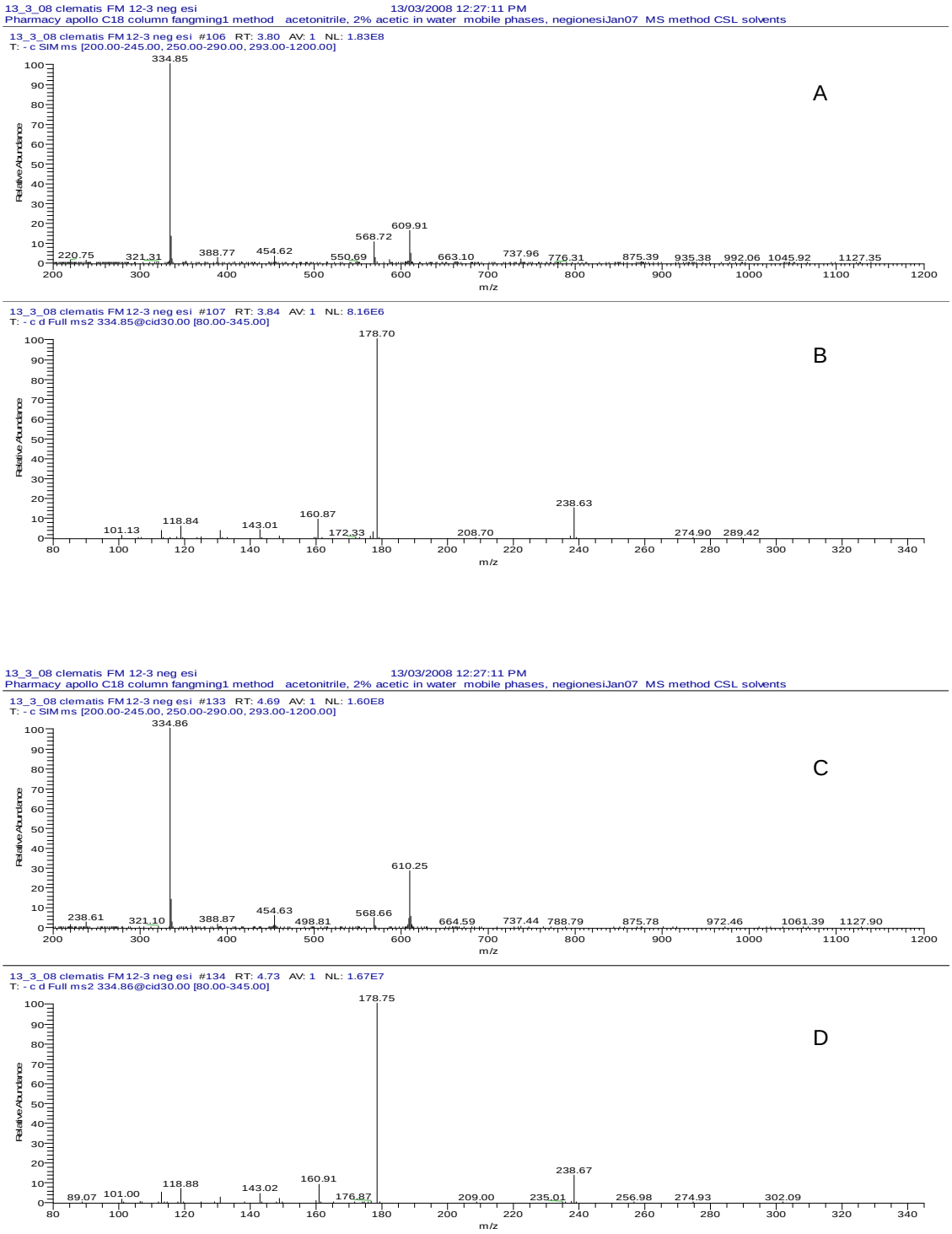

Figure 2.9 MS spectra of peak 1(the retention time was 3.80 minutes) and peak 2 (the retention time was 4.69 minutes). A is the MS spectrum of peak 1. B is the MS^2 spectrum of peak 1. C is the MS spectrum of peak 2 and D is the MS^2 spectrum of peak 2.

result provided evidence that the antitumour constituent was ranunculin and its isomer, and also confirmed that a further ranunculin-like isomer existed in CA-L.

As the number of effective Sephadex LH-20 fractions of *C. microphylla*-TN and *C. aristata*-L was quite similar, we hypothesise the effective constituents in the chromatographic cytotoxic active zone 1 and zone 2 (Figure 2.5) of CM-TNii were ranunculin and its isomer. The antitumour activity of Sephadex LH-20 fractions of CM-TNii14 probably were not obtained because there was not enough ranunculin.

Ranunculin was isolated and reported by Hill and van Heyningen in 1951.[169] It is a glucosidic precursor of protoanemonin. Protoanemonin is liberated enzymically from rancuculin when plant tissue is crushed. Protoanemonin is able to polymerize to a crystalline product, anemonin.

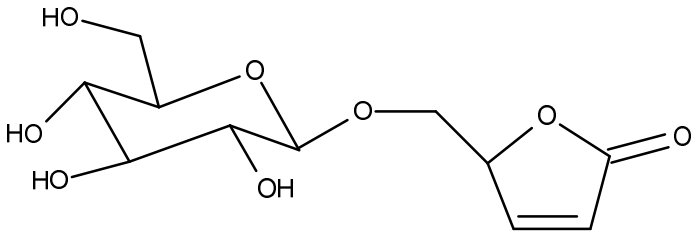

Ranunculin

Figure 2.10 Chemical structures of protoanemonin, anemonin and ranunculin.

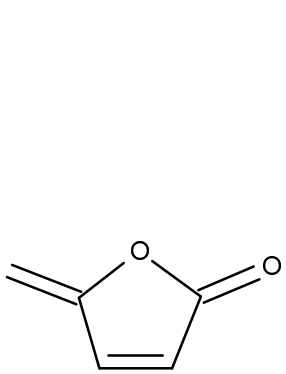

Protoanemonin

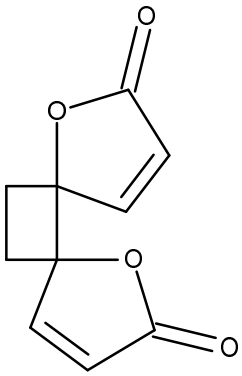

Anemonin

(continued).

In 1972 Tschesche and co-workers found ranunculin isomers, which were isoranunculin and ranunculoside (Figure 2.11).[(170)] In our study, although two ranunculin-like isomers were isolated, we have not undertaken any further study to determine the chemical structure of the ranunculin isomer. The MS^2 analysis could not detect the structure difference between ranunculin isomers.

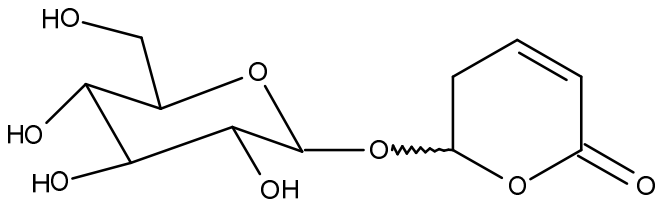

A

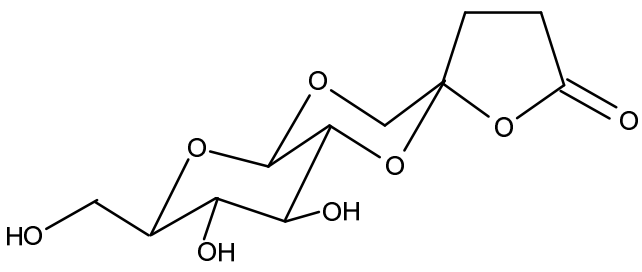

B

Figure 2. 11 Chemical structure of isoranunculin (A) and ranunculoside (B).

2.3.5 Isolation and purification of ranunculin and determination its antitumour IC_{50}

2.3.5.1 Isolation, purification and identification of ranunculin

Isolation of ranunculin was undertaken by C18 column fractionation (2.2.4.3) followed by Sephadex LH-20 column fractionation (2.2.3.5 method B). LH-20 fractions were analysed, by HPLC-ELSD using a carbohydrate column, for the purity of ranunculin. Sephadex LH-20 fractionation was repeated until purity was >95%. Sephadex LH-20 fractions having high purity of ranunculin were purified by recrystallization.[169]

Ranunculin was isolated as pale yellow crystals. The purity of ranunculin was 99.9% determined by HPLC-ELSD using a carbohydrate column and by UPLC-MS using the method described in 2.2.4.10. The UPLC-MS spectral data of this yellow crystalline product is presented in Figure 2.12.

The retention time of the only peak observed in Figure 2.12 A was 1.89 minutes. Positive ion electrospray MS data was collected for the 3 molecular species $[M+H]^+$, $[M+NH_4]^+$ and $[M+Na]^+$ at *m/z* 277, 294 and 299, respectively. Therefore, the molecular weight of M was 276, and the *m/z* at 97 was observed in Figure 2.12 B, which is consistent with protoanemonin. This analysis confirmed that ranunculin was successfully isolated from *C. aristata*-L.

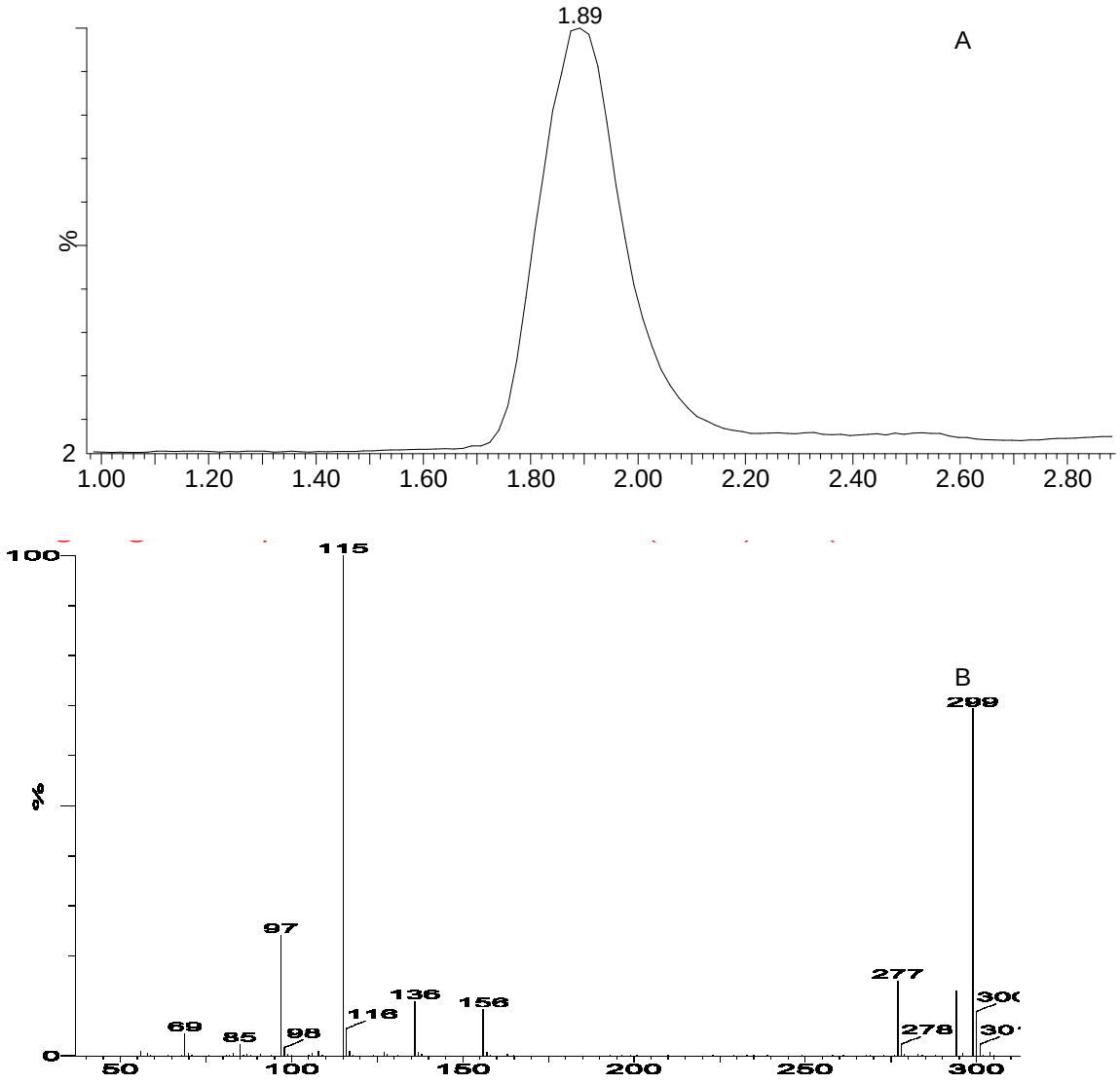

Figure 2.12 UPLC-MS of crystalline product. A is the UPLC chromatogram and B is the MS spectrum of the chromatographic peak observed in A.

2.3.5.2 Determination of cytotoxic IC_{50} of ranunculin

The antitumour dose response curve for ranunculin is shown in Figure 2.13. The positive control, 5-fluorouracil (5-FU), was employed in this experiment.

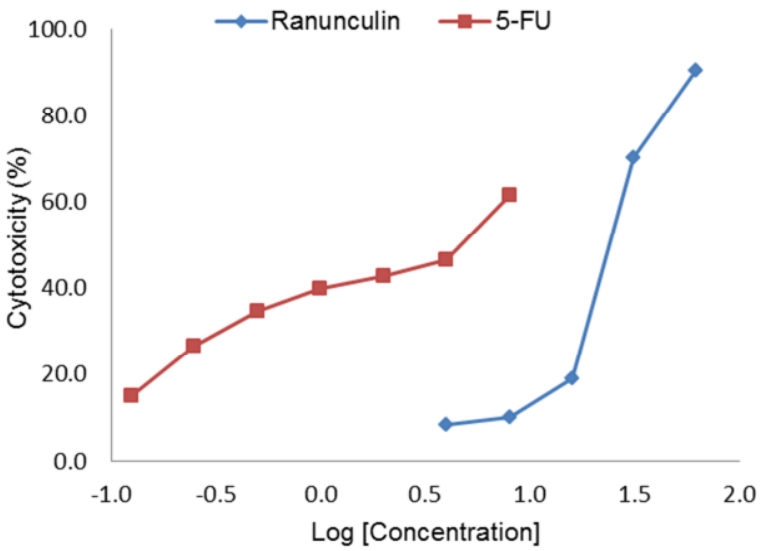

Figure 2.13 Dose-response curves of the cytotoxic activities ranunculin and 5-FU against P388 cells by ploting the cytotoxicity% versus log concentration of ranunculin and 5-FU (Log [Concentration]).

Interpolation from the dose response curves gave IC_{50} for ranunculin of 23.9 µg/ml and 4.7 µg/ml for 5-FU. This result showed that the antitumour activity of ranunculin against P388 cells was 5 times weaker than 5-FU.

The cytotoxicity of ranunculin and its mechanism of action against KB and Bel7402 cells were studied by Li.[131] The IC_{50} values of ranunculin against these two tumour cell lines was 0.21 and 0.35 µmol/L, respectively, and the mode of action was supposed as inhibition of DNA polymerase and increased oxygen free radical formation. When the unit was changed from µg/ml to µmol/L, the cytotoxic IC_{50} of ranunculin against P388 cells in our study was 86aµmol/L. The cytotoxic activity of ranunculin against P388 cells was hundreds of times weaker than that against KB and

Bel7402 cells. Furthermore, data of antitumour activity of ranunculin, protoanemonin and anemonin against the NCI tumour panel were reported in the NCI database.[171, 172] The IC_{50} value of ranunculin reported from NCI was 0.32 μmol/L, which was much less than that obtained in our study. The cytotoxic IC_{50} of 5-FU against P388 cells in our study, 4.7 μg/ml, was similar to reported data, 2.85 μg/ml. [167]

Ranunculin is an unsaturated lactone. In the 1970s, several studies reported that sesquiterpene lactones or ketones containing the system shown in Figure 2.14 had significant antitumour activities.[173-176] The inhibition of tumour growth by this type of compound was thought to occur due to the structure shown in Figure 2.14, alkylating by rapid Michael addition (a conjugate addition with the carbanion as the nucleophile) to the thiol group (-SH) of biological nucleophiles of key regulatory enzymes of nucleic acid and chromatin metabolism.[177] Loeb[178] claimed that nuclear DNA polymerase II and III possess an thiol group that is susceptible to inhibition by thiol reagents. Jone[179] demonstrated that P388 cells required sulfhydryl compounds for proliferation or colony formation. Therefore, the antitumour activity of ranunculin against P388 cells is likely to be contributed to by the inhibition of cell proliferation by inactive DNA polymerase, which was the same as the result obtained by Li[131] on the antitumour mechanism of ranunculin against KB and Bel7402 cells.

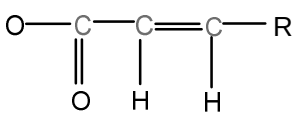

Figure 2.14 The antibacterial active structure in sesquiterpene lactones or ketones

The results from our study only demonstrated that ranunculin and its isomer were the antitumour active constituents in *C. aristata*-L and *C. microphylla*-TN. However, when 60 µg of CM-TNii and 72 µg of CA-Lii were fractionated by HPLC, there were more than two antitumour zones. The HPLC-ELSD chromatograms of these two samples showed that it was difficult to detect peaks in the other active zones. It was presumed that this was because the amount of cytotoxic constituents in those active zones was low. Therefore, in order to get enough of these cytotoxic compounds in HPLC fractions, an Apollo C18 HPLC semi-preparative column (250 mm x 10 mm) was used.

2.3.6 Antitumour activity of *C. microphylla*-TN Semi-preparative C18 HPLC column fractions

2.3.6.1 Antitumour activity of semi-preparative C18 HPLC column fractions of CM-TNII

To isolate more of the compounds corresponding to P388 activities observed in the HPLC fractions of CM-TNii, a larger quantity of *C. microphylla*-TN crude extract was fractionated on a C18 column, then the fraction 2 (CM-TNII), which was the appropriate fraction identified by HPLC, was fractionated using a semi-preparative C18 HPLC column. After a total of up to 5 injections (first fractionation applied in the study of 2.3.6.1) and 15 injections (second fractionation applied in the study of 2.3.6.2), similar fractions were evaporated to dryness and reconstited prior to P388 cytotoxicity assay. The antitumour effects of HPLC semi-preparative fractions of CM-TNII (first fractionation) are presented in Figure 2.15 A. Then two-fold dilution

of effective semi-preparative fractions was undertaken to determine their cytotoxic activity. Results are demonstrated in Figure 2.15 B, C and D.

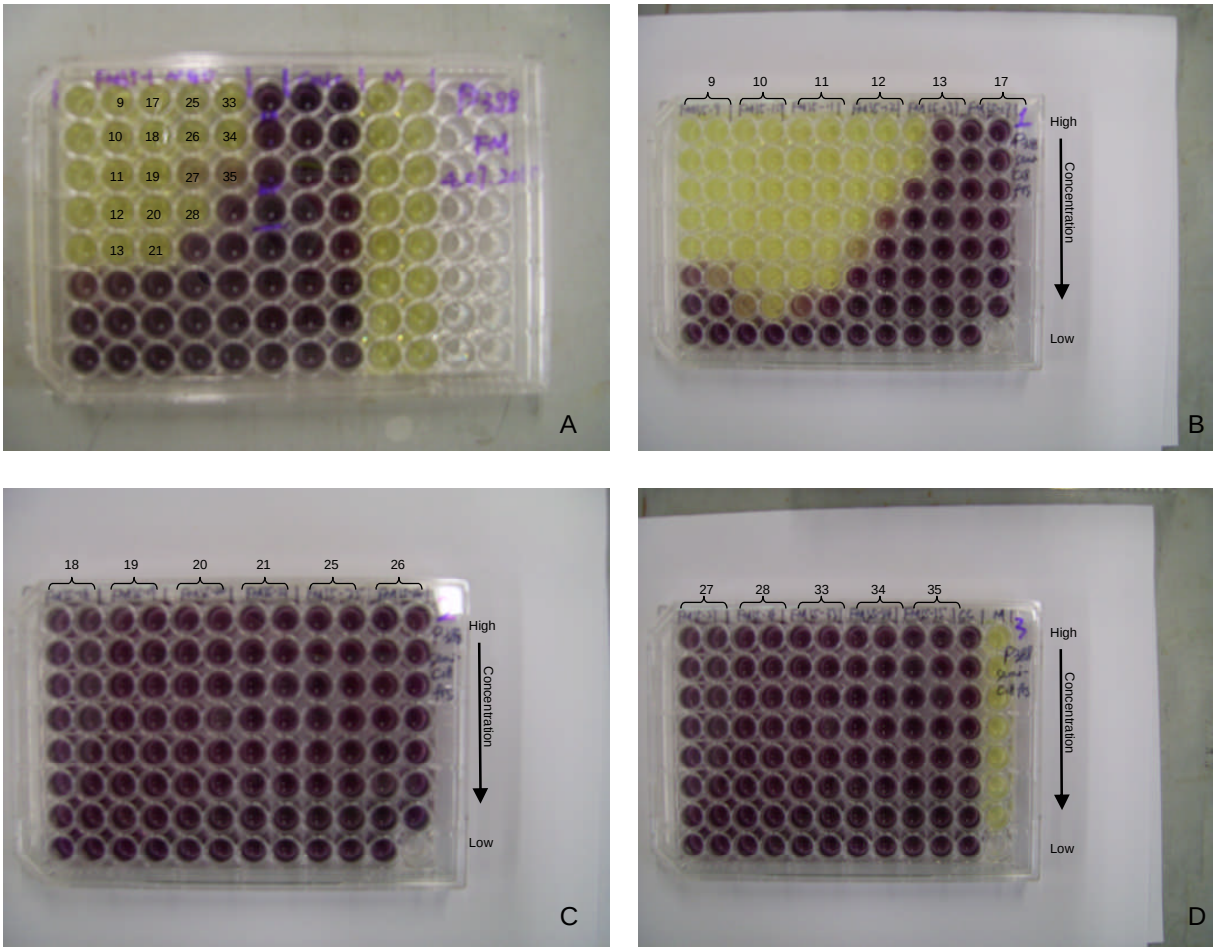

Figure 2.15 P388 cytotoxicity of semi-preparative fractions of CM-TNII (A) and the cytotoxic activities of effective semi-preparative fractions (B, C and D). In photo A, fractions were added into wells in first 5 rows following a vertical sequence from top to bottom. For photos B, C and D, the effective semi-preparative fractions from second column of photo A (yellow wells in columns 2-5) were added into the row A, having the same amount as those added in wells shown in photo A. Then a 2x serial dilution was performed. Each fraction was in duplicate.

Figure 2.15 A showed that the zones of inhibition in antitumour activities were observed in semi-preparative fractions of CM-TNII. However, the number of

antitumour active semi-preparative fractions was different from analytical column fractions. As the data presented in Figure 2.3 B, the effective analytical fractions were fractions 11, 12, 14, 15, 20, 21, 22, 27, 28 and 29. Following the results observed in Figure 2.15 A, the effective semi-preparative fractions were fractions 1, 2, 3, 4, 5, 9, 10, 11, 12, 13, 17, 18, 19, 20, 25, 26, 27, 28, 33, 34 and 35. These differences might be explained as the retention time of potential active chromatographic peaks shifted when eluted from the semi-preparative column compared with those eluted from the analytical column (Figure 2.16). But the initial semi-preparative fractions having the cytotoxic effects against P388 cells could not be explained in this stage of study.

A limitation of this experiment was that the concentration of each fraction applied was unknown. Although the larger HPLC column was employed in this study, the mass of each fraction after freezing dry was still not obtained. Fractions were collected in 20 ml glass vials, so the temperature or the humidity of vials may have influenced the weighing of fractions.

As the cytotoxicity% of each active semi-preparative fraction was almost 100%, in order to determine the antitumour activity level of each effective fraction, a serial dilution of each cytotoxic fraction from the second column shown in Figure 2.15 A was undertaken and their antitumour activities were investigated by the MTT assay. The results of this experiment were shown in Figure 2.15 B, C and D.

Figure 2.15 B, C and D show that only fractions 9, 10, 11 and 12 had antitumour activities. In these four effective fractions, fraction 10, which presented cytotoxicity% more than 90% in the most diluted fraction (column G), had the strongest cytotoxic activity against P388 cells. The result of fraction 13 was abnormal, i.e. the antitumour activity of the duplicate had big variation in the active amount. One gave cytotoxicity% of 100% (Figure 2.15 B column 9), but the other just had cytotoxicity% of 30% or lower (Figure 2.15 B column 10).

The cytotoxic distribution shown in Figure 2.15 B suggested that some cytotoxic results were possibly contributed to by neighbouring wells, such as the duplicates results of fraction 9, 11and 12. For a 96-well plate, rows from left to right are counted from 1 to 12 and coloums from top to bottom are counted from A to G. For fraction 12, the cytotoxic activity in wells 7D, 7E and 7F were larger than that in wells 8D, 8E and 8F, however, for fraction 9, the antitumour effects in wells 2F and 2G were stronger than that in 1F and 1G. The likely explanation was that some cytotoxic constituents could volatilise and spread to other neighbouring wells. The limitation of this experiment was still that the concentration of each fraction applied was unknown.

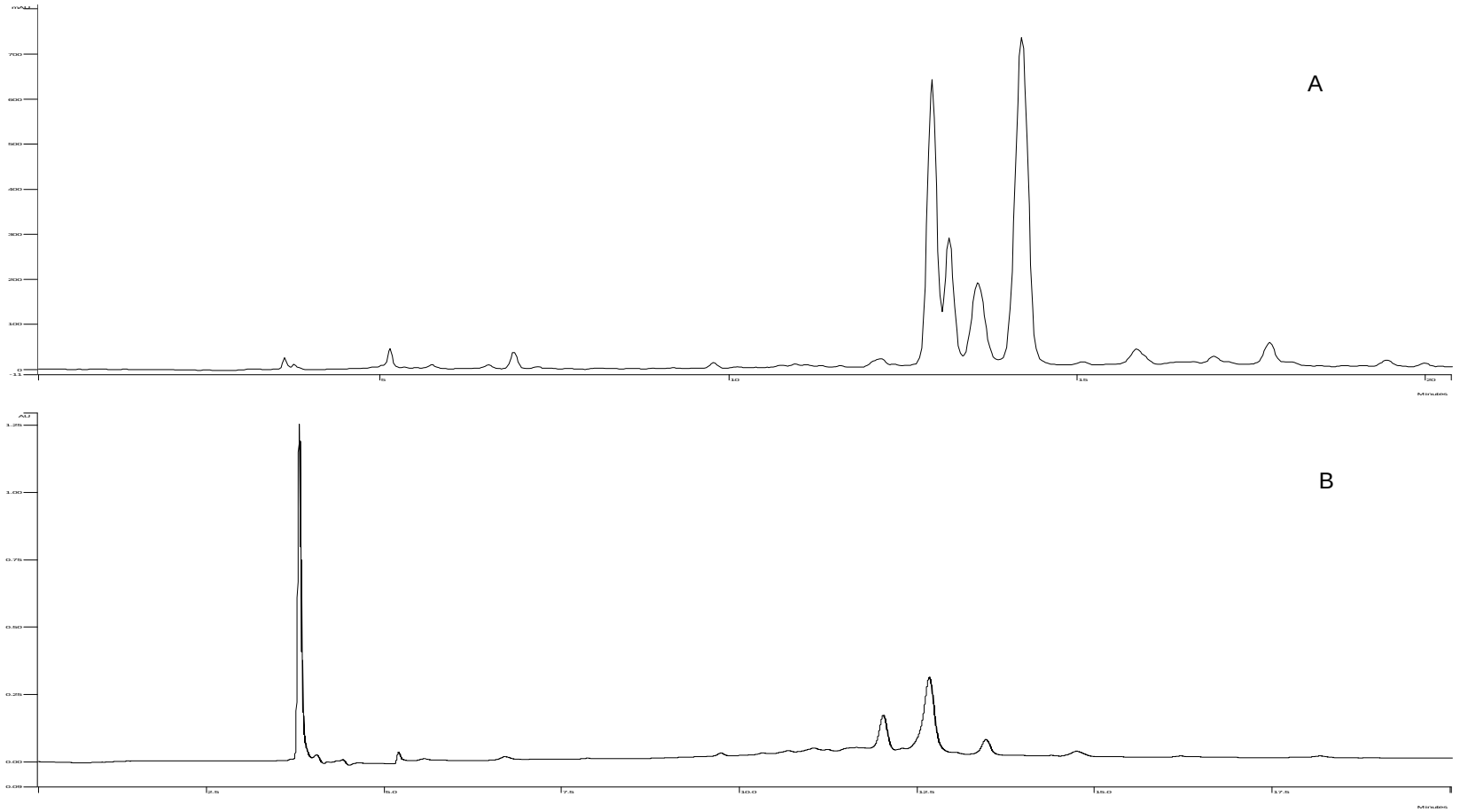

Figure 2.16 C18 semi-preparative HPLC-UV chromatogram of *C. aristata*-L C18 column fraction 2 (A) and C18 analytical HPLC-UV chromatogram of *C. aristata*-L SPE cartridge fraction 2 (B) at 254 nm.

2.3.6.2 Investigation of the cytotoxic vapour constituents in *C. microphylla*-TN.

In order to investigate the phenomenon observed in 2.3.6.1, assay was carried out, adding semi-preparative fractions of CM-TNII to only every second column of the plate. Cytotoxicity was observed in wells where no semi-preparative fraction was added. (Figure 2.17)

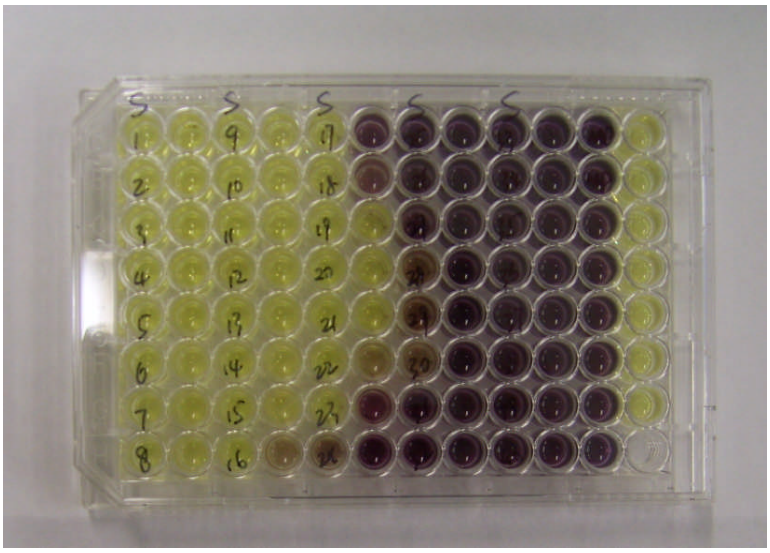

Figure 2.17 The P388 cytotoxicity of semi-preparative fractions of CM-TNii. Fractions were added into columns 1, 3, 5, 7 and 9. The numbers labelled on the microplate are the numbers of fractions.

Method in this assay was to transfer 100 µl of each semi-preparative fraction into 1.5 ml sterile Eppendorf tubes. Solvent was evaporated in the biosafety hood, then each fraction was redissolved by 10 µl of PBS. After seeding cell culture into a 96-well plate, these fractions were added into the plate.

The results in this experiment showed that P388 cytotoxicities were obtained in wells of columns 2 and 4 and part of wells of column 6 although there were no fractions

added to those wells. This result also suggested there existed volatile antitumour compounds which could influence P388 cells in adjacent wells. To test for volatile compounds, fractions 10, 11, 12, 13, 14 and 15, which had cytotoxicity% of more than 90%, were investigated. These fractions (100 µl of each) were evaporated to dryness and reconstituted to 10 µl by PBS. Each fraction was added into a single well (well 7D) using one microplate per fraction. The P388 cytotoxic results are demonstrated in Figure 2.18.

The results in Figure 2.18 showed that the fractions 11 and 12 had cytotoxic activity against P388 cells. The cytotoxicity% of fractions 11 and 12 were 97.1% and 98.1%, respectively. However, only fraction 12 influenced the P388 cells in adjoining wells, presumably by diffusing a volatile agent (eg. protoanemonin). The 27 wells surrounding fraction 12 showed significant inhibition of cell growth. Wells in the first column only contained RPMI-1640 complete medium, which was a negative control.

Based on results in this experiment, the relationship between dose and cytotoxicity% of fraction 12 was investigated. The method was modified slightly. The cell culture in well 7D of each 96-well plate was changed to RPMI-1640 medium. The purpose of this modification was to determine if the hydrolysis of fraction 12 was contributed to by P388 cells or RPMI-1640 medium alone. Four amounts of fraction 12 (100, 50, 25 and 12.5 µl) were transferred in to four 1.5 ml sterile Eppendorf tubes, respectively. MeOH was evaporated, then each fraction was dissolved by 10 µl PBS. The results, expressed as cytotoxicity%, are shown in Figure 2.19.

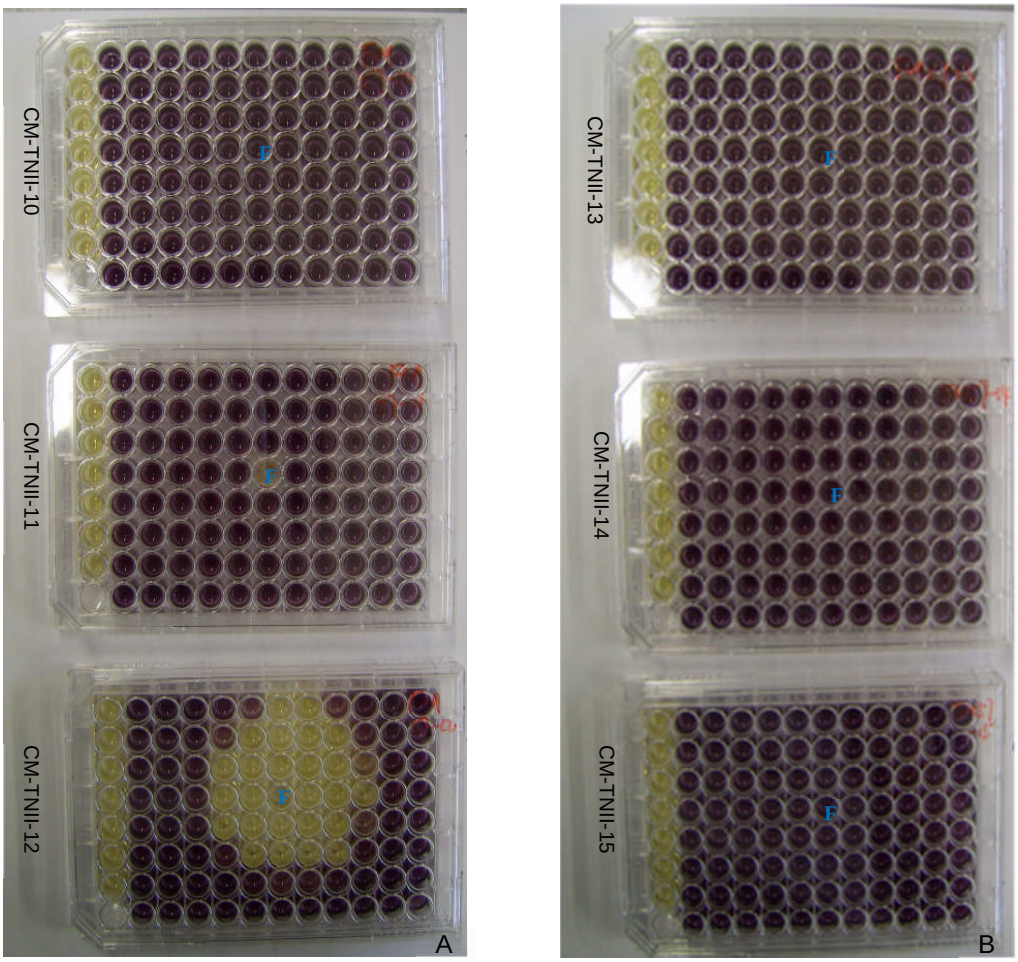

Figure 2.18 Antitumour and evaporation activity of semi-preparative C18 HPLC column fractions of 10, 11, 12, 13, 14 and 15 of CM-TNII. Fractions were added in well 7D (labeled as blue-coloured F). A shows the photo of cytotoxicity of fraction 10, 11 and 12 against P388 cells. B shows the photo of cytotoxicity of fractions 13, 14 and 15.

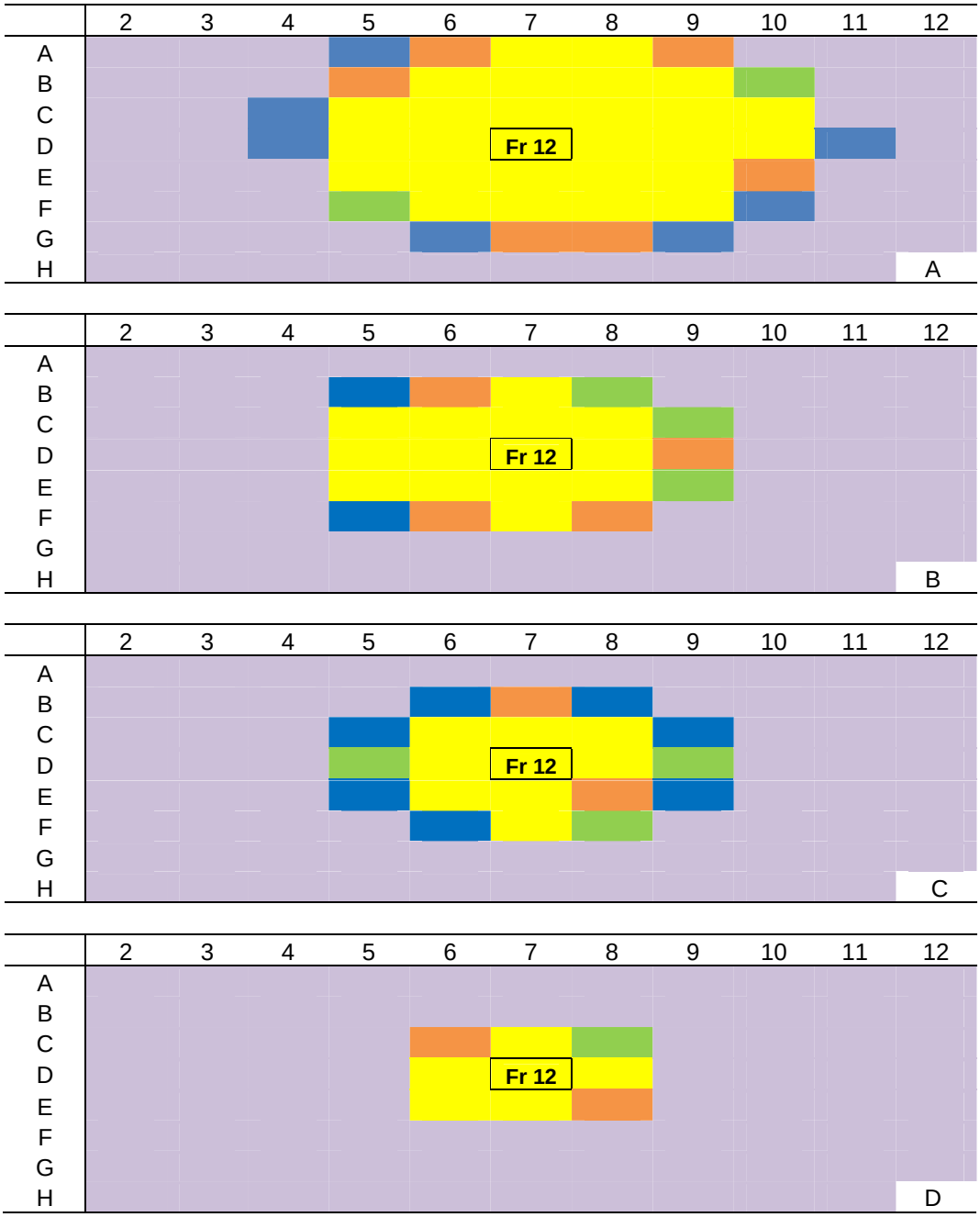

Figure 2.19 P388 cytotoxicity of semi-preparative HPLC fraction 12 of CM-TNii. Fraction in PRMI-1640 was in well 7D of each plate labelled as Fr12. A, B, C and D presented the P388 cytotoxicity of 100, 50, 25 and 12.5 µl of Fr12, respectively. Different colour represented the varied cytotoxicity% in each well (yellow — 81-100%, orange — 61-80%, green — 41-60%, blue — 21-40% and purple — 0-20%).

Figure 2.19 demonstrated that the hydrolysis of fraction 12 was contributed to by RPMI-1640 medium. The cytotoxicity and evaporation property was related to the amount of fraction. When the amount of fraction 12 decreased, the ability of fraction 12 influence surrounding wells decreased. The limitation of this experiment was that the concentration of each fraction applied was unknown. Fraction 12 was analysed by UPLC-MS to determine the chemical property. The result showed that the cytotoxic constituent was ranunculin (Figure 2.20).

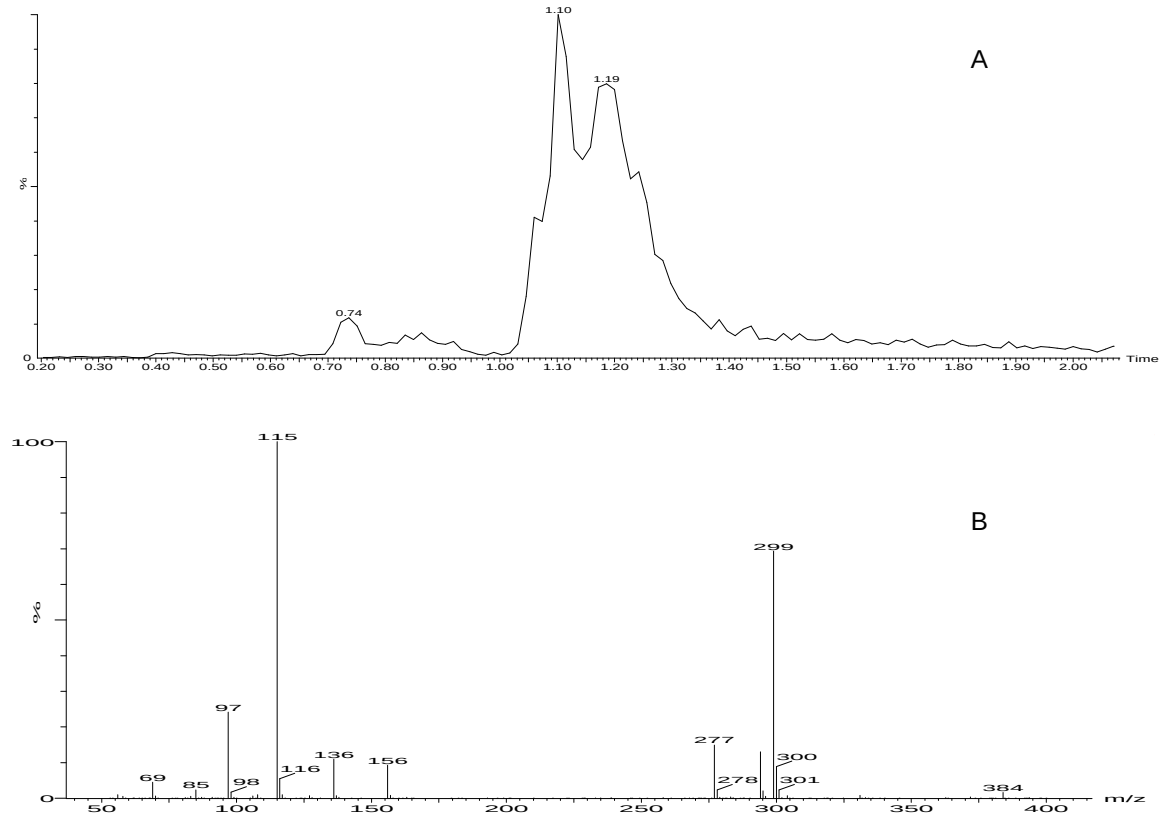

Figure 2.20 UPLC-MS chromatogram of semi-preparative HPLC fraction 12 of CM-TNII. A is the total ion current (TIC) chromatogram showing $[M+H]^+$ *m/z* at 277. B is the mass spectrum of peaks with retention time of 1.10 minutes and 1.19 minutes in A. Both chromagtographic peaks had the same MS spectrum.

2.3.7 Decomposition of ranunculin

Our study demonstrated that ranunculin had cytotoxic activity against P388 cells. However, ranunculin was not stable in RPMI-1640 medium and appeared to be hydrolysed to volatile compounds that were able to diffuse into wells adjacent to wells containing ranunculin, to exert cytotoxic effects on cells in these adjacent wells. It was hypothesised that ranunculin was hydrolysed to protoanemonin, which had cytotoxic activities. In order to confirm this hypothesis, the hydrolysis of ranunculin was investigated.

2.3.7.1 Decomposition of ranunculin facilitated by cell medium

The hydrolysis of ranunculin to protoanemonin facilitated by RPMI-1640 medium was determined by MTT assay. Cell culture in RPMI-1640 medium (100 µl) was put into each well, except wells of column 1 and 7D, which contained 100 µl of RPMI-1640 medium alone. Three different amounts of ranuculin (50, 25, 12.5 µg) in 10 µl PBS were added into well 7D of 3 different 96-well plates. The hydrolysis of ranunculin by cell medium was measured by determination of cytotoxicity% in the wells surrounding well 7D using the MTT assay. The results are presented in Figure 2.21.

Results in Figure 2.21 showed that when 50 µg (500 µg/ml) of ranunculin was added to well 7D, the cytotoxicity% of 100% was observed in the wells adjacent to 7D. When ranunculin was decreased to 25 µg (250 µg/ml), the P388 cytotoxicity of surrounding wells decreased to cytotoxicity% range of 21-60%. At a ranunculin

amount of 12.5 µg (125 µg/ml), there was not any cytotoxicity in the wells adjacent to 7D. This results show that the hydrolysis of ranunculin was facilitated by RPMI-1640 medium itself, since the well containing ranunculin contained only medium without any P388 cells.

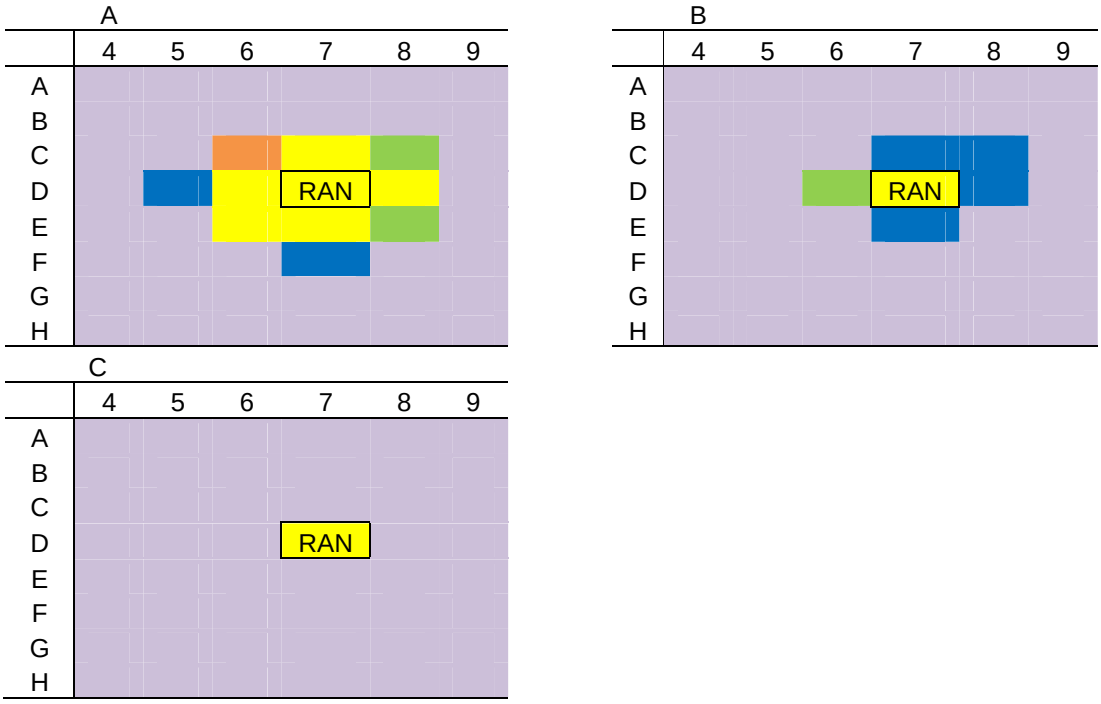

Figure 2.21 The determination of decomposing ranunculin to protoanemonin facilitated by RPMI-1640 medium using P388 cyototoxic assay indicated by MTT. Different amounts of ranunculin (RAN) prepared by 10 µl in PBS were added into well 7D of each 96-well plate. A, B and C presented the P388 cytotoxicity of 50, 25 and 12.5 µg of ranunculin, respectively. Different colour represented the varied CI % in each well (yellow — 81-100 %, orange — 61-80 %, green — 41-60 %, blue — 21-40 % and purple — 0-20 %).

2.3.7.2 The hydrolysis of ranunculin by cell medium, normal saline and phosphate buffered saline

Results in 2.3.7.1 demonstrated that ranunculin was not stable in RPMI-1640 medium. A further study was performed to determine if ranunculin was stable in other cell media or saline solution. Ranunculin was added to RPMI-1640 medium,

DMEM, phosphate PBS and normal saline to determine the stability of ranunculin in these solutions. The pH value of each solution was measured. The method was the same as that described in 2.3.7.1. There was no P388 cell in well 7D, which contained 100 µl of RPMI-1640, DMEM, PBS and normal saline in 4 plates, respectively. Ranunculin, 50 in 10 µl of PBS, was added into well 7D. Results are presented in Figure 2.22. Photos of microtitre plates are included in the Appendix II.

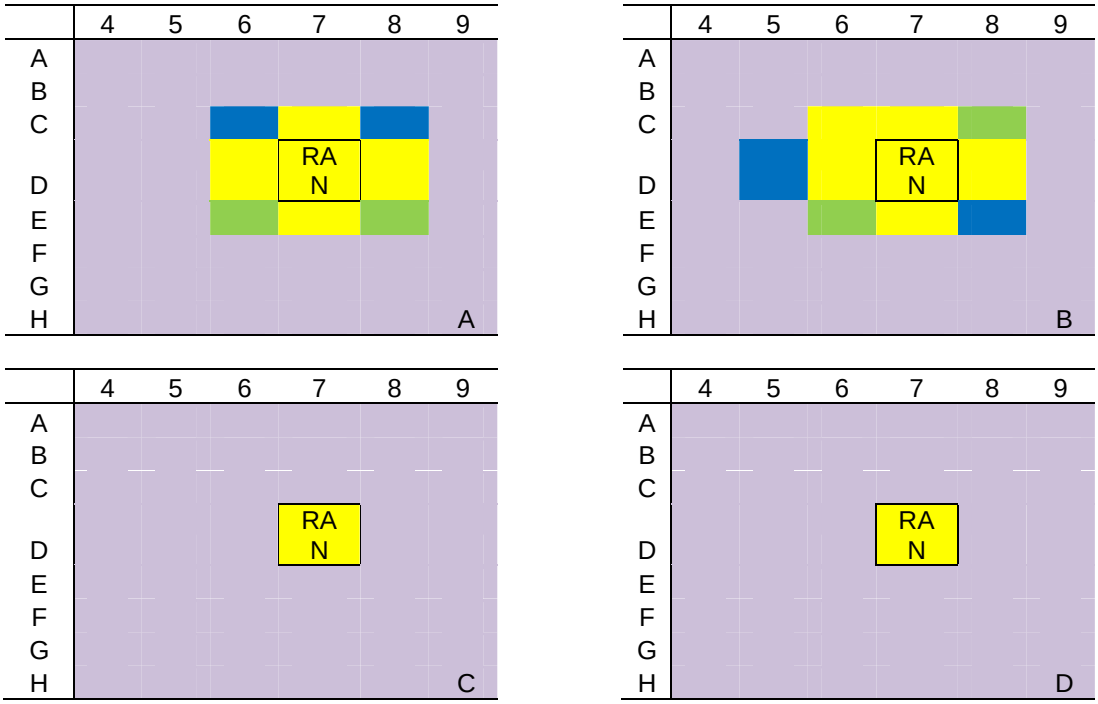

Figure 2.22 Hydrolysis ability of ranunculin by different matrices. A, B, C and D represent the P388 cytotoxicity of 50 µg of ranunculin in RPMI-1640, DMEM, PBS and normal saline, respectively. Different colour represented the varied CI% in each well (yellow — 81-100%, orange — 61-80%, green — 41-60%, blue — 21-40% and purple — 0-20%). The pH values of RPMI-1640, DMEM, PBS and normal saline were respectively 7.06, 7.14, 7.11 and 6.87.

The data showed that ranunculin could be hydrolysed to a volatile cytotoxic compound by both cell media, but evidence of hydrolysis was not observed in normal saline or PBS. In order to determine the chemical property of this volatile antitumour constituent, 1 mg of ranunculin was added into 2 ml of RPMI-1640 medium.

Headspace GC-MS SPME was applied to determine the mass spectrum of this volatile antitumour constituent. GC-MS data is shown in Figure 2.23 and 2.24.

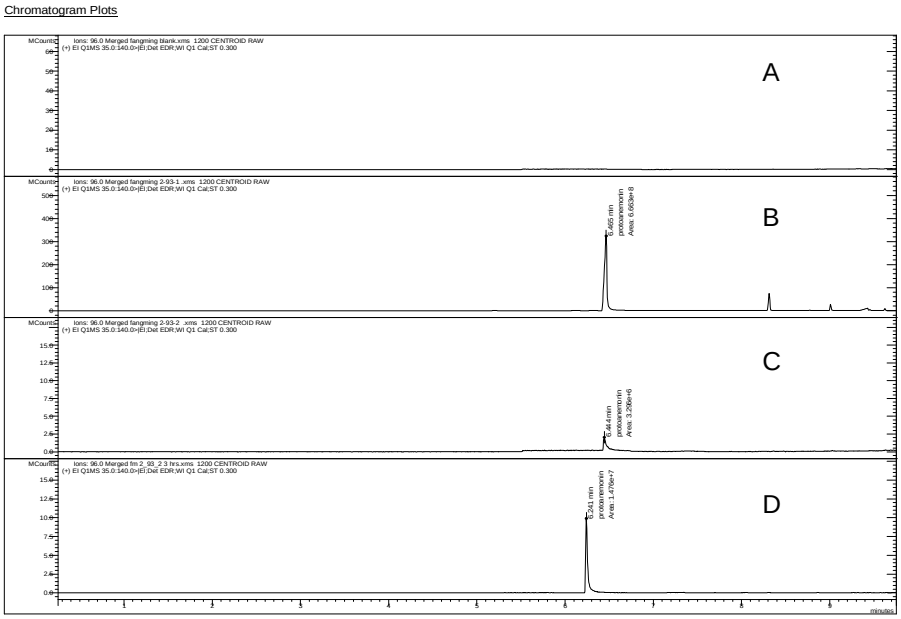

Figure 2.23 The Headspace GC-MS chromatogram of hydrolysed ranunculin by cell medium RPMI-1640. A is medium only blank; B is freshly crushed *C. microphylla*-TN leaf only; C is the ranunculin in RPMI-1640 without incubation; D is ranunculin in RPMI-1640 after 3 hours of incubation.

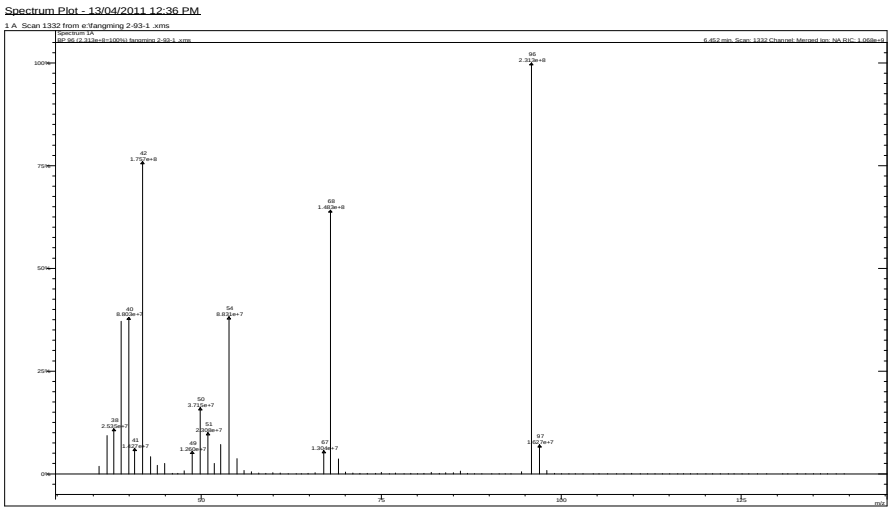

Figure 2.24 Mass spectrum of the chromatographic peak showing in Figure 2.23.

Protoanemonin had been determined by GC-MS in a previous study performed in this laboratory.[52] The mass spectrum in Figure 2.24 was consistent with that of protoanemonin. Peaks were observed at *m/z* (%): 96 (100), 68 (65), 54 (37), 42 (76). Therefore, chromatogramic peaks observed in Figure 2.23 were due to protoanemonin. This result revealed that protoanemonin was obtained from freshly crushed leaves of CM-TN and from ranunculin in RPMI-1640. The amount of protoanemonin detected after 3 hours incubation (Figure 2.23 D) was 4.5x greater than the amount detected from pre-incubation (Figure 2.23 C).

The pH of RPMI-1640, DMEM, PBS and normal saline were 7.06, 7.14, 7.11 and 6.87, respectively. Data in Table 2.6 showed that hydrolysis of ranunculin was not related to the pH values. The pH values of these four solutions were similar, but decomposition by ranunculin was only observed in DMEM and RPMI-1640.

Figure 2.25 Experimental photos of absorbing the volatile products produced from ranunculin presented RPMI-1640 medium. A hotplate with magnetic stirrer was used to maintain the temperature (37°C) of medium in the vial.

The result suggested that protoanemonin was the actual antitumour constituent in *Clematis* spp. Its glycoside, ranunculin, could be decomposed by RPMI-1640 and DMEM cell medium to produce protoanemonin. This result suggests that the cytotoxic activity of ranunculin and its mode of action investigated by Li[(131)] and the antitumour data of ranunculin against the NCI panel[(172)] were the antitumour effects and mechanism of protoanemonin rather than ranunculin. The IC_{50} value of ranunculin obtained in our study was hundards of times higher than that reported in the NCI website is likely that some protoanemonin was evpoarted in our experiment. Although this experiment demonstrated hydrolysis of ranunculin by RPMI-1640 medium and DMEM, the hydrolysis of ranunculin by other cell media is unknown.

Protoanemonin was obtained at the beginning of last century.[(180)] Its β-D-glucoside, ranunculin, was crystalized from different Ranunculus spp.[(169)] and authors also reported that ranunculin was stable both as a solid and in neutral aqueous solution, very stable in acid, but not stable in weak alkaline solution (sodium acetate) to yield protoanemonin. The stability of ranunculin under different conditions was reported. Protoanemonin was obtained in buffered solutions over a pH range of 4-8 and also in 0.1 N sodium hydroxide by means of UV absorption and chromatography.[(181)]

Based on the above reports, it is proposed that the hydrolysis of ranunculin by cell medium The contents of RPMI-1640[(182)] and DMEM[(183)] are listed in Table 2.4. The composition of cell media included amino acids, vitamins, inorganic salts and other components. As ranunculin was not stable in weak alkaline solution, it is

hypothesised that inorganic salts might contribute to the hydrolysis of ranunculin. But this has not been investigated in this study.

The antitumour study of *Clematis* spp. suggested that ranunculin has cytotoxic activity against P388 cells. However, the antitumour effect of ranunculin is contributed to by protoanemonin, achieved by hydrolysis of ranunculin by cell medium. The antitumour zones obtained in P388 assay of HPLC fractions were proposed to be due to protoanemonin. The strucutre shown in Figure 2.14 might contribute to the antitumour activity of protoanemonin by Michael addition to sulfhydryl biological nucleophiles of key regulatory enzymes of nucleic acid and chromatin metabolism.

Table 2.4 The formular of RPMI-1640 and DMEM.

RPMI-1640				DMEM			
COMPONENTS	Molecular Weight	Concentration (mg/L)	mM	COMPONENTS	Molecular Weight	Concentration (mg/L)	mM
Amino Acids				**Amino Acids**			
Glycine	75	10	0.133	Glycine	75	30	0.4
L-Arginine	174	200	1.15	L-Arginine hydrochloride	211	84	0.398
L-Asparagine	132	50	0.379	L-Cystine 2HCl	313	63	0.201
L-Aspartic acid	133	20	0.15	L-Glutamine	146	584	4
L-Cystine 2HCl	313	65	0.208	L-Histidine hydrochloride-H2O	210	42	0.2
L-Glutamic Acid	147	20	0.136	L-Isoleucine	131	105	0.802
L-Glutamine	146	300	2.05	L-Leucine	131	105	0.802
L-Histidine	155	15	0.0968	L-Lysine hydrochloride	183	146	0.798
L-Hydroxyproline	131	20	0.153	L-Methionine	149	30	0.201
L-Isoleucine	131	50	0.382	L-Phenylalanine	165	66	0.4
L-Leucine	131	50	0.382	L-Serine	105	42	0.4
L-Lysine hydrochloride	183	40	0.219	L-Threonine	119	95	0.798
L-Methionine	149	15	0.101	L-Tryptophan	204	16	0.0784
L-Phenylalanine	165	15	0.0909	L-Tyrosine disodium salt dihydrate	261	104	0.398
L-Proline	115	20	0.174	L-Valine	117	94	0.803
L-Serine	105	30	0.286				
L-Threonine	119	20	0.168				
L-Tryptophan	204	5	0.0245				
L-Tyrosine disodium salt dihydrate	261	29	0.111				
L-Valine	117	20	0.171				
Vitamins				**Vitamins**			
Biotin	244	0.2	0.00082	Choline chloride	140	4	0.0286
Choline chloride	140	3	0.0214	D-Calcium pantothenate	477	4	0.00839
D-Calcium pantothenate	477	0.25	0.00052	Folic Acid	441	4	0.00907
Folic Acid	441	1	0.00227	Niacinamide	122	4	0.0328
Niacinamide	122	1	0.0082	Pyridoxine hydrochloride	206	4	0.0194
Para-Aminobenzoic Acid	137	1	0.0073	Riboflavin	376	0.4	0.00106
Pyridoxine hydrochloride	206	1	0.00485	Thiamine hydrochloride	337	4	0.0119
Riboflavin	376	0.2	0.00053	i-Inositol	180	7.2	0.04
Thiamine hydrochloride	337	1	0.00297				
Vitamin B12	1355	0.005	3.7E-06				
i-Inositol	180	35	0.194				
Inorganic Salts				**Inorganic Salts**			
Calcium nitrate (Ca(NO3)2 4H2O)	236	100	0.424	Calcium Chloride (CaCl2) (anhyd.)	111	200	1.8
Magnesium Sulfate (MgSO4) (anhyd.)	120	48.84	0.407	Ferric Nitrate (Fe(NO3)3"9H2O)	404	0.1	0.00025
Potassium Chloride (KCl)	75	400	5.33	Magnesium Sulfate (MgSO4) (anhyd.)	120	97.67	0.814
Sodium Bicarbonate (NaHCO3)	84	2000	23.81	Potassium Chloride (KCl)	75	400	5.33
Sodium Chloride (NaCl)	58	6000	103.45	Sodium Bicarbonate (NaHCO3)	84	3700	44.05
Sodium Phosphate dibasic (Na2HPO4) anhydrous	142	800	5.63	Sodium Chloride (NaCl)	58	4750	81.9
				Sodium Phosphate monobasic (NaH2PO4-H2O)	138	125	0.906
Other Components				**Other Components**			
D-Glucose (Dextrose)	180	2000	11.11	D-Glucose (Dextrose)	180	4500	25
Glutathione (reduced)	307	1	0.00326	HEPES	238	5958	25.03
Phenol Red	376.4	5	0.0133				

2.4 Future work

For the future work, it might be worth to determine the composition in cell medium that contribute the decomposition of ranunculin, and investigate the reaction contributed to this decomposition. It might also be worth to investigate if ranunculin itself is cytotoxic. Our study only investigated the antitumour activities of leafs of Tasmania native *Clematis* spp., however, leafs were the least usage part of *Clematis* spp. in TCM, compared with roots and stems, and the most reported antitumour compounds (reviewed in Chapter 1) isolated from other *Clematis* spp were saponins, which were isolated from roots. Therefore, to investigate the antitumour activities of roots and stems of Tasmanian *Clematis* spp. would be worthy in the future.

2.5 Conclusion

This study demonstrated that Tasmanian native *Clematis* spp. had cytotoxic activities against P388 cells. Antitumour activities of *Clematis* spp. varied significants both between and within species of all investigated *Clematis* plants. *C. aristata*-L and *C. microphylla*-TN had the strongest antitumour activities. The cytotoxic pro-drug, ranunculin, was isolated by bioguided-fractionation. However, the actual cytotoxic compound against P388 cells was protoanemonin, which was generated from the decomposition of ranunculin in cell medium. The cytotoxic activity that was observed in fractions that did not contain ranunculin, and that were thought to contain additional cytotoxic compounds, was shown to be due to the diffusion of volatile

protoanemonin from adjacent wells that contained ranunculin. Ranunculin was responsibe for all cytotoxic constituents observed in the extract. The phenomenon of cell medium decomposition of ranunculin to protoanemonin also suggests that the antitumour activities of ranunculin determined from Li[131] and NCI[171, 172] was the antitumour effects of protoanemonin.

Chapter 3 Antibacterial Activity of Tasmanian *Clematis* Species.

Abstract

Leaf of some *Clematis* spp. has been used in TCM for the treatment of infections. The aim of this chapter was to investigate the antibacterial activities of Tasmanian native *Clematis* spp. and determine the potential active constituents. Minimum inhibitory concentrations (MICs) of extracts were determined by resazurin-indicated broth dilution in 96-well microplates. Isolation of active constituents from the most effective extracts included fractionation by SPE cartridge, HPLC columns and Sephadex LH-20 column chromatography. Identification was achieved by spectroscopic methods (UV, LC-MS and GC-MS). Scanning electron microscopy, Gram stain, antibiotic interaction with checkerboard, deoxycholate-induced lysis and the antibiotic resistant mechanism study of *Pseudomonas aeruginosa* were employed to study the antibacterial mechanism of the active constituent.

Varied antibacterial activities were obtained from different *Clematis* spp. extracts. Ranunculin was determined as an effective antibacterial constituent in the investigated *Clematis* spp. This compound is selective active against Gram negative bacteria. The MIC of ranunculin against clinically-isolated multi-drug resistant *Pseudomonas aeruginosa* strains (PAu19b and PA124) was the same as that against sensitive *P. aeruginosa* strain (PAO1). It was found that ranunculin is a pro-toxin of protoanemonin. The results of the antibacterial mechanism study revealed that the antibacterial mechanism of protoanemonin against sensitive and multi-drug resistant *P. aeruginosa* strains appears be different. The MexXY multidrug efflux system was detected in PAu19b and PA124, but this system did not confer resistance to

ranunculin (protoanemonin). This study provided experimental data demonstrating the antibacterial activity and suspected antibacterial mechanism of Tasmanian native *Clematis* spp. extract.

3.1 Introduction

Bacteria are microscopic, single-celled organisms belonging to Kingdom Monera. They can live practically everywhere and inhabit all kinds of environments, such as in soil, seawater, the stratosphere and even in bodies of other organisms. Most bacteria are not harmful to human beings and many are helpful. Some bacteria help to digest food, destroy disease-causing cells and provide the body with required vitamins. Bacteria are also used in making healthy foods like yogurt and cheese. But infectious bacteria cause illness to human beings. They reproduce quickly in the human body and many give off toxins, which are able to damage tissue and cause illness.

Antibiotics are the usual treatment for bacterial infections. Natural resources are a large treasury for the development of antibiotics. 'Chinese Materia Medica'[(3)] has recorded 8980 natural medicines, in which 596 have antibacterial functions. Most herbs with antimicrobial activity are classified as a group having the function of "clearing heat and expelling miasma". In TCM, bacterial infections are regarded as a heat disease due to the clinical symptoms like fever, yellow urine, red tongue and fast pulse. The theory of TCM regards fire as caused by heat. When evils invade human beings, symptoms like high fever appear, named "fire". In Western medicine, high fever is an early symptom of acute bacterial infection. In modern clinical practice of TCM, pure fire evils are purported to be Gram positive (G+) bacterial infections that are treated by herbs with the property of clearing heat; fire with damp evils are purported to be Gram negative (G-) bacterial infections that are treated by herbs with the property of clearing heat and expelling damp. Although *Clematis* spp. used in

TCM do not belong to the group of "clearing heat and expelling miasma" medicines, they have the function of expelling damp. And some of those recorded in 'Chinese Materia Medica' have antibacterial activity.

The literature review (section 1.4.1) indicated that a number of *Clematis* spp. including *C. cirrhosa*, *C. chinensis*, *C. vitalba*, etc, possess antifungal and antibacterial activities against some +ve and –ve bacteria. The potential active constituent was reported as protoanemonin. Previous studies performed in this laboratory have also showed that Tasmanian native *Clematis* spp. possesed antimicrobial activity. Their antibacterial effects were only found in polar fractions of solvent extracts and the antibacterial effects of leaf polar fractions were higher than those obtained in stem and root fractions. However, the antibacterial activities did not seem to be due to protoanemonin only. Results in this previous work provide a rational that Tasmanian native *Clematis* spp. leaf polar fractions may contain other antibacterial constituents.

Chapter 2 described the antitumour activities of Tasmanian native *Clematis* spp. and revealed the antitumour active constituent. In this chapter, the antibacterial activities of Tasmanian native *Clematis* spp. were studied by determination of minimum inhibitory concentrations (MICs) of extracts using resazurin-indicated broth dilution in 96-well microplates.

Resazurin was an indicator in this method. It is a blue non-fluorescent and non-toxic dye that becomes pink and fluorescent when reduced to resorufin by oxidoreductases

within viable cells. Resorufin is further reduced to uncoloured and nonfluorescent hydroresorufin. [184]

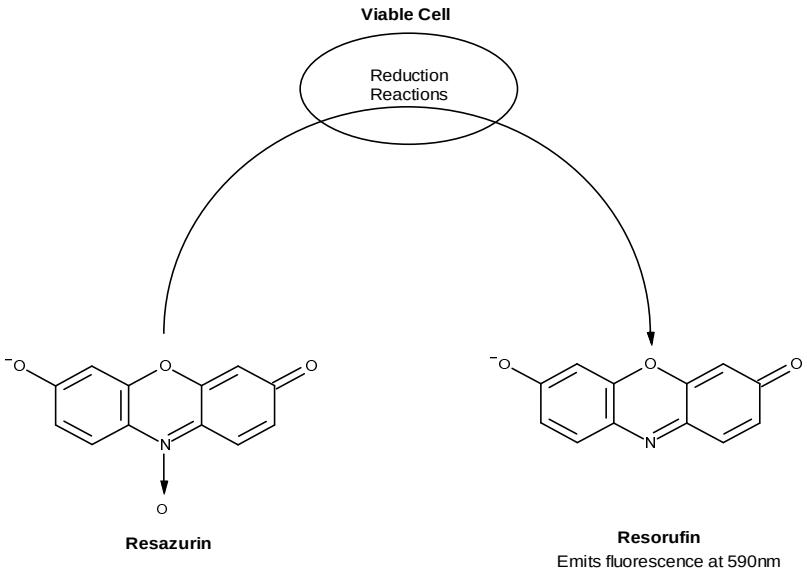

Figure 3.1 The change of resazurin to resorufin used for indicating bacterial viability.

The activity-guided isolation, identification and quantification of antibacterial compounds from native *Clematis* spp. collected and purchased from Hobart, Tasmania, and the antibacterial activities of Tasmanian native *Clematis* spp. and their potential active constituents were investigated in this study.

3.2 Experimental

3.2.1 Reagents

3.2.1.1 Extraction and isolation of plant material

The solvents used for extraction and isolation of plant material were the same as reagents used in Chapter 2. The only difference was the petroleum spirit (Polytreat, Australia) that was used for partitioning.

3.2.1.2 Antibacterial assay

Pipettes and pipettes tips of various sizes and material used in this study included: a multichannel pipette (200 µl) (Eppendorf, Australia); sterile 96-well/flat bottom microplates, sterile centrifuge tubes 14 ml and 50 ml (Iwaki, Japan); V-shaped reagent reservoirs (70 ml) (Socorex, Switzerland); sterile petridishes (Bioscience, Australia); universal bottles (Eppendorf, Australia); sodium deoxycholate, dimethy sulfoxide (DMSO), sterile normal saline, amoxicillin, gentamicin and resazurin powder (Sigma-Aldrich, Australia); Muller Hinton broth, Todd Hewit broth, agar technical, Gram's stain solutions and horse blood agar plates (Oxoid, Australia), sterile 0.22 µm MILLEX filters (Millipore, Ireland) and glutaraldehyde (Proscitech, Australia) were used in this study.

The resazurin solution was prepared by dissolving 20 mg powder into 100 ml sterile distilled water. This solution was filtered and stored in 10 ml sterile bottles, and frozen at -20°C. This solution was then thawed when required.

3.2.2 Instruments

Sonicator, rotary evaporator, HPLC, LC-MS, GC-MS, fraction collector, SPME fibre with holder, biosafety cabinet and CO_2 incubator were used, as described in Chapter 2.

Positive ion APCI was employed in the LC-MS analysis. Conditions were as follows; capillary temperature 165°C, APCI vaporizer temperature 360°C, needle voltage 6 KV, sheath gas 35 psi and capillary voltage 3 V. Ions from *m/z* 100 to 1500 were acquired, and data dependent MS_2 and MS_3 scans were acquired from the most intense ion with a collision energy of 25%.

3.2.2.1 Incubator

A EN 025 incubator (Nuve Inc., Turkey) was used for incubating bacteria. Temperature was set to 37°C.

3.2.2.2 Microscope

A LEICA DM 2500 microscope (Leica, Germany) was used for observing Gram stained bacteria.

3.2.2.3 Scanning Electron Microscope

A BalTec SCD 050 sputter coater (Capovani Brothers Inc., USA) and a FEI Quanta 600 MLA environmental scanning electron microscope (FEI, USA) were used for coating and observing bacteria.

3.2.2.4 Centrifuge

A MOO 18735 microcentrifuge (Denver Instrument Company, USA) and Model 7111 centrifuge (Surgical & Medical Products, Australia) were used for centrifuging bacterial suspensions.

3.2.3 Plant material

Two *C. aristata* cultivars and a *C. microphylla* cultivar were purchased from Plants of Tasmania Nursery, Ridgeway and a *C. aristata* cultivar was purchased from Lindisfarne Village Garden Centre, Lindisfarne in January 2008. Two cultivars of *C. aristata* were collected in the Weilangta Forest and Eaglehawk Neck, respectively, in March 2008. *C. vitalba* was collected from a private garden in Regent Street, Sandy Bay, and *C. gentianoides* was collected in University of Tasmania Hobart Campus in March 2008. All collected plants were identified by the Tasmanian Herbarium. Leaves were picked from fresh plants and cleaned with tap water, then were dried with paper towel. The leaves were weighed prior to extraction. These plants are summarised in Table 3.1.

Table 3.1 Resource of plant material

Species	Location	Date	Sample code
C. aristata	Tasmanian Nursery	11/01/08	CA-TN1
C. aristata	Tasmanian Nursery	11/01/08	CA-TN
C. aristata	Lindisfarne	11/01/08	CA-L
C. aristata	Eaglehawk Neck	14/02/08	CA-EN
C. aristata	Weilangta Forest	2/03/08	CA-WF
C. microphylla	Tasmanian Nursery	11/01/08	CM-TN
C. gentianoides	UTAS	7/03/08	CG-UTAS
C. vitalba	Regent Street	11/04/08	CV-RS

Different ages of CA-L leaf were collected. As the *Clematis* plant is a vine, in a branch, the leaf proximal to the main stem is older than those more distal from the stem. Leaves were removal from a single branch, at different distances from the main stem. They were labelled as 1, 2, 3, 4 and 5, from the youngest to oldest.

3.2.4 Extraction and fractionation

MeOH, MeOH-DCM and DCM extraction, SPE cartridge fractionation, analytical C18 HPLC column fractionation, carbohydrate HPLC column fractionation, analysis by HPLC-UV, HPLC–ELSD and LC-MS, Headspace-GC/MS-SPME were described in Chapter 2.

3.2.4.1 Partitioning

Clematis spp. solvent extract (5ml) in MeOH was added to a separating funnel with 15 ml MeOH and 40 ml petroleum spirit mixed and allowed to settle for 30 minutes until separation occurred. The top layer was discarded. Then 20 ml H_2O and 20 ml

DCM were added to the remaining liquid in the separating funnel, mixed and allowed to stand for 30 minutes until a good separation occurred. The aqueous partition was collected, evaporated and made up to 100 mg/ml in MeOH to give polar partitions.

3.2.4.2 Extraction and fractionation flow chart to determine the antibacterial constituents in *Clematis* spp.

The extraction and fractionation procedure in this chapter to determine the antibacterial constituents in Tasmanian native *Clematis* spp. against *E. coli* and *P. aeruginosa* (PAO1) are listed in Scheme 3.1 and Scheme 3.2, respectively.

3.2.5 Antimicrobial assay

3.2.5.1 Bacterial strains

Escherichia coli (American Type Culture Collection (ATCC) 8739), *Pseudomonas aeruginosa* (PAO1) (ATCC 27853), clinical isolates of *P. aeruginosa* 124 and u19b (Royal Hobart Hosptial, Hobart, Australia), *Klebsiella pneumoniae* (ATCC 10031), *Acinetobacter baumannii* (ATCC 19606), *Bacillus cereus* (ATCC 1778), *Staphylococcus aureus* (ATCC 6538), *Staph. saprophyticus* (ATCC 49907), *Streptococcus pyogenes* (ATCC 19615), and *Strep. mutans* (ATCC 35668) were used in this study.

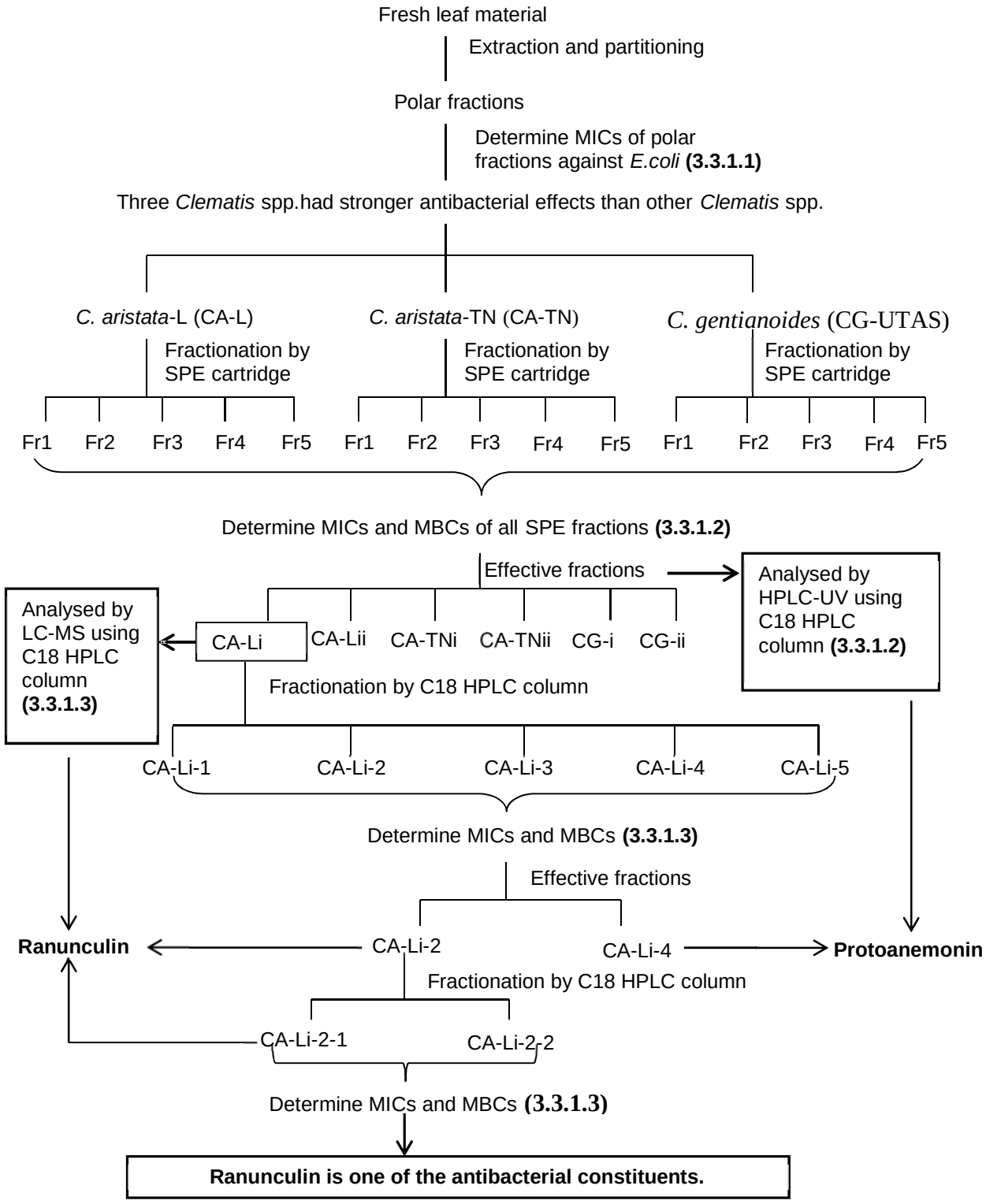

Scheme 3.1 Extraction and fractionation procedure to determine the antibacterial constituents in *Clematis* spp. against *E. coli*.

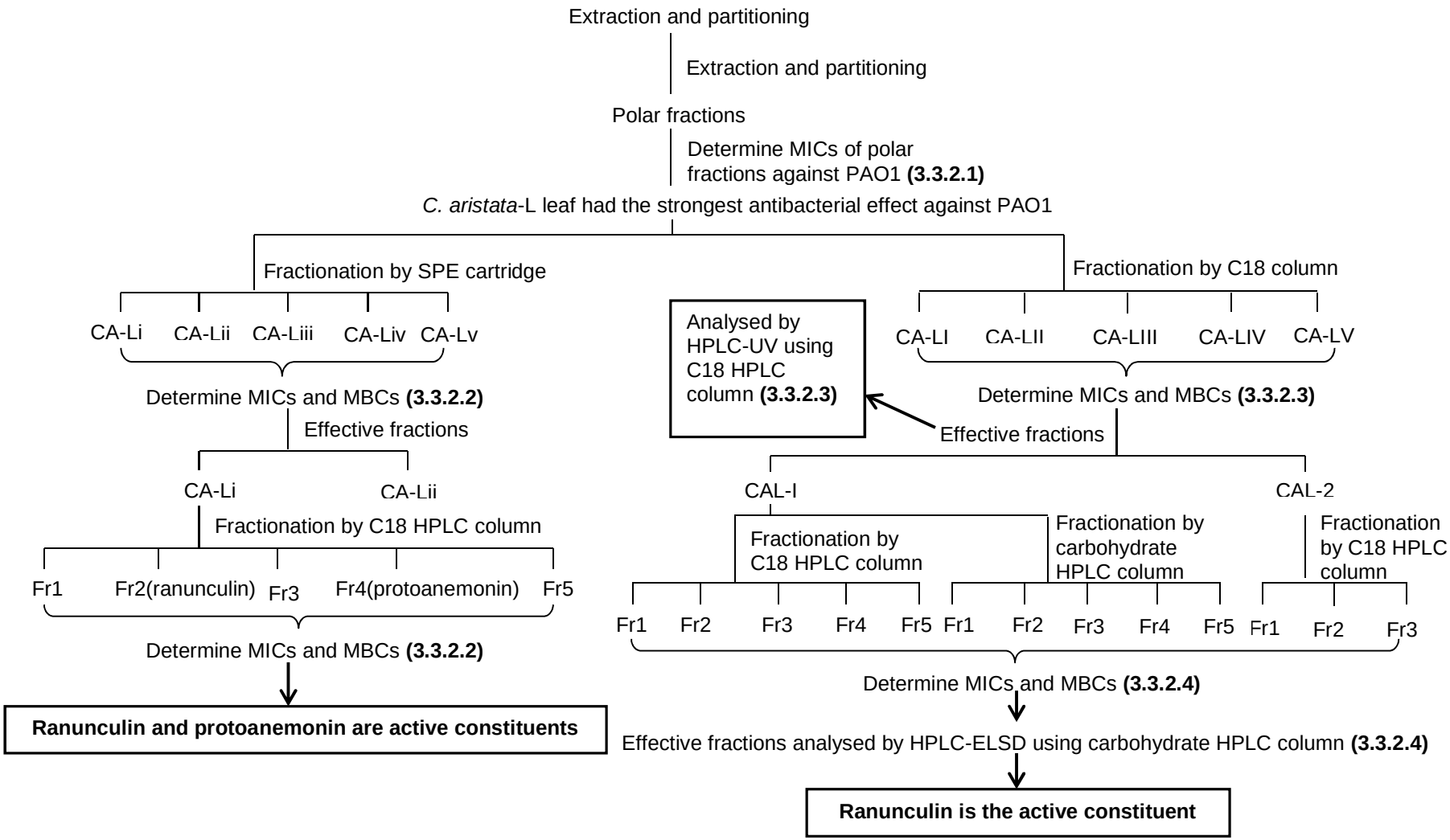

Scheme 3.2 Extraction and fractionation procedure to determine the antibacterial constituents in *Clematis* spp. against *P. aeruginosa* (PAO1).

3.2.5.2 Preparation of bacterial culture

Using aseptic techniques, a single colony was transferred into each of two 10 ml bottles of Muller Hinton broth (MHB), except *Streptococcus* strains which were incubated with Todd Hewit broth (THB). These were capped and placed in an incubator overnight at 37°C (*Streptococcus* strains were placed into a 37°C CO_2 incubator). After 18 hours of incubation, the broth was centrifuged at 4000 rpm for 5 minutes with appropriate aseptic precautions. The supernatant was discarded and the pellet was resuspended using 10 ml normal saline in each tube and centrifuged again at 4000 rpm for 5 minutes. This step was repeated until the supernatant was clear. The pellet was suspended in sterile normal saline and the turbidity adjusted to a 0.5 McFarland standard.

3.2.5.3 Minimum Inhibition Concentration

Minimum inhibition concentration (MIC) determinations followed the method from Satyajit.[184] Microplates (96-well) were prepared under aseptic conditions. A volume of 200 µl of test material in 10% (v/v) DMSO in normal saline (NS) was pipetted into the first column of plates. From the 2nd to the 12th test wells of each microplate row 100 µl of normal saline was added. Serial dilutions were performed by sequential transformation of 100 µl using a multichannel pipette. To each well 25 µl of resazurin indicator solution was added. Then four-fold strength MHB (50 µl) (or THB for *Streptococcus* strains) was added to each well to ensure that the final volume was single strength nutrient broth. Finally, 25 µl of bacterial suspension was added to each well. Plates were covered with lids. Each plate had a set of controls: a row with a

serial dilution of amoxicillin (starting at 256 μg/ml**)** as positive control for *E. coli* and G+ bacteria and gentamicin (starting at 256 μg/ml) as positive control for G- bacteria; a row containing all solutions with the exception of the test extract, containing 10% (v/v) DMSO in normal saline (NS) instead, was prepared as negative control; and a row containing all solutions with the exception of the bacterial solution but with 25 μl of nutrient broth instead was prepared as blank control . The layout of a 96-well microplate is presented in Figure 3.2.

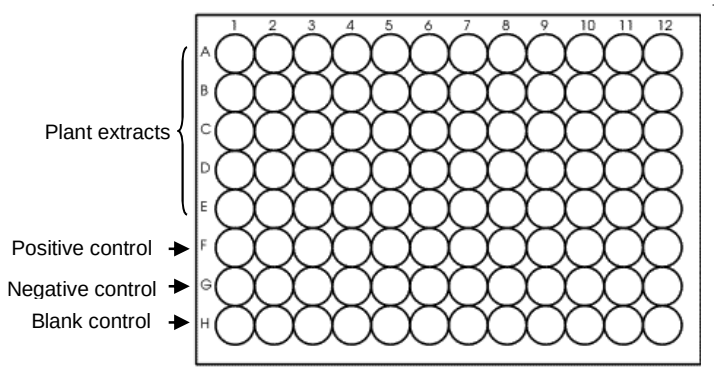

Figure 3.2 Typical layout of a 96-well microplate used in the antibacterial study.

The plates were prepared in duplicate, and placed in an incubator at 37°C for 24 hours. The colour change was then assessed visually. Any colour change from blue to pink or colourless was recorded as negative, meaning cells were still viable. The lowest concentration at which the colour change did not occur was taken as the MIC value, with the average of 2 values calculated. This value was the MIC for the test substance against that particular bacterial strain.

3.2.5.4 Minimum Bactericidal Concentration (MBC)

From the MIC microplates, bacterial culture of last two blue wells and the first pink well was performed by spreading 100 µl from the well across the entire surface of Mueller Hinton agar plate (or Horse Blood Agar plates for *Streptococcus* strains). Colonies grown on each plate were counted after 18 hours of incubation at 37°C. The concentration of extract where no colonies were obtained on the plate was recorded as the MBC.

3.2.5.5 Gram stains

Aliquots of bacterial culture (10 µl), which contained 2x MIC, MIC, ½ MIC and ¼ MIC of ranunculin, were applied to microscope slides. The slides were dried, then bacteria were stained using Gram's staining method. The G+ organisms retain crystal violet and stain blue; G- organisms do not retain crystal violet and stain pink due to the counterstain safranin.[185] The result was observed by microscopy at 1000x magnification.

3.2.5.6 Developing resistance by *P. aeruginosa* to the effects of ranunculin

The method was followed that of Bassaris[186] with slight modification. After MIC determination, the *P. aeruginosa* cultures (PAO1, PAu19b and PA124) treated by 0.25x MIC and 0.5x MIC of ranunculin were obtained. Then raunculin treated *P. aeruginosa* cultures were incubated with 0.25x MIC and 0.5x MIC of ranunculin for 2 weeks in 96-well microplates. Ranunculin (100 µl/well) and 3x MHB (50 µl/well) were freshly added to a row of wells in the microplate each day. Bacterial cultures

(25 µl/well) were transferred from the previous one day culture into a well containing fresh mediun and ranunculin. The MIC and MBC of ranunculin against ranunculin-treated *P. aeruginosa* strains were tested at day 7 (after 7 passages) and day 14 (after 14 passages).

3.2.5.7 Checkerboard study

The checkerboard technique was adapted to 96-well microplates. Serial dilutions in normal saline of antibiotic and ranunculin were made using concentrations proportional to the MICs of two antimicrobials used in the combination: the concentrations tested for each antimicrobial ranged from 8x dilutions below the MIC to 2x MIC using 2 fold dilutions. The concentrations tested for ranunculin ranged from 512x dilutions below the MIC to twice the MIC using 2 fold dilutions.Vertical columns of wells in the microplate contained the same concentraction of ranunculin except column one which contained antibiotic only. Horizontal rows of wells in the microplate contained the same concentration of antibiotic except row one which contained ranunculin only. Bacterial cultures without ranunculin and antibiotic were negative control. Broth alone was blank control. The layout of a 96-well microplate in this study is shown in Figure 3.3

The final volume was 200 µl in each well, 100 µl normal saline containing antimicrobials (50 µl of dilution of the antibiotic plus 50 µl of dilution of ranunculin) except those of the first horizontal row and those of the first vertical column which

contained antibiotics or ranunculin alone in normal saline. A 50 µl aliquot of 4x MHB, 25 µl of resazurin solution and 25 µl of bacterial suspension were added to each well.

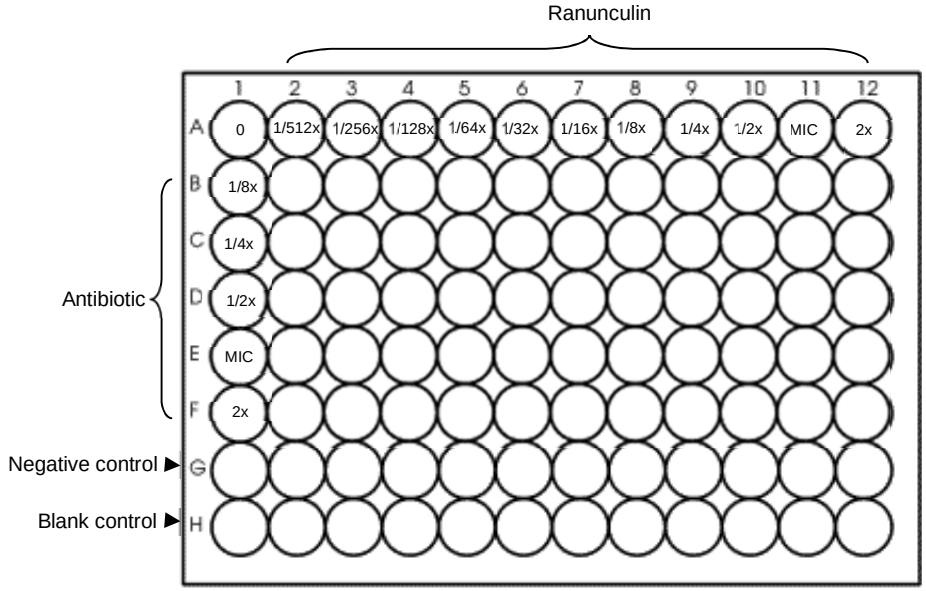

Figure 3.3 Layout of a 96-well microplate in the checkerboard study of ranunculin with antibiotic. Concentration of ranunculin decreased from column 12 to column 2 using 2x dilution. Concentration of antibotic decreased from row F to row B using 2x dilution. Wells covered by blue shadow contained both ranunculin and antibiotic at the indicated concentrations.

The results obtained were determined after incubation at 37°C for 24 hours. The FIC (Fractional Inhibitory Concentration) index used to report the results of studies of antimicrobial combinations was calculated according to the following formula:

FIC Index = $A/MIC_A + B/MIC_B = FIC_A + FIC_B$

Where A is the concentration of antibiotic in a well which is the lowest inhibitory concentration in its row; MIC_A is the MIC of the microorganism to the antibiotic alone; B is the concentration of ranunculin in a well which is the lowest inhibitory concentration in its row and MIC_B is the MIC of the microorganism of ranunculin alone. Total synergism (FIC<0.5), partial synergism (0.5<FIC<0.75), no effect

(0.75<FIC<2) or antagonism (FIC>2) between antibiotic and active fraction was assumed from the values of the FIC index.[187]

3.2.5.8 Scanning electron microscopy

Scanning electron microscopy (SEM) was applied to determine the morphologial changes in *P. aeruginosa* treated by ranunculin. The method followed a published method by Prior.[188] The methods of bacterial culture preparation and amount of active fraction added were developed from previous MIC and MBC studies. In this method, sterile Eppendorf tubes were used instead of 96-well plates in order to yield more bacterial cells to prepare specimens for SEM. Ranunculin (250 µl) with concentrations of 1.5x MIC, MIC, 0.5x MIC and 0.25x MIC was incubated with 187.5 µl of 2.6x strength MHB and 62.5 µl of bacterial suspension for 24 hours at 37°C.

After incubation, treated bacterial culture was centrifuged at 800x g for 10 minutes and the pellets were immediately resuspended in 2% glutaraldehyde with 0.05 M phosphate buffer and 4% sucrose, pH 7.3. These bacterial cultures were kept at 4°C overnight for fixation. The specimens were centrifuged at 800x g for 10 minutes, followed by washing four times in distilled water. They were placed on aluminium stubs, air-dried, sputter-coated, and examined with a scanning electron microscope.

3.2.5.9 Disruption of the outer membrane of *P. aeruginosa*

The assay followed the method described by Vaara.[189] Bacterial cultures in Eppendorf tubes were prepared in the same way as described in 3.2.5.9.

After incubation for 0.5, 1, 3, 6 and 24 hours, 100 µl of each cell culture was transferred to Eppendorf tubes, respectively. Then cells were pelleted (7000x g, 15 minutes) at room temperature and resuspended in 100 µl of 0.5% sodium deoxycholate in saline. Each cell suspension was transferred to a 96-well microplate, then incubated at 37°C for 10 minutes. Cell lysis was measured as a decrease in optical density at 450 nm (OD_{450}) by a microplate reader. Results were expressed as the percentage of OD_{450} of controls (cells not exposed to ranunculin).

3.2.5.10 Headspace-GCMS-SPME

Ranunculin (250 µl) at its MIC was incubated with 187.5 µl of 2.6x strength MHB and 62.5 µl of bacterial suspension in 30 ml sterile vials for 24 hours at 37°C. Broth with and without ranunculin were controls in this experiment. A blank SPME fibre run was performed before exposure to the sample to eliminate carryover from previous exposures. After incubation for 0.5, 1, 3 and 6 hours, the fibre was exposed to each sample for 10 minutes. Samples were stirred during the adsorption. After absorption, the fibre was introduced into a GC/MS for thermal desorption (3 minutes) and analysis.

3.2.5.11 Study of resistant mechanism of *P. aeruginosa*

The study of mechanisms of multi-drug resistance in *P. aeruginosa* strains was performed in collaboration with the School of Medicine, UTAS and the School of Pharmacy, Aichi Gakuin University, Japan. Experiments to determine MexXY multidrug efflux system activity in the multi-drug resistant *P. aeruginosa* strains (PA124 and PAu19b) were undertaken in Japan. The MexXY deficient mutant was produced from PA124 using plasmid pTEM424 for deletion of *mex*XY, and the determination of MICs of amikacin, gentamicin and tobramycin against PA124 and MexXY deficient PA124 were undertaken in Muller-Hinton broth by the twofold dilution method. [(190)] The DNA sequence of MexZ was studied in PA124 and PAu19b.[(191)]

3.3 Results and Discussion

3.3.1 Antibacterial activity of *Clematis* spp. against *E. coli*.

3.3.1.1 Antibacterial effects of polar fractions of *Clematis* crude extracts

Preliminary study performed in this laboratory showed that *Clematis* spp. polar fractions of solvent partitioning had inhibitory action against *E. coli*.[52] In this study the MIC values for the polar fractions of crude extracts of investigated *Clematis* plants were investigated and results are shown in Table 3.2.

Table 3.2 Antibacterial activities of polar fractions of *Clematis* spp. leaf crude extracts against *E. coli*. (n=2)

	18hours	24hours	40hours
Samples	MIC (mg/ml)	MIC (mg/ml)	MIC (mg/ml)
CA -TN	0.39	0.39	0.39
CA -L-1	1.56	1.56	1.56
CA -L-2	0.39	0.39	0.39
CA -L-3	0.78	0.78	0.78
CA -L-4	0.78	0.78	0.78
CA-L-5	0.78	0.78	0.78
CM-TN	1.56	1.56	1.56
CG-UTAS	0.39	0.39	0.39
CA-TN 1	x[a]	x	x
CV-RS	x	x	x
CA -WF	3.13	3.13	x
CA-EN	1.56	1.56	1.56
Amoxicillin	0.016	0.016	0.016
10% DMSO	x	x	x

[a]X means that extract does not have antibacterial activity.

Data in Table 3.2 revealed that the MIC values of polar fractions of *Clematis* spp. crude extracts were found to be in the range of 0.39-3.13 mg/ml. MICs at different incubation times (18 hours, 24 hours and 40 hours) were evaluated in this study. The purpose of this evaluation was to determine the stability of antibacterial effects of

these fractions. The MIC of amoxicillin, which was the positive control, was 0.016 mg/ml. The negative control (10% DMSO/NS) did not show any antibacterial activity.

From this experiment, variation of antibacterial effects in different species and cultivars were indicated. The most effective fractions were CA-TN, CA-L-2 and CG-UTAS. Their MICs were all 0.39 mg/ml. However, compared with amoxicillin (0.016 mg/ml), MICs of the polar partitions of these three *Clematis* spp. were about 24x higher. MICs of investigated *Clematis* polar fractions against *E. coli* were sequenced from strongest to weakest: CGUTAS, CA-TN, CA-L-2 > CA-L-3, 4, 5 > CA-L-1, CM-TN, CA-EN > CA-WF. CA-TN1. CV-RS had no effects against *E. coli* at tested concentrations. These activities were stable in various incubation times except CA-WF whose antibacterial effect was lost at 40 hours incubation.

The antibacterial activities of 5 different ages of CA-L leaf were studied. From the youngest to the oldest they were marked as 1, 2, 3, 4 and 5, respectively. The results showed that the antibacterial activities from 3 to 5 were the same. Their MICs were all 0.78 mg/ml. The antibacterial activity of 2 was 0.39 mg/ml, however, the youngest leaf (CA-L-1) showed the lowest cytotoxic activity against *E. coli* in the five different ages of leaf (1.56 mg/ml). The difference between antibacterial activities of leaf 5, 4, 3 and leaf 2 was only 2-fold dilution, and the difference between antibacterial activities of leaf 2 and leaf 1 was 2-fold dilution. Following the determination of MIC end points in the approved standard of "Methods for dilution Antimicrobial Susceptibility Tests for Bacteria That Grow Aerobically" released by the Clinical and

Laboratory Standards Institute in 2009,[(192)] this result revealed that only 4 and 5 had different antibacterial activities against *E. coli*.

These results also suggested that the amount of antibacterial constituents may differ with different ages of leaf. The level of effective constituents was the same in 5, 4 and 3. But the level of active constituents in 2 was greater than that in 1. Another hypothesis is that CA-L-2 contained antibacterial compounds that were absent in the other ages of leaf.

Based on the above results, CA-L-1 to 5 were analysed by HPLC with UV detection. The chromatograms at 254 nm are shown in Figure 3.4. The concentration and volume of injection was the same for each sample.

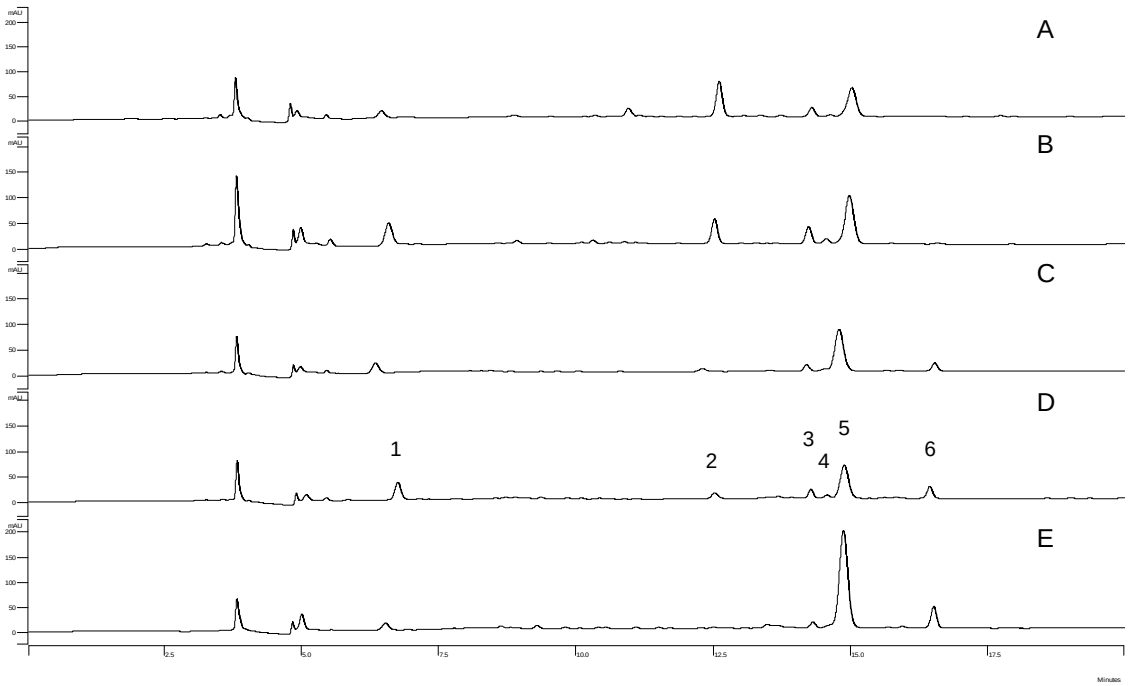

Figure 3.4 HPLC chromatograms of *C. aristata*-L of different age leave determined at 254 nm. A is CA-L-1 (the youngest leaf); B is CA-L-2; C is CA-L-3; D is CA-L-4; and E is CA-L-5 (the oldest leaf).

The chromatograms obtained from polar fractions of five ages of CA-L leaf showed that peaks were adequately separated and that there was some age-related variation. The chromatograms in Figure 3.4 only showed the first 20 minutes of HPLC trace, as all of the peaks eluted before 20 minutes. The main chromatographic peaks were named as 1-6, as labelled in the Figure 3.4 D. The early peaks (retention time between 3.5 and 6.0 minutes) were solvent peaks, so they were not employed in this analysis. The individual total relative area (%) of these 6 peaks in each chromatogram is summarized in Figure 3.5.

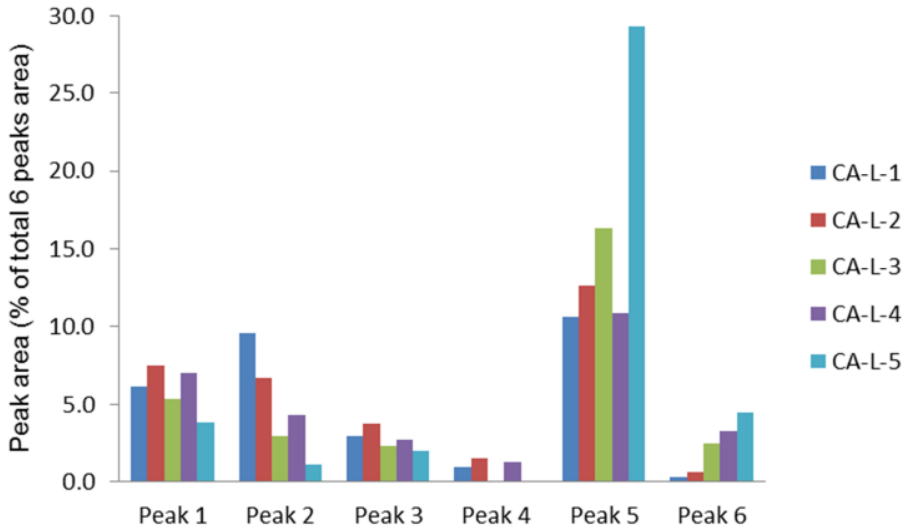

Figure 3.5 The individual areas of six different chromatographic peaks in 5 CA-L leaves of different age. CA-L-1 to CA-L-5 is from young to old.

Results in Figure 3.5 suggested that the ratio of leaf constituents content varied in five ages of *C. aristata*-L leaf. The content of constituents contained in chromatographic peaks 1 and 3 was similar in the five ages of leaves. Constituent contained in peak 4 was not obtained in CA-L-3 and 5. Content of compound in peak 5 obtained in the youngest leaf was twice that detected in the other four ages of

leaves. But this compound would not be the constituent leading to the varied antibacterial activities in different ages of leaf as the antibacterial effects of CA-L-5 was similar to the other four ages of leaves. At the same time an interesting phenomenon obtained in Figure 3.5 was that the yield of peak 3 decreased following increasing leaf age; but yield of peak 6 increased following increasing leaf age. The results of identification these two compounds will be described in Chapter 5. Result in this analysis did not reveal the chemical constituents variation leading to the different antibacterial activitiy against *E. coli* between CA-L-1 (MIC=1.56 mg/ml) and CA-L-2 (MIC=0.39 mg/ml).

3.3.1.2 Antibacterial effects of SPE cartridge fractions

Based on antibacterial results of *Clemtis* spp. polar fractions against *E. coli*, the three most potent *Clematis* spp., CA-TN, CG-UTAS and CA-L were fractionated by SPE cartridge. The antibacterial activities of each fraction and polar partitions of the three *Clematis* spp. are listed in Table 3.3.

Table 3.3 MICs and MBCs of CA-TN, CG-UTAS and CA-L SPE cartridge fractions against *E. coli*. And the MICs of these three *Clematis* spp.polar partitions against *E.coli*. (n=2)

Fraction	CA-TN		CG-UTAS		CA-L	
	MIC (mg/ml)	MBC (mg/ml)	MIC (mg/ml)	MBC (mg/ml)	MIC (mg/ml)	MBC (mg/ml)
PF[a]	0.4		0.4		0.8	
Fr 1	0.9	0.9	0.8	1.6	0.6	1.2
Fr 2	0.9	0.9	1	2	0.8	1.6
Fr 3	x[b]	x	x	x	x	x
Fr 4	x	x	x	x	x	x
Fr 5	x	x	x	x	x	x
amxoycilin	0.03	0.03	0.03	0.03	0.03	0.03
10% DMSO	x	x	x	x	x	x

[a]PF means polar fraction. [b]X means that fraction did not have antibacterial activity at the tested concentration.

Results in this study demonstrated that SPE fraction 1 and fraction 2 of each *Clematis* spp. polar fraction (by partitioning) had antibacterial activity. In this experiment the minimum bactericidal concentrations (MBCs) were determined at the same time. The MICs and MBCs of CA-TN SPE fraction 1 and fraction 2 (CA-TNi and CA-TNii) were both 0.9 mg/ml. The MICs of *C. gentianoides* SPE fractions 1 and 2 (CG-UTASi and CG-UTASii) were 0.8 mg/ml and 1.0 mg/ml, respectively and the MBCs of both fractions were respectively 1.6 mg/ml and 2.0 mg/ml. The MICs of *C. aristata*-L SPE fraction 1 and fraction 2 (CA-Li and CA-Lii) were 0.6 and 0.8 mg/ml, respectively, and their MBCs were 1.2 and 1.6 mg/ml, respectively. When comparing MICs of SPE fractions with the polar fraction of each *Clematis* spp. in Table 3.3, it was revealed that the antibacterial activities of active SPE fractions were similar to the polar fractions.

The chemical constituents of the polar partition and SPE fractions 1 and 2 of CA-L, CA-TN and CG-UTAS were determined by HPLC-UV. The HPLC-UV chromatograms at 254 nm are presented in Figures 3.6, 3.7 and 3.8, respectively.

Chromatograms in Figure 3.6-3.8 revealed that there were fewer constituents obtained in SPE cartridge fraction 1 than in SPE fraction 2 and the polar fraction using 254 nm UV detection. The data in Table 3.3 suggested that there were no differences in antibacterial effects in the polar fraction, SPE fractions 1 and 2 in each individual plant. These results suggest that the antibacterial active constituents in polar fraction, SPE fractions 1 and 2 might be similar. As the SPE fraction 1

contained the lesser number of chemical constituents, *C. aristata*-L leaf SPE fraction 1 was used to undertake further study to isolate the effective antibacterial constituents.

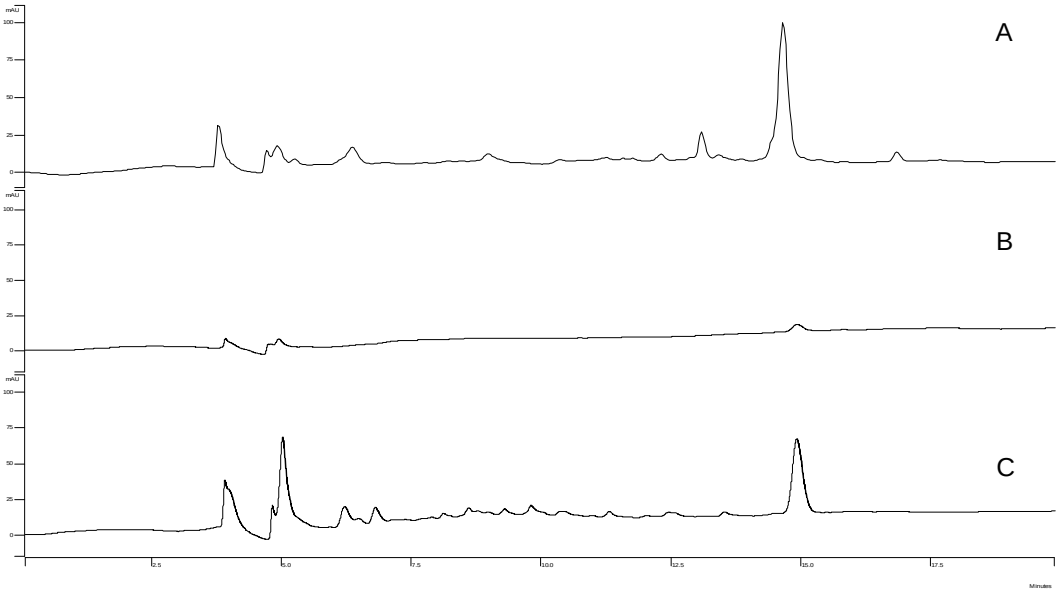

Figure 3.6 HPLC chromatograms of polar partition (A), SPE fraction 1 (B) and SPE fraction 2 (C) of *C. aristata*-TN at 254 nm.

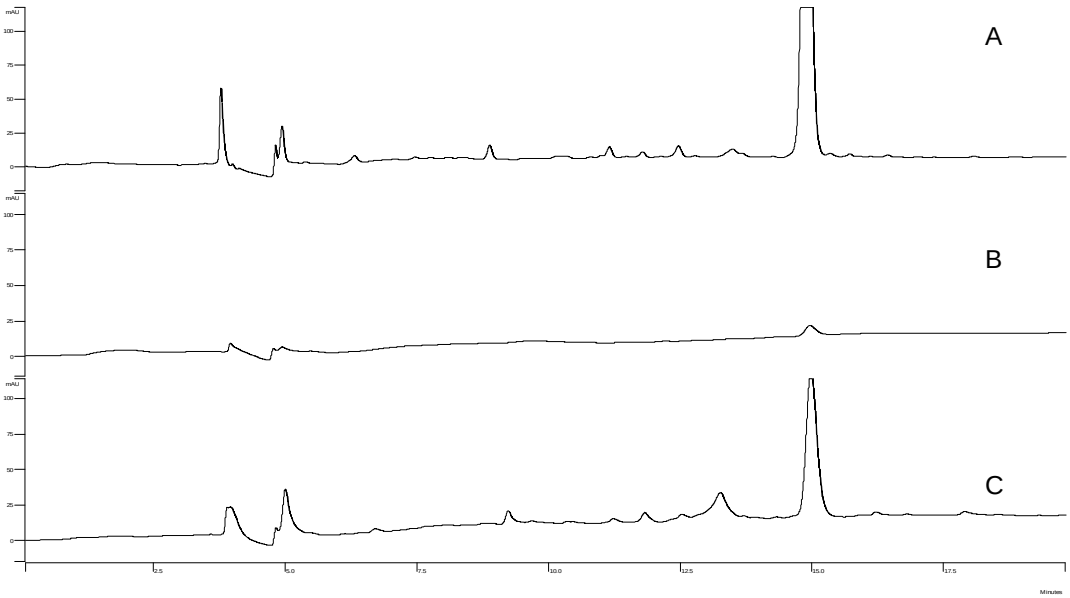

Figure 3.7 HPLC chromatograms of polar partition (A), SPE fraction 1 (B) and SPE fraction 2 (C) of *C. gentianoides* at 254 nm.

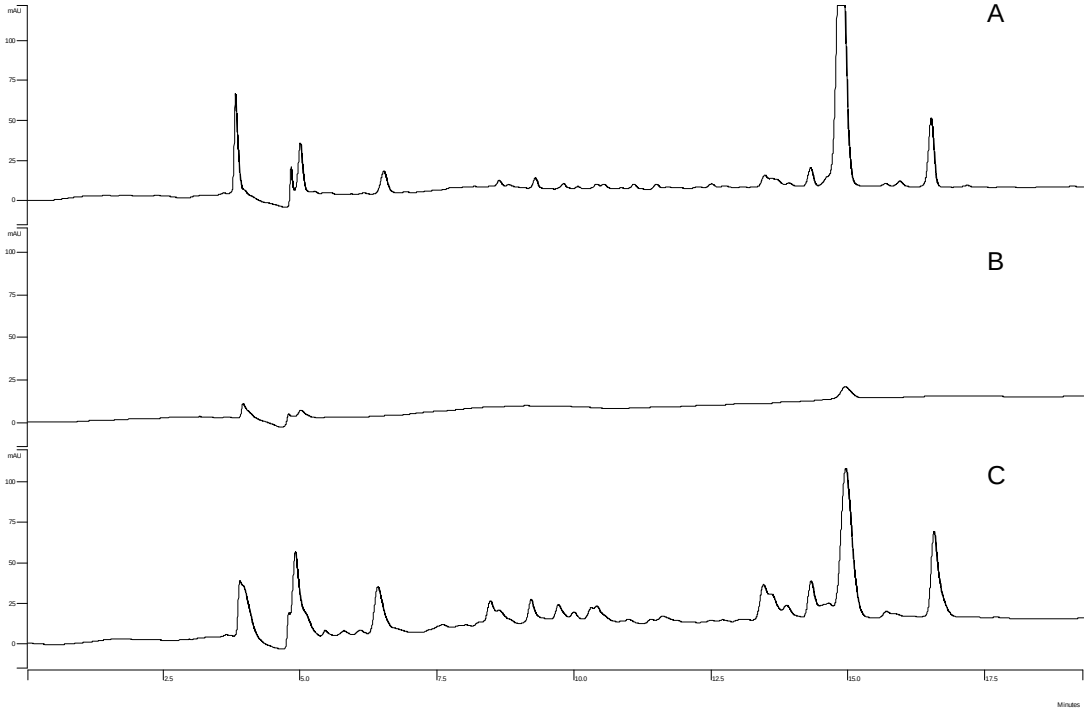

Figure 3.8 HPLC chromatograms of polar partition (A), SPE fraction 1 (B) and SPE fraction 2 (C) of *C. aristata*-L at 254 nm.

3.3.1.3 Antibacterial effects of bioassay-directed liquid chromatography fractions

Previous experiments conducted in this study showed that *C. aristata*-L SPE fraction 1 (CaL-i), which had the least number of compounds, had the same antibacterial activity against *E. coli* as the polar fraction and SPE fraction 2. Further fractionation was performed by gradient elution HPLC on a reverse-phase C18 column which generated 5 fractions in the first 20 minutes (i.e. 4 minutes per fraction). All of the 5 fractions were assayed for antibacterial effects against *E. coli* by evaluating their MICs and MBCs. Results are shown in Table 3.4.

Table 3.4 The antibacterial activity (MIC and MBC) of C18 HPLC column fractions of CA-Li (n=2)

Sample	MIC (mglmL)	MBC (mglmL)
CA-Li-1 (0-4min)	x	x
CA-Li-2 (4-8min)	0.3	0.3
CA-Li-3 (8-12min)	x	x
CA-Li-4 (12-16min)	1.8	x
CA-Li-5 (16-20min)	x	x
CA-Li	0.62	1.24
Amoxicillin	0.015	0.03
10% DMSO	x	x

Table 3.4 revealed that C18 HPLC fractions 2 (CA-Li-2) and 4 (CA-Li-4) had antibacterial activity against *E. coli*. The MIC and MBC of CA-Li-2 were both 0.3 mg/ml. The MIC of CA-Li-4 was 1.8 mg/ml, but this fraction did not show bactericidal activity. Comparison of the antibacterial effects of active CA-Li HPLC fractions with CA-Li demonstrated that CA-Li-2 had the similar antibacterial activity to CA-Li, but the bactericidal effect of CA-Li-4 was weaker than CA-Li. This result suggested that the constituents in CA-Li-2 were responsible for most of the antibacterial activity of CA-L.

To identify potential antibacterial constituents in CA-L, LC-MS analysis was performed on CA-Li. The mass spectrum of the main peak detected in CA-Li was at *m/z* 276 (Figure 3.9). As ammonium was employed in the LC-MS analysis, the possibility of forming $[M+NH_4]^+$ was enhanced. The mass spectrum at *m/z* 277, 294, 553 and 570 corresponded to $[M + H]^+$, $[M + NH_4]^+$, $[2M + H]^+$ and $[2M + NH_4]^+$ (Figure 3.9B). According to MS^2 of *m/z* at 293 in positive mode presented in Figure 3.9C, *m/z* at 277 and 97 confirmed that M was ranunculin as *m/z* 97 consistent with protoanemonin. Therefore, ranunculin was the antibacterial constituent in CA-Li-2,

but the ranunculin isomer detected in tge P388 cytotoxicity studies was not obtained in this experiment.

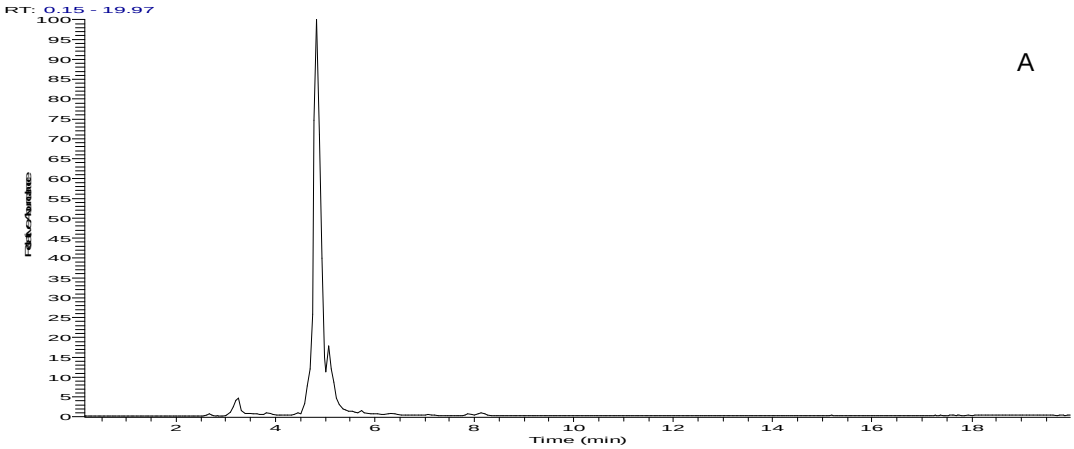

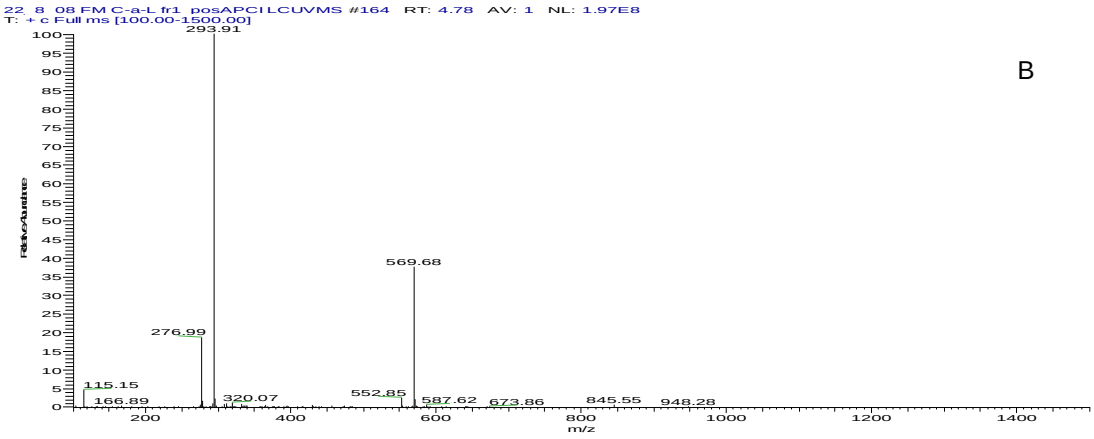

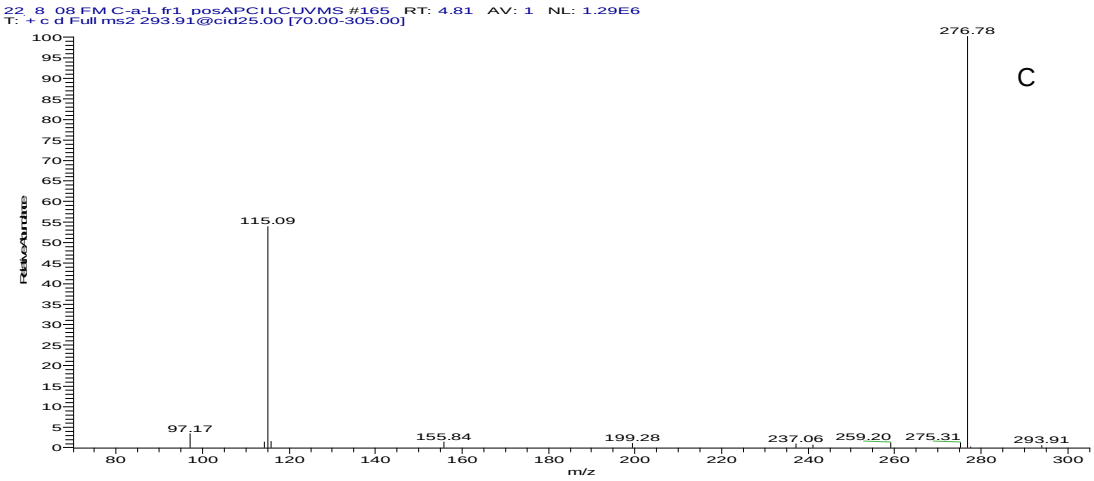

Figure 3.9 LC-MS chromatogram of CA-Li (A) and the MS (B) and MS/MS (C) spectrum of *m/z* 276.

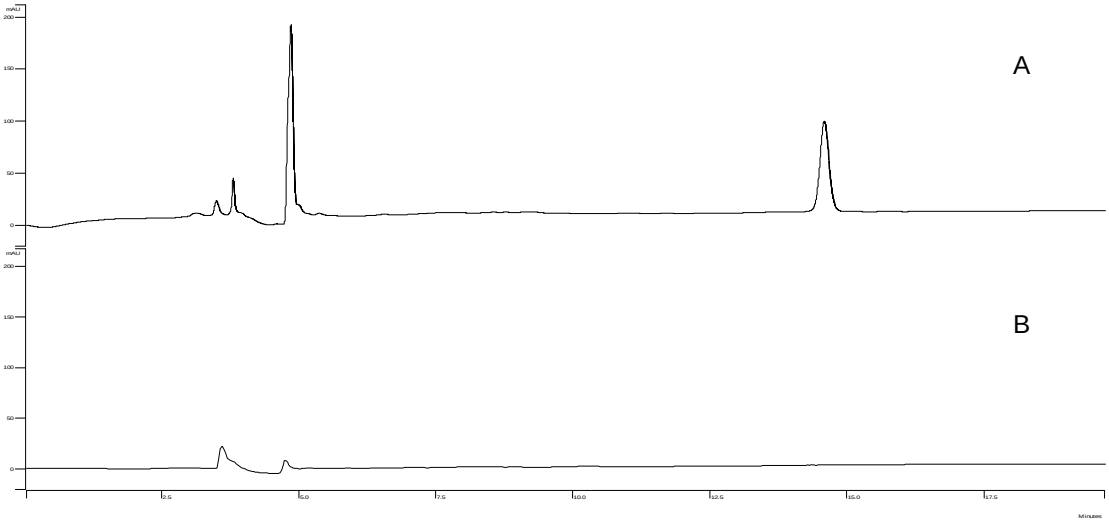

Figure 3.10 HPLC-UV chromatograms of CaL-i (A) and MeOH (B) at 254 nm.

The retention time of ranunculin obtained in the positive mode of LC-MS analysis was 4.78 min (Figure 3.9A). There was no peak obtained at 4.78 min in the HPLC chromatogram of CA-Li, but an obvious peak was observed at 4.95 minutes (Figure 3.10A). This peak would be ranunculin peak mixed with solvent peak as it was also obtained in the chromatogram of the negative control (MeOH) (Figure 3.10B).

The only peak obtained in CA-Li-4 had a retention time of 14.9 minutes. Its UV spectrum was consistent with protoanemonin (λ_{max}= 260 nm).[193] Therefore, protoanemonin was deemed to be the active constituent in CA-Li-4 and it was the other antibacterial constituent in *C. aristata*-L SPE fraction 1 against *E. coli*, but with a weaker effect than ranunculin.

Protoanemonin has been reported to have antibiotic effects against a broad range of bacteria[187] and fungi[194]. The reported MICs of protoanemonin against microbes are

presented in Tables 3.5 and 3.6. These data showed that the antimicrobial effects of protoanemonin were varied with different bacterial and fungi. The MIC values obtained with fungi ranged from 0.0192 mg/ml to 0.072 mg/ml. The MIC values obtained with bacteria ranged from 0.008 mg/ml to 0.125 mg/ml. The highest antibacterial activity was observed with a strain of *Serratia marcescens*. The lowest antibacterial effects were obtained with *Eubacterium lentum* and *Fusobacterium nucleatum*.

Table 3.5 MICs and MBCs of protoanemonin obtained with fungi adapt from Mares *et al*[194]

Test organism	MIC (mg/ml)	MBC (mg/ml)
Saccharomyces cerevisiae	0.0624	0.0960
Schizosaccharomyces pombe	0.0288	0.0528
Rhodotorula glutinis	0.0192	0.0365
Candida albicans	0.0269	0.0480
Trichophyton mentagrophytes	0.0720	0.0960
Trichophyton rubrum	0.0576	0.0096
Epidermophyton floccosum	0.0240	0.0480
Microsporum cookei	0.0288	0.0528

Protoanemonin was reported to be the antifungal constituent in *Ranunculus sceleratus*[195] and *Clematis apiifolia* DC.[125] Protoanemonin, an unsaturated lactone, contains the structure shown in Figure 3.11 A. Mares[194] proposed that the mechanism of action of the substances containing a system shown in Figure 3.11 B (especially sesquiterpene lactones) or a system shown in Figure 3.11 A (especially coumarin and protoanemonin) was based on the capacity of these substances to

interact with –SH groups by a Micheal-type addition. The biological effects of –SH with protoanemonin was discussed in Chapter 2. The MIC of protoanemonin against

Table 3.6 MICs of protoanemonin obtained against bacteria, adapted from Didry *et al*.[187]

Strains	MIC (µg/ml)
Staphylococcus aureus ATCC 25923	31.25
Staphylococcus aureus MSSA1[a]	31.25
Staphylococcus aureus MSSA2[a]	31.25
Staphylococcus aureus MSSA1[b]	62.5
Staphylococcus aureus MSSA2[b]	31.25
Staphylococcus epidermidis	31.25
Streptococcus faecalis	62.5
Streptococcus mutans ATCC 25175	31.25
Streptococcus mitis	62.5
Streptococcus sanguis	62.5
Acinetobacter calcocaceticus	62.5
Citrobacter freundii	15.625
Enterobacter cloacae	31.25
Escherichia coli ATCC 25922	62.5
Klebsiella pneumoniae	31.25
Proteus hauseri	62.5
Providencis stuartii	15.625
Pseudomonas aeruginosa ATCC 27853	62.5
Pseudomonas aeruginosa 1	62.5
Pseudomonas aeruginosa 2	31.25
Pseudomonas aeruginosa 3	15.625
Pseudomonas aeruginosa 4	31.25
Pseudomonas aeruginosa 5	15.625
Serratia marcescens IPP 6093	15.625
Serratia marcescens 1	15.625
Serratia marcescens 2	8
Peptostreptococcus anaerobius ATCC 14956	62.5
Peptostreptococcus anaerobius 1	31.25
Peptostreptococcus anaerobius 2	31.25
Streptococcus intermedius	31.25
Clostridium perfringens ATCC 129247	62.5
Bifidobacterium bifidum	15.625
Bifidobacterium longum ATCC 15707	15.625
Propionibacterium intermedium ATCC 14072	31.25
Propionibacterium acnes ATCC 6920	31.25
Eubacterium limosum ATCC 8486	31.25
Eubacterium lentum	125
Veillonella parvula	31.25
Bacteroides oralis	15.625
Bacteroides fragilis ATCC 25285	125
Bacteroides thetaiotaomicron ATCC 29741	62.5
Bacteroides fragilis	62.5
Bacteroides vulgatus ATCC 8482	62.5
Fusobacterium nucleatum	125

[a] Human pathogenic strains susceptible to methicillin

[b] Human pathogenic strains resistant to methicillin

E. coli in this study was 1.8 mg/ml that was much higher than its reported MIC (0.0625 mg/ml). The decreased antibacterial effect of protoanemonin in our study might be caused by the fractionation procedure. Protoanemonin is volatile, so it may evaporate during fractionation and rotary evaporation.

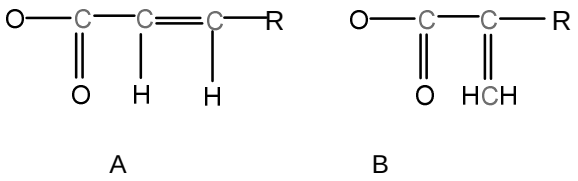

Figure 3.11 The antibacterial structures of unsaturated lactones.

Results in this study exerted that the CaL-i-2 had the greatest antibacterial activity against *E. coli*, and the active constituent was ranunculin. In order to confirm this result, the active chromatographic peak with retention time 4.95 minutes in HPLC analysis was separated by HPLC by fraction collection. CaL-i-2 was fractionated into 2 fractions using the same column and same gradient elution. The first sub-fraction (CaL-i-2-1) was ranunculin (4-6 minutes HPLC fraction) and the second sub-fraction (CaL-i-2-2) started from the end of ranunculin and finished at 8 minutes (6-8 minutes HPLC fraction). The antibacterial activities of these fractions against *E. coli* are shown in Figure 3.12. The CaL-i-2-1 (ranunculin fraction) showed antibacterial activity against *E. coli*. Its MIC and MBC were both 0.52 mg/ml. Compared with the MIC of CaL-i-2 (0.3 mg/ml), their antibacterial activity were similar.

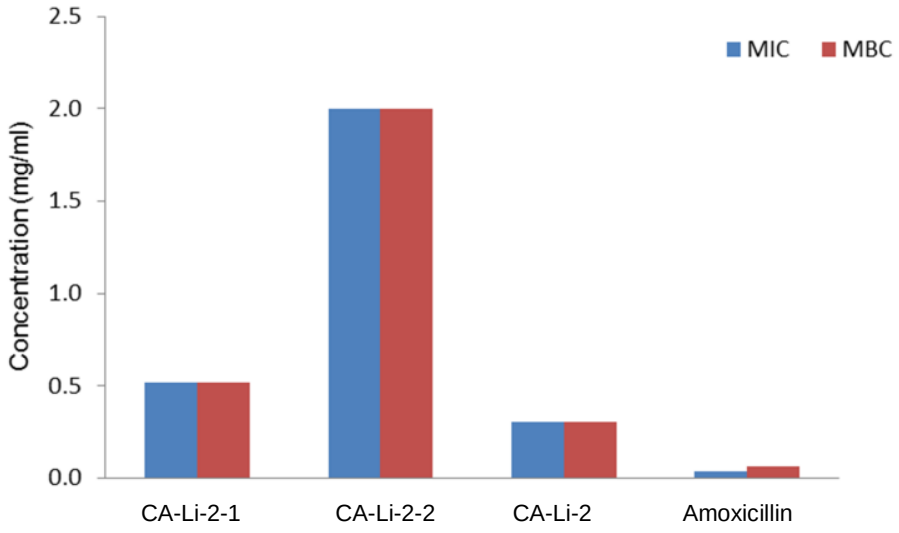

Figure 3.12 Antibacterial activity of C18 HPLC fraction 2 of *C. aristata*-L and its sub-fractions against *E. coli*.

Results in the antibacterial screening of *Clematis* spp. against *E. coli* and the determination of the potential active constituents revealed that the antibacterial activities of different *Clematis* spp. and cultivars against *E. coli* were different and ranunculin and protoanemonin were active constituents. Based on these results, another G- bacterium *Pseudomonas aeruginosa* was employed to assess the antibacterial effects of Tasmanian *Clematis* spp.

3.3.2 Antibacterial activity of *Clematis* spp. against *Pseudomonas aeruginosa*

3.3.2.1 Screening of antibacterial activity of *Clematis* spp.

Previous results exhibited that *Clematis* spp. had antibacterial activities against *E. coli* and ranunculin and protoanemonin contributed to this effect. In this part of the study, another G- bacterium, *P. aeruginosa*, was employed to study the antibacterial activities of *Clematis* spp. *P. aeruginosa* is a common bacterium that can cause

disease in humans. It is found in soil, water, skin flora, and most man-made environments throughout the world, and it is one of the leading nosocomial pathogens, responsible for 10-15% of nosocomial infections worldwide. In humans, this pathogen can cause life-threatening infections in individuals who are compromised because of immune deficiencies, and those suffering from burn wounds, cancer and cystic fibrosis.[196-198] At this stage of the study, a commonly used laboratory strain of *P. aeruginosa*, PAO1, was used for screening antibacterial effects of *Clematis* spp. by determination of MIC. At the same time, the evaluation of the relationship between leaf ages and antibacterial activity was investigated by determining the MIC of age 1, 2, 3, 4 and 5 *C. aristata*-L leaves. The results are summarised in Table 3.7. Amoxicillin was the positive control. Ten percent DMSO in normal saline, which was used to dissolve plant extracts, was the negative control.

Table 3.7 Antibacterial activities of *Clematis* spp. polar fractions against PAO1

Name	MIC(mg/ml)	MBC(mg/ml)
CA-L-1(Y)	0.31	0.62
CA-L-2	0.31	0.62
CA-L-3	0.31	0.62
CA-L-4	0.31	0.62
CA-L-5 (O)	0.31	0.62
CA-WF	1.6	3.2
CA-TN	0.8	1.6
CA-TN 1	6.25	12.5
CA-EN	0.8	1.6
CM-TN	1.6	3.2
CG-UTAS	0.8	1.6
CV-RS	x	x
Negative control	x	x
Amoxicillin	0.063	x

Results in this experiment showed that the antimicrobial effects of various species are different. CA-L polar fraction had the strongest activity against PAO1 whose MIC

was 0.31 mg/ml and MBC was 0.62 mg/ml. The antibacterial activities of *Clematis* spp. against PAO1 from high to low can be sequenced as follows: CA-L > CA-TN, C A-EN, CG-UTAS > CM-TN, CA-WF > CA-TN1. CV-RS did not show any antibacterial activity against PAO1. MIC of amoxicillin against PAO1 was 0.063 mg/ml and its MBC was not observed in this study. There was no antibacterial effect from the negative control. This variation was deemed to be due to the environmental condition, species difference or form variation within a species. For example, the leaf of CA-L was wider than CA-TN1, which is demonstrated in Figure 3.13.

Figure 3.13 Plant of CA-L (left) and CA-TN1 (right).

Comparing the MIC of *Clematis* spp. crude extracts against PAO1 with *E. coli* (Figure 3.14), *C. aristata*-TN, *C. aristata*-WF, *C. aristata*-EN and *C. gentianoides*-UTAS showed a 2x diluted concentration difference between PAO1 and *E. coli*. *C. microphylla*-TN had the same MIC against *E. coli* and PAO1 and *C. vitalba* did not have antibacterial effects against *E. coli* and PAO1. This result suggested antibacterial effects of these 6 *Clematis* spp. against *E. coli* and PAO1 were similar. For the 5 different leaf ages of *C. aristata*-L, the MIC of age 2-5 leaves against PAO1

was only 2x or less than 2x diluted concentration lower than that against *E. coli*; the MIC of youngest leaf against PAO1 was 4x diluted concentration lower than that against *E. coli*. This result suggested that the different antibacterial activities of 5 different ages of *C. aristata*-L leaves against *E. coli* and PAO1 was obtained in the youngest leaf. *C. aristata*-TN1 did not have antibacterial activity against *E. coli*, but its MIC against PAO1 was 6.25 mg/ml. These results suggested that the antibacterial activity of *Clematis* spp. against *E. coil* and *P. aeruginosa* were similar, except *C. aristata*-TN1 and the youngest leaf of *C. aristata*-L.

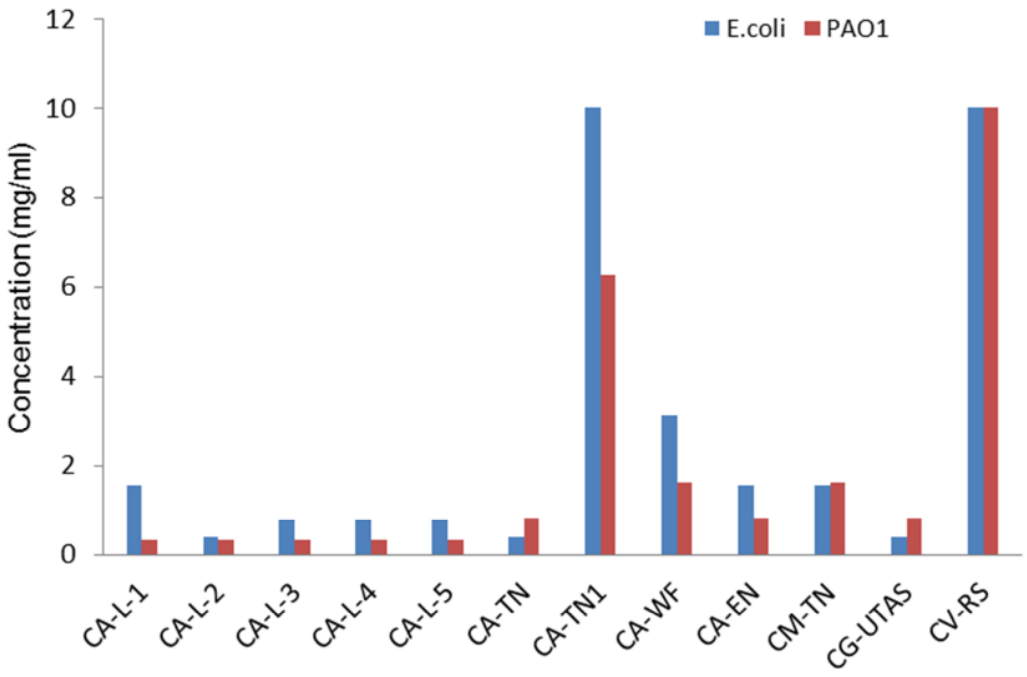

Figure 3.14 Comparsion of MICs (mg/ml) of *Clematis* spp. crude extracts against *E. coli* (blue) and PAO1 (red).

3.3.2.2 Antibacterial activities of *C. aristata*-L by SPE cartridge and C18 HPLC column fractions

Based on the screening results in 3.3.2.1, *C. aristata*-L polar partition had the strongest antibacterial activity against PAO1. In this part of the study the bioactive-guided fractionation of *C. aristata*-L polar partition by SPE cartridge and HPLC column was employed to determine the antibacterial constituents against PAO1. The procedure of fractionation was similar to the bioactive-fractionation procedure of *Clematis* polar fraction to *E. coli*, and the results are shown in Figure 3.15.

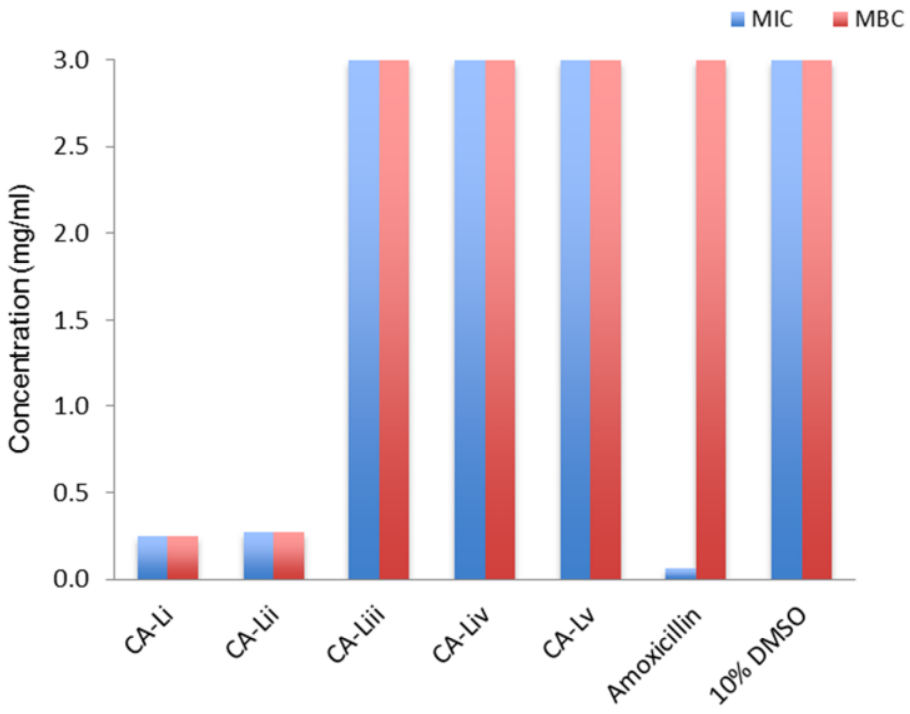

Figure 3.15 Antibacterial activities of five SPE cartridge fractions of *C. aristata*-L polar partition (CaL-i, CaL-ii, CaL-iii, CaL-iv and CaL-v) against PAO1. Blue represented the MIC and red reprented the MBC. All values of 3 mg/ml mean that there were no antibacterial activities detected at that concentration.

MICs of CA-Li and CA-Lii were 0.25 and 0.28 mg/ml, respectively. Their values of MBCs were the same as MICs. The remaining three fractions did not show any antibacterial activity against PAO1. Negative control (10% DMSO in normal saline) did not have antibacterial activity. MIC of amoxicillin was 0.0625 mg/ml, but the MBC of amoxicillin against PAO1 was not detected in this experiment. The trend of the antibacterial activity of SPE cartridge fractions against PAO1 was the same as *E. coli*, i.e. only SPE fraction 1 and fraction 2 had cytotoxicity to G- bacteria, and PAO1 was more sensitive to both fractions than *E. coli*. This result suggested that ranunculin might be the antibacterial constituent against PAO1. The HPLC chromatographic fractionation by C18 analytical HPLC column was undertaken and the antibacterial activity of these HPLC fractions is shown in Figure 3.16.

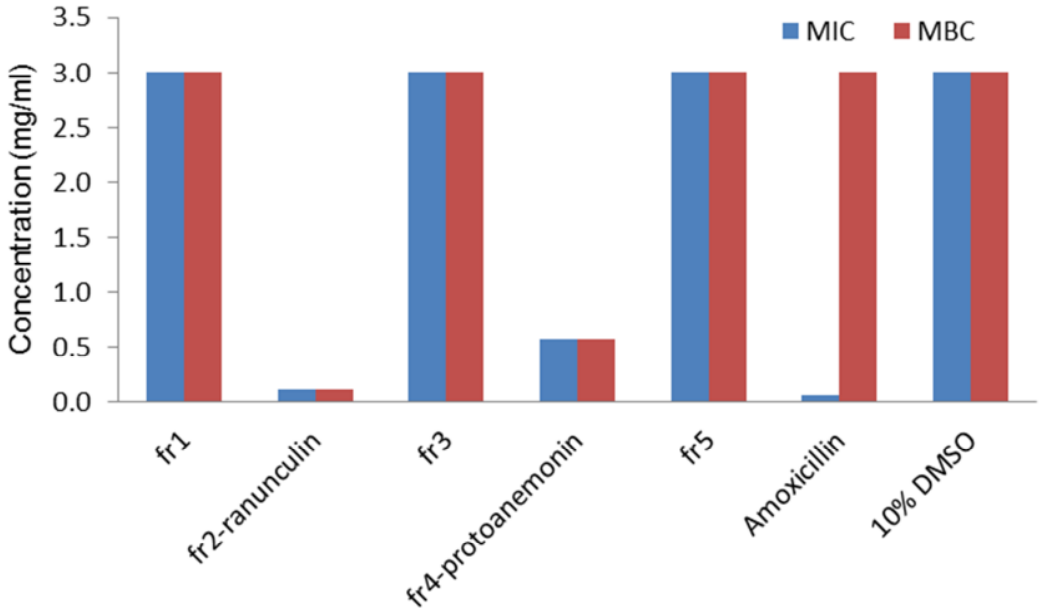

Figure 3.16 Antibacterial activities of C18 HPLC fractions of CaL-i against PAO1. All values of 3 mg/ml mean that there were no antibacterial activities detected at that concentration.

The trend of antibacterial effects of HPLC fractions against PAO1 was similar to those obtained in the antibacterial activities of HPLC fractions against *E. coli*. The ranunculin fraction and the protoanemonin fraction had antibacterial effects. The antibacterial effects of CaL-i HPLC fractions against *E. coli* in previous study exhibited that the MICs of ranunculin and protoanemonin fractions were 0.3 and 1.8 mg/ml, respectively. MBC of ranunculin fraction was 0.3 mg/ml, and MBC of protoanemonin was not detected. Both MIC and MBC of ranunculin fraction against PAO1 were 0.12 mg/ml, and MIC and MBC of protoanemonin fraction on PAO1 were 0.57 mg/ml. The MIC of amoxicillin against PAO1 was 0.063 mg/ml, which is 4x higher than its MIC against *E. coli*. This result evidenced that ranunculin and protoanemonin are antibacterial constituents in *Clematis* spp. The antibacterial activities of ranunculin against *E. coli* and PAO1 were similar, but the antibacterial activity of protoanemonin against PAO1 might be slightly stronger than that against *E. coli*.

Didry *et al*[187] demonstrated antibacterial activities of protoanemonin against 6 strains of *P. aeruginosa* and *E. coli*. In their study, MICs of protoanemonin against 6 *P. aeruginosa* strains were from 15.63 to 62.5 μg/ml, and the MIC of protoanemonin against *E. coli* was 62.5 μg/ml. Their report suggested that the antibacterial activity of protoanemonin against *P. aeruginosa* was the same or stronger than in against *E. coli*, which is consistent with the results from this study. However, the antibacterial activity of protoanemonin in Didry's report was much higher than the result obtained in this study. As previously discussed, protoanemonin is a volatile compound. The

decrease in antibacterial effect of protoanemonin in this current study was likely to be influenced by the extraction and fractionation procedure.

A review paper from Tschesche mentioned that ranunculin did not have antimicrobial activity,[199] but the original data was unpublished. The conflicting result presented in this study is that ranunculin is an antibacterial compound. Therefore, it was decided to undertake more work to confirm the antibacterial activity of ranunculin against *P. aeruginosa*.

3.3.2.3 Antibacterial activities of bioactive fractions of *C. aristata*-L by C18 column

In order to confirm our previous results that ranunculin was suspected to be the antibacterial constituent, a silica gel C18 coated column with 5.4 cm of height and 1.9 cm of diameter was employed in this study instead of a SPE cartridge. The C18 column could load larger amounts of polar fraction (1.1527 g) than a SPE cartridge (30 mg) The amounts of C18 column fractions 1 (CA-LI) and 2 (CA-LII) eluted from the column were 442 mg and 154 mg, respectively, which was much greater than CA-Li (18.4 mg) and CA-Lii (10.2 mg). HPLC chromatograms of CA-LI and CA-LII by comparison with CA-Li and CA-Lii at 254 nm are shown in Fig.3.17 and 3.18.

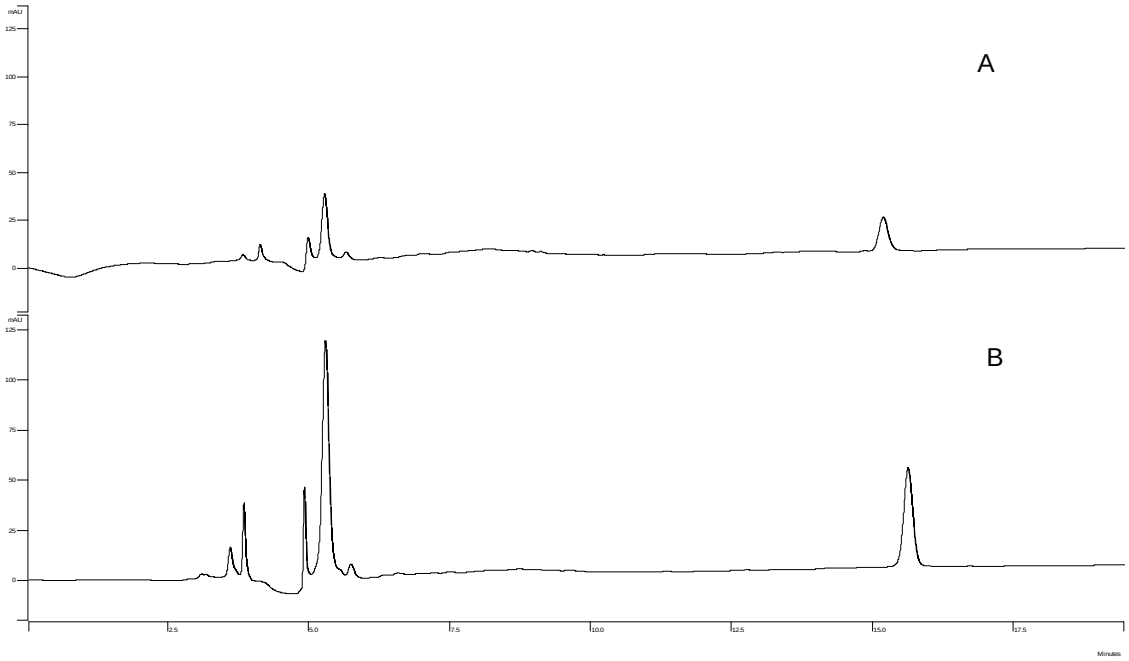

Figure 3.17 HPLC chromatograms of CA-LI (A) and CA-Li (B) at 254 nm.

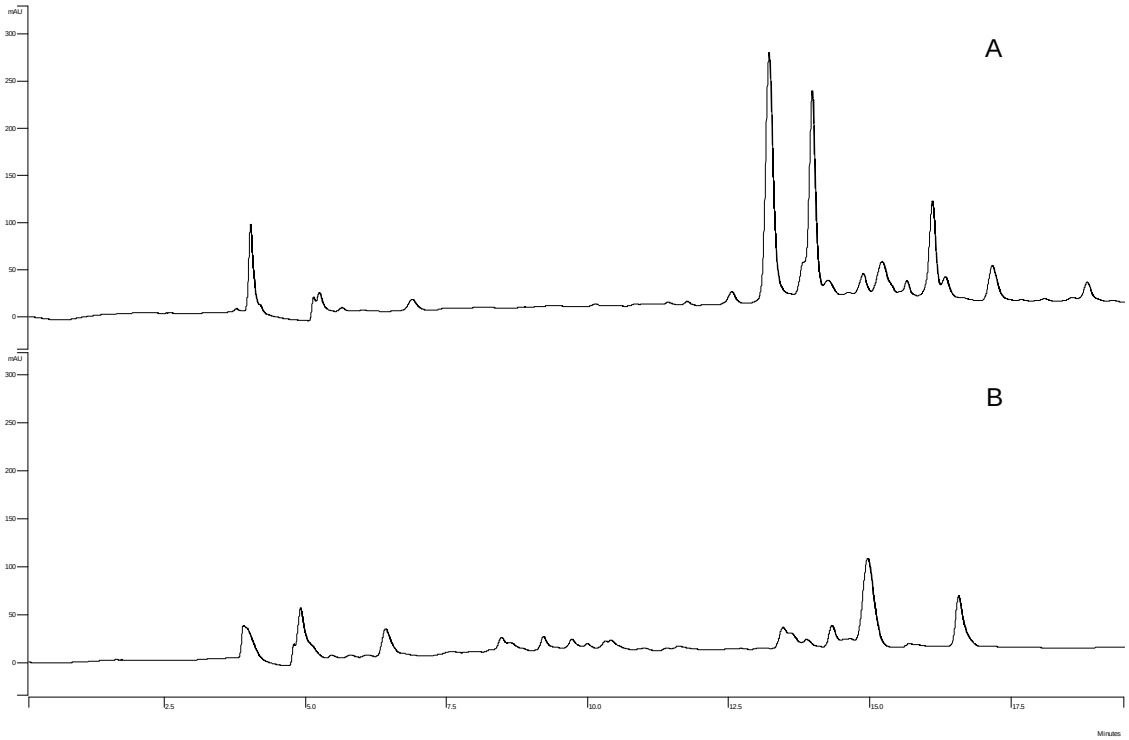

Figure 3.18 HPLC chromatograms of CA-LII (A) and CA-Lii (B) at 254 nm.

The HPLC spectrum of CA-LI was in complete agreement with the HPLC chromatogram of CA-Li. Only ranunculin and protoanemonin were present in both fractions 1. The HPLC chromatogram of CA-LII was similar to the HPLC chromatogram of CA-Lii. Both chromatograms before 7.5 minutes were the same. The chromatogram of CA-LII between 7.5 and 20 minutes had more peaks than that of CA-Lii in that period of time. As CA-Lii also exhibited antibacterial activity against *E. coli* and PAO1 in previous results, in this study, the antibacterial activities of both CA-LI and CA-LII against PAO1 were determined and a comparison of these effects with previous antibacterial results of CA-Li and CA-Lii are presented in Figure 3.19.

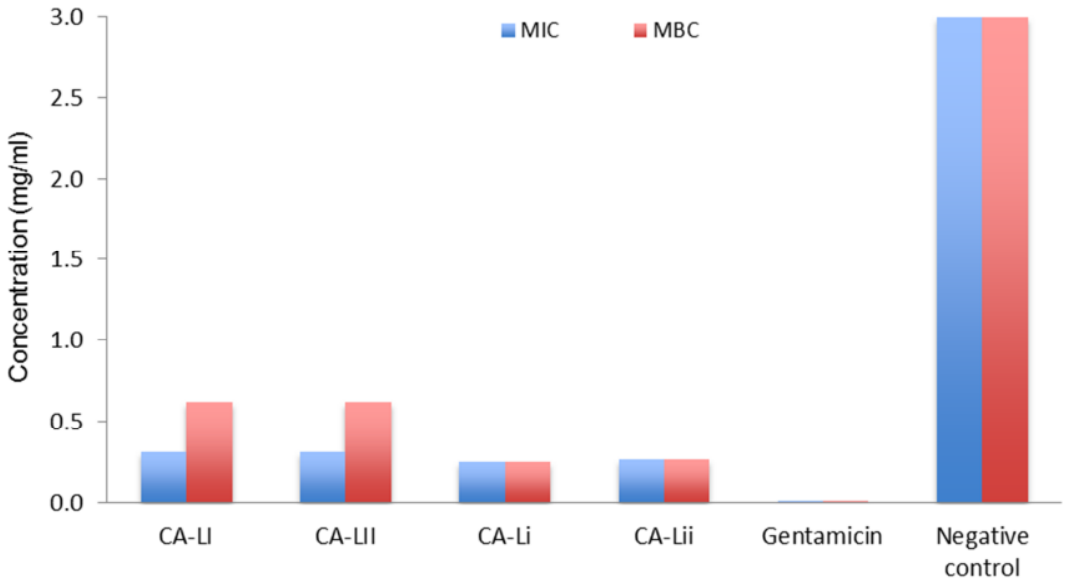

Figure 3.19 The antibacterial activities of CA-LI, CA-LII, CA-Li and CA-Lii against PAO1. Blue bars are MICs and red bars are MBCs. All values of 3 mg/ml mean that there were no antibacterial activities detected at that concentration.

Results in Figure 3.19 showed that MICs of CA-LI and CaL-II were both 0.31 mg/ml, and their MBCs were both 0.62 mg/ml. This results revealed that the antibacterial

activity of C18 column fractions were the same as SPE cartridge fractions. The slight difference may be due to the concentration of sample added in the first well of each row being different.

CA-LI and CA-LII had the same inhibitory and bactericidal activities against PAO1. HPLC chromatograms of both fractions demonstrated that fraction 1 where only ranunculin and protoanemonin were present had fewer compounds than fraction 2, therefore, it was hypothesised that the antibacterial constituents in C18 column fractions of CA-L polar partition were still ranunculin and protoanemonin.

The positive control was changed to gentamicin in this experiment as amoxicillin could only inhibit the growth of PAO1 rather than contribute bactericidal activity. This result is shown in Figure 3.20. The colour of well F3 and F4 was blue (left image) but colonies were obtained when bacterial culture of these two wells was subcultured on to an agar plate (right image). The MIC of gentamicin against PAO1 was 1 µg/ml and MBC was 2 µg/ml, which was consistent with the report from Krogfelt.[200] The negative control did not have antibacterial effects against PAO1. Amoxicillin was used as positive control in previous experiment. It had bactericidal effects against *E. coli*, but only inhibited the growth of PAO1.

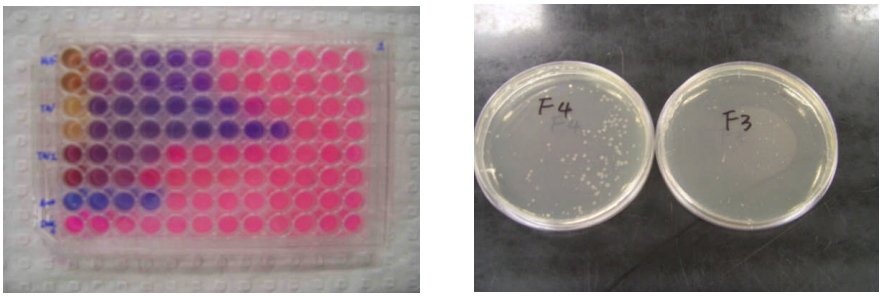

Figure 3.20 Photos of experiment of determining MIC of *Clematis* spp. and amoxicillin against PAO1 (left) and MBC of amoxicillin (right)

3.3.2.4 Antibacterial activity of fractions from HPLC columns

To summarise the above results, ranunculin and protoanemonin were antibacterial constituents in *Clematis* spp. Protoanemonin has been reported to be the antimicrobial compound in many studies. Therefore this study targeted ranunculin, which has been reported as having no antimicrobial effects.[199] Work in Chapter 2 described that ranunculin could be eluted from a carbohydrate column with a longer retention time than that obtained by C18 column chromatography. Based on these results, an HPLC carbohydrate column was employed to fractionate CA-LI and CA-LII to confirm if ranunculin was the active constituent.

The antibacterial constituents were present in the 6-9 minutes HPLC carbohydrate column fractions of CA-LI and CA-LII, and 0-10 minutes HPLC C18 column fraction of CA-LI (Figure 3.21). Photographs of experimental work are in the appendix III. MICs of the active HPLC carbohydrate column fractions of CA-LI and CA-LII were respectively 0.43 and 0.50 mg/ml. MIC of the active HPLC C18 column

fraction of CA-LI was 0.31 mg/ml. The chemical constituents of these 3 active HPLC fractions were determined by HPLC-ELSD.

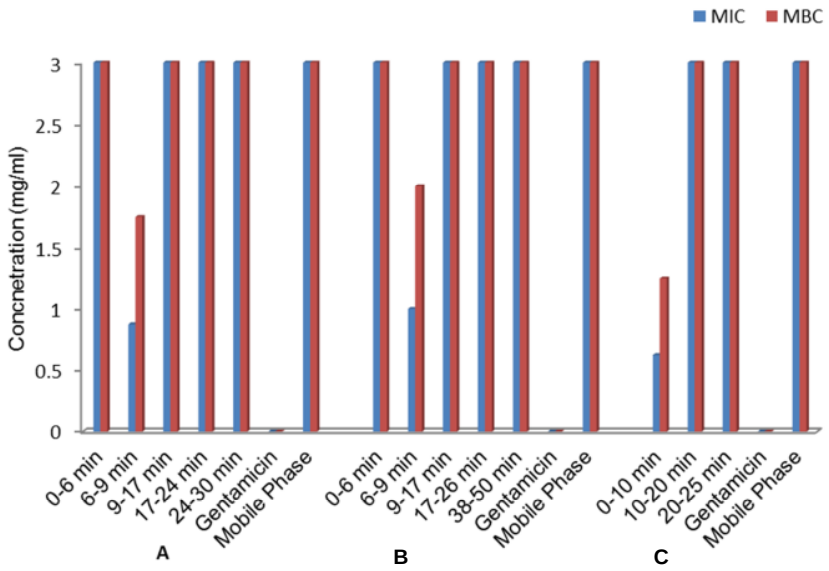

Figure 3.21 Antibacterial activity of analytical HPLC column fractions of CA-LI and CA-LII against PAO1**.** A shows the antibacterial activities of carbohydrate HPLC column fractions of CA-LI. B shows the antibacterial activities of carbohydrate HPLC column fractions of CA-LII. C shows the antibacterial activities of C18 HPLC column fractions of CA-LI. All values of 3 mg/ml mean that there were no antibacterial activities detected at that concentration.

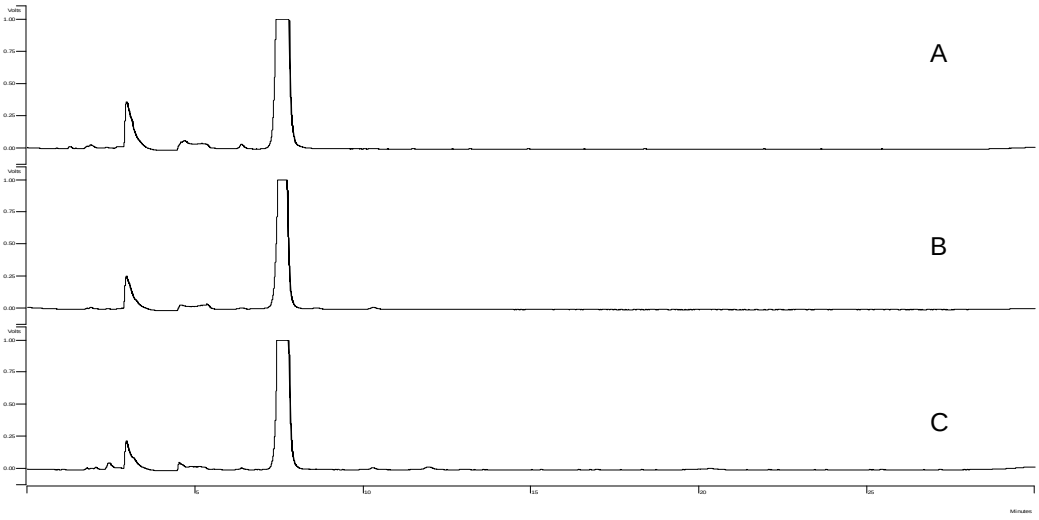

Figure 3.22 Amino HPLC-ELSD chromatograms of CA-L antibacterial active 6-9 minutes HPLC carbohydrate column fraction of CA-LI (A) and CA-LII (B) and 0-10 minutes C18 HPLC column fraction of CA-LI (C).

Chromatograms in Figure 3.22 demonstrated that the chemical constituents of these 3 active fractions were the same. The peak with retention time of 7 minutes of each chromatogram was determined to be ranunculin by LC-MS as interpreted in Chapter 2. Results of this experiment confirmed that ranunculin was responsible for the antibacterial activity in our study and that there were no other antibacterial constituents in the active fractions. The apparent variation of MICs of the 3 active HPLC fractions in Figure 3.16 is possibly because the initial concentration of fractions added in the first well were different. Based on all the above results, determination of the antibacterial activity of ranunculin against some G+ and G- bacteria and investigation of its antibacterial mechanism was performed in the following study.

3.3.3 Antibacterial activity of Ranunculin

3.3.3.1 Antibacterial activity of ranunculin against G+ and G- bacteria

The antibacterial effects of ranunculin against G- and G+ bacteria are listed in Table 3.8. Gentamicin was the positive control for G- bacteria and amoxicillin was the positive control for G+ bacteria.

In this experiment, ranunculin exhibited antibacterial activity against all tested G- strain. For the G+ species tested, ranunculin only had inhibitory and bactericidal effects against *B. cereus*. The MICs for PAO1 and *P. aeruginosa* u19b (PAu19b), a multi-drug resistant strain isolated from cystic fibrosis patient, were both 0.25 mg/ml.

Table 3.8 Antibacterial activity of ranunculin against G+ and G- bacteria

Strain of bacteria	Ranunculin		Gentamicin		Amoxicillin	
	MIC(mg/ml)	MBC(mg/ml)	MIC(mg/ml)	MBC(mg/ml)	MIC(mg/ml)	MBC(mg/ml)
PAO1	0. 25	0.5	0.001	0.002		
P. aeruginosa 124	0.5	0.5	>0.5	>0.5		
P. aeruginosa u19b	0. 25	0.5	>0.5	>0.5		
Klebsiella pneumoniae	2.5	2.5	0.5	0.5		
Acinetobacter baumannii	0.62	x[a]	0.004	0.008		
Bacillus cereus	2.5	2.5			0.001	0.002
Staphylococcus aureus	x[a]	x			0.0005	0.001
Staphylococcus saprophyticus	x	x			0.001	0.002
Streptococcus pyogenes	x	x			0.002	0.002
Streptococcus mutans	x	x			0.001	0.002

[a]x no antibacterial activity

For *P. aeruginosa* 124 (PA124), the other multi-drug resistant strain isolated from a sink in a neurosurgical unit in the Royal Hobart Hospital (Hobart, Australia), the MIC was 0.5 mg/ml. Ranunculin also inhibited the growth of other G- bacteria such as clinically isolated multi-drug resistant strains of *K. pneumoniae* and *A. baumannii* but only one G+ strain, *B. cereus*. These data point to an antibacterial spectrum specific to G- bacteria. In this study, MICs of gentamicin against G- bacteria were in the range between 0.001 mg/ml to more than 0.5 mg/ml and MICs of amoxicillin against G+ bacteria were in the range between 0.0005 and 0.002 mg/ml.

MBCs of ranunculin for three strains of *P. aeruginosa* were all 0.5 mg/ml. The value of MBCs for PAO1 and PAu19b was 2 fold their value of MICs. MBC for PA124 was equal to MIC. This result suggested that the antibacterial activity of ranunculin against sensitive *P. aeruginosa* (PAO1) and multi-drug resistant *P. aeruginosa* strains (PAu19b and PA124) was the same. The weak bactericidal effects of ranunculin against *K. pneumoniae* and *B. cereus* were the same (2.5 mg/ml). The inhibitory activity of ranunculin for *A. baumannii* was obtained but we did not observe any bactericidal effects of ranunculin against this bacterium at tested concentrations up to 5 mg/ml.

Protoanemonin had antimicrobial activity against a broad range of microbes, including G-, G+ and fungi. In this study, ranunculin only exhibited antibacterial effects against G- bacteria, and the antibacterial activity of ranunculin against PAO1 (0.25 mg/ml) was weaker than the reported data of antibacterial activity of

protoanemonin against PAO1 (0.015-0.0625 mg/ml). This result revealed that the antibacterial activity of ranunculin was different from protoanemonin.

The difference between G- and G+ bacteria are that G+ bacteria possess a thick cell membrane containing many layers of peptidoglycan and teichoic acids. By contrast, G- bacteria have a relatively thin cell membrane consisting of a few layers of peptidoglycan surrounded by a second lipid membrane containing lipopolysaccharides and lipoproteins.[201] This suggested that the major difference between G+ and G- bacterial is in their membranes. Therefore, it is hypothesised that the difference in antibacterial activity between protoanemonin and ranunculin was due to the ability of both compounds to penetrate bacterial membranes. Protoanemonin could penetrate both G+ and G- bacterial membranes, but ranunculin might only have the ability to penetrate G- bacterial membranes. Ranunculin is an unsaturated lactone. It is known that the ability of unsaturated lactones to act as inhibitory substances against several microorganisms is due to the ability of the molecule to penetrate the microbial cell and this ability depends on the lipophilicity.[202]

It is worth pointing out that the antibacterial activity of ranunculin against two multi-drug resistant strains of *P. aeruginosa* was stronger than the effects obtained from gentamicin in this study. PA124 and PAu19b are known to be resistant to gentamicin. A study by Bradbury[203, 204] demonstrated that in the eleven investigated antibiotics, PAu19b, isolated from a cystic fibrosis patient respiratory tract, was

resistant to nine antibacterial agents and intermediate to the other two antibiotics. Antibiotics that PAu19b was resistant to include carbenicillin, ticarcillin, timentin, ceftazidime, cefepime, aztreonam, imipenem, amikacin and gentamicin. Antibiotics intermediate to PAu19b were tobramycin and ciprofloxacin. PA124 was isolated from a neurosurgical unit (NSU) sink. It is resistant to carbenicillin, ticarcillin, aztreonam, amikacin, gentamicin, tobramycin and ciprofloxacin. It is intermediate to ceftazidime and cefepime and sensitive to timentin and imipenem.

Results in Bradbury's study revealed that PA124 and PAu19b are resistant to a broad range of antibiotics, except timentin and imipenem, to which PAu19b was also sensitive. Ranunculin showed antibacterial activity against both *P. aeruginosa* strains, therefore, it was decided to evaluate if PA124 and PAu19b are able to produce resistance to ranunculin.

3.3.3.2 Evaluation of multi-drug resistant *P. aeruginosa* strains generating resistance to ranunculin

After incubation of PAO1, PA124 and PAu19b with 0.5x MIC and 0.25x MIC of ranunculin for 2 weeks, the changing of antibacterial activity was evaluated. The results are presented in Table 3.9. The MICs and MBCs of *P. aeruginosa* strains to ranunculin after extended exposure of *P. aeruginosa* to 0.5x MIC and 0.25x MIC of ranunculin were tested at day 7 and day 14.

Table 3.9 The susceptibility of *P. aeruginosa* to ranunculin after extended exposure of *P. aeruginosa* to sublethal concentration of ranunculin**.**

Bacterial Strain	DAY 0		Conc. of RAN mg/ml	DAY 7		DAY 14	
	MIC mg/ml	MBC mg/ml		MIC mg/ml	MBC mg/ml	MIC mg/ml	MBC mg/ml
PAO1	0.25	0.5	0.125	0.5	1	0.5	1
			0.0625	0.5	1	0.5	1
PAu19b	0.25	0.5	0.125	0.5	>1	0.5	>1
			0.0625	0.5	1	0.5	1
PA124	0.5	1	0.25	0.5	1	0.5	1
			0.125	0.5	1	0.5	1

After incubation for 7 days (after 7 passages), the MIC and MBC of ranunculin against PAO1 just increased by a factor of 2 at both incubated concentrations of ranunculin (MIC of 0.25 mg/ml increased to 0.5 mg/ml and the MBC of 0.5 mg/ml increased to 1 mg/ml). The MIC of ranunculin against PAu19b also increased by a factor of 2 at both incubated concentrations of ranunculin (from 0.25 mg/ml to 0.5 mg/ml). The MBC of PAu19b increased to more than 1 mg/ml at 0.125 mg/ml of incubated concentration of ranunculin and 1 mg/ml at 0.0625 mg/ml incubated concentration of ranunculin. The MIC and MBC of PA124 did not change after incubation with ranunculin for 7 days (7 passages) or after 14 days (14 passages).

Carenti-Etesse *et al*[(205)] studied the effect of β-lactam antibiotics (cefepime, cefpirome, ceftazidime, cefotaxime, peperacillin and imipenem) on the *in vitro* development of resistance in *P. aeruginosa*. The initial and final MICs and number of passages required to reach resistance are listed in Table 3.10.

Table 3.10 Initial and final MICs (µg/ml) and number of passages required to reach resistance in the nine strains of *P. aeruginosa* adapted from Carenti-Etesse *et al*. [205]

	Cefepime			Cefpirome			Ceftazidime		
Strain	MIC start	MIC end	n[c]	MIC start	MIC end	n	MIC start	MIC end	n
Ps1	1.0	64.0	39	1.5	62.0	17	1.0	62.0	22
Ps2	0.3	64.0	26	0.3	64.0	13	0.2	64.0	18
Ps3	0.4	8.0	NR[a] (33)	0.7	64.0	22	0.3	64.0	22
Ps4	2.0	64.0	16	2.7	64.0	9	0.9	64.0	10
Ps5	3.0	64.0	39	6.0	ND	ND	1.0	20.3	NR(17)
Ps6	6.0	64.0	ND[b]	12.0	128.0	—	1.5	64.0	17
Ps7	4.0	64.0	6	16.0	ND	—	3.0	64.0	8
Ps8	4.0	64.0	8	32.0	—	—	16.0	—	—
Ps9	1.5	64.0	13	32.0	—	—	12.0	—	—
	Cefotaxime			Piperacillin			Imipenen		
Strain	MIC start	MIC end	n	MIC start	MIC end	n	MIC start	MIC end	n
Ps1	16.0	ND	ND	4.0	ND	ND	1.0	64.0	24
Ps2	1.3	64	4	0.4	64.0	9	0.3	13.3	NR(21)
Ps3	2.7	64	4	0.8	64.0	11	0.3	4.3	NR(14)
Ps4	4.1	64	2	1.2	64.0	11	0.5	8.2	22
Ps5	4.0	64	3	1.5	ND	ND	0.5	10.9	32
Ps6	4.0	64	10	512.0	ND	ND	0.8	12.3	23
Ps7	192.0	—	—	512.0	—	—	6.0	—	—
Ps8	512.0	—	—	12.0	—	—	0.5	64.0	7
Ps9	512.0	—	—	128.0	—	—	0.4	20.0	35

[a]NR not reached. Number in parentheses is total number of serial passages.

[b]ND, not determined

[c]n, number of passages to reach resistance.

Carenti-Etesse showed that the final MICs of these antibiotics were much greater than the initial MICs, and cefepime and imipenem had slowest appearance of resistance. Data in Table 3.10 also suggested cefotaxime resulted in the most rapid appearance of resistance, with a mean of 3.3 passages required. Piperacillin also rapidly developed resistance with a mean of 10.3 passage required. Our study only undertook 14 passages and the final MICs of ranunculin only increased by a factor of 2 when compared with its initial MICs. Results in our study suggested that PAO1, PA124 and PAu19b could not generate resistance to ranunculin after 14 passages. The only

difference was observed in the MBC of PAu19b incubated with 0.125 mg/ml ranunculin. This difference could not be explained in this stage of study.

PA124 and PAu19b are multi-drug resistant *P. aeruginosa* strains, but PA124 is sensitive to timentin and imipenem. Timentin and imipenem fall within the larger class of β-lactam antibiotics. Imipenem is the oldest of the carbapenems and is typically very active against *P. aeruginosa*.[206] The antibacterial mechanism of imipenem against *P. aeruginosa* is due to penicillin-binding protenis (PBPs) that inhibit the transpeptidase activities of PBPs-1A, -B and -4, and the D-alanine carboxypeptidase activities of PBPs-4 and -5.[207] The MexXY-OprM efflux pump (to be discussed in 3.3.3.3.6) does not give rise to resistance to imipenem. Timentin is ticarcillin (carboxypenicillin) combined with clavulanate potassium, and works by preventing cross-linking of peptidoglycan during cell wall synthesis.

As the antibacterial activity of ranunculin has not been reported in any other research and the resistance mechanisms of PA124 and PAu19b are still unknown, we could not explain the mode of action of antibacterial activity of ranunculin against *P. aeruginosa*. This activity was equal between sensitive and multi-drug resistant strains. Ranunculin has specific stronger effects against *P. aeruginosa* than other bacteria screened in this study, and the sensitivity of the lab control level strain (PAO1) to ranunculin is the same as the sensitivity of the multi-drug resistant strains (PAu19b and PA124). The antibacterial activity of ranunculin against multi-drug

resistant strains is better than gentamicin. Based on these results, a study of the antibacterial mechanism of ranunculin against *P. aeruginosa* was carried out.

3.3.3.3 Study of antibacterial mechanism of ranunculin

3.3.3.3.1 Combination of ranunculin and gentamicin against sensitive and multidrug-resistant P. aeruginosa

A study of antibacterial activity of a combination of ranunculin and gentamicin against PAO1, PA124 and PAu19b was undertaken. The FIC indexes obtained with PAO1, PAu19b and PA124 were 1, 2 and 2, respectively. These values suggested that no synergistic effect was observed with the combination of ranunculin with gentamicin for all three tested *P. aeruginosa* strains. In this experiment the MICs of either gentamicin or ranunculin used alone for PAO1 were 0.001 mg/ml (MIC_A) and 0.25 mg/ml (MIC_B), respectively; when both ranunculin and gentamicin was combined, the minimum inhibition of PAO1 was obtained in the presence of 0.0005 mg/ml of gentamicin (A) plus 0.125 mg/ml of ranunculin (B). Thus the FIC index calculated was 1, which fits within the no effect range between 0.75 and 2.[187] The FIC index of 2 is included in no effect. Images from this experiment are shown in Figure 3.23.

The purpose of this study was to evaluate the effect of combinations of ranunculin and antibiotics to detect possible synergism, difference or antagonism, and to provide possible data regarding the mode of action of ranunculin. Gentamicin is an

aminoglycoside antibiotic and its antibacterial mechanism is inhibition of bacterial protein synthesis. The antibacterial mechanism of ranunculin has not been reported, but its specific activity on G- bacteria might suggest that the permeability of G- and G+ bacterial membranes to ranunculin is different. It was not evident that ranunculin increased the permeability of *P. aeruginosa* membrane to gentamicin, or vice versa.

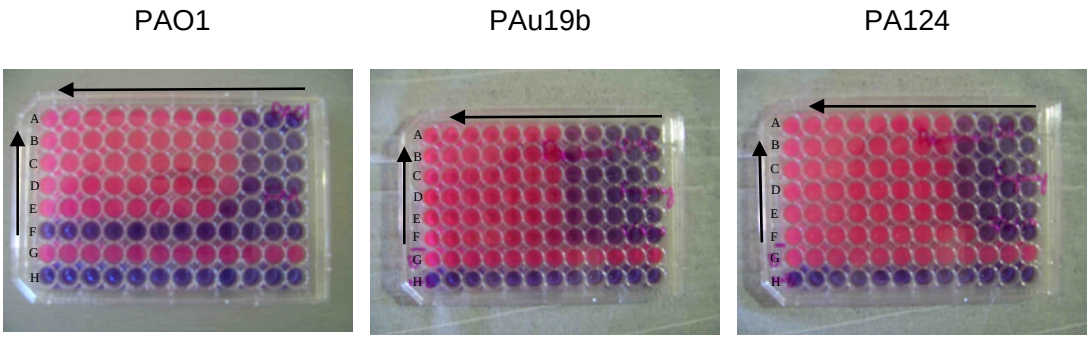

Figure 3.23 Antibacterial activity of combination of ranunculin with gentamicin against PAO1 (left), PAu19b (middle) and PA124 (right). In each image, the 2x diluted concentration of gentamicin was labeled as a vertical arrow, and the 2x diluted concentration of ranunculin was labeled as a horizontal arrow. The first row wells in each image were ranunculin only, and wells A-F of the first column were gentamicin only. Row G was negative control and row F was blank control.

Although ranunculin had no effect in combination with gentamicin in this study, its hydrolysis product, protoanemonin, was reported to have antibacterial activity that was totally or partially synergistic with some antibiotics.[187] The most significant effect was decreased inhibitory concentration of cefamandole against *Streptococcus mutans* from 1 μg/ml to 0.125 μg/ml, and the MICs of protoanemonin dropped from 31.25 to 7.81 μg/ml, giving an FIC of 0.375. The FIC of protoanemonin with ceftazidime and ticarcillin was in the range of 0.625 to 0.75. The results from Didry's study also suggested that protoanemonin is able to increase gentamicin penetration of

the G+ microbial wall. They did not perform a study to evaluate the effects of a combination of protoanemonin with gentamicin on G- bacteria.

Table 3.11 FIC index calculated from protoanemonin-antibiotic combinations adapted from Didry, *et.al* (187)

Strain	Antibiotic combined		MIC (g/ml)			FIC[e] index
	with protoanemonin	A[a]	MIC_A[b]	B[c]	MIC_B[d]	values
Staphylococcus aureus	Cefamandole	0.015	0.125	15.625	31.25	0.625
ATCC 25923	Oxacillin	0.062	0.5	15.625	31.25	0.625
Staphylococcus aureus	Cefamandole	0.125	1	7.81	31.25	0.375
MSSA	Oxacillin	0.062	0.25	15.625	31.25	0.75
Staphylococcus aureus	Cefamandole	0.031	0.25	15.625	31.25	0.625
MSSA2	Oxacillin	0.031	0.25	15.625	31.25	0.625
Streptococcus mutans	Erythromycin	0.004	0.008	3.9	31.25	0.625
ATCC 25175	Gentamycin	0.25	1	15.625	31.25	0.75
	Doxycyclin	0.031	0.25	15.625	31.25	0.625
	Amoxicillin	0.037	0.15	15.625	31.25	0.75
Pseudomonas aeruginosa	Ceftazidime	0.25	1	15.625	62.5	0.75
ATCC 27853	Ticarcillin	8	16	7.81	62.5	0.625
Pseudomonas aeruginosa 1	Ceftazidime	0.25	1	31.25	62.5	0.75
	Ticarcillin	16	32	7.81	62.5	0.625
Pseudomonas aeruginosa 2	Ceftazidime	1	2	7.81	31.25	0.75
	Ticarcillin	32	64	3.9	31.25	0.625
Serratia marcescens	Cefotaxime	0.015	0.125	7.81	15.625	0.625
IPP 6093	Amikacin	0.062	1	7.81	15.625	0.56
Serratia marcescens 1	Cefotaxime	0.062	0.125	7.81	15.625	1
	Amikacin	0.125	1	7.81	15.625	0.625
Serratia marcescens 2	Cefotaxime	0.5	2	4	8	0.75
	Amikacin	0.5	1	2	8	0.75

a A is the concentration of antibiotic in a microtube which is the lowest inhibitory concentration in its row.

b MICA is the MIC of the microorganism to the antibiotic alone.

c B is the concentration of protoanemonin in a microtube which is the lowest inhibitory concentration in its row.

d MICB is the MIC of the microorganism to protoanemonin alone

e FIC index is the Fractional Inhibitory Concentration index.

3.3.3.3.2 Gram stain

Photographes of Gram stain results are shown in Figure 3.24, 3.25 and 3.26. Elongation in bacterial cellular morphology was observed in this experiment.

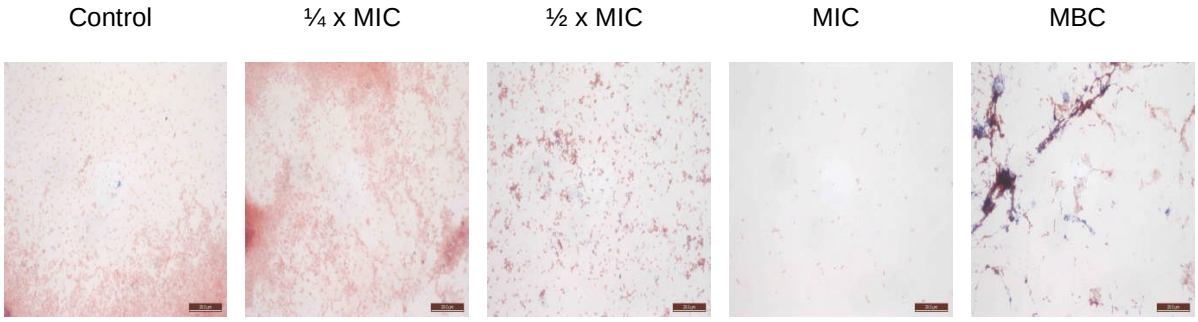

Figure 3.24 Gram stain images of different concentrations of ranunculin for PAO1

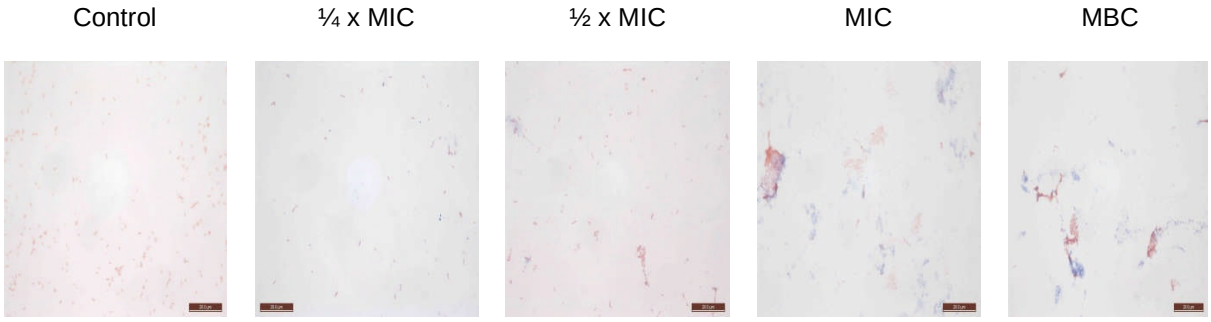

Figure 3.25 Gram stain images of different concentrations of ranunculin for PAu19b

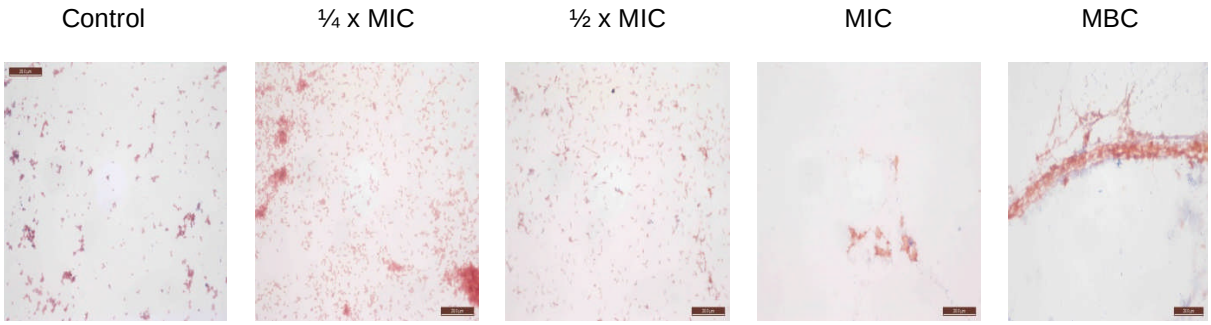

Figure 3.26 Gram stain images of different concentrations of ranunculin for PA124

Gram staining is a bacteriological staining technique that distinguishes between two groups of bacteria by the identification of differences in the structure of their cell walls. The technique, named after its developer, Danish bacteriologist Christian Gram, has become an important instrument in bacterial classification, distinguishing

between G+ bacteria, which keep the colour of the primary stain after the staining procedure, and G- bacteria, which keep the colour of the counter-stain. As *P. aeruginosa* is a G- bacterium, it exhibited a pink colour after staining. *P. aeruginosa* was observed as a rod measuring 0.5 to 0.6 μm by 1.5 to 2.5 μm. When ranunculin was applied to *P. aeruginosa*, cellular elongation was observed at sub-MIC levels for all three strains and at MIC levels for PAO1. There were no bacterial cells observed at MIC for PAu19b and PA124 and at bactericidal concentrations for all three strains.

This experiment showed that there was a change of *P. aeruginosa* cellular morphology caused by treatment with ranunculin. Images were not clear enough under optical microscopy to perform a statistical analysis to compare the level of elongation because we could not determine the length of a single cell in the images. For example, dividing cells could not be distinguished from elongated cells. Therefore, scanning electron microscopy was employed for further investigations.

3.3.3.3.3 Scanning electron microscopy of ranunculin-treated P. aeruginosa

Electron micrographs of ranunculin-treated sensitive and multi-drug resistant *P. aeruginosa* strains are shown in Figures 3.27, 3.28 and 3.29.

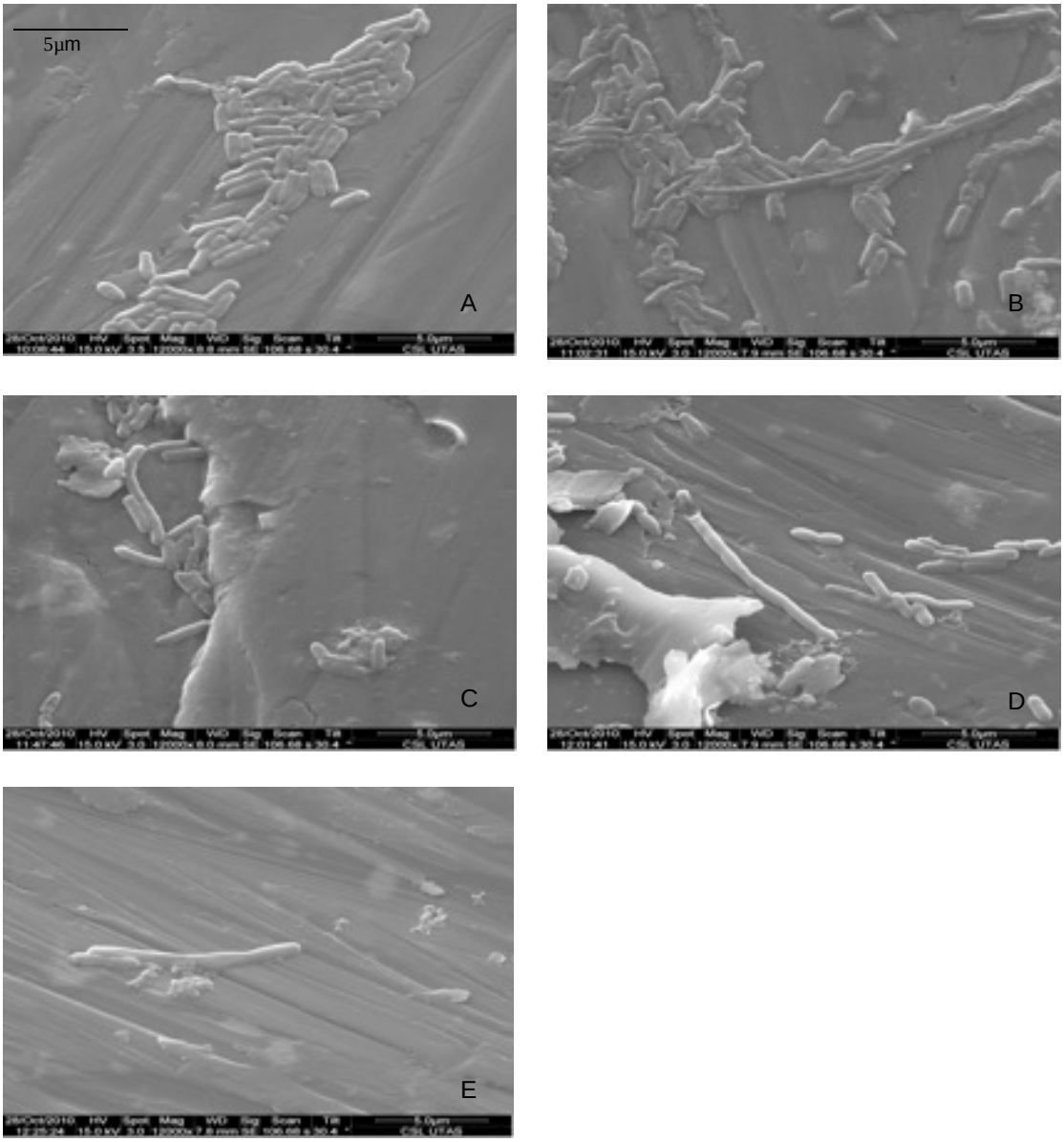

Figure 3.27 Electron micrograph of PAO1 cells after treatment with different concentrations of ranunculin. Control (A), 0.5x MIC (B), MIC (C), 1.5x MIC (D) and MBC (E). The magnification is 12000x.

Figure 3.27 shows images of PAO1 cells after treatment with different concentrations of ranunculin. Control cells (A) are rod shaped, smooth walled and of similar size. After incubation with different concentrations of ranunculin, elongation of some cells was observed. In the images D (1.5 x MIC) and E (MBC), cell debris was observed.

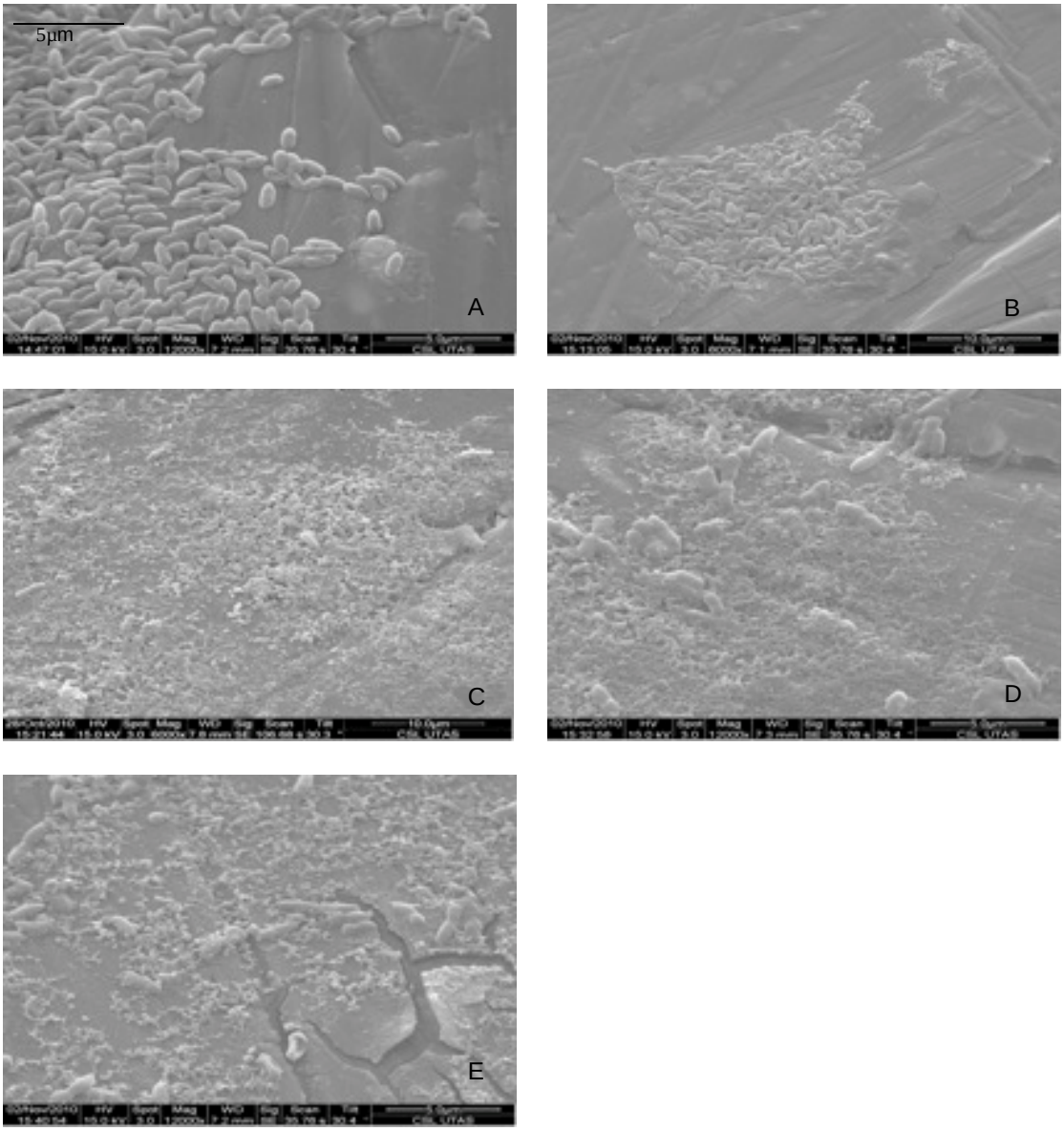

Figure 3.28 Electron micrograph of PAu19b cells after treatment with different concentrations of ranunculin. Control (A), 0.5x MIC (B), MIC (C), 1.5x MIC (D) and MBC (E). The magnification of A, D and E were all 12000x. The magnification of B and C were both 6000x.

Figure 3.28 shows the images of PAu19b cells after treatment with different concentrations of ranunculin. Control cells are rod shaped, smooth walled and of similar size. After incubation with different concentrations of ranunculin, cellular lysis was obtained in most of them as shown in B, C, D and E.

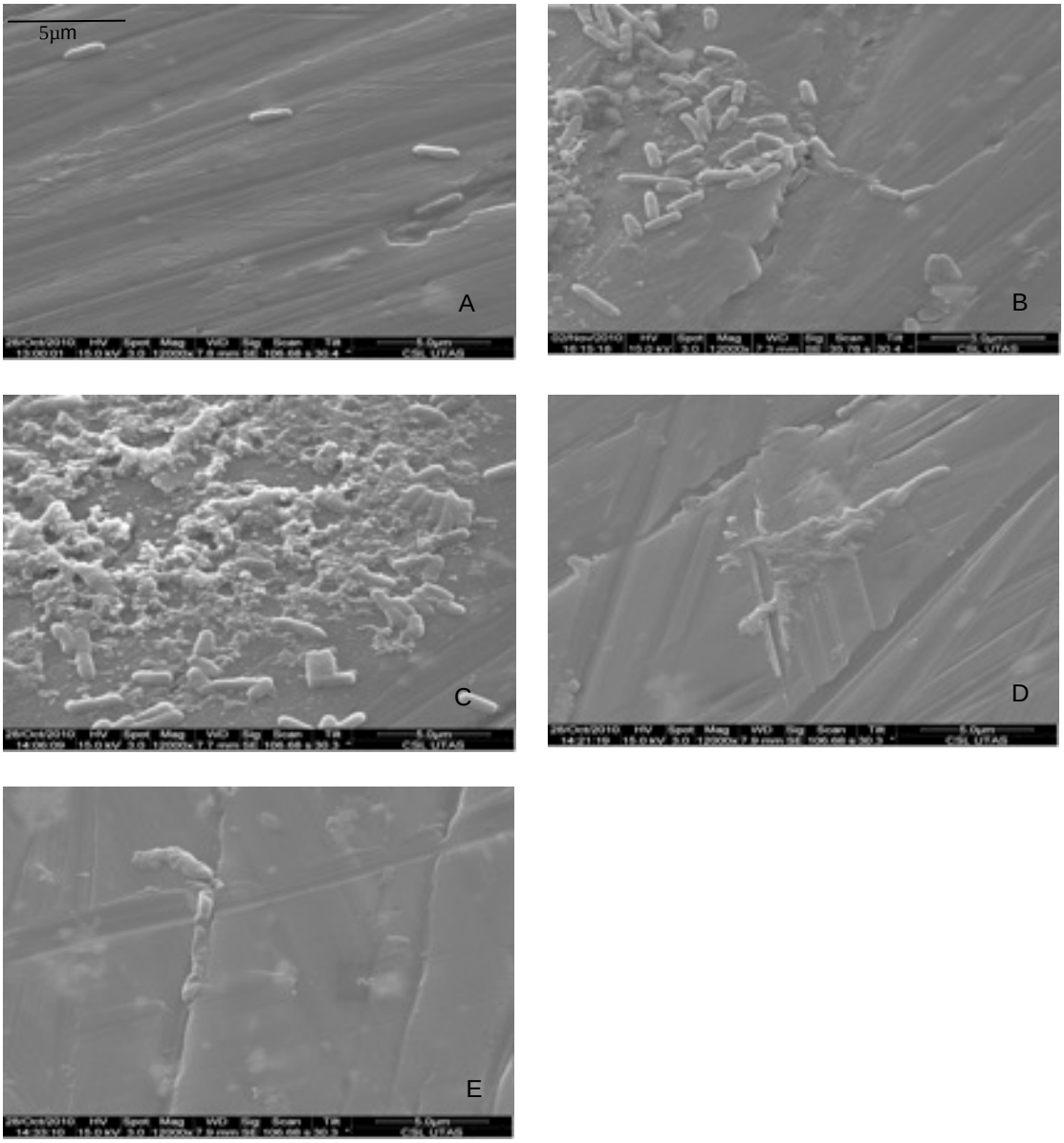

Figure 3.29 Electron micrograph of PA124 cells after treatments with different concentrations of ranunculin. Control (A), 0.5x MIC (B), MIC (C), 1.5x MIC (D) and MBC (E). The magnification was all 12000x.

Figure 3.29 shows the images of PA124 cells after treatment with different concentrations of ranunculin. Control cells are rod shaped smooth walled and similar size. Little change was obtained when treated by sub-MIC. After incubation with

MIC of ranunculin, cellular lysis was obtained in most, which is shown in image C and cellular elongation was obtained in D and E.

When examined by SEM, the control images of PAO1, PAu19b and PA124 were generally smooth-walled, rod shaped and free from each other. After 24 hours of incubation with ranunculin, the main effects observed in the three *P. aeruginosa* strains were different. The significant change in PAO1 cells was cellular elongation. The main difference in ranunculin-treated PAu19b and PA124 observed in images was celluar debris. A comparison of cellular length of ranunculin-treated three strains of *P. aeruginosa* is presented in Figure 3.30.

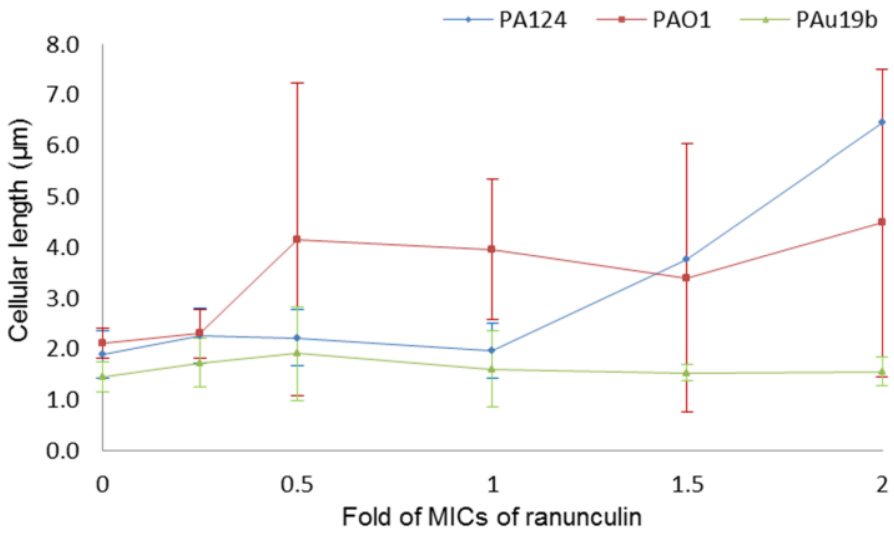

Figure 3.30 Increased length of sensitive and multi-drug resistant *P. aeruginosa* after incubation with ranunculin for 24 hours ($n_{0\text{-}0.5}$=40, n_1=20, $n_{1.5\text{-}2}$=5, but for PA124 $n_{1.5\text{-}2}$=1).

Figure 3.30 compared the cellular length of three *P. aeruginosa* strains before and after treatment by ranunculin. For PAO1, the average length of control cells was 2.12

± 0.30 μm and the average width of control cells was 0.60 ± 0.06 μm. In the concentration of 0.25x MIC, the average length of cells (2.30 ± 0.49 μm) was similar to control cells. Cellular elongation was observed at more than 0.5x MIC of ranunculin treated PAO1. Statistical analysis by Mann-Whitney U test showed that a significantly increased cell length was obtained at 0.5x, 1x and 2x MIC of ranunculin ($P<0.05$). The width of ranunculin treated PAO1 cells was the same as control cells. This result suggested that ranunculin could significant elongate PAO1 cells.

For PAu19b, the length and width of cells were measured in the absence and presence of ranunculin. In the absence of raunuclin, the average length and width of control cells were 1.46 ± 0.29 μm and 0.56 ± 0.05 μm, respectively. In the presence of ranunculin at tested concentrations, the cellular length and width of ranunculin treated PAu19b were the same as control cells. The Mann-Whitney U test did not show any difference between ranunculin-treated groups and controls.

For PA124, the average length of control cells was 1.89 ± 0.46 μm and the average width was 0.56 ± 0.05 μm. In the presence of 0.25x, 0.5x and 1x MIC of ranunculin, the cellular length and width of ranunculin treated PA124 was the same as control cells. In the concentration of 1.5x MIC and MBC only a single cell was measured, as it was hard to observe cells at this concentration of ranunculin. With 0.75 mg/ml ranunculin the length of the cell was 3.76 μm and the width was 0.52 μm. In the concentration of 1.0 mg/ml ranunculin the length of the cell was 6.64 μm and the width was 0.63 μm. The result did not show any difference between ranunculin-

treated groups of sub-MIC and MIC with controls. Statistical analysis could not be performed in 1.5x MIC and MBC because only single cells were measured.

As can be seen in image C, D and E of Figure 3.27, 3.28 and 3.29, at the MIC of ranunculin, there was evidence of greater amounts of cell debris present in the SEM images of PAu19b and PA124 than PAO1. The membrane disruption image, 24000x magnification, of PA124 and PAu19b at MIC of ranunculin is shown in Figure 3.31 in order to demonstrate more clearly the images of membrane disruption.

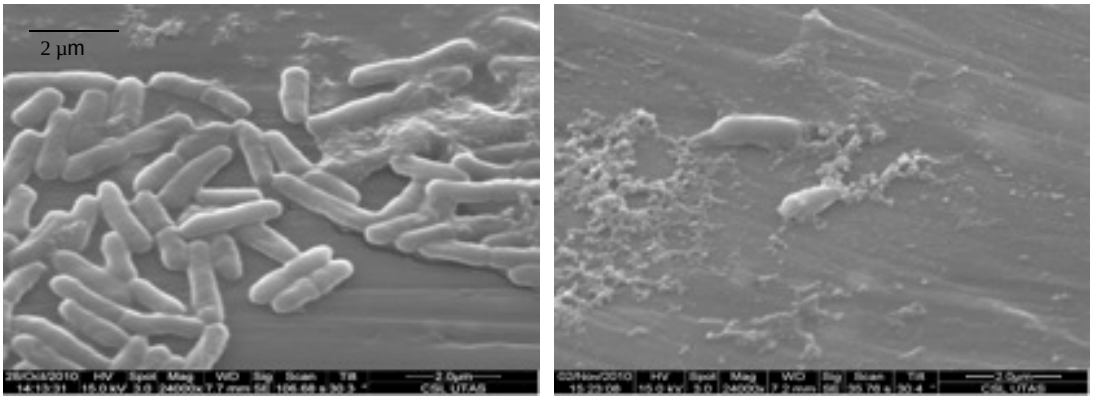

Figure 3.31 SEM images of ranunculin-treated PA124 (left) and PAu19b (right) at 24000x magnification. The concentration of ranunculin presented in PA124 was 0.5 mg/ml and the concentration of ranunculin presented in Pau19b was 0.25 mg/ml.

Based on SEM results, we hypothesise that the antibacterial mechanisms of ranunculin against sensitive (PAO1) and multi-drug resistant strains (PAu19b and PA124) of *P. aeruginosa* were different. Ranunculin treated sensitive *P. aeruginosa* cells were elongated compared with control ($P<0.05$), but for multi-drug resistant *P. aeruginosa* cells, the antibacterial mechanism of ranunculin was possibly because of membrane disruption due to cellular lysis, as observed in Figure 3.31.

Mares and co-workers[208] reported that protoanemonin at a sub-lethal dose inhibited the growth of *Euglena gracilis*. *E. gracilis* is a unicellular alga which was used as it revealed characteristics particularly useful in the preliminary study of the action mechanisms of cytotoxic substances. This result suggested that protoanemonin could cause most nuclei to be arrested in G_2/M phase (gap 2/mitosis phase) of the cellular cycle. In this phase, the nucleus of *E. gracilis* is characterized by a high scattering of chromosomes, broken down into small chromatic mass. Another study from Mares[209] reported the electron microscopy of dermatophyte *Microsporum cookie* after '*in vitro*' treatment with protoanemonin. This study showed that mitochondria, nuclei and vacuoles could be affected by protoanemonin. In particularly, the observed alteration in shape and polarity of the hyphae lead to the assumption that –SH groups of cytoplasmic microtubules could be particularly affected by protoanemonin.

In our study, elongation was also observed in ranunculin treated PAO1. This result may suggest that ranunculin might cause most nucleoids of PAO1 to be arrested in a phase analogous to G2/M phase of cellular cycle in order to stop cells dividing, analogous to protoanemonin against *E. gracilis*. Results in this study provide a hypothesis that the antibacterial effects of ranunculin are due to protoanemonin. Results in this study also suggested that the antibacterial mechanisms of ranunculin against sensitive and multi-drug resistant *P. aeruginosa* strains are different.

3.3.3.3.4 Ability of ranunculin to disrupt the outer membrane of P. aeruginosa

Previous electron microscopic evidence suggest that ranunculin was able to disrupt the membrane of *P. aeruginosa* cells. This ability was higher for multi-drug resistant strains than for PAO1.

In this study, sodium deoxycholate was employed to evaluate the effect of ranunculin disruption of *P. aeruginosa* membranes. Sodium deoxycholate is an ionic detergent that is especially useful for disrupting and dissociating protein interactions. It is most frequently used as a component of cell lysis buffer. This agent penetrates the intact enterobacterial outer membrane only poorly, but does so easily when the outer membrane is defective.[189] Therefore, the sensitivity of these three strains of *P. aeruginosa* cells to sodium deoxycholate during exposure to ranunculin could reflect any membrane disruption caused by ranunculin.

A determination of the relationship between dosage of ranunculin with the level of membrane disruption of PAO1, PAu19b and PA124 after incubation for 0.5, 1, 3, 6 and 24 hours is shown in Figure 3.32. Before 1 hour of incubation, there was no effect on the optical density of either sensitive or resistant bacteria under the test conditions (Figure 3.32 A and B). When incubated for 3 hours, cellular lysis appeared to start. As can be seen in Figure 3.32 C, the concentration of ranunculin that gave the strongest cellular lysis of PA124 was at 0.125 mg/ml. The OD decreased to 80% of the control. The concentration of ranunculin that gave the highest cell lysis of PAO1 and PAu19b was 0.25 mg/ml, with an OD decrease to 85%

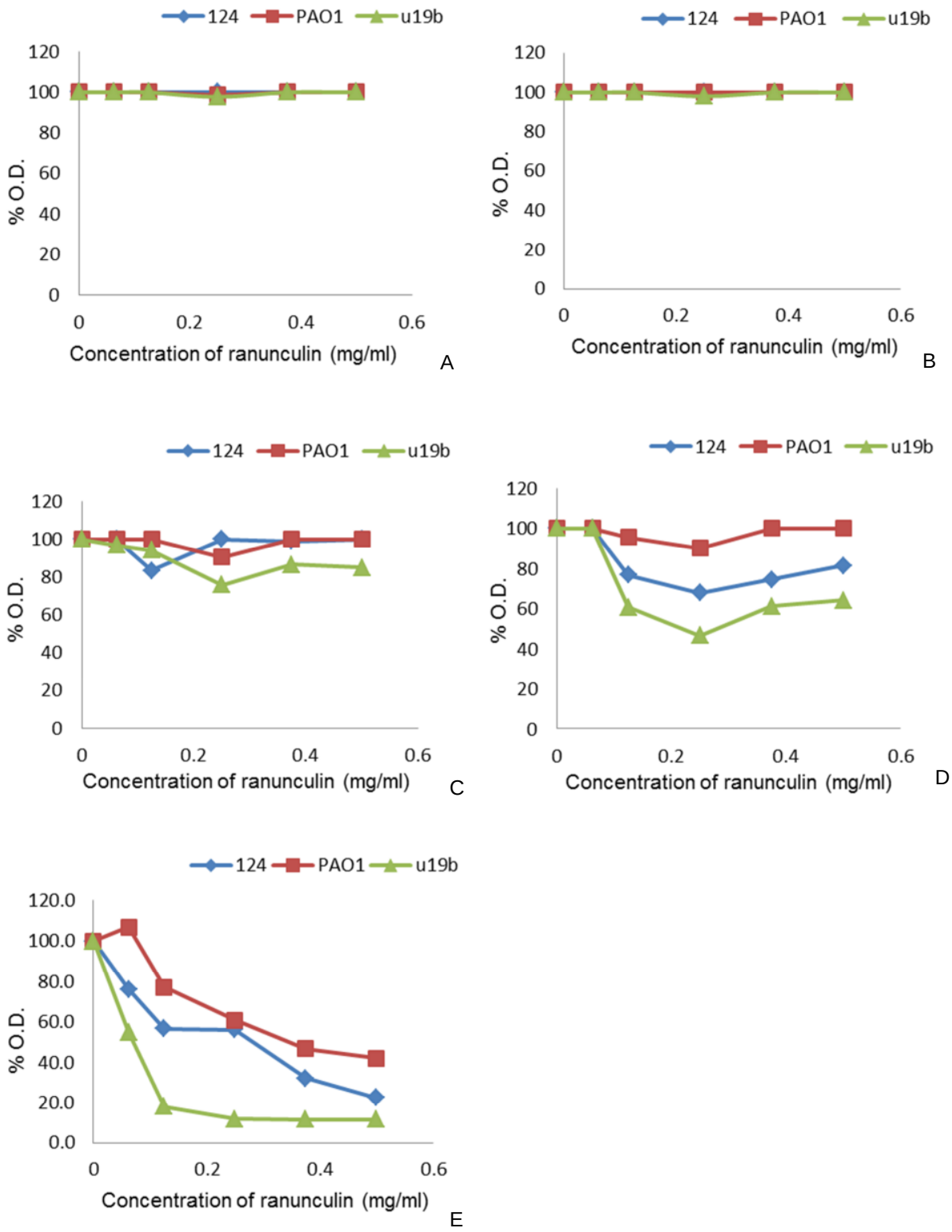

Figure 3.32 Dose- response curve of membrane disruption of PAO1, PAu19b (u19b) and PA124 (124) after incubation for 0.5 hour (A), 1 hour (B), 3 hours (C), 6 hours (D) and 24 hours (E). Cell lysis was measured as a decrease in the optical density at 450 nm. Results were expressed as the percentage of OD of controls (cells not exposed to ranunculin).

and 78% of the control. Membrane disruption of PAu19b and PA124 was greater than PAO1.

After 6 hours of incubation (Figure 3.32 D), maximum membrane disruption happened at 0.25 mg/ml of ranunculin-treated PAO1, PAu19b and PA124. The membrane disruption was strongest in ranunculin-treated PAu19b. This tendency was presented in the dose-response curves of 24 hours incubation of ranunculin with three *P. aerugiosa* strains (Figure 3.32 E). The strongest membrane disruption observed in PAu19b. In the MIC, the OD of PAu19b, PA124 and PAO1 were 15%, 21% and 60% of the control.

Figure 3.33 demonstrates the relationship between incubation time and the level of membrane disruption of PAO1, PAu19b and PA124 at different concentrations of ranunculin. At the concentration of 0.0625 mg/ml, the OD did not exhibit change in the first 6 hours. As the concentration of ranunculin increased, membrane disruption appeared. The membrane of PAO1 cells was not disrupted by ranunculin after 3 hours except at the concentration of 0.25 mg/ml. At this concentration, the percentage of OD was the similar for both PA124 and PAO1 at 24 hours of incubation.

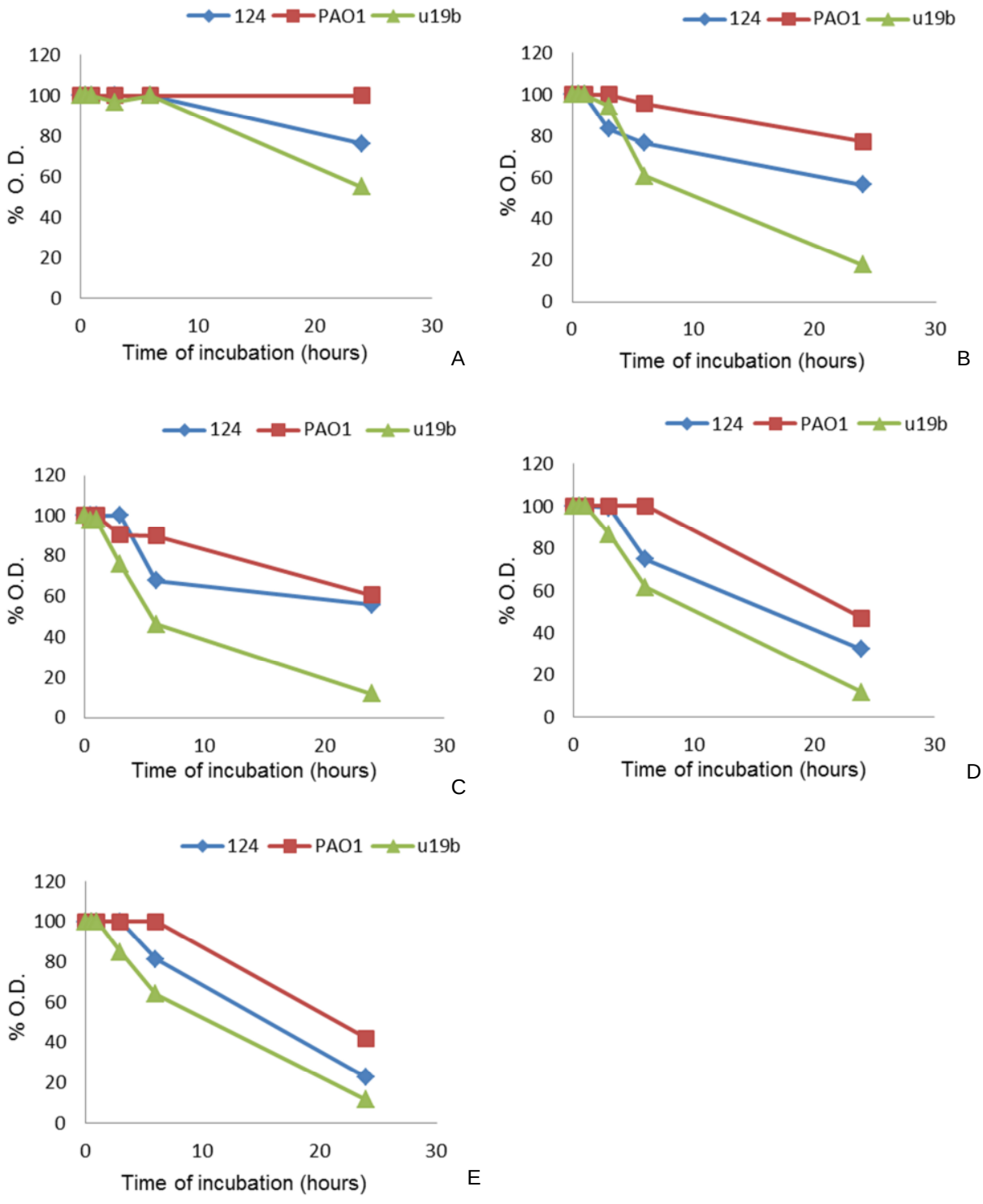

Figure 3.33 Time-response curve of membrane disruption of PAO1, PAu19b (u19b) and PA124 (124) incubated with ranunculin at 0.0625 mg/ml (A), 0.125 mg/ml (B), 0.25 mg/ml (C), 0.375 mg/ml (D) and 0.5 mg/ml (E). Cell lysis was measured as a decrease in the optical density at 450 nm. Results were expressed as the percentage of OD of controls (cells not exposed to ranunculin).

As the MIC of ranunculin for PA124 was different from PAO1 and PAu19b, curves in Figure 3.33 did not show the comparison between membrane disruption when exposed to ranunculin at equivelent doses, related to the MIC. Therefore, the time-response curves have been redrawn based on 0.25x MIC, 0.5x MIC and MIC for the three *P. aeruginosa* strains (Figure 3.34).

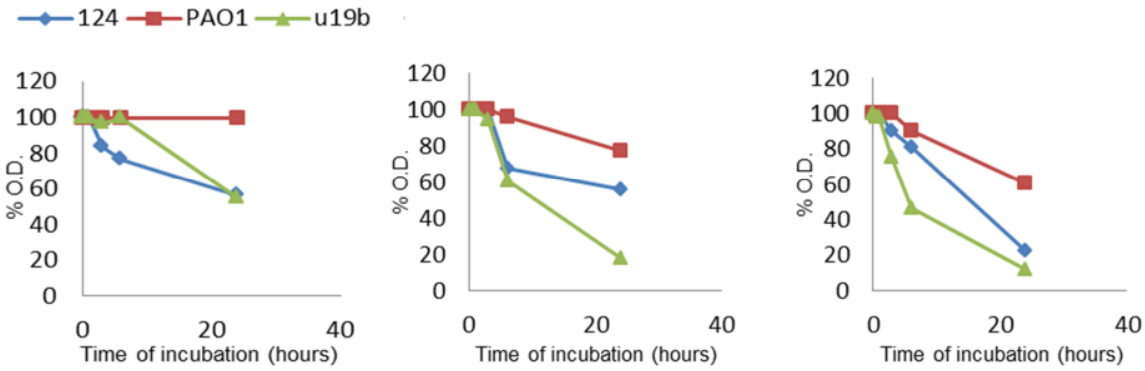

Figure 3.34 Membrane disruption after 0.25x (left), 0.5x (middle) and 1x MIC (right) of ranunculin-treated PAO1, PAu19b (u19b) and PA124 (124). Cell lysis was measured as a decrease in the optical density at 450 nm. Results are expressed as the percentage of OD of controls (cells not exposed to ranunculin).

Figure 3.34 clearly demonstrates that the ability of ranunculin to cause membrane disruption was different for the three strains of *P.aerugions.* Results from this experiment confirmed the observations by SEM. Ranunculin at the concentration of 0.25x MIC caused stronger membrane disruption in PA124 than that in PAu19b and PAO1 (Figure 3.31 A). At the concentration of 0.5x MIC, the ability of ranunculin disrupt PA124 membranes was similar to its effect on PAu19b before 6 hours (Figure 3.31 B). At the MIC, ranunculin caused membrane disruption in all three strains of *P. aerguinosa*. The greatest membrane disruption was observed in PAu19b and the least

membrane disruption was observed in PAO1. These results suggest that ranunculin causes membrane disruption in PAO1 and PAu19b which is dose dependent. However, the membane disruption in PA124 caused by ranunculin was not dose dependent to the same extent. At 6 hours, the OD% of ranunculin treated PA124 was 78%, 69% and 82% at 0.25x MIC, 0.5x MIC and MIC of ranunculin, respectively.

The results of both cellular morphological changes of *P. aeruginosa* observed by scanning electron microscopy and ranunculin-induced sodium deoxycholate sensitivity indicate that ranunculin has multiple toxic pathways against *P. aeruginosa*. The mode of action against the sensitive strain (PAO1) and multi-drug resistant strains (PAu19b and PA124) are speculated to be different. Although no report has described bacterial membrane disruption by ranunculin, the mechanism of protoanemonin producing antimicrobial effects was reported by Mares.[(194)] It was found that protoanemonin has an inactivating effect against bacterial enzyme systems due to blocking of SH groups. Additionally, Rotter and Gruber[(210)] reported that protoanemonin was able to alter the permeability of the bacteria. Mares and his co-workers' study showed that protoanemonin is able to arrest *Euglena gracilis* nuclei in the G2/M phase of the cell cycle. Although the structure of bacteria is different from *E. gracilis*, the elongation of undivided *P. aeruginosa* cells observed in our SEM study suggested that ranunculin, or possibly protoanemonin, was able to arrest bacterial cellular division.

Based on the above results, it was speculated that the antibacterial activity of ranunculin might be in fact be contributed to by protoanemonin from ranunculin hydrolysis in the medium or within the cells. A determination of protanemonin from ranunculin-treated *P. aeruginosa* cell culture was performed by headspace-GC-MS-SPME.

3.3.3.3.5 Headspace-GC-MS SPME

In this experiment, protoanemonin peaks were detected in MIC of ranunculin-treated medium with or without *P. aeruginosa* cellular culture (Figure 3.35). The MS spectrum is shown in the Appendix V.

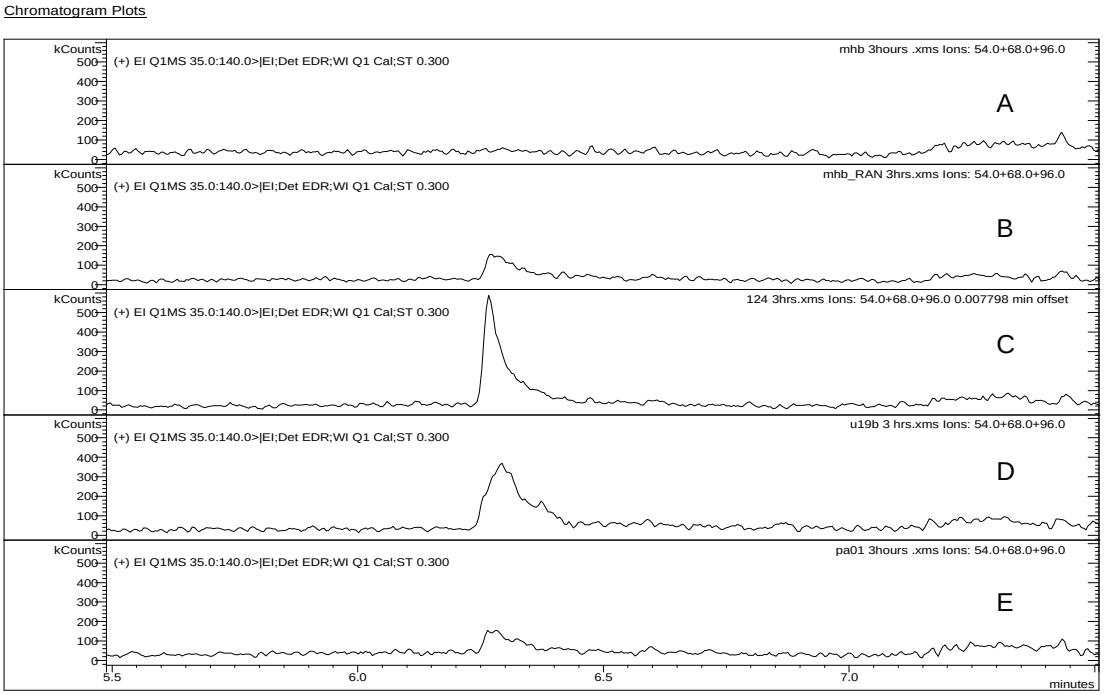

Figure 3.35 GC-MS-SPME chromatograms of ranunculin-treated *P. aeruginosa* cellular culture after 3 hours incubation. A is control; B is ranunculin (0.25 mg/ml) in MHB; C is ranunculin (0.5 mg/ml) in PA124 bacterial culture; D is ranunculin (0.25 mg/ml) in PAu19b bacterial culture; E is ranunculin (0.25 mg/ml) in PAO1 bacterial culture.

From the GC-MS chromatograms exhibited in Figure 3.35, protoanemonin peaks with retention time of 6.3 minutes were detected when ranunculin was present in MHB and PAO1, PAu19b and PA124 bacterial culture after incubation for 3 hours. MHB without ranunculin was a blank control, whose GC-MS chromatogram was shown in Figure 3.35 A, i.e. no protoanemonin peak was observed. Figure 3.35 B was the chromatogram after 3 hours of incubation of ranunculin in MHB and E was ranunculin incubated with PAO1 bacterial culture in MHB. Both B and E seemed to produce a similar amount of protoanemonin by comparing the area under curve (AUC) of protoanemonin. The protoanemonin detected under the same conditions but with PA124 (Figure 3.35 C) and PAu19b (Figure 3.35 D) bacterial culture, exhibited more protoanemonin than that obtained from PAO1 (Figure 3.35 E). A comparison of the AUC of protoanemonin obtained after incubation in MHB or *P. aeruginosa* culture is shown in Figure 3.36. All GC chromatograms are shown in Appendix V.

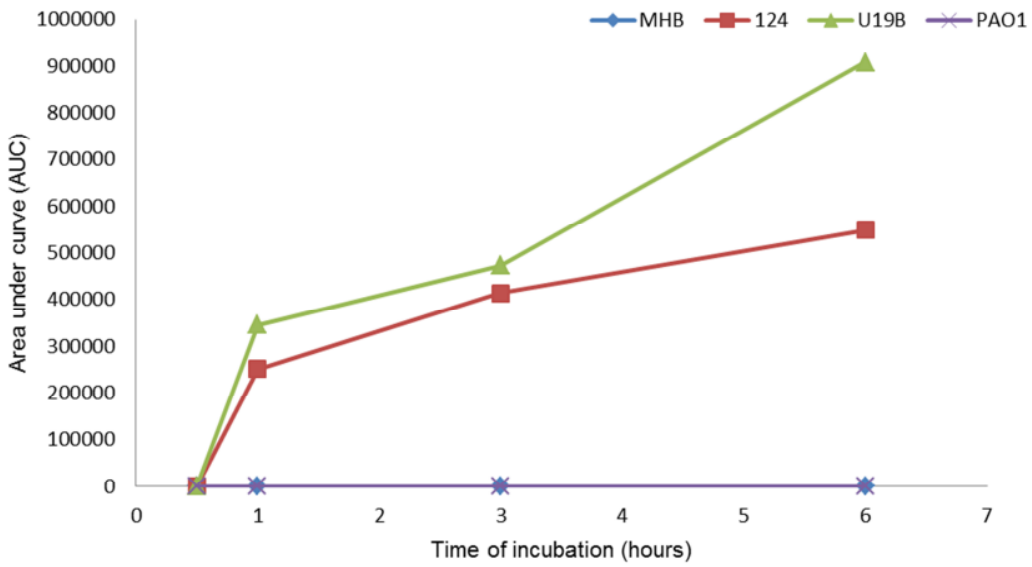

Figure 3.36 The AUC of protoanemonin detected from incubation of MHB, PAO1, PAu19b (u19b) and PA124 (124) bacterial culture containing ranunculin.

Figure 3.36 demonstrates that different amounts of protoanemonin were obtained in MHB, PAO1, PAu19b and PA124 bacterial culture. The AUC of protoanemonin was insignificant in PAO1 bacterial culture and control MHB. The protoanemonin obtained from PAu19b was greater than that obtained from PA124 at any detection time of more than 0.5 hours. The amount of protoanemonin obtained from PA124 and PAu19b was greater than the amount obtained from PAO1.

This result provides evidence that the antibacterial activity of ranunculin was contributed to by protoanemonin and suggests that ranunculin might be stable in MHB. This result also demonstrated that the ability of the three strains of *P. aeruginosa* to liberate protoanemonin from ranunculin was different. This difference could be due to the different rate of hydrolysis of ranunculin by PAO1, PAu19b and PA124, or may be related to the cellular membrane integrity to protoanemonin produced intracellularly. As seen earlier ranunculin produced stronger membrane disruption of PAu19b and PA124, and more protoanemonin was released from these bacterial cultures. This result also supported previous results from the study of membrane disruption.

The result from the GC-MS-SPME study provided evidence that ranunculin penetrated bacterial membranes and moved into the cells, and hydrolysis of ranunculin occurred within the cells to produce protoanemonin. Protoanemonin has cytotoxic activity against *P. aeruginosa*. Protoanemonin was released into the broth, which may have happened when the bacterial membrane was disrupted. Broth itself

did not cause significant hydrolysis of ranunculin. Membrane disruption of PAO1 was not as significant as that of PAu19b and PA124, and protoanemonin detected in PAO1 was less than that obtained from PA124 and PAu19b under the same conditions. This may be because of less disruption of PAO1 membrane or due to less hydrolysis of ranunculin by PAO1.

Ranunculin may penetrate *P. aeruginosa* through porins in the outer membrane of G- bacteria. The outer membrane of a variety of G- bacteria acts as a permeabile barrier to macromolecules, hydrophobic antibiotics and dyes, and hydrophilic substances above approximately 600 daltons in molecular weight. There are essentially two pathways that antibiotics can take throught the outer membrane: a lipid-mediated pathway for hydrophobic antibiotics, and general diffusion through porins for hydrophilic antibiotics.[211] Porins are a type of protein in the outer membrane. β-lactam antibiotics are generally taken through the outer membrane by porins.[212, 213] Ranunculin is a glycoside, and consequently hydrophilic. Such compounds are able to diffuse through porins.

The hypothesis, that ranunculin crosses G- bacteria outer membrane via porins, might be used to explain why ranunculin only had antibacterial activity against G- bacteria but protoanemonin had antibacterial activity against both G+ and G- bacteria. Protoanemonin could diffuse into G- and G+ bacteria, but ranunculin could only penetrate G- bacterial membranes because porins only exist in G- membranes. A previous part of this chapter discussed the antibacterial mechanism of protoanemonin

being related to the reaction of protoanemonin with –SH by Michael addition. As several key enzymes, like DNA polymerase, phosphofructokinase, and microtubular proteins of the mitotic apparatus contain exposed –SH groups, protoanemonin may interact with –SH groups to inactivate sulphydryl-containing enzymes necessary for cellular replication.[194] Electron microscopic images exhibited that elongation was obtained in ranunculin-treated PAO1, therefore, it is supposed that this may be related to ranunculin interaction with –SH group in DNA polymerase, or possibly microtubular proteins.

3.3.3.3.6 Study of the antibiotic resistance mechanism of P. aeruginosa strains 124 and u19b

Treatment of *P. aeruginosa* infection may be hampered as the bacteria show inherent and acquired resistance mechanisms when treated by antimicrobial agents. The intrinsic resistance mechanisms include the chromosomal β-lactamases, active efflux pumps and impermeable membranes. Acquired resistance mechanisms may include membrane permeability changes, mutations in type II topoisomerase enzymes and aminoglycoside modifying enzymes. [214]

Results in our study suggest that one of the major aminoglycoside resistance mechanisms in PA124 is the MexXY multidrug efflux system. Figure 3.37 shows the MICs of amikacin, gentamicin and tobramycin against PAO1, PAu19b, PA124 and a MexXY deficient mutant from PA124. MICs of amikacin, gentamicin and tobramycin against PA124 were 128, 1024 and 256 μg/ml, respectively. When

MexXY was deficient, the MICs of amikacin and gentamicin against PA124 were 8 and 8 μg/ml, respectively. This result revealed a 16 and 128 times decrease in the MICs of amikacin and gentamicin when MexXY is deficient.

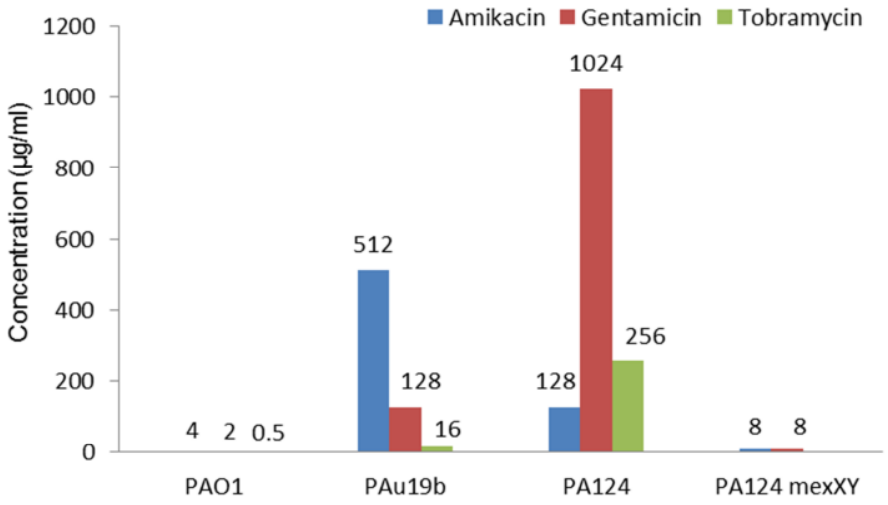

Figure 3.37 Antibacterial activities (MIC) of amikacin (blue), gentamicin (red) and tobramycin (green) against *P. aeruginosa* strains. The MICs are labelled in this Figure. *P. aeruginosa* strains used in this study included PAO1, PAu19b, PA124 and a mexXY deficient mutant from PA124 (PA124 mexXY).

MexXY is a component of an resistance-nodulation-division (RND)-type multidrug efflux pump in *P. aeruginosa*. The MexXY multidrug efflux pump system was firstly reported by Mine, *et.al.* in 1999. [215] The RND transporter MexY interacts with the outer membrane channel OprM and the periplasmic adaptor protein MexX to actively extrude various antibiotics from the intracellular compartment to the external medium.[216] At the gene level, the MexX and MexY proteins are encoded by a single transcriptional unit, *mex*XY.[215] The MexXY-OprM active efflux pump system is implicated in resistance to a broad range of antibiotics including β-lactam agents,

macrolides, glycylcycline, lincosamides, chloramphenicol, fluoroquinolones and aminoglycosides, but not imipenem.

Furthermore, the sequence of *mexZ* in PA124 and PAu19b was undertaken. MexZ is a transcriptional regulator of the *mex*XY multidrug transporter operon. Expression of *mex*XY is negatively regulated by the production of the divergently transcribed *mex*Z gene.[217] Upregulation of the MexXY-OprM pump often results from mutations occurring in *mex*Z.[218] Silent mutations were found in *mex*Z of PA124, but frame shift mutation was found in *mex*Z of PAu19b. This result suggested that PAu19b was an agrZ-type mutant. Studies by another group found that PA124 also has acquired sulfhydryl variable group extended spectrum β-lactamases,[219] conferring resistance to a wide range of β-lactam agents up to and including the third generation cephalosporins.

Results in this study only revealed one of the major aminoglycoside resistant mechanisms of PA124 and PAu19b. The MICs of ranunculin (and protoanemonin) against PAO1, PA124 and PAu19b were 0.25, 0.5 and 0.25 mg/ml, respectively, which suggested that the antibacterial activity of ranunculin (and protoanemonin) against sensitive and multi-drug resistant *P. aeruginosa* were the same. When combining both results, it clearly provides a hypothesis that a MexXY multidrug efflux system in PA124 and PAu19b does not confer resistance to ranunculin (and protoanemonin).

The result of the checkerboard study suggested that there was no change of the antibacterial activity of gentamicin against PA124 and PAu19b when combining ranunculin (and protoanemonin) with gentamicin. When introducing this result to the resistance mechanism study of multi-drug resistant *P. aeruginosa*, it provided a suggestion that although the MexXY-OrpM efflux pump system did not influence the antibacterial effect of ranunculin (and protoanemonin), ranunculin (and protoanemonin) could not prevent the effects of the MexXY-OrpM efflux pump system on aminoglycoside antibiotics.

However, results in this study could not explain the phenomenon observed in the SEM images. This study showed that membrane disruption of PA124 and PAu19b when treated by ranunculin (protoanemonin) was greater than that of PAO1. Therefore, this result might provide another hypothesis that there is a relationship between the MexXY-OrpM efflux pump system and cellular lysis when PA124 and PAu19b were treated by ranunculin (and protoanemonin), or other mechanisms exist that contribute to the results observed from SEM images.

3.4 Future work

Further studies on the antibacterial mechanism of ranunculin (and protoanemonin) against PA124 and PAu19b would be worthwhile. Firstly, it would be necessary to study how ranunculin penetrates G- bacterial membranes. This investigation might provide information that ranunculin only has antibacterial activity against G- bacteria. Secondly, investigate chemical decomposition of ranunculin to protoanemonin acting as an antibacterial pro-cytotoxin.

Further investigation of the antibacterial mechanism of protoanemonin against sensitive (PAO1) and multi-drug resistant *P. aeruginosa* strains (PAu19b and PA124) would be interesting. Protoanemonin could elongate PAO1 cells and this result was supposed to be due to inhibition of cellular division. Therefore, flow cytometry could be employed in a study to investigate this hypothesis. If positive results were obtained, this experimental method might be applied to tumour cells to observe if the cellular division of tumour cells could be stopped by protoanemonin. For multi-drug resistant *P. aeruginosa* strains (PA124 and PAu19b), protoanemonin causes cellular lysis. In our study, MexXY-OrpM multidrug efflux system was detected in PAu19b and PA124. Therefore, it would be interesting to investigate if there is any relationship between protoanemonin and this efflux pump system that contributes to the cellular lysis of both multi-drug resistant *P. aeruginosa* strains.

Ranunculin was a pro-toxin with antibacterial activity isolated from Tasmanian *Clematis* spp. and different cultivars. Determination of the relationship between

antibacterial activity of *Clematis* polar fraction and the content of ranunculin in each *Clematis* would confirm if ranunculin is the only antibacterial constituent existing in *Clematis* spp. leaf, or if there are other antibacterial constituents. The antifungal activity of ranunculin and toxicity of ranunculin would be worth investigating.

3.5 Conclusion

The antibacterial activities of collected Tasmanian native *Clematis* spp. were screened and an antibacterial constituent was successfully isolated and identified. The antibacterial activity of this active compound, ranunculin, was determined on G+ and G- bacteria, including multi-drug resistant strains. Ranunculin showed cytotoxic effect against G- bacteria, particularly for clinically isolated multi-drug resistant *P. aeruginosa*. The antibacterial mechanisms of ranunculin against *P. aeruginosa* were determined by a series of experiments. A complicated action of ranunculin against sensitive (PAO1) and multidrug resistant *P. aeruginosa* strains (PAu19b and PA124) was observed. Ranunculin elongated PAO1 possibly by arresting bacterial cells in a certain phase to stop cellular division; and interrupted the bacterial membrane integrity of PA124 and PAu19b. The mechanism of this activity is not understood at this stage. Another finding was that this complicated antibacterial effect of ranunculin was contributed to by protoanemonin. The resistance mechanism study showed that the MexXY multidrug efflux system was a major contributor to aminoglycoside resistance in PAu19b and PA124. This result also implied that the MexXY multidrug

efflux system in PA124 and PAu19b does not confer resistance to ranunculin (and protoanemonin).

Chapter 4 Anti-inflammatory Activity of Tasmanian *Clematis* Species

Abstract

Clematis species have a history of use as anti-inflammatory agents worldwide and have been used in the treatment of rheumatoid arthritis in TCM for hundreds of years. Tasmania has some native *Clematis* spp. However, neither biological effects of Tasmanian native *Clematis* spp. nor their active constituents have been studied. In order to elucidate the anti-inflammatory activities of Tasmanian native *Clematis* spp., the present study was designed to examine their effects on inhibition of NO production from lipopolysaccharide (LPS)-stimulated Raw 264.7 cells and to undertake bioassay-guided fractionation to isolate their active constituents. The effects of *C. aristata*-L on basal (unstimulated) and LPS and phytohaemagglutinin A (PHA)-stimulated cytokine release from peripheral blood mononuclear cells (PBMC) were also investigated.

The varied inhibition of NO production by different Tasmanian *Clematis* spp. was obtained. The IC_{50} of cartridge fraction 2 of each investigated species was determined. The strongest NO inhibition effects were obtained in *C. aristata*-L, *C. aristata*-TN and *C. microphylla*-TN, whose IC_{50} of SPE cartridge fractions 2 were 0.34, 0.2 and 0.24 μg/ml, respectively. Ranunculin and its isomer were identified as two active constituents. But the IC_{50} vaule of ranunculin (0.54 μg/ml) was higher than the three most effective *Clematis* spp. SPE cartridge fractions 2. This result suggested that there may be other active constituents in those three *Clematis* spp. extracts.

C. aristata-L cartridge fraction 2 was able to significantly decrease the release of IL-1β ($P<0.01$) and TNF-α ($P<0.05$) from PBMC in the presence of LPS and PHA at 10

μg/ml. This study demonstrated *in vitro* anti-inflammatory activities of Tasmanian native *Clematis* spp.

4.1 Introduction

Arthritic diseases, such as osteoarthritis (OA) and rheumatoid arthritis (RA) are the most common inflammatory diseases.[220] They are diseases of joints, specifically the diarthrodial or synovial joints that enable movement and locomotion. OA is characterized by degeneration of articular cartilage, changes in the subchondral bone and synovial inflammation. It is by far the most common form of arthritis, with radiologic evidence of the disease detectable in 80% of individuals over the age of 75.[221, 222] By contract, RA is a systemic autoimmune disease characterized by symmetric polyarticular joint disorders that primarily affects the small joints of hands and feet.[221, 223] *Clematis* spp. have been used in TCM to treat arthritis for thousands of years. Evidence is accumulating to suggest that they have good activity in OA and RA.[3]

A number of preclinical and clinical studies worldwide have revealed the anti-inflammatory values of *Clematis* spp. mainly *C. chinensis*, *C. intricate*, *C. mandshurica*, *C. vitalba* and some Australian *Clematis* spp. including *C. pickeringii*, *C. glycinoides* and *C. microphylla*. Various kinds of saponins isolated from different *Clematis* plants were found to be the active constituents. However, saponins mainly exist in stems and roots of *Clematis* spp. Leaf of some *Clematis* plants are also used in TCM for anti-inflammatory purpose (Table 1.1). Worked by Li *et al* [133] indicated the inhibitory effects of the ethanol extract of three Australian native *Clematis* spp. to COX-1, COX-2 and 5-LOX. However, their study did not identify potential active constituents. Therefore, it is hypothesised that *Clematis* spp. native to Tasmania may have anti-inflammatory activity. There have been no investigations into the anti-

inflammatory value of Tasmanian native *Clematis* spp. This chapter mainly focused on the anti-inflammatory activities and their potential chemical constituents of Tasmanian native *Clematis* spp. leaf material.

The evaluation of the anti-inflammatory activities of Tasmanian native *Clematis* spp. was undertaken from two aspects, including inhibition of NO and influence of the release of interleukin-1 beta (IL-1β), interleukin-4 (IL-4), interleukin-10 (IL-10), tumour necrosis factor-alpha (TNF-α) and monocyte chemotactic protein 1 (MCP-1). NO and these cytokines have been reported to play important roles in OA and RA. NO production induced by LPS through iNOS expression in Raw 264.7 cells, a mouse macrophage cell line, may reflect the degree of inflammation and may provide a measure of assessing the effects of test drugs on the inflammatory process.[(224)] The screening of NO inhibiton by all collected *Clematis* spp. was undertaken and the IC_{50} was determined in our study. Through bioassay-guided fractionation, protoanemonin was isolated as one of the active constituents. In the cytokines study, the effects of *C. aristata*-L SPE cartridge fraction 2 on basal (unstimulated) and LPS- and PHA-stimulated cytokine release from peripheral blood mononuclear cells (PBMC) were investigated.

NO is an effector molecule released by murine macrophages and other cells after immunological activation. It is synthesized from the amino acid L-arginine (L-Arg) by a family of enzymes, including a constitutive NO synthase and an inducible one (Figure 4.1). The human iNOS gene contains 26 exons spanning 37kb, and was

assigned to chromosome 17cen-q11.2.[225] The expression of inducible NOS (iNOS) is induced by pro-inflammatory stimuli such as bacterial LPS or cytokines.[226-229]

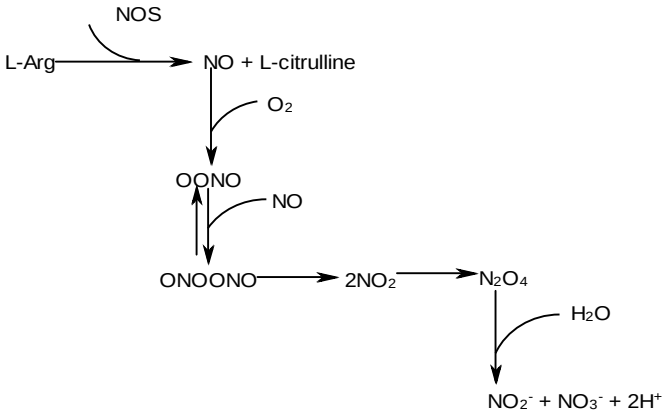

Figure 4.1 The procedure by which L-Arg produces nitrite and nitrate.

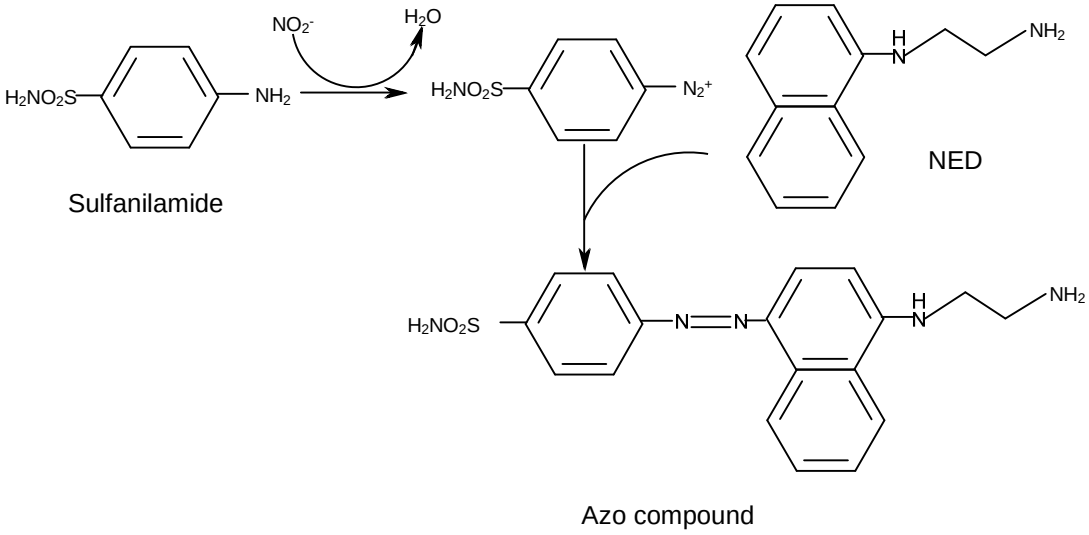

Figure 4.2 Chemical reactions involved in the measurement of nitrite using the Griess reagent system.

Griess assay was used to determine NO formation by measuring nitrite (NO_2^-), which is one of two primary, stable and non-volatile breakdown products of NO. This assay relies on a diazotization reaction that was originally described by Griess in 1879. It uses sulphanilamide and 1-N-napthylethylenediamine dihydrochloride (NED) under acidic (phosphoric acid) conditions. The chemical reaction was shown in Figure 4.2.

The UV spectrum of the azo compound determined in this study showed a range of absorbance between 420 nm and 610 nm and the maximum absorbance was exhibited at 550 nm. Therefore, the recommended a filter was between 520-550 nm. As the microplate reader in this laboratory did not have filter with that range of wavelength, absorbance was read at 490 nm. The relative strength of absorbance at 490 nm is up to 84% of the maximum absorbance.

4.2 Experimental

4.2.1 Plant material

Plant materials used in this study are the same as that described in Chapter 2. The collecting of varied ages of leaf was the same as described in Chapter 3.

4.2.2 Reagents

4.2.2.1 Extraction and isolation of plant material

Reagents for extraction and isolation of plant material were the same as reagents described in Chapter 2.

4.2.2.2 Antiinflammatory assay (Raw 264.7 Cell Line)

MTT, gentamicin, L-glutamine, and phosphate buffered saline tablets were purchased from Sigma-Aldrich (Australia). RPMI-1640, DMEM and foetal bovine serum (FBS) were purchased from Invitrogen Corporation, Australia. Tissue culture flasks, 96-well flat bottom microplates, 15 ml centrifuge tubes with triple seal cap and 50 ml centrifuge tubes with triple seal cap were purchased from Iwaki (Japan). Sterile disposable plastic pipettes (10 ml) were purchased from Sterilin (UK). Autoclavable V-shaped reagent reservoirs (70 ml) were purchased from Socorex (Switzerland).

4.2.3 Instruments

Instruments including sonicator, rotary evaporator, HPLC-UV, HPLC-ELSD, CO_2 incubator, biosafety cabinet, microscope, haemocytometer and microplate reader were the same as those described in Chapter 2.

4.2.4 Procedure of fractionation

Methods of MeOH, MeOH-DCM and DCM extraction, SPE cartridge fractionation, C18 HPLC analytical column fractionation were the same as extraction and fractionation methods used in the antitumour study which was described in Chapter 2.

4.2.5 Assays to determine the anti-inflammatory activity

4.2.5.1 Determine the inhibition of NO production by *Clematis* spp. by Griess assay

4.2.5.1.1 Cell culture

Raw 264.7 cells, which are a transformed murine macrophage cell line, were obtained from the Menzies Research Institute (UTAS, Australia). Cells were maintained by twice-weekly passage in RPMI 1640 medium supplemented with 10% FBS, L-glutamine and gentamicin.

4.2.5.1.2 Nitrite measurement (Method A)

The method followed was that described by Zhao [230] and Lee [231] with slight changes to suit our laboratory facilities. Cell aliquots of 200 µl/well (5 x 10^5 cells/ml)

were seeded in 96-well plates, and cultured for 24 hours. Then the medium was changed to serum-free DMEM for another 1 hour to render the attached cells quiescent. To assess the effects on LPS-induced NO production, 10 µl/well of *Clematis* spp. extracts were added in the absence or presence of LPS. The final concentration of LPS was 200 ng/ml in each well. Plates were incubated for a further 24 hours. As a parameter of NO synthesis, nitrite concentration was assessed in the supernatant of Raw 264.7 macrophages by the Griess reaction. Briefly, after incubation, 100 µl of cell culture supernatant was removed to a new 96-well plate. At the same time, aliquots of 3 serial diluted sodium nitrite standard solutions (100 µl/well) starting from 125 µM were added into columns 1 to 3 of the plate. Then 100 µl/well 1% sulphanilamide in 5% H_3PO_4 (SAN) was added, and the plate was kept in a dark space for 10 minutes. After that, 100 µl/well 0.1% NED in H_2O was added, then the plate was placed in dark place for 10 minutes, followed by spectrophotometric measurement at 490 nm using a Bio-Rad Model 3550 Microplate reader. The inhibition of NO production induced by LPS was calculated by the NO_2^- levels as follows:

Inhibition (%) = 100 x $(A_{untreated}-A_{sample})/A_{sample}$ where A is the absorbance. The data were expressed as mean ± standard deviation (SD) when each experiment was done independently three times. The cell viability was determined by MTT assay.

4.2.5.1.3 Nitrite measurement (Method B)

The method of this experiment was similar to 4.2.5.1.2 with a slight modification. Cell aliquots 200 µl/well (5 x 10^5 cells/ml) were seeded in 96 well plates, then

ranunculin with the concentrations of 100, 50 and 25 µg/ml was added into the plate (10 µl/well) in triplicate. The plate was incubated for 24 hours. Then cell culture supernatant was discarded and wells were washed with PBS twice. Serum-free DMEM (200 µl/well) was added into plate wells and incubated for 1 hour to render the attached cells quiescent. To assess the effects on LPS-induced NO production, LPS (at a final concentration of 200 ng/ml in each well) was added. Plates were incubated for a further 24 hours. As a parameter of NO synthesis, nitrite concentration was assessed in the supernatant of Raw 264.7 macrophages by the Griess reaction described in 4.5.5.1.2. The cell viability was determined by MTT assay.

4.2.5.1.4 Cell viability assay for Raw 264.7 cells

Cytotoxicity of extracts was measured by MTT assay. After culture, 100 µl of supernatant was removed for nitrite measurement as described above. Then MTT solution (20 µl) was added into each well containing 100 µl of Raw 264.7 cell culture. The plates were incubated at 37°C in a humidified 5% CO_2 incubator for 4 hours. Following the incubation, MTT solvent (100 µl/well) was added to dissolve the precipitate and the absorbance was read using a microplate reader at 490 nm. The percentage of suppression was calculated by comparing the absorbance of sample-treated cells with that of non-treated cells. The method of calculating cell viability was described in Chapter 2.

4.2.5.2 Inflammatory cytokine assay

The effects of CA-L SPE fraction 2 (CA-Lii) on IL-4, TNF-α, IL-1β, IL-10 and MCP-1 release from PBMC obtained from five healthy human volunteers were measured after *in vitro* exposure to the mitogens, PHA or LPS. This experiment was undertaken by a collaborator in the School of Human Life Sciences, UTAS.

Frozen cell suspensions were thawed at 37°C and centrifuged at 2000 g for 3 minutes. Pellets were washed twice in RPMI-1640 containing 10% FBS at 2000 g for 3 minutes and cell viability determined using trypan blue exclusion. Samples with viability less than 80% were discarded. Cell suspensions were resuspended in complete RPMI containing 2 mM L-glutamine, 100 U penicillin, 100 U streptomycin and 10% FBS in 24-well cell culture plates. Cells were then incubated in the absence (blank) and presence of PHA (5 µg/mL), LPS (5 µg/mL), or CA-Lii (1, 4 and 10 µg/mL) for 24 hr at 37°C in 8% CO_2 in a Heraeus HERAcell 150 incubator (Thermo Fisher Scientific, USA). Finally, cell suspensions were centrifuged at 1400 g for 6 minutes, and the supernatants collected and stored at -80°C until required.

Supernatant concentrations of TNF-α, IL-4, IL-10, TNFα, MCP-1 and IL-1β were determined using a Procarta® Cytokine Profiling Kit (Affymetrix Inc, Fremont, USA). The assay was performed according to the manufacturer's instructions and analyzed on a Luminex®100 flow cytometer (Luminex Corporation, USA). Statistical differences were determined by Student's unpaired t-test. A value of P less than 0.05 was regarded as statistically significant.

4.3 Results and Discussion

4.3.1 Screening of NO inhibition activity of *Clematis* spp.

The inhibition of NO by Tasmanian *Clematis* species was investigated by Griess assay. Five SPE cartridge fractions of CA-TN and CA-W1 leaf crude extracts were used in initial screening to determine suitable concentrations for the screening of NO inhibition of all collected *Clematis* spp. in the following stage. NO inhibition activities (inhibition%) of CA-TN and CA-W1 cartridge fractions were listed in Table 4.2. Data was expressed as mean ± SD. The concentration of nitrite in control cells culture in this experiment was determined to be 23.4 ± 3.9 µM. The concentration of nitrite in blank medium was 3.1 ± 2.3 µM. Photos of the NO inhibition effects of CA-TN from laboratory work are shown in Appendix VI.

Results in this study showed that the SPE cartridge fraction 1 and fraction 2 of *C. aristata*-TN and *C. aristata*-W1 exhibited inhibitory activities on the production of NO induced by LPS. As shown in Table 4.2, more than 50% NO inhibition was observed in *C. aristata*-TN SPE fraction 1 (57%) at 0.54 µg/ml and fraction 2 (52%) at 0.45 µg/ml; *C. aristata*-W1 SPE fraction 1 exhibited 55% inhibition of NO production at 2.05 µg/ml and SPE fraction 2 had 56% inhibition of NO production at 1.05 µg/ml. The negative control, PBS, did not show any NO inhibitory activity. Cell viabilities were determined by MTT assay and the results showed that cell viability was more than 90% of the cells in this study. SPE fractions 3, 4 and 5 did not show NO inhibition activity.

Table 4.1 NO inhibition activities and cytotoxicity of SPE cartridge fractions of CA-TN and CA-W1 leaf crude extracts (mean ± SD, n=3)

	CA-TN			CA-W1		
Sample	Conc. (µg/ml)	NO inhibition (%)	cytotoxicity (%)	Conc. (µg/ml)	NO inhibition (%)	cytotoxicity (%)
Fr 1	17.5	85 ± 2	8 ± 1	11.5	70 ± 4	1 ± 6
	8.5	78 ± 8	0 ± 1	8.3	70 ± 6	1 ± 6
	4.3	91 ± 1	4 ± 5	4.1	61 ± 7	0 ± 10
	2.2	88 ± 3	0 ± 3	2.1	55 ± 6	6 ± 4
	1.1	83 ± 4	7 ± 7	1	39 ± 6	4 ± 3
	0.54	57 ± 2	5 ± 13	0.50	27 ± 8	2 ± 6
	0.27	40 ± 12	3 ± 10	0.25	11 ± 2	3 ± 6
	0.14	4 ± 2	8 ± 3	0.13	0 ± 4	0 ± 9
Fr 2	14.5	87 ± 8	1 ± 2	10	70 ± 4	5 ± 3
	7.3	83 ± 4	0 ± 4	5.0	62 ± 4	3 ± 8
	3.6	89 ± 1	0 ± 1	2.5	65 ± 1	0 ± 3
	1.8	81 ± 3	5 ± 3	1.3	56 ± 4	3 ± 2
	0.91	68 ± 19	6 ± 1	0.63	30 ± 15	4 ± 5
	0.45	52 ± 1	3 ± 13	0.31	36 ± 2	7 ± 2
	0.23	39 ± 2	6 ± 4	0.16	12 ± 3	0 ± 4
	0.11	31 ± 11	1 ± 5	0.08	7 ± 7	2 ± 3
Fr 3	6.3	0 ± 19	0 ± 8	6.0	0 ± 5	7 ± 2
	3.1	1 ± 17	0 ± 7	3.0	10 ± 6	2 ± 3
	1.6	9 ± 3	0 ± 12	1.5	18 ± 6	3 ± 5
	0.78	15 ± 7	6 ± 4	0.75	14 ± 1	1 ± 4
	0.39	17 ± 9	5 ± 6	0.38	0 ± 6	7 ± 6
	0.19	18 ± 3	14 ± 5	0.19	5 ± 6	4 ± 10
	0.10	6 ± 6	3 ± 8	0.09	0 ± 4	3 ± 2
	0.05	0 ± 5	0 ± 19	0.05	0 ± 10	7 ± 8
Fr 4	6.3	0 ± 7	0 ± 6	5.0	0 ± 30	5 ± 2
	3.1	0 ± 6	0 ± 9	2.5	0 ± 25	0 ± 4
	1.6	5 ± 1	4 ± 7	1.3	0 ± 7	0 ± 2
	0.78	5 ± 3	0 ± 1	0.63	2 ± 11	5 ± 3
	0.39	0 ± 26	9 ± 2	0.31	0 ± 9	3 ± 5
	0.19	0 ± 14	2 ± 2	0.16	2 ± 1	2 ± 6
	0.10	0 ± 7	1 ± 4	0.08	5 ± 5	7 ± 4
	0.05	0 ± 7	4 ± 3	0.04	0 ± 7	2 ± 4
Fr 5	6.3	0 ± 3	6 ± 3	7.5	0 ± 1	2 ± 5
	3.1	12 ± 2	4 ± 10	3.8	0 ± 3.	0 ± 9
	1.6	0 ± 3	1 ± 4	1.9	0 ± 7.25	4 ± 7
	0.78	0 ± 4	0 ± 1	0.95	0 ± 7	0 ± 5
	0.39	2 ± 17	9 ± 5	0.48	0 ± 3	8 ± 3
	0.19	3 ± 27	7 ± 1	0.24	2 ± 5	3 ± 3
	0.10	5 ± 3	0 ± 3	0.12	4 ± 10	2 ± 3
	0.05	1 ± 7	2 ± 3	0.08	0 ± 7	3 ± 4
PBS	10µl	0 ± 5	3 ± 6	10µl	0 ± 8	4 ± 4

Results in this experiment also showed that the NO inhibitory activity of CA-TN was stronger than CA-W1. At the concentration of around 1 µg/ml, the effect of NO inhibition produced by CA-TN SPE fraction 1 (82%) was 2 times stronger than that produced from CA-W1 SPE fraction 1 (38%). At the concentration of 0.27 µg/ml of CA-TN SPE fraction 1 and 0. 25 µg/ml of CA-W1 SPE fraction 1, the percentage of NO inhibition was 40% and 11%, respectively. The same pattern of activity was observed in the SPE cartridge fraction 2 of both *Clematis* spp. Based on the data from this experiment, concentrations of 1 and 0.2 µg/ml of *Clematis* spp. SPE fractions were chosen for further screening of *Clematis* spp. extracts. The screening results are shown in Table 4.3. Data was expressed as mean ± SD. The concentration of nitrite in control cells culture in this experiment was detected as 28 ± 9 µM. The concentration of nitrite in blank medium was 4 ± 3 µM.

Table 4.2 The NO inhibition activity of Clematis spp. SPE cartridge fractions 2 (1 µg/ml and 0.2 µg/ml) determined by the nitrite concentration in Raw 264.7 cell culture and the Raw 264.7 cell cytotoxicity of these fractions. The results of NO inhibition are expressed as percentage of NO inhibition compared with control 264.7 cell culture (NO inhibition%). The results of Raw 264.7 cell cytotoxicity are expressed as cytotoxicity%. Assay was undertaken in triplicate and data are expressed as mean ±SD.

Plant	SPE	1 µg/ml		0.2 µg/ml	
	fraction	NO inhibiton %	cytotoxicity %	NO inhibiton %	cytotoxicity %
CA-L 1	fraction 1	35 ± 4	11 ± 4	20 ± 1	5 ± 14
	fraction 2	51 ± 3	3 ± 6	18 ± 2	0 ± 1
	fraction 3	15 ± 1	1 ± 6	7 ± 1	0 ± 4
	fraction 4	22 ± 3	6 ± 7	2 ± 1	0 ± 6
	fraction 5	19 ± 1	2 ± 9	4 ± 1	9 ± 9
CA-L 2	fraction 1	17 ± 6	9 ± 8	8 ± 4	5 ± 9
	fraction 2	23 ± 0	7 ± 6	15 ± 3	0 ± 8
	fraction 3	0 ± 3	2 ± 5	0 ± 6	9 ± 3
	fraction 4	0 ± 4	9 ± 8	0 ± 3	16 ± 4
	fraction 5	19 ± 3	0 ± 4	16 ± 1	6 ± 2

Table 4.2 (continued)

Species	Samples	1 µg/ml		0.2 µg/ml	
		NO inhibiton %	cytotoxcity %	NO inhibiton %	cytotoxicity%
CA-L 3	fraction 1	88 ± 5	0 ± 7	27 ± 6	7 ± 4
	fraction 2	82 ± 9	2 ± 2	32 ± 3	5 ± 5
	fraction 3	0 ± 3	3 ± 3	0 ± 3	4 ± 6
	fraction 4	5 ± 2	13 ± 4	1 ± 9	5 ± 2
	fraction 5	11 ± 4	0 ± 4	13 ± 6	2 ± 2
CA-L 4	fraction 1	22 ± 2	0 ± 19	15 ± 2	8 ± 12
	fraction 2	69 ± 4	0 ± 20	28 ± 4	10 ± 15
	fraction 3	22 ± 1	0 ± 17	5 ± 2	4 ± 9
	fraction 4	20 ± 3	6 ± 13	12 ± 1	16 ± 10
	fraction 5	13 ± 5	8 ± 14	10 ± 3	8 ± 13
CA-L 5	fraction 1	8 ± 2	0 ± 17	7 ± 1	3 ± 6
	fraction 2	54 ± 3	9 ± 1	14 ± 1	11 ± 8
	fraction 3	23 ± 5	15 ± 3	12 ± 5	17 ± 5
	fraction 4	11 ± 4	20 ± 9	12 ± 3	18 ± 18
	fraction 5	0 ± 0	0 ± 0	0 ± 0	0 ± 0
CA-TN	fraction 1	72 ± 8	0 ± 16	7 ± 7	0 ± 13
	fraction 2	87 ± 5	0 ± 11	34 ± 18	0 ± 16
	fraction 3	15 ± 4	0 ± 10	22 ± 4	1 ± 14
	fraction 4	0 ± 5	0 ± 7	0 ± 13	0 ± 9
	fraction 5	7 ± 8	8 ± 4	12 ± 3	15 ± 25
CA-TN1	fraction 1	62 ± 5	9 ± 7	13 ± 5	8 ± 10
	fraction 2	100 ± 3	15 ± 4	56 ± 3	12 ± 10
	fraction 3	8 ± 3	24 ± 8	6 ± 1	15 ± 10
	fraction 4	1 ± 7	22 ± 13	2 ± 3	15 ± 7
	fraction 5	0 ± 5	18 ± 8	0 ± 2	21 ± 6
CA-W1	fraction 1	5 ± 4	12 ± 4	3 ± 8	12 ± 4
	fraction 2	60 ± 3	12 ± 13	22 ± 7	8 ± 15
	fraction 3	0 ± 2	1 ± 2	0 ± 3	0 ± 19
	fraction 4	13 ± 2	6 ± 9	13 ± 9	0 ± 7
	fraction 5	22 ± 4	7 ± 8	7 ± 3	9 ± 5
CA-W2	fraction 1	13 ± 12	11 ± 9	3 ± 2	7 ± 9
	fraction 2	24 ± 9	8 ± 8	5 ± 3	8 ± 4
	fraction 3	0 ± 4	6 ± 8	0 ± 13	4 ± 5
	fraction 4	4 ± 6	0 ± 4	5 ± 4	6 ± 3
	fraction 5	11 ± 13	0 ± 7	9 ± 3	3 ± 18

Table 4.2 (continued)

Species	Samples	1 µg/ml		0.2 µg/ml	
		NO inhibiton %	cytotoxicity %	NO inhibiton %	cytotoxicity %
CA-EN	fraction 1	0 ± 7	5 ± 9	0 ± 12	0 ± 14
	fraction 2	18 ± 8	0 ± 9	6 ± 24	0 ± 1
	fraction 3	17 ± 7	0 ± 15	5 ± 9	0 ± 3
	fraction 4	4 ± 10	0 ± 13	7 ± 10	0 ± 2
	fraction 5	9 ± 7	0 ± 8	9 ± 13	0 ± 5
CA-W3	fraction 1	4 ± 13	0 ± 19	4 ± 6	0 ± 18
	fraction 2	13 ± 4	0 ± 8	6 ± 3	1 ± 11
	fraction 3	7 ± 9	8 ± 8	0 ± 4	0 ± 7
	fraction 4	14 ± 2	0 ± 16	7 ± 3	0 ± 6
	fraction 5	17 ± 2	4 ± 5	5 ± 3	14 ± 4
CM-TN	fraction 1	36 ± 5	4 ± 3	11 ± 2	3 ± 4
	fraction 2	95 ± 4	3 ± 1	32 ± 3	1 ± 2
	fraction 3	11 ± 5	4 ± 5	5 ± 10	5 ± 1
	fraction 4	1 ± 5	1 ± 6	2 ± 7	3 ± 3
	fraction 5	1 ± 7	1 ± 4	3 ± 4	3 ± 3
CM-B	fraction 1	14 ± 22	0 ± 5	6 ± 14	0 ± 1
	fraction 2	23 ± 8	3 ± 13	8 ± 3	1 ± 14
	fraction 3	9 ± 2	3 ± 5	10 ± 5	5 ± 7
	fraction 4	13 ± 7	9 ± 10	18 ± 11	8 ± 11
	fraction 5	5 ± 14	4 ± 7	14 ± 18	3 ± 8
CG-UTAS	fraction 1	36 ± 12	0 ± 6	25 ± 9	0 ± 21
	fraction 2	64 ± 19	0 ± 10	25 ± 15	0 ± 21
	fraction 3	25 ± 9	8 ± 5	21 ± 7	3 ± 17
	fraction 4	23 ± 11	7 ± 4	8 ± 10	2 ± 10
	fraction 5	12 ± 17	0 ± 13	6 ± 22	0 ± 19
CV-RS	fraction 1	10 ± 4	6 ± 4	3 ± 13	9 ± 6
	fraction 2	9 ± 9	0 ± 21	11 ± 4	0 ± 11
	fraction 3	12 ± 14	1 ± 6	17 ± 9	2 ± 7
	fraction 4	6 ± 25	0 ± 20	8 ± 26	1 ± 12
	fraction 5	4 ± 20	0 ± 10	0 ± 19	2 ± 1
PBS	1	12 ± 7	0 ± 9	12 ± 6	4 ± 5
	2	0 ± 6	14 ± 17	1 ± 8	14 ± 8
	3	4 ± 12	0 ± 1	0 ± 10	0 ± 15

The NO inhibitory activities were varied in different *Clematis* SPE cartridge fractions. NO inhibitory effects produced by each fraction 2 of investigated *Clematis* spp. was stronger than other fractions. When the inhibition produced by 1 µg/ml of each fraction was compared, CA-L 1, 3, 4 and 5, CA-TN and –TN1, CA-W1 and CG-UTAS produced more than 50% of NO inhibition. Fractions sequenced from strong to weak are presented in Figure 4.3.

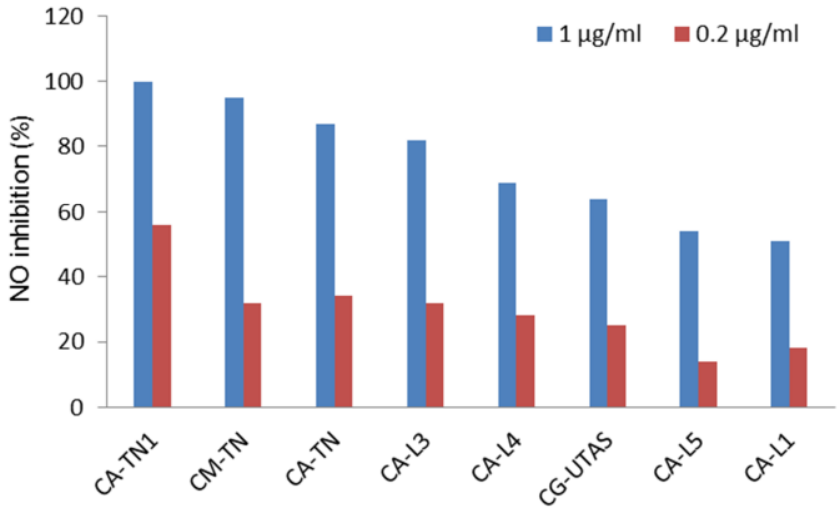

Figure 4.3 Sequence of NO inhibition (%) by *Clematis* spp. SPE fractions 2 from strong to weak. Data excludes the SPE fractions 2 at 1 µg/ml producing less than 50% of NO inhibition.

Figure 4.3 showed that CA-TN1 SPE cartridge fraction 2 (CA-TN1ii) had the strongest NO inhibitory effect, with 100% NO inhibition at 1 µg/ml and 56% at 0.2 µg/ml. In this study, we also investigated the NO inhibitory activity of CA-L leaves at different ages. From young to old they were marked as 1 to 5. Figure 4.3 also showed that the NO inhibitory effects varied from young to old leaf. In fractions 2, the strongest inhibitory activity was obtained in age 3, giving 82% of NO inhibition

at 1 μg/ml. Leaf age 2 showed the weakest NO inhibitory activity, whose NO inhibition% is 23% at 1 μg/ml. Fractions 1 of CA-L-1 (35%) and 3 (88%) also inhibited NO production (Table 4.3). Cell viabilities were determined by MTT assay.

A relatively large standard deviation was obtained in the Griess assay. Relative standard deviation of NO inhibition obtained from this experiment was between 1 and 26. We speculated that this was caused by the following factors.

The amount of NO formation induced by LPS in cultured murine macrophages was affected by the pH of the medium. NO formation by iNOS in LPS-activated murine macrophages is optimal at pH 7.2. The environmental pH affects both transcriptional and posttranscriptional factors that influence inducible NO formation. Acidosis favors expression of iNOS mRAN and alkalosis favors expression of iNOS. The optimal pH necessary for NO production appears to be a balance between alkalosis promoting expression of iNOS protein and acidosis promoting expression of iNOS mRNA. [(232)] The pH value of freshly prepared completed RPMI-1640 medium was around 7.2, but the pH of the medium gradually increased following storage at 4°C. This experiment was undertaken 2 times, the second after storage leading to a slight difference in the pH. We observed that the maximum control NO produced in freshly prepared complete medium (38 μM) in our experiments was much higher than in the medium stored at 4°C for 10 days (14 μM). Once this was discovered, the completed medium used in the following work was freshly prepared (within 3 days).

In the Griess assay, the RPMI-1640 medium was changed to DMEM that did not contain FBS for several reasons. Nitrite level in the medium is affected by endotoxin and ferric nitrate.[230, 232] Endotoxin contained in FBS is able to inhibit the induction of iNOS. Nitrate would swamp any small amount of NO oxidized to nitrate. DMEM contains 0.1 mg/L of ferric nitrate, but RPMI-1640 contains 100 mg/ml of calcium nitrate, which is 1000x the nitrate content in DMEM.

The NO inhibitory effects of crude extracts of *Clematis* spp. were not investigated in this study. The purpose of our study was isolation and identification of the anti-inflammatory constituents in *Clematis* spp. and the isolation methods included solvent extraction, SPE cartridge fractionation and HPLC column fractionation. In the anti-inflammatory study, we screened the anti-inflammatory effects of cartridge fractions of all collected *Clematis* spp. without first investigating the NO inhibition by the crude extracts. The assumption made was that skipping the analysis of *Clematis* spp. crude extracts did not result in the failure to detect antiinflammtory compounds.

4.3.2 IC_{50} of SPE of *Clematis* spp. cartridge fractions 2

As the previous screening results of SPE fraction 1 to fraction 5 demonstrated that each fraction 2 had stronger activity than the other fractions, the IC_{50} of each SPE cartridge fraction 2 of each species was determined. The dose-response curves are shown in Figure 4.4.

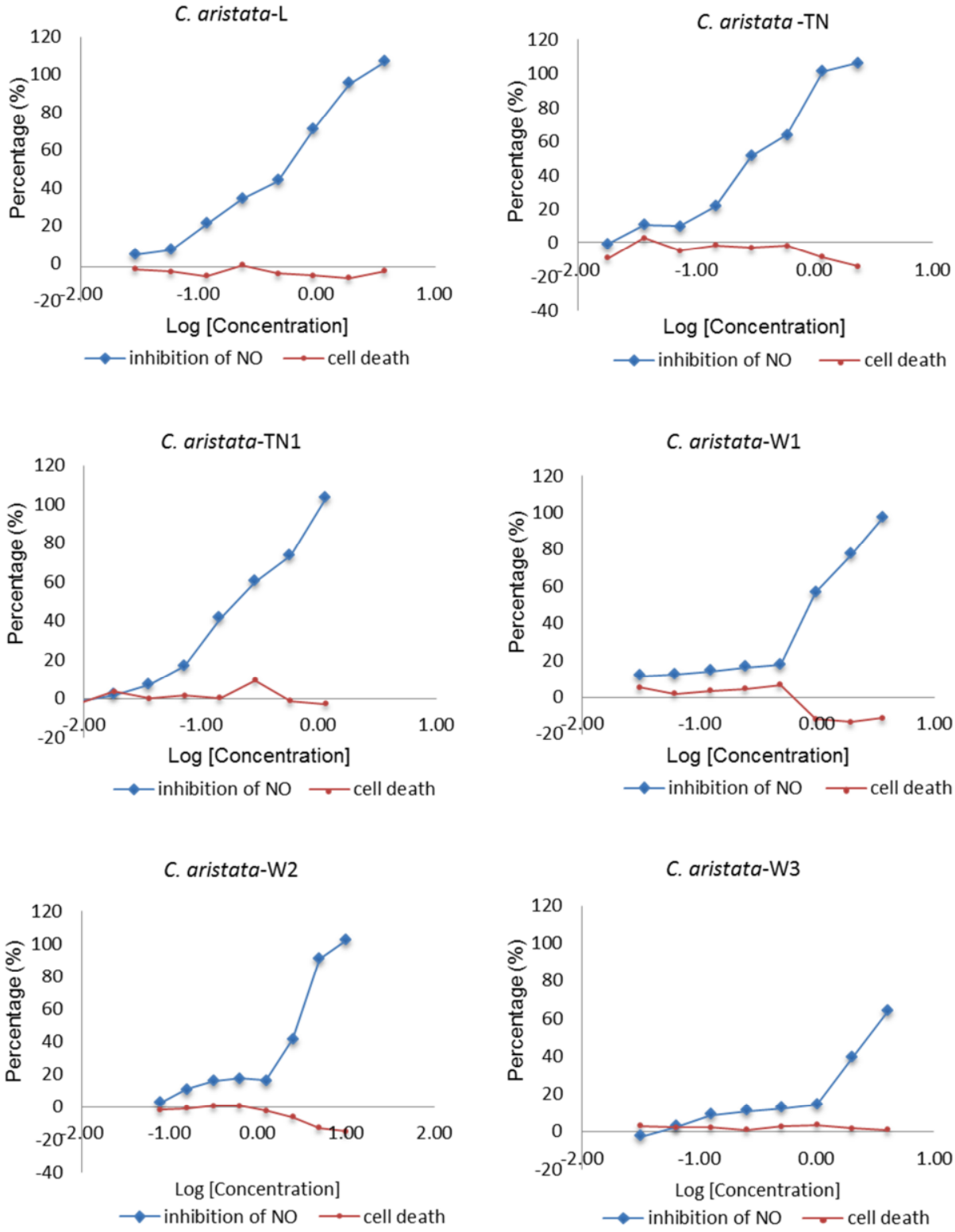

Figure 4.4 Dose-response curves of SPE cartridge fraction 2 of *Clematis* spp. by ploting the concentration of SPE cartridge fraction 2 (log [Dose]) versus the inhibition% NO production by LPS stimulated Raw 264.7 cells (blue). Cell viabilities of Raw 264.7 cells in each well are also plotted as cell death % (red).

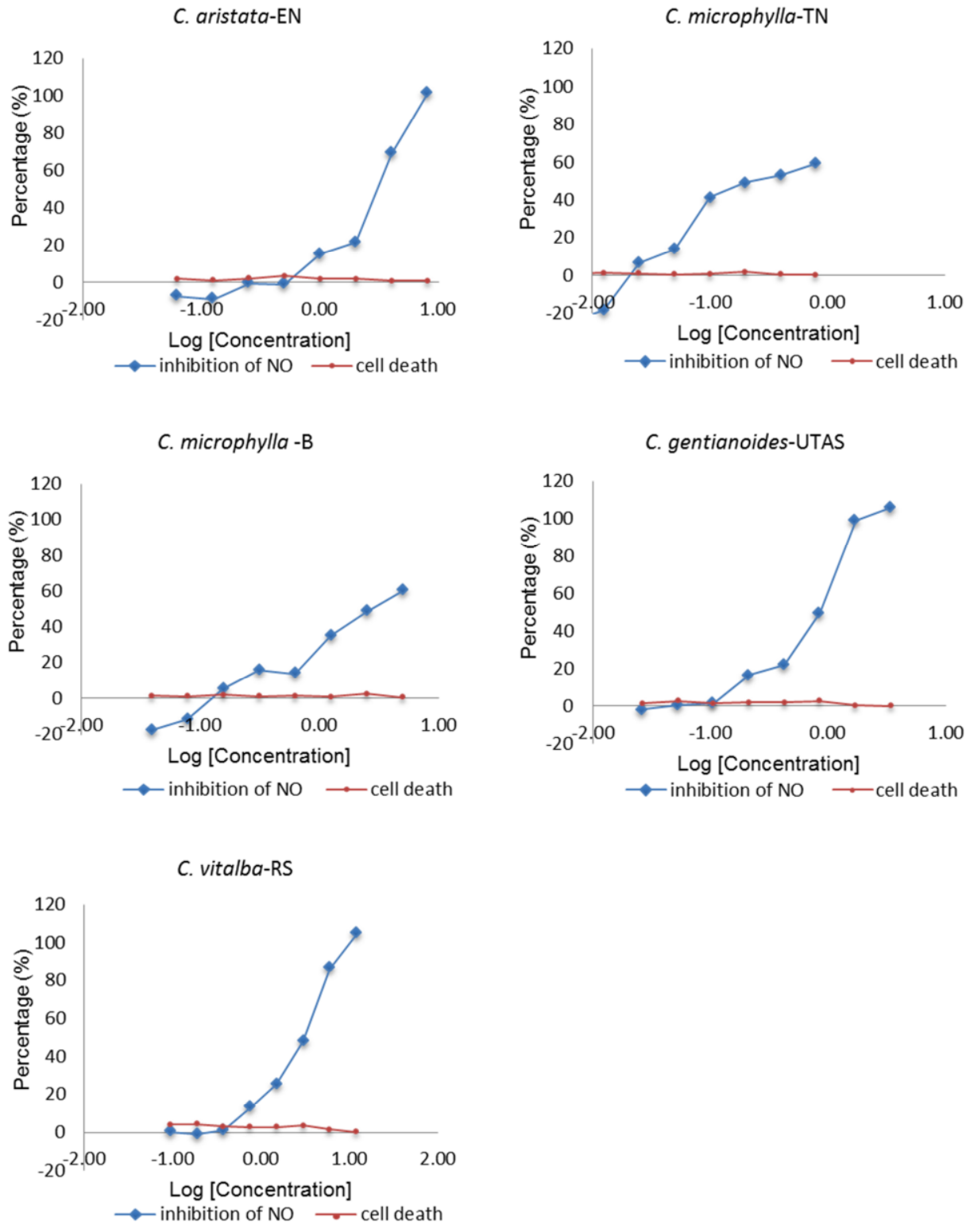

Figure 4.4 (continued)

In the Griess assay, NO production was measured as nitrite concentration. The percentage of NO inhibition of each sample was calculated by comparing the amount of NO produced by vehicle control of cell culture with that obtained from cells cultured in the presence of test substances. Without LPS, Raw 264.7 cells released undetectable levels of NO after 24 hours incubation (data not shown). When LPS was added to Raw 264.7 cells, NO produced in cell culture was 25 ± 2 μM. PBS, which was used to dissolve fractions, did not affect the NO production induced by LPS. As shown in Figure 4.4, fraction 2 of each *Clematis* spp. extract in various concentrations attenuated NO production in concentration-related manner. The IC_{50} of each fraction 2 for inhibition of NO production was calculated from the equation which was set up by the linear trendline using the percentage (%) data on dose-response curves where the 50% of NO inhibitory was included in the trendline. The IC_{50} values are shown in Figure 4.5.

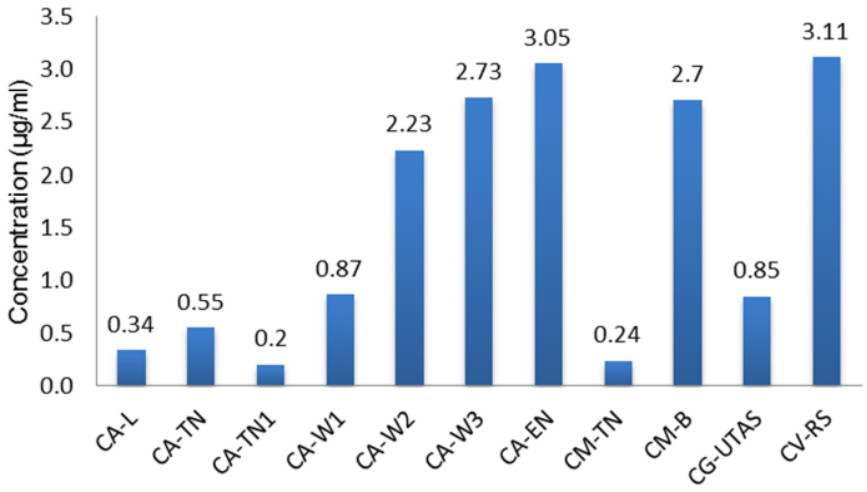

Figure 4.5 The IC_{50} values for *Clematis* spp. (extract SPE fraction 2) for inhibition of NO production from LPS stimulated Raw 264.7 cells.

The MTT assay was used to detect the cytotoxicity of the test fractions against Raw 264.7 cells. Results indicated that both various concentrations of *Clematis* spp. SPE fractions 2 (0.01-10.5 μg/ml) and vehicle control in the presence of LPS had no adverse effects on the viabilities of Raw 264.7 macrophages.

Figure 4.5 shows differences in IC_{50} for NO inhibition for each *Clematis* spp. SPE fraction 2. The strongest activity was obtained from CA-TN1, whose IC_{50} was 0.2 μg/ml. The one with lowest effect was CV-RS (3.11 μg/ml). The inhibitory effects from high to low were sequenced as CA-TN1 > CM-TN > CA- L > CA-TN > CG-UTAS > CA-W1 > CA-W2 > CM-B > CA-W3 > CA-EN > CV-RS. A positive control was not employed in this experiment as the target of study in this stage was to isolate the active constituents.

A study by Lee and co-workers reported that the IC_{50} of *C. crassifolia* extract inhibiting NO produced by LPS stimulated Raw 264.7 cells was 1.60 ± 0.28 mg/ml.[231] The ethanol extract of *C. mandshurica* root at 100 μg/ml was found to significantly block the production of NO in LPS -stimulated mouse peritoneal macrophages by up to 77%.[233] Besides *Clematis* spp., *Ventilago maderaspatane*, *Rubia cordifolia* and *Lantana camara* were reported to have an IC_{50} values of 168.3, 153.7 and 145.3 μg/ml, respectively. The positive control of curcumin had an IC_{50} of 6.8 μg/ml.[234] SKI306X, an extract purified from a mixture of three Oriental herbal medicines (*C. mandshurica, Trichosanthes kirilowii* and *Prunella vulgaris*), was studied in Korea for anti-inflammatory and analgesic efficacy. Its IC_{50} for inhibition

of NO production was 280 ± 17.8 µg/ml.[144] In our study, the IC_{50} value of 6 out of 11 species was below 1 µg/ml, and the NO inhibitory activity of all investigated effective *Clematis* spp. extracts was higher than the reported IC_{50} of curcumin.

4.3.3 Bio-active fractionation by HPLC column

To identify the active agents in *Clematis* spp., the fractionation of SPE cartridge fractions 2 of CA-L (CA-Lii), -TN1 (CA-TN1ii) and CM-TN (CM-TNii) by C18 HPLC column was undertaken to obtain 56 HPLC fractions. The inhibitory activities of NO production by these HPLC fractions were presented in Figure 4.6. Each sample was tested in duplication and results were expressed as mean.

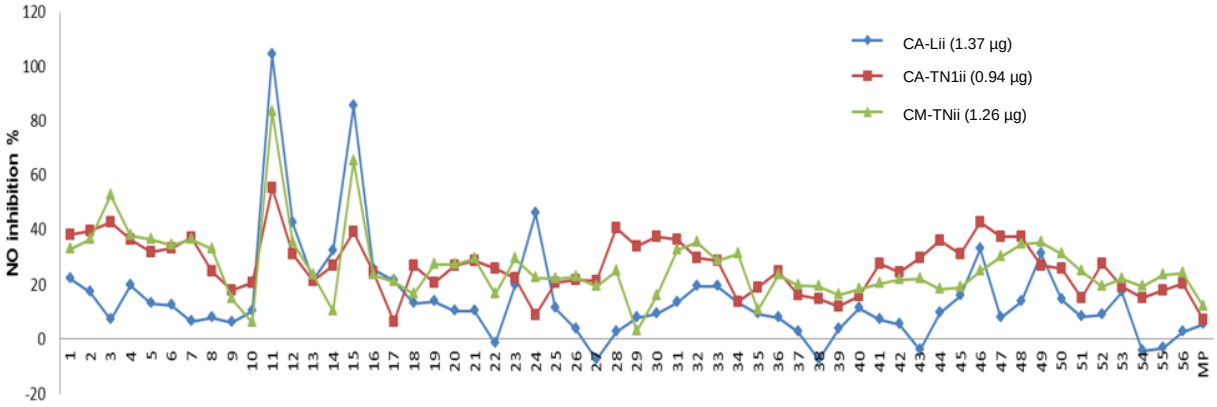

Figure 4.6 Inhibition of NO production (NO inhibition%) by HPLC fractions of CA-Lii, CA-TN1ii and CM-TNii. Blue lines represent the NO inhibitory produced by CA-Lii HPLC fractions. Amount of CA-Lii is 1.37 µg. Red lines represent the NO inhibitory produced by CA-TN1ii HPLC fractions. Amount of CA-TN1ii is 0.94 µg. Green lines represent the NO inhibitory produced by CM-TNii HPLC fractions. Amount of CM-TNii is 1.26 µg.

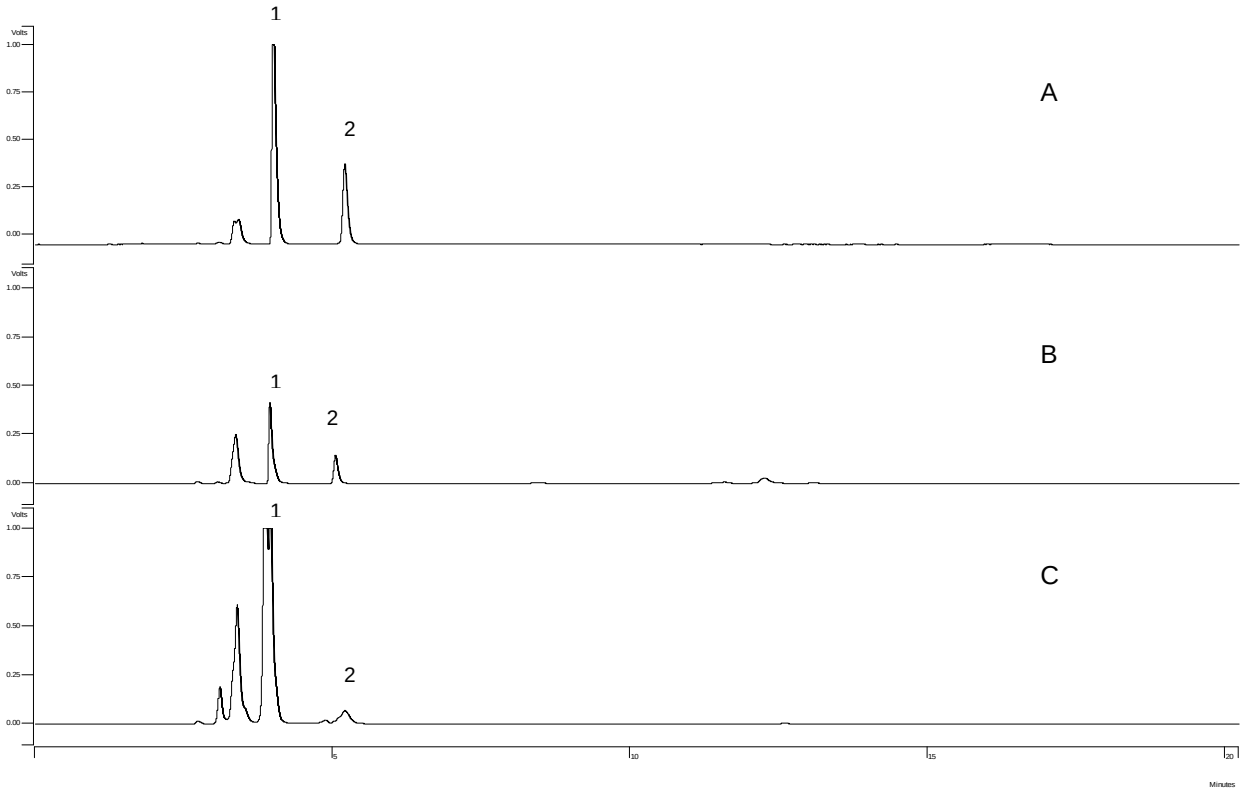

Figure 4.7 HPLC-ELSD chromatograms of *Clematis* spp. SPE cartridge fractions 2. A is CM-TNii. B is CA-TN1ii and C is CA-Lii. Amount of each *Clemaits* spp. was 10 µg.

In this experiment, the concentration of nitrite in control cell culture was found to be 23.8 µM. The concentration of nitrite in blank medium was 0.3 µM. The Raw 264.7 cell viabilities were more than 90% for all fractions tested (data not shown). Data in Figure 4.6 exhibited that fractions 11 and 15 had higher NO inhibition (%) than other fractions in the three investigated *Clematis* spp. The chromatographic peaks in fractions 11 and 15 correspond to peak 1 and 2 in Figure 4.7. In previous LC-MS analysis of CA-Lii *and* CM-TNii in Chapter 2, peak 1 and 2 were ranunculin and one of its isomers. This suggests that the NO inhibitory activities of HPLC fraction 11 and fraction 15 were contributed to by ranunculin and its isomer.

Excluding HPLC fractions 11 and 14, the NO inhibitory effects of the other 54 fractions in the investigated *Clematis* spp. are summarized in Figure 4.8.

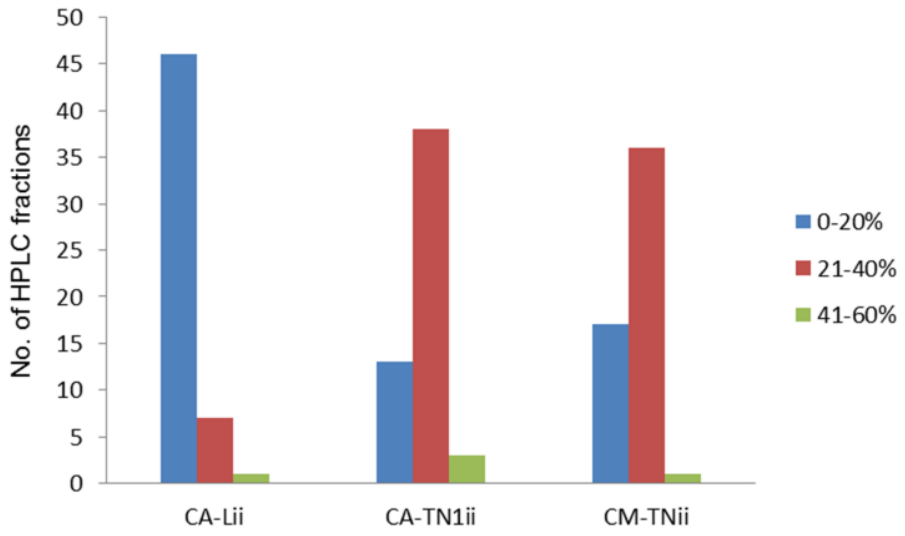

Figure 4.8 Distribution of NO inhibitory activities of CA-Lii, CA-TN1ii and CM-TNii HPLC fractions (except fractions 11 and 15). Blue represents fractions having NO inhibition (%) between 0-20%. Red represents fractions having NO inhibition (%) between 21-40%. Green represents fractions having NO inhibition (%) between 41-60%.

Data in Figure 4.8 showed that the number of fractions with NO inhibitory more than 20% obtained in CA-TN1ii and CM-TNii was more than those obtained in CA-Lii. This result suggests that it is likely exist other active consitiuents in CA-TN1ii and CM-TNii. As shown in Figure 4.7, there were no large, and only a few minor peaks evident in the chromatograms after peak 2. ELSD is proportional to the mass of compound, therefore, results in this experiment also suggested that if active constituents existed in other active HPLC fractions, their potencies were higher than ranunculin and its isomer.

Ranunculin and one of its isomers were two of the effective compounds, but it seems that there were other active constituents. The number of HPLC fractions of CA-TN1ii and CM-TNii having NO inhibition% in the range of 21-60% were more than CA-Lii, which would contribute that CA-TN1ii and CM-TNii had lower value of IC_{50} than CA-Lii, since there are other active constituents, which inhibit NO production, in CA-TN1ii and CM-TNii.

Hyun-Woo *et al.*[235] reported the NO inhibitory activity of phenolic compounds from the fruit of *Actinidia arguta*. The reported IC_{50} values of protocatechuic acid, caffeic acid, caffeoyl-β-D-glucopyranoside, esculetin, quercetin, quercetin 3-*O*- β-D-glucopyranoside were 52.27, 27.95, 73.09, 64.77, 17.40 and 41.99 μg/ml, respectively. The investigated *Clematis* spp. contain unknown phenolic compounds and some of these are identified as caffeic acid based phenolic compounds. They will be described in chapter 5. It is suspected that these unknown phenolic compounds might contribute to the NO inhibitory activities.

Results in this study revealed that ranunculin and its isomer were two active constituents in Tasmanian *Clematis* spp. to inhibit NO produced by LPS stimulated Raw 264.7 cells. Therefore, the effect of ranunculin on inhibition of NO production was investigated in the following work.

4.3.4 The activity of inhibition of NO production by ranunculin

4.3.4.1 Effect of ranunculin inhibiting NO production

The dose response curve for ranunculin (0.04-5 µg/ml) follows a concentration-dependent relationship, as shown in Figure 4.9.

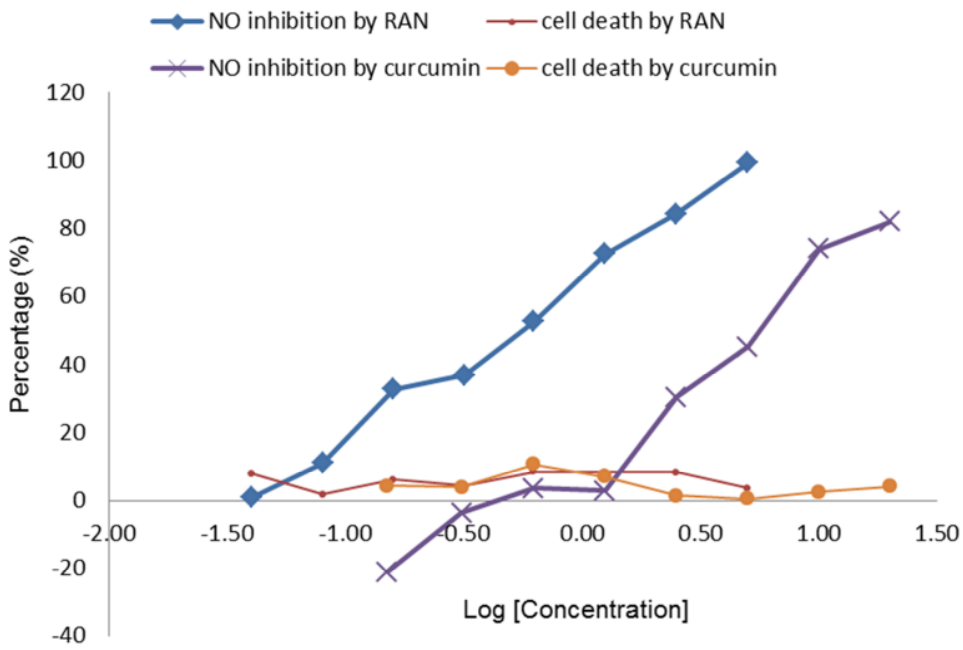

Figure 4.9 The dose-response curves of ranunculin (RAN) and curcumin for NO inhibitory activity. Percentage of NO inhibition (percentage%) versus the concentration (Log[Concentration]) of ranunculin (blue) and curcumin(purple), respectively, are ploted. The cytotoxicity of ranunculin (red) and curcumin (orange) against Raw 264.7 cells are also ploted. Data shows percentage (%).

The value of IC_{50} of ranunculin was determined as 0.54 µg/ml. Curcumin was employed as a positive control in this experiment and its IC_{50} was 5.60 µg/ml. The results revealed that the NO inhibitory activity of ranunculin was almost 10 times higher than curcumin. Cell viabilities of both ranunculin and curcumin treated cells were more than 90%.

Lee *et al.*[231] reported that anemonin was the potent and selective iNOS inhibitor in *C. crassifolia*. The IC_{50} of anemonin inhibiting NO production by LPS stimulated Raw 264.7 cells was 5.37± 0.39 μM. In this study, the IC_{50} of ranunculin was 7.67 μM, which is similar to the NO inhibitory activity of anemonin.

The mechanism of anemonin inhibiting NO production reported from Lee *et al.*[231] study was the suppression of NO production by inhibition of iNOS protein expression. The expression of iNOS is mainly regulated at the transcriptional level. Lee *et al*[231] also reported that the highest increases of iNOS mRNA expression were obtained after LPS stimulation for 6 hours. After 6 hours treatment, anemonin markedly suppressed the LPS-induced iNOS mRNA levels in a concentration-dependent manner without affecting mRNA expression for GAPDH, a house-keeping gene product. Their study also exhibited that anemonin did not modify the activity of eNOS.

As discussed previously, NO is synthesised from the semi-essential amino acid L-arginine by the action of a family of isoenzymes known as NO synthase (NOS).[228] There are three NOS isoforms, namely endothelial, neuronal and inducible. Two Ca^{2+}/calmodulin-dependent isoforms (endothelial and neuronal) are constitutively expressed in endothelium of blood vessels and the neurons of the brain. These isoforms synthesize small amounts of NO in response to various agonists that increase intracellular Ca^{2+}. The high output isoform, iNOS, is expressed in various cell types following its transcriptional induction.[236] LPS is the most important

stimulus for induction of iNOS.[237, 238] LPS-elictited induction of arterial iNOS results in subsequent overproduction of NO, which causes vascular hyporesponsiveness to vasoconstrictors, vascular damage, and disseminated intravascular coagulation. This ultimately leads to multiple organ dysfunction and death.[239, 240] Non-selective NOS inhibitors may increase organ ischemia and mortality in experiment models of endotoxic shock.[241] The results might be contributed to by the inhibition of eNOS, which is constitutively present in the endothelial cells and produces physiological levels of NO, leading to the maintenance of vascular tone via its antioxidant and vasorelaxant effects.[242] Therefore, it was postulated that pharmacological inhibition of selective iNOS might be of therapeutic value to improve the vascular hyporeactivity in LPS-induced inflammation.

The study by Lee *et al.*[231] evidenced that anemonin was able to inhibit iNOS expression. Anemonin is the dimer of protoanemonin, and ranunculin is the glucoside of protoanemonin. Although the study to evaluate iNOS expression has not been undertaken, it is possible that one of the mechanisms of ranunculin inhibition of NO production would be the suppression of NO production by inhibiting iNOS protein expression. The previous work described in the antitumour and antibacterial Chapters demonstrated that ranunculin has cytotoxic activity against P388 cells and some bacteria. Therefore, we hypothesise that ranunculin at a very low concentration was able to influence Raw 264.7 cells possibly by the action on iNOS, leading to the decreased release of NO after LPS stimulation.

In this study, the persistent NO inhibition of ranunculin on Raw 264.7 cells was determined. The inhibition of NO production determined by the Griess assay using method B was compared with method A (Figure 4.10). Method A and B were respectively described in 4.2.5.1.2 and 4.2.5.1.3. The main difference between method A and B in this experiment was the way of adding ranunculin. In method A, ranunculin was added into a 96-well microplate after an initial 24 hours incubation of cell culture, followed by a further 24 hours incubation. In method B, ranunculin was added into plates before the initial 24 hours incubation. Then cell culture supernatant was discarded and wells were washed by PBS twice, followed by a further 24 hours incubation with media not containing ranunculin.

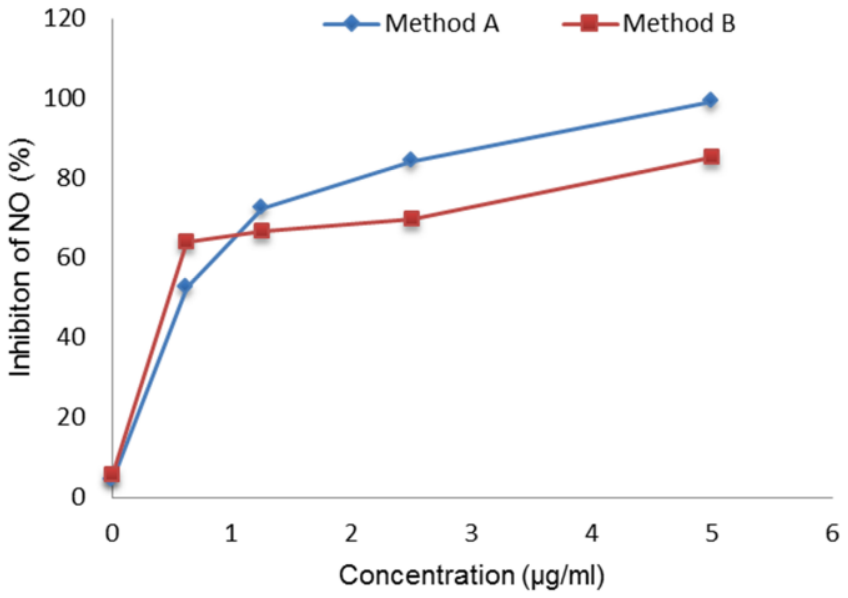

Figure 4.10 The NO inhibitory activity of ranunculin (inhibition of NO%) determined by two methods. Five concentrations of ranunculin were employed in this study. Blue is the curve showing the percentage of NO inhibition by these 5 concentrations of ranunculin using method A. Red is the curve showing the percentage of NO inhibition by these 5 concentrations of ranunculin using method B.

Results in Figure 4.10 showed that the NO inhibition effects of ranunculin determined by both methods were the same. At 5 µg/ml of ranunculin, the percentage of NO inhibition was only decreased 14% in method B compared with method A. At 2.5 and 1.25 µg/ml of ranunuclin, this decrease was respectively 15% and 6%. At 0.625 µg/ml of ranunculin, the percentage of NO inhibition was increased 12% from method B to method A. This result suggested that Raw cells did not recover their ability to produce NO for 24 hours after removal of ranunculin. From the previous results in Chapter 2, ranunculin could be hydrolysed to protoanemonin by DMEM and RPMI-1640 medium. In this study, we proposed that the NO inhibitory activity of ranunculin was contributed to by protoanemonin. The result in the study is likely to be contributed to by protoanemonin permanent (covalent binding) inhibition of iNOS.

Anemonin is the dimer of protoanemonin, and ranunculin is the glucoside of protoanemonin. Based on the comparison of chemical structure of ranunculin, anemonin and protoanemonin and results of stability of ranunculin in medium described in Chapter 2, it is suspected that the NO inhibitory mechanism, whether ranunculin or anemonin, was contributed to by protoanemonin. It is possibly related to the reaction of protoanemonin with –SH groups, which might exist in iNOS mRNA.

NO is an important regulatory and effector molecule with various biological functions. It exhibits a wide range of important functions *in vivo*, acting as a releasing

factor mediating vasodilation, as a neuronal messenger molecule, and as a major regulatory molecule and principal cytotoxic mediator of the immune system. NO has been implicated as playing a role in many pathological conditions, including allergic airway diseases, pneumonitis, vasculitis, acute rejection of allograft and toxic shock syndrome.[243-249] Macrophages play major roles in inflammation and host defence mechanisms against bacterial and viral infections.[250] During acute and chronic inflammation, excessive production of NO may cause severe injury to host cells and tissues.[251] Furthermore, NO is known to cause mutagenesis and deamination of DNA bases[252] and play an important role in the formation of carcinogenic N-nitroso compounds in vivo.[253] NO rapidly and spontaneously reacts with triplet oxygen ($^3O_2$) to form stable anoins, nitrite and nitrate.[254] These compound non-enzymatically N-nitrosylate primary and secondary amines to produce carcinogenic nitrosamines.[253] Moreover, under inflammatory conditions, macrophages can greatly increase their production of both NO and the superoxide anion (O_2^-) stimultaneously, which rapidly react with each other to form the peroxynitrite anion ($ONOO^-$), and thus play a role in inflammation and also possible in the multistage process of carcinogenesis.[255] The peroxynitrite anion activates the constitutive and inducible forms of cyclooxygenase (COX-1 and COX-2, respectively), which are rate-determining enzymes for prostaglandin biosynthesis during the inflammatory process.[256]

More evidence is accumulating that NO is produced locally within human osteoarthritic and rheumatoid joints. Inflammation and loss of articular cartilage are

two main pathophysiological processes that predominate in arthritic joints. By observing that articular chondrocytes produce large amounts of NO in response to interleukin-1 (IL-1) and endotoxin, Stadler and his co-workers provided the first evidence implicating NO in joint disease.[257] Further evidence supports NO involvment in human arthritis. Articular chondrocytes can be reproducibly stimulated to produce large amounts of NO. Biochemical studies confirm that NOS is expressed at high levels in human articular cartridge obtained from patients with OA but not in cartilage obtained from normal individuals.[258] Studies from Farrell *et. al*[259] showed that concentrations of nitrite and nitrate are elevated within synovial fluids obtained from patients with RA and OA. These elevations probably reflect quite high levels of local NO production. Ialenti *et al.*[260] found that T lymphocytes recovered from adjuvant rats treated with $_{L}$-N^{G}-nitro arginine methyl ester, an inhibitor of NO synthase, had reduced reactivity to antigen, suggesting a role for NO in immune recognition of arthritogenic epitopes.

NO is not only related to joint inflammation, but also plays roles in cartilage loss. Loss of articular cartilage may result from increased matrix catabolism, decreased anabolism, or both. Although the mechanisms are presumed to be complicated, one of the factors might involve certain cytokines, especially IL-l, that induce NO production in articular chondrocytes.[257, 261] Studies with human[262] and rabbit[263] cartilage have confirmed that NO suppresses the synthesis of cartilage proteoglycans. NO also influence the production of cytokines and prostanoids by chondrocytes. In the presence of $_{L}$-N^{G}-monomethyl arginine, alginate cultures of human articular

chondrocytes synthesise much more IL-6, a mediator of the acute phase response and a B-cell growth factor, and prostaglandin E2 which may play a protective role in cartilage.[264] Furthermore, NO causes apoptosis in articular chondrocytes. This result contributes to the loss of articular chondrocytes that occurs during aging and the development of OA.[265]

As NO plays an important role in arthritis, this study demonstrated the NO inhibitory activity by Tasmanian *Clematis* spp., and provides experimental *in vitro* evidence to support the therapeutic use of *Clematis* spp. in TCM in the treatment of arthritis. Protoanemonin is one of the active constituents having the ability to inhibit NO production by LPS stimulated Raw 264.7 cells. It is proposed that the NO inhibitory activity of protoanemonin was possible as it inhibits iNOS. Results in this study also demonstrated that the NO inhibitory activity of cartridge fraction 2 of *C. aristata*-L and –TN1, *C. microphylla*-TN had stronger NO inhibitory activity than ranunculin. This suggests the possible presence of additional active constituents in *C. aristata*-L and –TN1, *C. microphylla*-TN.

4.3.5 Investigation of anti-inflammatory activity of *Clematis aristata*-L fractions on molecular targets

RA is a systemic autoimmune disease characterized by chronic inflammation of joints. RA pathology is mediated by a number of cytokines (TNF-a, IL-1, IL-6, IL-17, etc.), chemokines (MCP-1, MCP-4, CCL18, etc.), cell adhesion molecules (ICAM-1,

VCAM-1, etc.) and matrix metalloproteinases. In this section, the influence of *CAristata*-L SPE cartridge fraction 2 on cytokines and chemokines was investigated.

4.3.5.1 Cytokines and chemokines

Cytokines (IL-1β, IL-10, IL-4 and TNF-a) and a chemokine (MCP-1) were investigated in this study. The results showing *C. aristata*-L SPE cartridge 2 (CL) influencing IL-1β, IL-10, IL-4 and TNF-α and MCP-1 from PMBC are shown in Figure 4.11. Statistical comparison was performed using Students T-test.

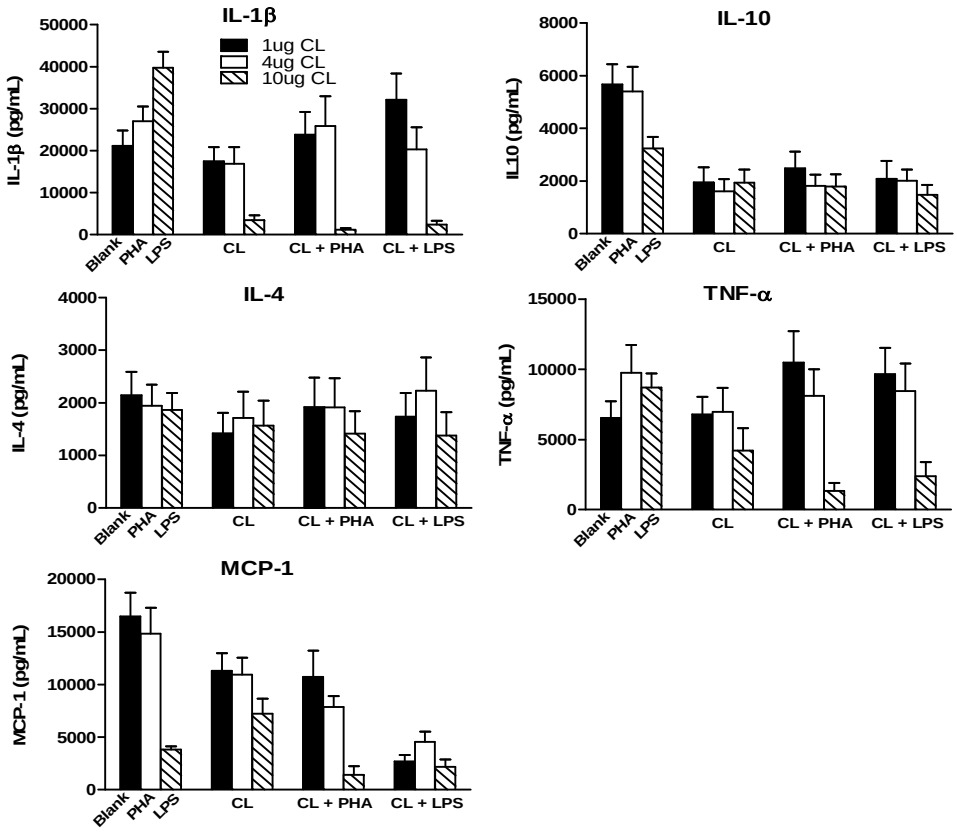

Figure 4.11 The anti-inflammatory activity of *C. aristata*-L SPE cartridge fraction 2 (CL) (1, 4 and 10 µg) on IL1-β, TNF-α, IL-4, IL-10 and MCP-1 measured from the unstimulated or stimulated PMBC by LPH and PHA. Results are presented as means ± SD.

IL-1β

LPS stimulated the expression of IL-1β compared with blank. The level of IL-1β was decreased by CL at 1, 4 and 10 µg. In blank and LPS stimulated cultures, the level was reduced in a dose dependent manner. At 4 µg, IL-1β level was reduced to 50% of the control for LPS presented culture. At 10 µg, IL-1β level was significantly decreased compared with the control in blank, PHA and LPS stimulation ($P<0.01$). The IL-1β level dropped to 17.6%, 3.6% and 7.3% of the control in blank, PHA and LPS stimulation, respectively.

IL-10

Stimulation of IL-10 by PHA and LPS was not observed. However, CL significantly decreased IL-10 compared with blank and PHA controls ($P<0.05$). This decrease was independent of the dose. A similar IL-10 concentration was seen in all CL treated samples, representing inhibition ranging from ~ 30 to 60% of the controls.

IL-4

CL did not change IL-4 levels. Stimulation was not observed by PHA or LPS. IL-4 level in blank culture was reduced to ~70 to 90% of the control in the presence of CL and this effect was independent from dosages. In the PHA and LPS presented cultures, IL-4 level did not change in the presence of 1 and 4 µg of CL, but the level decreased around 25% compared with control at 10 µg but this was not significant.

TNF-α

TNF-α levels were stimulated by PHA and LPS ($P<0.05$). CL changed TNF-α level in dose dependent manner. The level of TNF-α in blank and PHA and LPS stimulated cultures did not change in the presence of 1 and 4 µg of CL. However, in the presence of 10 µg of CL, level of TNF-α in PHA and LPS stimulated cultures were reduced to 14% and 30.5% of the control ($P<0.05$).

MCP-1

MCP-1 decreased in the presence of LPS ($P<0.05$). The decrease of MCP-1 by CL alone and in the presence of PHA followed a dose-dependent manner. The significant decrease in MCP-1 level was observed at 10 µg of CL in PHA presented culture ($P<0.05$).

IL-1 plays an important role in immune and inflammatory processes. It mediates inflammation by recruiting neutrophils, activating macrophages, and stimulating growth and differentiation of T cells and B cells. Moreover, IL-1 induces proteolytic enzymes that degrade extracellular matrix, resulting in tissue destruction.[(266)] There is strong evidence that links IL-1 to RA.(267) Animal studies demonstrated that intra-articular administration of IL-1 causes arthritis and synovitis.[(268)] IL-1 is clinically detectable in the plasma and synovial fluid of patients with RA and its concentration in plasma has been correlated with RA disease activity.[(269)]

TNF-α has emerged as a dominant proinflammatory mediator and important molecular target for therapy.[(270)] Additional evidence of the role of TNF-α in arthritis

comes from studies of transgenic mice. Mice that over-express TNF-α spontaneously develop an erosive, inflammatory arthritis.[271]

The results in our study show that CL is able to decrease the level of IL-1β in culture with or without the presence of PHA and LPS. These results imply that the therapeutic mechanisms of *Clematis* spp. in treatment of RA are probably multiple. They not only inhibit NO production, but also decrease the level of inflammatory cytokines (IL-1β and TNF- α), which play important roles in the pathology of RA. This ability is the strongest at high dose (10 μg) in stimulated cultures. The ability of CL to reduce TNF-α level in culture was not as strong as its effects on IL-1β.

IL-4 and IL-10 are anti-inflammatory cytokines. IL-4 has marked inhibitory effects on the expression and release of the proinflammatory cytokines. It is able to block or suppress the monocyte-derived cytokines, including IL-1, TNF-α, IL-6, IL-8, and macrophage inflammatory protein (MIP)-1a.[272-275] IL-4 has also been shown to suppress macrophage cytotoxic activity, parasite killing, and macrophage-derive nitric oxide production.[276] In contrast to its inhibitory effects on the production of proinflammatory cytokines, it stimulates the synthesis of the cytokine inhibitor IL-1ra.[277] Our study showed that CL did not change IL-4 level.

Although IL-10 is able to inhibit IL-1β and TNF-α release from TH1 cells and APC,[278, 279] as a cytokine that inhibits multiple modulatory effects on the immune system, it has altered expression in many autoimmune diseases.[280, 281] High serum levels of IL-10 have been reported in human autoimmune diseases. In systemic lupus

erythematosus (SLE) patients, high IL-10 levels have been shown to correlate with disease activity,[282, 283] and studies indicate that cultured PBMC from lupus patients spontaneously produce high levels of IL-10.[280] Production of high levels of IL-10 has also been demonstrated in synovial T-lymphocytes of RA patients, in the serum of systemic sclerosis, Kawasaki disease, and autoimmune lymphoproliferative syndrome (ALPS) patients, as well as in the cultured cells of polymyositis and dermatomyositis patients.[281] High IL-10 levels have been found in the blister fluid of pemphigus vulgaris and bullous pemphigoid patients and in the mucosal T cells in ulcerative colitis.[232, 281, 284-290] Increased expression of IL-10 mRNA by PBMCs and/or various other tissues was associated with Sjogren's syndrome, Grave's disease, myasthenia gravis, psoriasis and ALPS.[280, 281, 286, 290, 291] Taken together, these studies indicate that deregulated expression of IL-10 plays a significant role in autoimmune diseases. CL decreased IL-10 in a dose independent manner, which might provide a rationale that CL may have therapeutic value in the treatement of autoimmune diseases.

Chemokines are chemotactic cytokines that regulate leukocyte migration during inflammatory responses, as well as homeostatic trafficking of lymphocytes and dendritic cells.[292, 293] In the setting of RA, chemokines and their receptors appear to play an important role in cell migration and the positioning of leukocytes within the inflamed rheumatoid synovium.[294, 295] Monocyte chemotactic protein-1 (MCP-1)/CCL2, macrophage inflammatory protein-1α (MIP-1α)/CCL3 and MIP-1β /CCL4, are implicated in RA pathogenesis via recruitment and retention of monocytes and T

lymphocytes in the joints.[296] Monocyte chemotactic protein -1/CCL2 (a ligand of CCR2) can attract monocytes, T cells, NK cells, and basophils. MCP-1/CCL2 is highly expressed in synovial tissue and synovial fluid from RA patients, and synovial tissue macrophages are the dominant source of MCP-1/CCL2 production.[297] MCP-l levels in culture supernatants were significantly correlated with the amounts of IL-1β, IL-6 and IL-8 following incubation of RA patient's synovial cells. Furthermore, the expression of MCP-1 mRNA by cultured synovial cells was stimulated by IL-1β and TNF-α.[298] Analysis of FLS from patients with RA showed that MCP-1/CCL2 enhanced IL-6 and IL-8 production.[299]

The activity of CL inhibition of NO production and the effects on IL-1β, IL-4, TNF-α and MCP-1 in this investigation provided *in vitro* experimental data on the potential therapeutic value of *Clematis* spp. used in TCM, mainly as an anti-inflammatory medicine. The therapeutic mechanisms arise through multiple pathways. CL not only inhibits NO production, but also modifies the cytokines and chemokines. CL is able to suppress the expression of proinflammatory cytokines of IL-1β, TNF-α and chemokines, MCP-1, which play an important role in the inflammatory. CL did not influence the IL-4 expression at low and medium levels. This effect would potentially be of benefit in inflammation, as the role of IL-4 is to block IL-1, TNF-α, IL-6, IL-8 and stimulate the synthesis of cytokine inhibitor IL-1ra.

NO and inflammatory cytokines are important factors leading to the human joint inflammation, especially because IL-1 can induce NO production in articular

chondrocytes.[257, 261] Results in our study showed that CL had inhibitory effects on both IL-1β and NO. This finding may provide a rationale for the use of Tasmanian native *Clematis* spp. in the treatment of RA. Currently, medicines inhibiting TNF-α and IL-1 are used in the clinic for treatment of RA. Anti-TNF medicines like adalimumab and infliximab are monoclonal antibodies directed against TNF-α while etanercept is a construct of two molecules of TNF-α receptor (p75 receptor) linked to the Fc portion of IgG1, to give rise to an immunoglobulin-like molecule. Clinical trials with the three agents demonstrated high efficacy in RA patients who failed traditional non-biologic disease-modifying anti-rheumatic drugs. The anti-IL-1 agent used clinically is anakinra. It antagonizes the biologic activity of IL-1 by competitively inhibiting IL-1 binding to its type 1 receptor, therefore blocking cell signalling.[223]

It is likely that there may be multiple therapeutic targets of *Clematis* spp. in RA. It not only inhibits NO production, but also inhibits cytokines, like IL-1, TNF, IL-10 but has no influence on IL-4. Molecular targets of RA treatments are numerous, as shown in Figure 4.12. Monocytes are attracted to the RA joint, where they differentiate into macrophages and become activated. They secrete TNF and IL-1. TNF increases the expression of adhesion molecules on endothelial cells, which recruit more cells to the joint. Chemokines, such as MCP-1 and IL-8 are also secreted by macrophages and attract more cells into the joint. IL-1 and TNF induce synovial fibroblasts to express cytokines (such as IL-6), chemokines (such as IL-8), growth factors (such as granulocyte-macrophage colony-stimulating factor, GM-CSF) and

matrix metalloproteinases (MMPs), which contribute to cartilage and bone destruction. TNF contributes to osteoclast activation and differentiation. In addition, IL-1 mediates cartilage degradation directly by inducing the expression of MMPs by chondrocytes. That means IL-1, TNF and MCP-1 are secreted by macrophages. It is not described that IL-4 is related to macrophages. And in the NO study, NO is also secreted from macrophages. Therefore, it is supposed that the multiple therapeutic targets might be simplified to be the action of CL on macrophages. This kind of action could lead to decrease the secretion of cytokines, or even NO from cells.

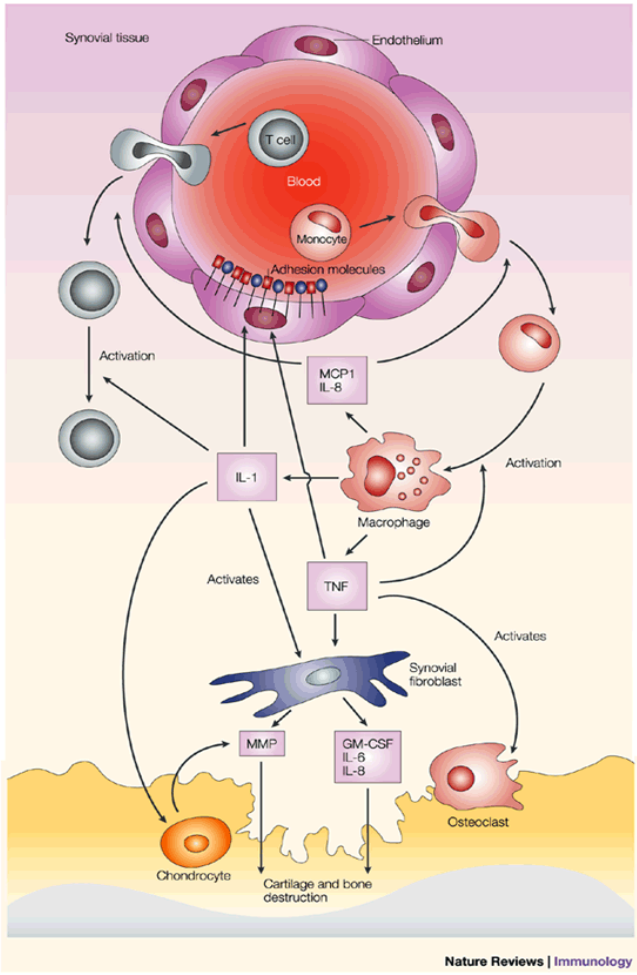

Figure 4.12 Overview of the pathogenesis of rheumatoid arthritis, adapted from Pope *et.al.*[300]

It is interesting to point out that CL decreases IL-10 level and this effect is dose independent. Increasingly research has revealed the relationship of IL-10 and autoimmune diseases, which have been discussed previously. Results in this study showed that CL decreased IL-10 level by a dose-independent manner and IL-4 level could not be changed by CL. IL-10 level of SLE patients is increased and their IL-4 mRNA expression is decreased.[(301)] Therefore, the result in this study would provide a rationale that it would be worth to investigate the therapetuc effects of CL in SEL or other autoimmune diseases. In TCM, *Clematis* spp. has been used in the preparation for some autoimmune diseases, such as SLE, psoriasis, myasthenia gravis, systemic scierosis, asthma and Slogren's syndrome. However, to our knowledge, there is no experimental evidence that demonstrates the activity of *Clematis* spp. on these autoimmune diseases.

The name of *Clematis chinensis* in TCM is 'Wei Ling Xian", that means panacea. The inhibition of NO and influence of cytokines implied the therapeutic activities might be not only in arthritis, but also in other diseases related to NO and cytokines. In the present study, LPS was used as an iNOS stimulator, however, some inflammatory cytokines, such as IFN-γ, TNF-α and IL-1β, generated during the inflammatory reaction in macrophages, hepatocytes and endothelial or smooth muscle cells are able to stimulate iNOS as well.[(236)] NO as a reactive radical directly damages functional normal tissues; when excessively produced by iNOS, it has been implicated in a variety of pathophysiological processes including carcinogenesis. It can also react with superoxide anion to form an even stronger oxidant, peroxynitrite,

which contributes to DNA damage and nitration of protein and nucleic acids.[302] The investigated *Clematis* spp. were able to inhibit NO production, therefore, they may be useful in therapeutic strategies against various diseases promoted by overproduction of NO, such as asthma, atherosclerosis, multiple sclerosis, myocarditis, septic shock, Alzheimer's disease and Parkinsonism.[303]

This study primarily suggests there is a biochemical basis to the potential therapeutic value of Tasmanian *Clematis* spp. in inflammatory diseases. Positive *in vitro* results were achieved in this pilot investigation which warrants more detailed investigation in futrue work.

4.4 Future work

Determination of the IC_{50} of protoanemonin on NO inhibition would be the first next step. Results in the study of NO inhibitory activity exerted that ranunculin is one the active constituents, however, it might be conceived as a "pro-drug" as it decomposes to protoanemonin in cell medium as found in the antitumour investigation (Chapter 2). Further work should also evaluate the NO inhibition effects of the 3 potent species, CA-L, CA-TN1 and CM-TN, and whether these effects are contributed to by protoanemonin or other active constituents. The relationship between protoanemonin and NO inhibitory effects could also be confirmed by the determination of protoanemonin in all investigated *Clematis* material by GC-MS. If the NO inhibitory activity corresponds to the protoanemonin content, determination of the potential of cysteine reverse activity of protoanemonin inhibiting production of NO via –SH group could be undertaken.

The cytokines study revealed cartridge fraction 2 of *C. aristata*-L had positive activity, however, the active constituents have not been determined in this present study. In future work, bioactive fractionation would need to be performed to determine the active constituents (effects on inflammatory cytokines, pro-inflammatory cytokines and chemokines using the present experimental method). Further investigations into active constituents influencing cytokines in the whole blood culture of patients with RA and SLE patients would be worthwhile

4.5 Conclusion

The anti-inflammatory activity of Tasmanian native *Clematis* spp. was investigated through NO inhibition in LPS stimulated Raw 264.7 cells and the influence of cytokine levels released by PBMC. Varied NO inhibitory effects were obtained in different *Clematis* spp. giving a range of IC_{50} from 0.2 µg/ml to 3.11 µg/ml. Ranunculin is one of the active constituents in the inhibition of NO production and its IC_{50} was 0.54 µg/ml. The cytokine study demonstrated that 10 µg of CL could significantly decrease the level of IL-1 β ($P<0.01$) and TNF-α ($P<0.05$) from PBMC in the presence of LPS and PHA. The decreasing of IL-10 by CL follows a dose-independent manner. CL did not influence IL-4 level. This study provids a basis to support Tasmanian native *Clematis* spp. having therapeutic value not only in inflammatory diseases, but also in autoimmune diseases.

.

Chapter 5 Remaining compounds of interest not identified by activity guided fractionation

Abstract

In this chapter the chemical constituents in Tasmanian native *Clematis* spp. were investigated. The chemical constituents of SPE cartridge fractions of each investigated *Clematis* leaf were analysed by HPLC, LC-MS and LTQ-Orbitrap-MS. Flavonoids and hydroxycinnamate esters obtained in these investigated *Clematis* spp. The amounts of nine hydroxycinnamate esters were varied in each *Clematis* leaf material and in the different ages of *C. aristata*-L leaf samples. Isomers of (-)-4-(E)-caffeoyl-D-glyceric acid were observed in this study. This study is the first to describe the hydroxycinnamate esters in Tasmanian *Clematis* spp. and the first to observe the isomers of (-)-4-(E)-caffeoyl-D-glyceric acid.

5.1 Introduction

The Australian continent is one of the vast repositories of medicinal plants that have been used in traditional medicine. Australian native species of *Clematis* include *C. aristata, C. gentianoides, C. glycinoides, C. microphylla, C. fawcettii, C. microphylla* var. *leptophylla* and *C. pubescens*, from which, *C. aristata, C. microphylla* and *C. gentianoides* are Tasmanian native species. To our knowledge, investigation and comparison of the chemical constituents in Tasmanian *Clematis* species have yet not been undertaken.

Studies described in Chapter 2, 3 and 4 provided basic experimental data of the investigation of biological activities of Tasmanian native *Clematis* spp. In the determination of potential active constituents, some novel compounds were observed. This chapter will describe the chemical properties of these novel compounds and the fundamental investigation of chemical constituents in Tasmanian *Clematis* spp.

LC-MS and linear ion trap quadrupole-orbitrap-mass spectrometry (LTQ-Orbitrap-MS) were employed in this study for determination of the molecular formula of novel compounds. Liquid chromatography is a fundamental separation technique in the life sciences and related field of chemistry. It can effectively separate a very wide range of organic compounds, from small-molecule drug metabolites to peptides and proteins. For most compounds, mass spectrometers are more sensitive and far more specific than all other LC detectors. They work by ionising molecules and then sorting and identifying the ions according to their mass-to-charge (*m/z*) ratios.[304] In

this study, electrospray ionization was used in LC-MS. Electrospray relies in part on chemistry to generate analyte ions in solution before the analyte reaches the mass spectrometer.[304] LTQ-Oribtrap-MS delivers single-stage mass analysis providing molecular high resolution mass information, two-stage mass analysis (MS/MS) and multi-stage mass analysis (MS^n) delivering structural information.[305]

This chapter identifies the chemical structure of some novel constituents in the investigated *Clematis* spp. by LC-MS and LTQ-Orbi-trap-MS. The differences in chemical constituents in Tasmanian native *Clematis* species were compared by HPLC analysis in this chapter.

5.2 Experimental

5.2.1 Reagents used

Reagents used in extraction, isolation and determination were the same as those described in Chapter 2 (2.2.1.1).

5.2.2 Instruments

Sonicator, rotary evaporator, HPLC and LC-MS were described in Chapter 2**.** Only a C18 analytical HPLC column was used in this study.

5.2.2.1 LTQ-Orbitrap-MS

This system consisted of an Alliance 2690 Separations Module (Waters, USA) equipped with a quaternary pump, a photodiode array detector (PDA) and a thermostated autosampler, coupled to a ThermoFischer LTQ Orbitrap high resolution Tandem Mass Spectrometer (Thermo Scientific, Australia) equipped with an ESI source in negative mode.

5.2.2.2 UV-visible spectrophotometer

A CARY IE UV-visible spectrophotometer (Varian, Australia) was used in the determination of the UV absorption of plant fractions.

5.2.3 Plant material

Plant materials used in this study were the same as those described in Chapter 2.

5.2.4 Extraction, isolation and determination techniques

The methods of MeOH, MeOH-DCM and DCM Extraction and SPE cartridge fractionation were the same as the extraction and fractionation methods described in Chapter 2.

5.2.4.1 Analysis of chemical constituents by LC-MS

The column, flow rate, injection volume, mobile phase and elution gradient applied for LC-MS were the same as for HPLC. The detection wavelength was 220 -400 nm.

Negative ion electrospray ionisation (ESI) was applied to the samples. Conditions for negative ESI were as follows; needle voltage 4 KV, capillary voltage -15V, capillary temperature 220°C, sheath gas (nitrogen) 65 psi, auxiliary gas (nitrogen) 20 psi. The full scan range from *m/z* 200 to 1200, and data dependent MS^2 and MS^3 scans were acquired from the most intense ion with 30% collision energy. $[M-H]^-$ and $[M+CH_3COO]^-$ ions were typically observed in this mode. Data was analyzed by Xcalibur® software.

5.2.4.2 Determination of HCAs by LC-MS Orbitrap mass spectrometry

Further characterization of novel compounds was performed on the LC/ESI-LTQ-Orbitrap-MS. A Nova C18 column (150 mm x 2.1mm, i.d., 5 µm; Waters, USA) was used. Gradient elution was performed with methanol (solvent A) and 2% acetic acid in water (solvent B) at a constant flow rate of 0.2 ml/min, and injection volume was 5 µl. The elution gradient was from 5% A and 95% B to 35% A and 65% B at 15 minutes, then to 100% A at 25 minutes.

The mass spectrometer, equipped with an ESI source in negative mode, was used to acquire mass spectra in profile mode with a setting of 30000 resolution at *m/z* 500. Operation parameters were as follows: source voltage, 3.5 kV; sheath gas, 30 units; and capillary temperature, 275°C. The capillary voltage was -5.00 V; the tube lens voltage was set to -57.36 V. Samples were first analyzed in full MS mode with the Orbitrap resolution set at 30000 at *m/z* 500. The successive analysis was performed in MS^n mode with the Orbitrap resolution set at 15000 at *m/z* 500. An isolation width of 2 mu was used and precursors were fragmented by collision-induced dissociation (CID) with normalized collision energy of 35 % and activation time of 30 ms. The maximum injection time was set to 50 ms with three micro scans for MS mode and to 1000 ms with one micro scan for MS^n mode. The mass range was from *m/z* 150-1000. Data were analyzed by Xcalibur® software.

5.2.4.3 HPLC analysis of HCAs by HPLC and quantification of HCAs in each *Clematis* leaf material

SPE cartridge fraction 2 of each *Clematis* leaf crude extract was analyzed by HPLC-UV. Partial loop injection mode was applied to inject 20 µl of SPE cartridge fraction 2. The solvent A was ACN and solvent B was 2% acetic acid in water for HPLC. The elution gradient was from 5% A and 95% B to 25% A and 75% B at 15 minutes, then to 40% A and 60% B at 25min, then to 100 % A at 35 minutes. The flow rate was 0.8 ml/minutes. The detection wavelength was between 200 nm and 400 nm.

Approximate quantification of HAC compounds was performed at 254 nm by using *C. microphylla*-TN SPE fraction 2 (CM-TNii) (0.056 mg/ml) as a standard, assuming a similar molar extinction coefficient for HCAs. The caffeoglucose extinction coefficient of ε_{330nm} is 23000.[306] Results are expressed in microgram per gram of fresh leaf material for each identified HCA compound.

5.3 Results and Discussion

5.3.1 Determination of chemical constituents of SPE cartridge fraction 2 of *C. aristata*-L leaf solvent extract

From the results obtained in the antimicrobial, anticancer and anti-inflammatory chapters, *C. aristata*-L appeared to be the most interesting cultivar to investigate. Therefore, Chemical constituents in *C. aristata*-L leaf SPE cartridge fraction 2 (CA-Lii) were screened by LC-MS. Results are summarized in Table 5.1 and the LC-MS chromatogram is shown in Figure 5.1. MS spectra of all compounds in Table 5.1 are shown in Appendix VII. UV spectra of HCAs are shown in Appendix VIII.

Table 5.1 The chemical constituents in CA-Lii.

Compound ID	RT (min)	UV/vis	MS (*m/z*)	MS^2 (*m/z*)	MS^3 (*m/z*)
1	3.8		275	179	89,101,107,113,119,131, 143,149,161
2	4.69		275	179	89,101,107,113,119,131, 143,149,161
3	10.49	HCA[1]	503	341, 179	179, 161,135
4	10.93	FL[2]	787	626	
5	11.15	HCA	503	341, 179	179, 161,135
6	11.7	HCA	341	179	
7	12.14	FL	949	788	625
8	12.47	HCA	341	179, 135, 161	135
9	12.58	HCA	297	179, 135, 117	
10	13.35	HCA	341	179, 135	135
11	14.78	HCA	267	179, 161, 105	
12	15.66	HCA	267	179, 161, 135, 105	
13	16.41	HCA	267	179, 161, 135, 105	

[1]HCA is hydroxycinnamic acid
[2]FL is flavonol

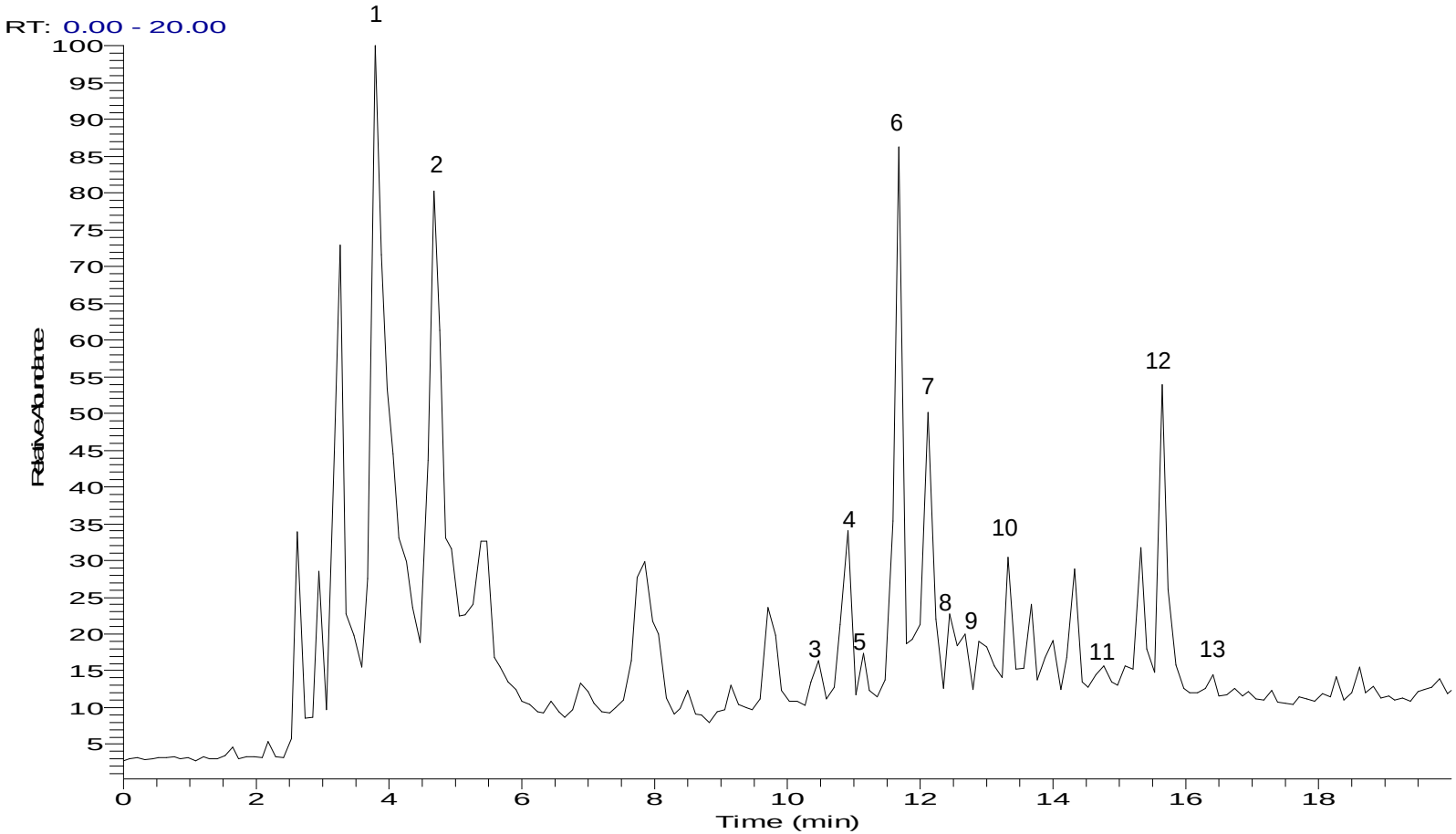

Figure 5.1 LC-MS chromatogram illustrating the chemical constituents of CA-Lii using an Apollo C18 HPLC column. The number labeled in the chromatographic peaks corresponds to the compound ID in Table 5.1.

Compounds 3, 5, 6, 8, 9, 10, 11, 12 and 13 had typical hydroxycinnamic acid UV spectra with absorbance maxima (λ_{max}) of 242, 293 (sh) and 330 nm.[307] Compounds 4 and 7 had typical UV spectra of flavonoids with compound 4 having λ_{max} of 254nm and 337 nm; and compound 7 having λ_{max} of 266 and 347 nm. Compounds 8, 11, and these two flavonoids had been detected in *Clematis* spp. in a previous study performed in this laboratory.[52] Their UV spectra are exhibited in Figure 5.2.

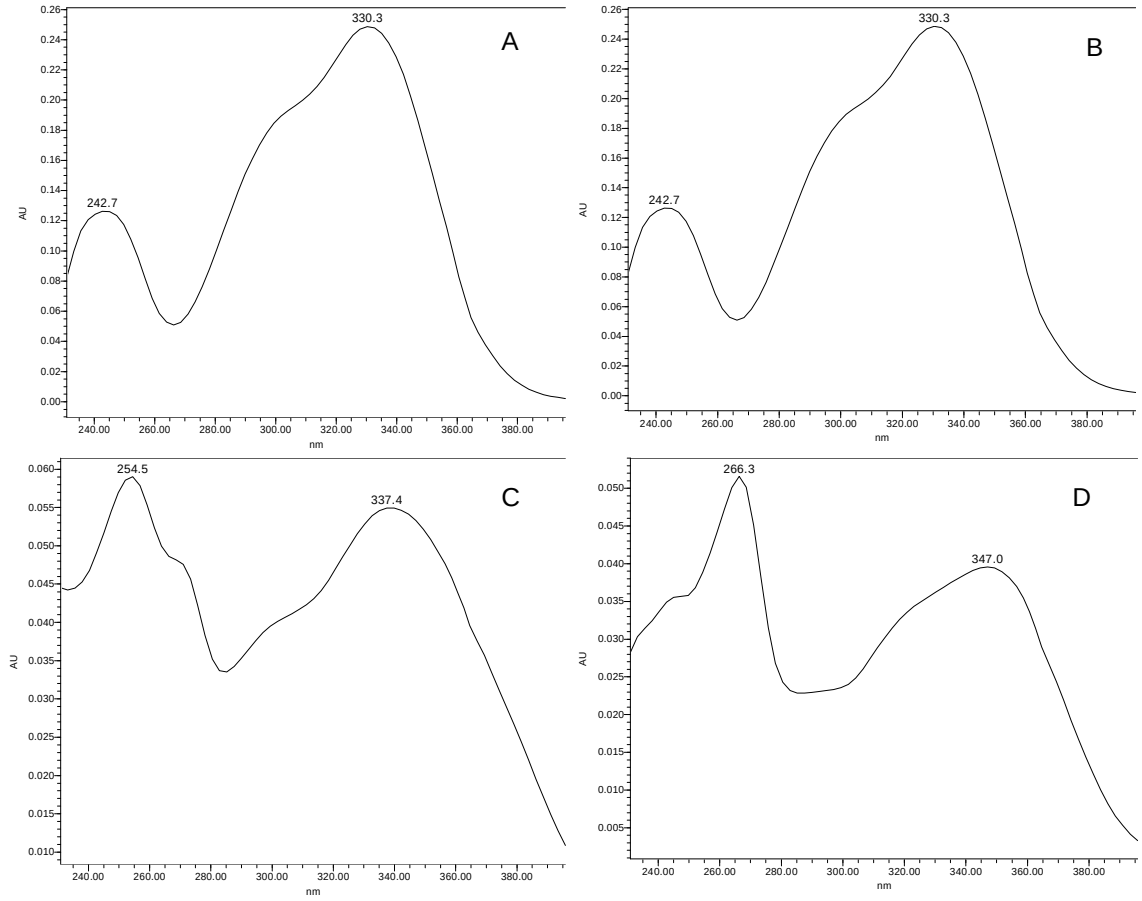

Figure 5.2 UV spectra of compounds 8 (A), 11 (B), 4 (C) and 7 (D).

The LC-MS data presented in Table 5.2 showed that the MW of two flavonoids, compounds 4 and 7, were 788 and 950, respectively. Compound 4 had the MS^2 at *m/z* 625, which is [787-glucose]$^-$. Compound 7 had MS^2 at *m/z* 787, which is [949-

glucose]$^-$; and MS^3 at *m/z* 625, which is [787-glucose]$^-$. This result suggested that compound 7 had one more glucose than compound 4. Data from this analysis matched with a previous study in this laboratory. The previous study performed in our laboratory[52] (Table 5.2) demonstrated that the aglycone was consistent with quercetin, which is the usual one found in *Clematis* spp.[76, 77, 79, 80, 308] The molecular structure of quercetin is shown in Figure 5.3. MS spectra of flavonoids were presented in Appendix VII .

Table 5.2 Chemical constituents of *Clematis* species leaves determined by LC-MS

Compound ID	MW	Aglycone	Glycoside	Molecular formula (proposed)
4	788	quercetin	3xC_6 sugars	$C_{33}H_{40}O_{22}$
7	950	quercetin	4xC_6 sugars	$C_{39}H_{50}O_{27}$

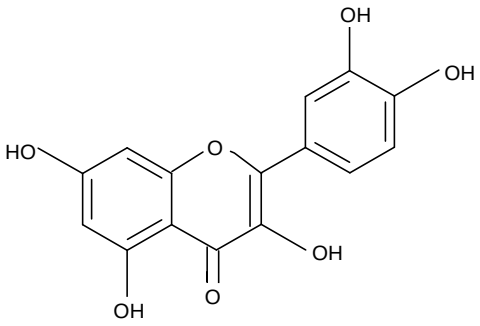

Figure 5.3 Molecular structure of quercetin

In previous studies determining antibacterial, anticancer and anti-inflammatory effects of *C. aristata*-L SPE cartridge fraction 2, the biological activities of these two flavonoids were not observed. However, quercetin, which is a flavonol, was reported

to widely exist in fruit and vegetables and have antioxidant activity.[309] Its content in apples, plums, cranberries, strawberries and grapes was 34, 12, 170, 39 and 31 mg/kg, respectively.

Mass spectrometry data of compounds 1 and 2 showed *m/z* at 275 corresponding to $[M-H]^-$. Therefore, the molecular weight of both compounds are 276. MS^2 produced an ion at *m/z* 179 and MS^3 produced ions at *m/z* 89, 101, 107, 113, 119, 131, 143, 149 and 161. MS^3 data indicated that *m/z* at 179 was due to a sugar. The difference between 275 and 179 is 96, which is consistent with the molecule weight of protoanemonin. The above data revealed that these 2 compounds had the same MS data consistent with ranunculin. The UV spectra of both compounds were not obtained in the UV range of 220-400nm. The λ_{max} of ranunculin is 204 nm[310] with little absorbance at longer wavelengths, which is consistent with the results of the current study. As discussed in Chapter 2, ranunculin and its isomers had been reported in 1972 by Techesche and co-workers.[170]

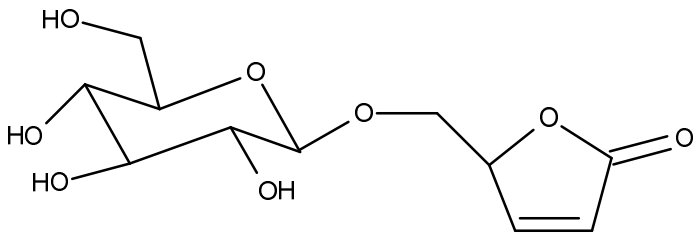

Figure 5.4 The chemical structure of ranunculin

Data in Table 5.1 showed that all compounds having typical hydroxycinnamic acid UV spectra had similar fragment ions at *m/z* 179, 161 and 135. Besides, compound 8

had another fragment ion at *m/z* 117 and compounds 11, 122 and 13 had another fragement ion at *m/z* 105.

Compounds 3 and 5 are isomers with MW of 504 and similar MS fragmentation that indicated the loss of 162 unit mass, consistent with the loss of a sugar. Compound 6, 8 and 10 are isomers with MW of 342 and similar MS fragmentation that indicated the loss of 162 unit mass, consistent with the loss of a sugar. Compound 9 has the MW of 298. Its MS fragmentation indicates the loss of a 108 mass unit. Compound 11, 12 and 13 are isomers with MW of 268. Their MS fragementation indicates that the loss of a 88 mass unit. Mass spectra of compounds 1-13 are presented in Appendix VII.

The result in this study showed that *C. aristata*-L SPE fraction 2 not only had ranunculin and one of its isomers, but also had novel flavonoids and hydroxycinnamic acids with the basic MW of 342, 298 and 268. This study also found the presence of isomers of MW 342 and 268 compounds. In order to determine their potential chemical structures, they were analysed by LTQ-Orbitrap-MS.

5.3.2 Investigation of chemical structure of HCA compounds

The CA-Lii was analysed by LTQ-orbitrap-MS. The molecular formulas of the compounds with MW of 342, 298 and 268 were determined.

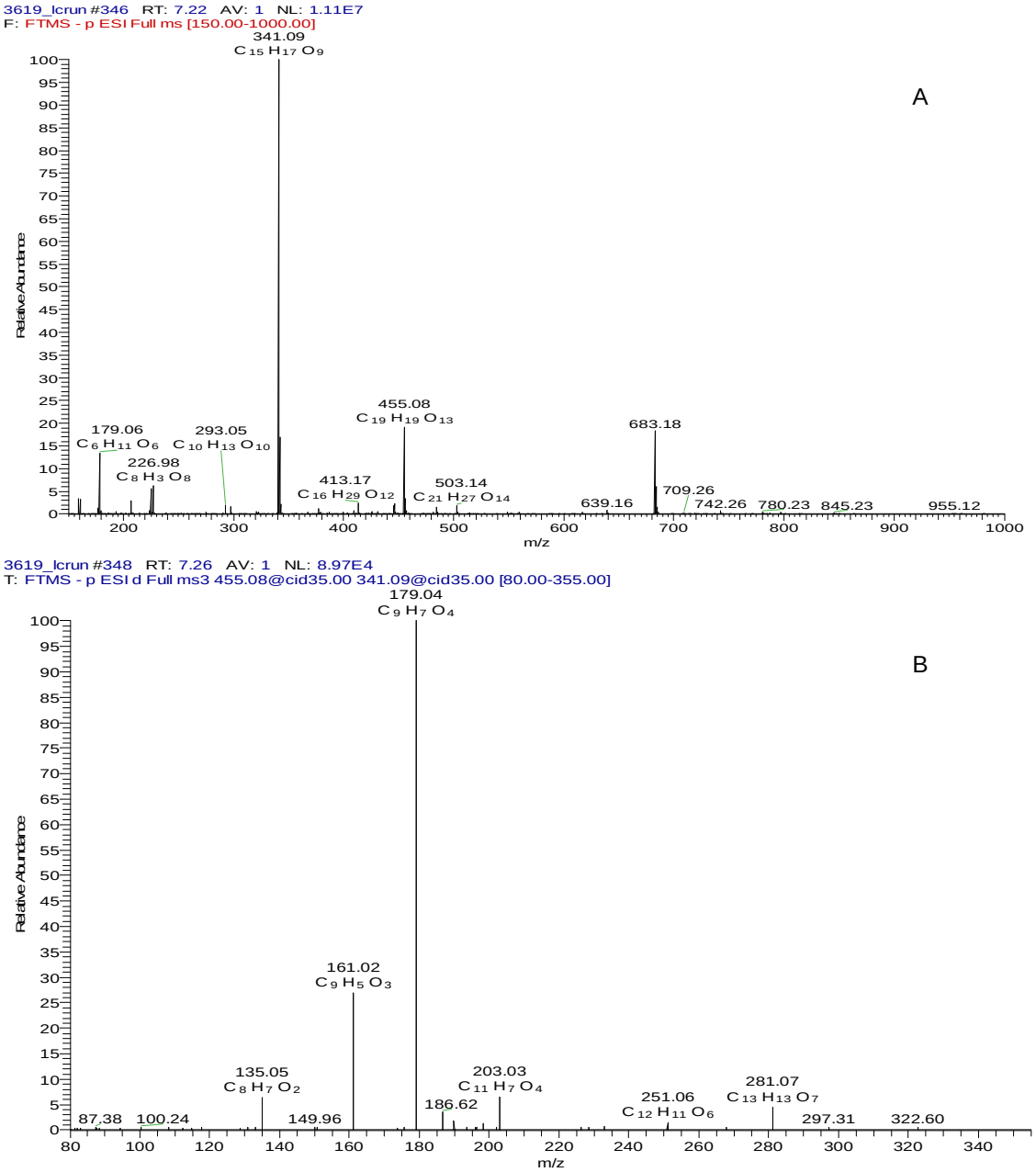

Figure 5.5 Orbitrap fingerprints of compounds with MW 342 (A) and MS^2 data of molecular ion of 341 (B).

Figure 5.5 demonstrates that the molecular formula of compounds with MW 342 was $C_{15}H_{18}O_9$. The MS^2 spectrum of *m/z* 341 gave peaks at *m/z* 179 ($C_9H_7O_4$), 161 ($C_9H_5O_3$), and 135 ($C_8H_7O_2$). The above mass spectrometry data of compounds with MW 342 are consistent with the MS data of caffeoylglucose.[305, 311] Based on the

previous LC-MS study, the UV spectrum of the MW 342 compound was a typical hydroxycinnamic acid UV spectrum. Therefore, it was supposed that fragmentation of compounds with *m/z* at 341 producing daughter MS data at *m/z* 179 giving molecular formula $C_9H_7O_4$ corresponded to [caffeic acid-H], *m/z* 161 ion giving molecular formula $C_9H_5O_3$ corresponded to [caffeic acid-H_2O] and *m/z* 135 ion giving molecular formula $C_8H_7O_2$ corresponded to [caffeic acid-COOH].

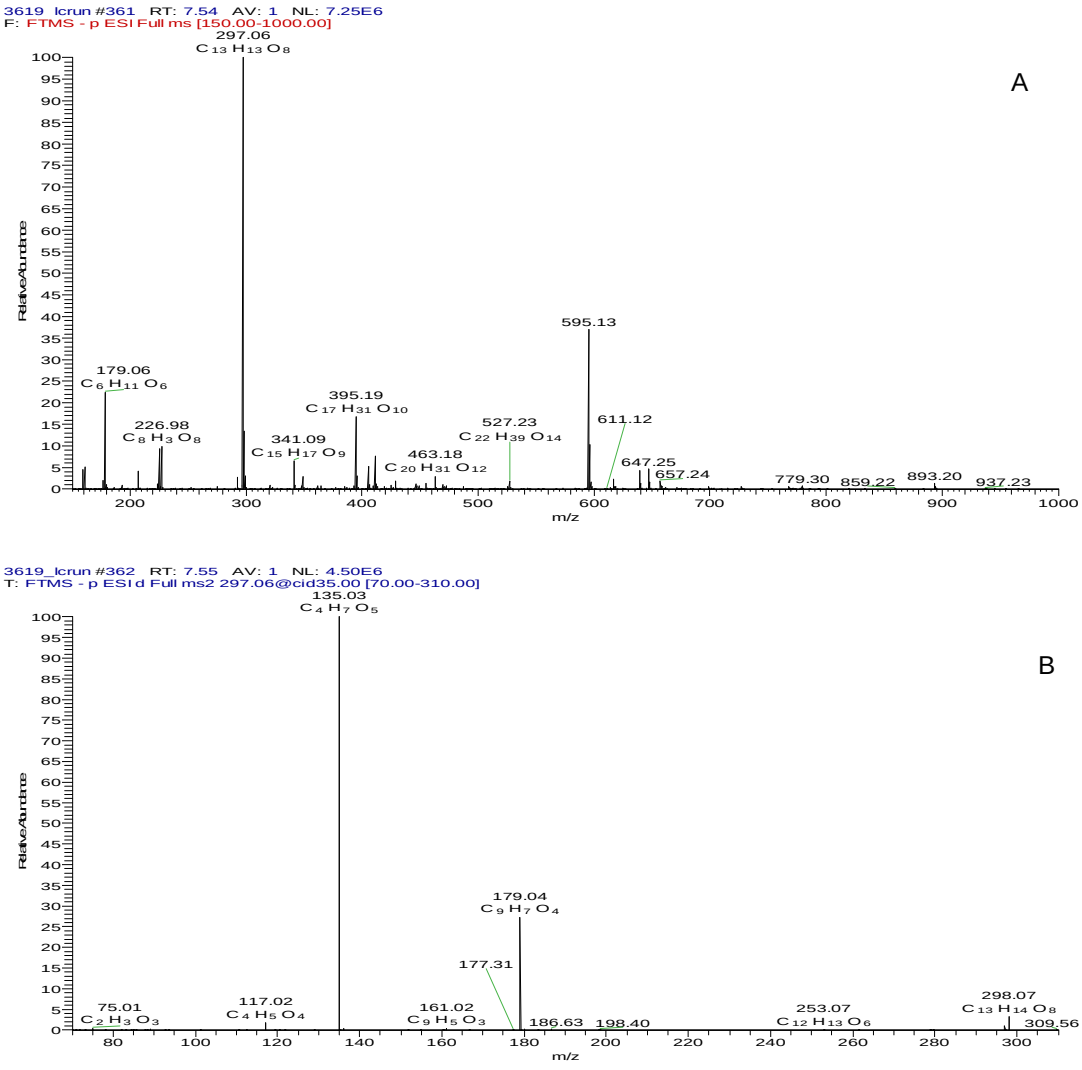

Figure 5.6 Orbitrap mass spectral fingerprints of compounds with MW 298 (A) and MS^2 data of molecular ion of 297(B).

The mass spectra in Figure 5.6 presented the molecular formula of compounds with MW298 as $C_{13}H_{14}O_8$. For MS^2 spectra of *m/z* 297, the molecular formula of *m/z* 179 was $C_9H_7O_4$, the molecular formula of *m/z* 161 was $C_9H_5O_3$, the molecular formula of *m/z* 135 was $C_4H_7O_5$ and the molecular formula of *m/z* 117 was $C_4H_5O_4$. Based on the previous LC-MS study, the UV spectrum of MW 297 was a typical hydroxycinnamic acid UV spectrum.

Mass spectrometry data of the compound having $[M-H]^-$ at *m/z* 297 was consistent with the MS data of 2-O-caffeoylthreonic acid.[312] Parveen's study identified and described the data of negative-ion ESI-MS of 2- O-caffeoylthreonic acid which showed a molecular ion of *m/z* 297 $[M-H]^-$ and *m/z* 595 $[2M-H]^-$, indicating the molecular formula $C_{13}H_{14}O_8$ that matched the formula of this MW 298 compound given by the orbitrap analysis in our study. Parveen's study found that the MS^2 of the molecular ion *m/z* 297 gave *m/z* 179 [caffeic acid-H], *m/z* 135 ion [threonic acid-H] and 117 [M- caffeic acid]. Therefore, in this study, it was supposed that fragmentation of compounds with *m/z* at 297 producing daughter MS data at *m/z* 179 giving molecular formula $C_9H_7O_4$ corresponded to [caffeic acid-H], *m/z* 161 ion giving molecular formula $C_9H_5O_3$ corresponded [caffeic acid-H_2O], *m/z* 135 ion giving molecular formula $C_4H_7O_5$ corresponded to [M-caffeoyl] and *m/z* 117 ion giving molecular formula $C_4H_5O_4$ corresponded to [M-caffeic acid].

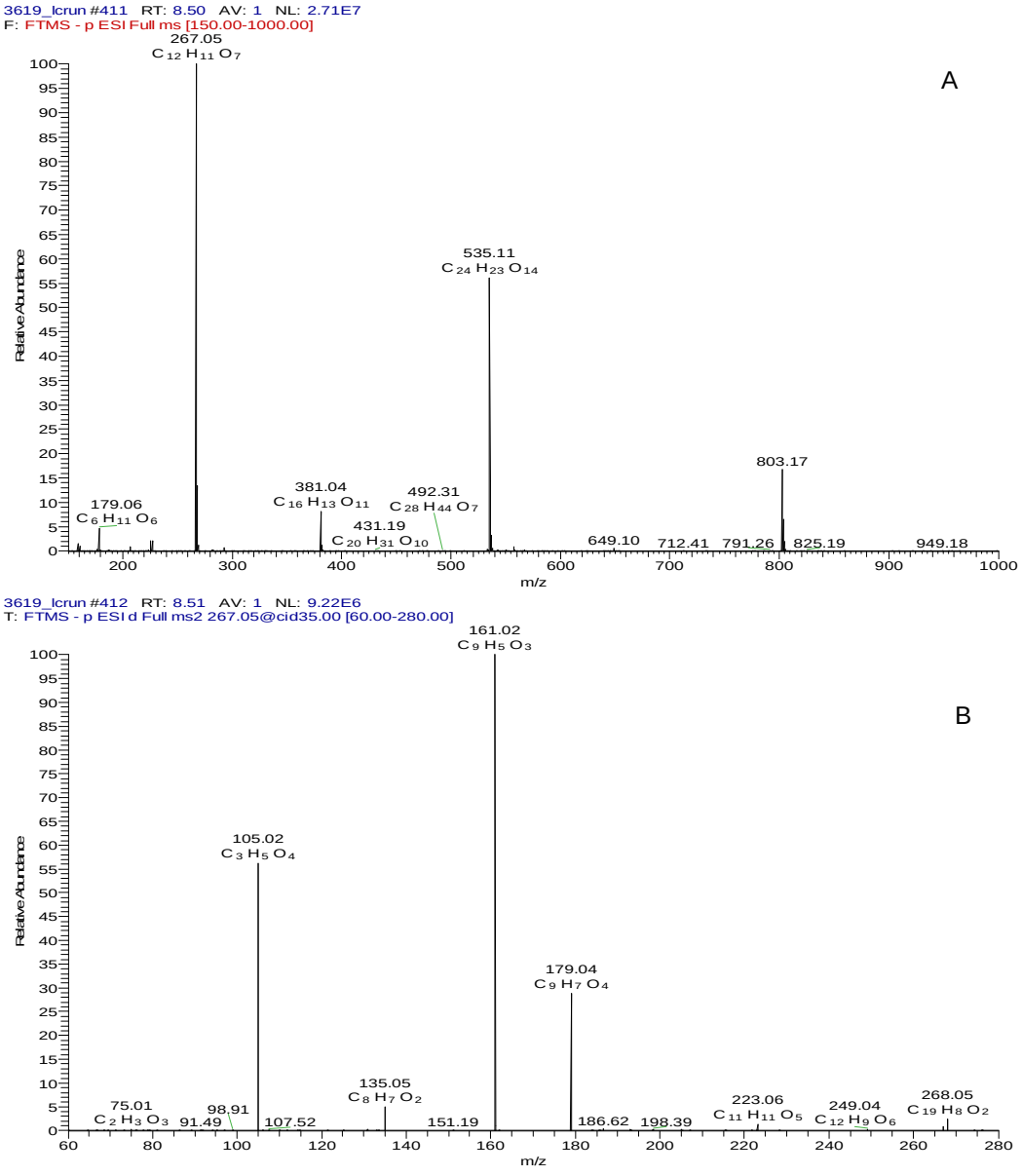

Figure 5.7 Orbitrap fingerprints of compound with MW 268 (A) and MS^2 data of molecular ion of 267(B).

The mass spectra in Figure 5.7 presented the molecular formula of compounds having MW of 268 as $C_{12}H_{12}O_7$. For MS^2 spectra of *m/z* 267, the molecular formula of *m/z* 179 was $C_9H_7O_4$, the molecular formula of *m/z* 161 was $C_9H_5O_3$, the molecular formula of *m/z* 135 was $C_8H_7O_2$ and the molecular formula of *m/z* 105 was $C_3H_5O_4$.

Based on the previous LC-MS study, the UV spectrum of MW 268 was a typical hydroxycinnamic acid UV spectrum.

Mass Spectrometry data of the compound having [M-H] at *m/z* 267 matched the MS data of (-)-2-(E)-Caffeoyl-D-glyceric acid.[313] Therefore, in this study, it was proposed that fragmentation of compounds with *m/z* at 267 producing daughter MS data at *m/z* 179 giving molecular formula $C_9H_7O_4$ corresponded to [caffeic acid-H], *m/z* 161 ion giving molecular formula $C_9H_5O_3$ corresponded to [caffeic acid-H_2O], *m/z* 135 ion giving molecular formula $C_8H_7O_2$ corresponded to [caffeic acid-COOH] and *m/z* 105 ion giving molecular formula $C_3H_5O_4$ corresponded to [M-caffeoyl].

In this study, five compounds having ions at *m/z* 341, 179, 161 and 135 were detected. They were listed as compounds 3, 5, 6, 8 and 10 in Table 5.1. Compounds 6, 8 and 10 were expected to be isomers of caeffic acid attached to a sugar. Compound 3 and 5 have one more sugar substituent than compounds 6, 8 and 10 giving $[M-H]^-$ at *m/z* 503. The expected molecular formula of both isomers is $C_{21}H_{28}O_{14}$. Compounds 11, 12 and 13, all with MW 268, were expected to be (-)-2-(E)-Caffeoyl-D-glyceric acid isomers.

There are 12 previously reported compounds consistent with the molecular formula of $C_{21}H_{28}O_{14}$ that have the chemical structure of caffeic acid with two sugar attachments. They are listed in Figure 5.8.

CP1:**β-D-Glucopyranose,6-O-β-D-glucopyranosyl-, 1-[(2E)-3-(3,4-dihydroxyphenyl)-2-propenoate]**

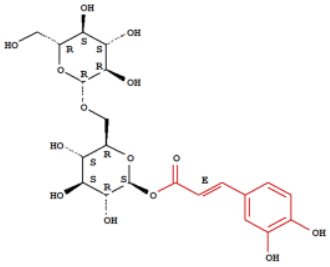

CP2:**β-D-Glucopyranose,6-O-β-D-glucopyranosyl-, 1-[3-(3,4-dihydroxyphenyl)-2-propenoate]**

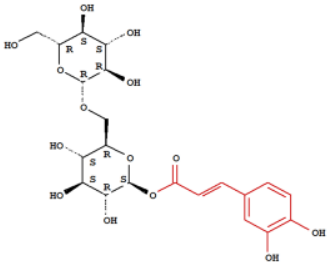

CP3:**β-D-Glucopyranose**, **3-O-β-D-glucopyranosyl-, 1-[3-(3,4-dihydroxyphenyl)-2-propenoate]**

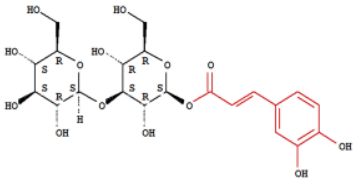

CP4: **α-D-Glucopyranoside,β-D-fructofuranosyl,6-[(2E)-3-(3,4-dihydroxyphenyl)-2-propenoate]**

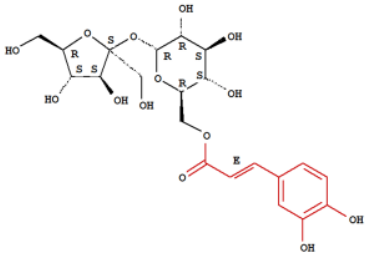

CP5:**D-Glucose,2-O-β-D-glucopyranosyl-, 6-[(2E)-3-(3,4-dihydroxyphenyl)-2-propenoate]**

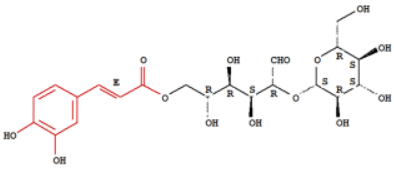

CP6:**D-Glucose,2-O-β-D-glucopyranosyl-, 6-[3-(3,4-dihydroxyphenyl)-2-propenoate]**

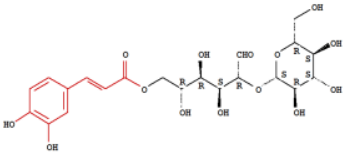

CP7:**D-Glucose,6-O-β-D-glucopyranosyl-, 6-[(2E)-3-(3,4-dihydroxyphenyl)-2-propenoate]**

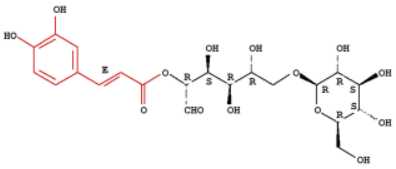

CP8:**β-D-Glucopyranose,1-[3-[3-(β-D-glucopyranosyloxy)-4-hydroxyphenyl]-2-propenoate]**

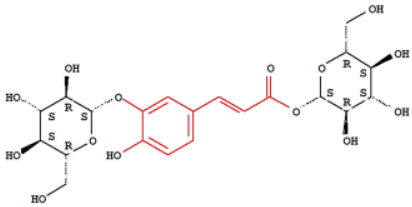

CP9:**β-D-Glucopyranose,1-[(2E)-3-[3-(β-D-glucopyranosyloxy)-4-hydroxyphenyl]-2-propenoate]**

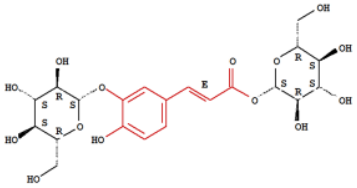

CP10:**β-D-Glucopyranose,1-[(2E)-3-[4-(β-D-glucopyranosyloxy)-3-hydroxyphenyl]-2-propenoate]**

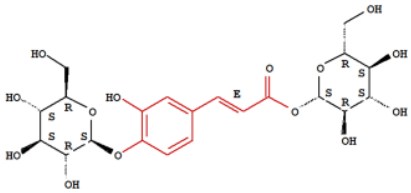

CP11:**2-Propenoic acid,3-[3-[6-O-β-D-glucopyranosyl-β-D-glucopyranosyl)oxy]-4-hydroxypenyl]-,(2E)-**

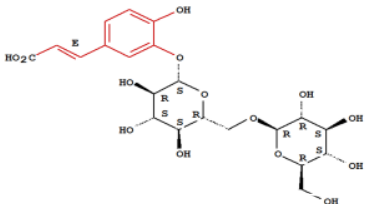

CP12:**2-Propenoic acid, 3-[3,4-bis(β-D-glucopyranosyloxy)phenyl]-**

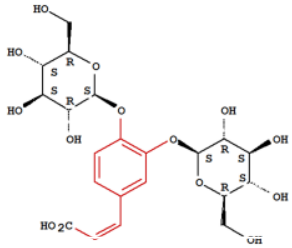

Figure 5.8 The chemical strucutres and CA index names of the 12 reported compounds (CPs) that have the molecular formula of $C_{21}H_{28}O_{14}$ and have the chemical structure of caffeic acid with two sugar substituents.

On the biological activities of 12 compounds in Figure 5.8, CP4 was reported to have moderate activity as an antioxidants in the DPPH test and metmyoglobin test.[314] CPs 5 and 6 were reported to have antihyperglycemic effects. [315, 316] CP7 was reported to have antioxidant activity and it was suspected that it played an important functional role in red vinegar as do anthocyanins and other components.[317]

There are 24 reported compounds consistent with the molecular formula of $C_{15}H_{18}O_9$ and that have the chemical structure of caffeic acid with a sugar attachments. In these 24 compounds, six were reported to have biological effects. The chemical strucutres of these 6 compounds are listed in Figure 5.9.

CP1:**2-Propenoic acid, 3-[3-(β-D-glucopyranosyloxy)-4-hydroxyphenyl]-**

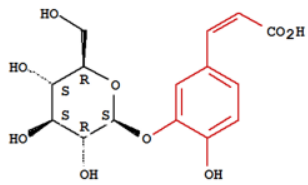

CP2:**2-Propenoic acid, 3-[4-(β-D-glucopyranosyloxy)-3-hydroxyphenyl]-**

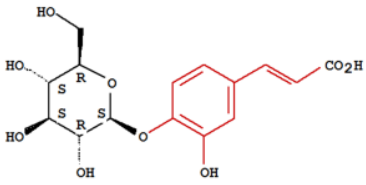

CP3: **β-D-Glucopyranose, 1-[3-(3,4-dihydroxyphenyl)-2-propenoate]**

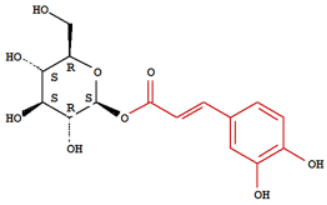

CP4: **β-D-Glucopyranose, 1-[(2E)-3-(3,4-dihydroxyphenyl)-2-propenoate]**

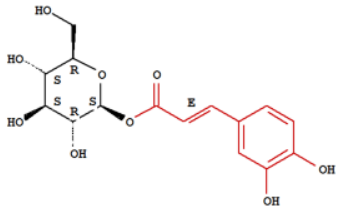

CP5: **D-Glucose, 6-[3-(3,4-dihydroxyphenyl)-2-propenoate]**

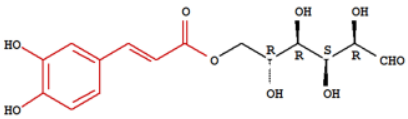

CP6: **D-Glucose, 6-[(2E)-3-(3,4-dihydroxyphenyl)-2-propenoate]**

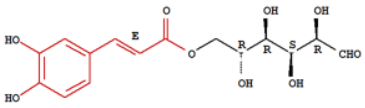

Figure 5.9 The chemical strucutres and CA index names of the 6 reported compounds (CPs) which have the molecular formula of $C_{15}H_{18}O_9$ and have the chemical structure of caffeic acid with a sugar attachemnt.

In Figure 5.9, CP1 was detected in apple and kiwi fruit.[318, 319] CP2 existed in herbal plants, vegetables and fruits, such as *Linum usitatissimum*, *Clematis trichotoma*, kiwi fruit, red currant, and Brazilian species.[75, 318, 320-322] Both compounds have antioxidant effects.[318, 321] CP4 exists in some plants, such as leave of *Coussarea hydrangeifolia*,[323] flower of *Moricandia arvensis*,[324] flower of *Spiraea thunbergia*,[325] rhizome of *Balanophora fungosa*[326] and *Balanophora harlandii*.[327] Study from Iwai, *et al* showed that this compound had α-glucosidase-inhibiting effects. It could supress maltose-induced increase in blood glucose in a diabetic mouse model.[328] CP5 was detected in the bark of *Prunus grayana*.[329] CP6 was obtained in serveral plants, like *Petrorhagia velutina* leaves, whole plants of *Caryopteris incana*, *Alsophila spinulosa* leaves and bark of *Prunus buergeriana* and this compound had antioxidant activity.[330-333] In all 6 compounds listed in Figure 5.10, CP3 is the most well studied one. The common name of CP3 is caffeoylglucose.

Caffeoylglucose, one of the phenolic compounds, is the glucose ester of caffeic acid and it has been identified in some plants, vegetables, tea and fruits like berries, *Annona crassifulora* and kiwi fruit. It often has been detected in the strawberry,[334, 335] red and yellow gooseberry,[336] raspberry and arctic bramble[337] and contributes almost 40% of total measured phenolic acid derivate in black currant fruit.[338] It is rarely found in vegetables. The content of caffeoylglucose in different varieties of tomatoes, bell pepper and eggplant is less than 2 mg/kg.[339] It is also found in olive[340-342] and tobacco[343]. Furthermore, the caffeoylglucose exists in some plants, such as *Begonia* species,[344] several species of fern,[345] leaves of *Phaseolus vulgaris*

var Pinto (pinto bean),[346] *Thymus* spp.,[347] Orchidaceae,[348] and *Petunia hydrida*[349] *et.al*. It was also detected in a Traditional Chinese herb shengma (*Cimicifuga foetida*).[350]

Biological studies of caffeoylglucose have shown that this compound has antioxidant and anti-inflammatory activities. Bastos[351] studied the phenolic antioxidants from yerba mate and green tea and detected caffeoylglucose in them. But his study did not show an antioxidant effect of caffeoylglucose. Du[352] screened the water soluble antioxidant compounds in fruits of *Luffa cylindrica* (L.) Roem by the DPPH radical scavenging activity assay. His research showed that the DPPH radical scavenging activity of 1 mg of caffeoylglucose is 90.4%. Tominaga[353] investigated the 50% scavenging concentration (SC_{50}) of several phenylpropanoid compounds and their glycoside derivatives, in which caffeic acid and caffeoylglucose had SC_{50} value of 8 μM and 29 μM, respectively. This study exerted that the scavenging activity tended to decrease slightly after introducing a β-glucose moiety. A similar result was obtained by Kati who evaluated the antioxidative capability of tomato skin.[354] He suggested that the antioxidant acivity of caffeoylglucoside was less than caffeic acid because of a comparatively short conjugated δ-electron chain.

Furthermore, caffeoylglucose has been shown to have anti-inflammatory activity. Lim studied the nitric oxide production inhibitory effects of phenolic compounds from the fruits of *Actinidia arguta* and the result showed that the IC_{50} of caffeoylglucose decreasing NO release was 27.95 μg/ml.[355] Yuko[356] investigated

the anti-inflammatory effects of extracts from some crude natural drugs. These results suggested that caffeoylglucose would be one of the constituents responsible for the anti-inflammatory activity of *Balanophora japonica*.

There are 4 reported compounds consistent with the molecular formula of $C_{13}H_{14}O_8$. The CA index names and chemical structures of these 4 compounds are listed in Figure 5.10.

CP1: **Butanoic acid,2-[[(2E)-3-(3,4-dihydroxyphenyl)-1-oxo-2-propen-1-yl]oxy]-3,4-dihydroxy-, (2R,3S)-**

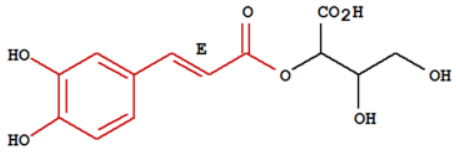

CP2: **Butanoic acid,4-[[3-(3,4-dihydroxyphenyl)-1-oxo-2-propen-1-yl]oxy]-3,4-dihydroxy-, (2R,3S)-**

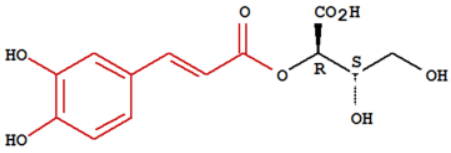

CP3: **Butanoic acid,4-[[3-(3,4-dihydroxyphenyl)-1-oxo-2-propen-1-yl]oxy]-2,3-dihydroxy-, (2R,3S)-**

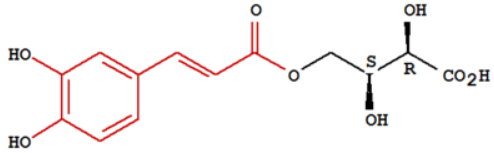

CP4: **Butanoic acid,4-[[(2E)-3-(3,4-dihydroxyphenyl)-1-oxo-2-propen-1-yl]oxy]-2,3-dihydroxy-, (2R,3S)-**

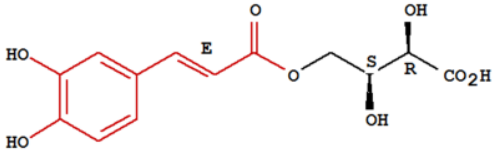

Figure 5.10 The chemical strucutres and CA index names of the 4 reported compounds that have the molecular formula of $C_{13}H_{14}O_8$.

There is only 1 reported compound consistent with the molecular formula of $C_{12}H_{12}O_7$. Its CA index name and the chemical structure of this compound are showed in Figure 5.11. Another name of this compound is (-)-2-(*E*)-caffeoyl-*D*-glyceric acid.

2-Propenoic acid,3-(3,4-dihydroxyphenyl)-,
1-carboxy-2-hydroxyethylester, [R-(E)]-(9Cl)

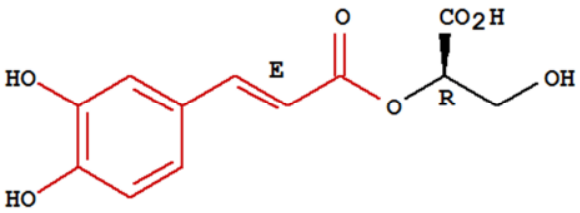

Figure 5.11 The chemical strucutres and CA index names of the reported compound that has the molecular formula of $C_{12}H_{12}O_7$.

Compared with the study of biological activities of caffeoylglucose, the biological studies of compounds listed in Figure 5.10 and 5.11 are fewer in number. The CPs 2 and 3 in Figure 5.10 were reported to have inhibition of neutrophil elastase activity.[357] As neutrophil elastase is secreted by neutrophils during inflammation, it would provide a rational that this compound may have anti-inflammatory effects. Compound shown in Figure 5.11 ((-)-2-(*E*)-caffeoyl-*D*-glyceric acid) was only identified in *Chelidonium majus* by Hahn in 1992,[313] and its biological activity and existance of isomers have not been reported. As (-)-2-(*E*)-caffeoyl-*D*-glyceric acid was isolated from *C. majus*, it might play a role in the therapeutic effects of *C. majus* which traditionally is used against diseases of the liver, the gallbladder and various skin disorders.

In our study of the anti-inflammatory activity of *Clematis* spp., the IC_{50} values of SPE fraction 2 of *C. aristata*-L (0.34 μg/ml), -TN1 (0.2 μg/ml) and *C. microphylla*-TN (0.24 μg/ml) inhibiting NO production were less than the IC_{50} value of ranunculin

(0.54 μg/ml). Based on the reported inhibitory NO production of caffeoylglucose, it provides a rationale that HCA compounds in *Clematis* spp. contribute to the anti-inflammatory activities of the plant extracts. The current work did not obtain the NO inhibitory effects of these HCA compounds. It was suspected that the concentration of HCA compounds in our study was not enough to achieve significant inhibit NO production from LPS stimulated Raw 264.7 cells. The HPLC fractionation method in the anti-inflammatory study of *Clematis* spp. was by timing (22 seconds/fraction). Therefore, HCA compounds were fractionated into several wells and even a single HCA compound was fractionated into two wells and thus the NO inhibitory effects of these HCA compounds was not obtained.

In this study, 3 isomers of (-)-2-(*E*)-caffeoyl-*D*-glyceric acid were detected in *C. aristata*-L. To our knowledge, there are no reports on the isomers of (-)-2-(*E*)-caffeoyl-*D*-glyceric acid. The chemical structures of these HCA compounds have not been investigated in this study. Thus, it might be worth to identify their chemical structures and their biological activities.

5.3.3 Comparison of the hydroxycinnamate esters in Tasmanian *Clematis* species

The chemical constituents study in the *C. aristata*-L revealed that HCA compounds were obtained in *C. aristata*-L SPE cartridge fraction 2. In this part of study, the investigation of HCA compounds in the collected Tasmanian *Clematis* species was undertaken by HPLC-UV.

In the absence of a caffeoglucose standard, the UV absorbance of *C. microphylla*-TN SPE cartridge fraction 2 (CM-TNii) (0.056mg/ml) was determined by UV spectrophotometry as this fraction had the least colour. The approximate concentration of total HCAs in CM-TNii, calculated using Beer's Law ($A=\varepsilon cl$) with $\varepsilon=23000$ at 330nm, was 0.0039mg/ml. The percentage of total HCAs in CM-TNii was estimated to be 7%, using the concentration of total HCAs divided by the concentration of CM-TNii. The amount of CM-TNii used in HPLC analysis was 40 µg, thus the amount of HCAs was 2.8 µg. Total AUC of HCAs obtained in HPLC chromatogram of CM-TNii at 254 nm was 9541082. The total amount of HACs divided by AUC of total HCAs gave a converting factor (CF), which was used to convert the total AUC of HCAs to the total amount of HCAs.

For each *Clematis* spp., the amount of fresh leaves used in the HPLC analysis was obtained by calculation. The amount of HCAs in each *Clematis* spp. fresh leaf sample was then estimated from the AUC of total HCAs multiplied by CF. The amount of individual HCA compounds in the *Clematis* spp. fresh leaves was estimated from the individual compound AUC.

The approximate amounts of individual HCA in each *Clematis* spp. fresh leaf material are summarized in Table 5.3.

Table 5.3 Distribution of nine hydroxycinnamate ester compounds in *Clematis* spp. leaf material. Results are given in microgram of individual hydroxycinnamate ester per gram of fresh leave.

Plant	CP[a]3	CP5	CP6	CP8	CP9	CP10	CP11	CP12	CP13
CA-L-1	146	45	304	93	29	28	26	10	5
CA-L-2	80	69	264	147	59	38	12	24	9
CA-L-3	53	131	111	87	x	0.4	34	94	12
CA-L-4	67	99	142	88	42	13	32	107	13
CA-L-5	64	63	46	74	x	0.6	13	169	15
CA-TN	1	x	1	x	x	x	x	x	x
CA-TN1	x[b]	x	136	38	x	10	x	2	x
CA-W1	37	7	140	21	x	x	x	1	x
CA-W2	31	13	283	40	x	x	x	1	x
CA-W3	x	x	x	x	x	x	x	x	x
CA-EN	79	x	75	x	x	x	x	x	x
CM-TN	9	15	191	x	x	4	x	x	8
CM-B	x	x	246	x	x	x	x	x	x
CG-UTAS	25	x	107	35	x	x	x	x	x
CV-RS	x	x	120	x	197	x	x	x	x

[a]CP means compound
[b]X means the compound was not detected.

Data in Table 5.3 showed that the distribution of nine hydroxycinnamate esters varied in four *Clematis* spp. CA-L-1, 2 and 4 contained all nine compounds; CG-UTAS, CM-B and -TN and CV-RS contained less than five hydroxycinnamate esters. Beside the difference in interspecies, the distribution of hydroxycinnamate esters varied within the same species collected from different location. CA-L had almost all nine hydroxycinnamate esters; however, no hydroxycinnamate ester was obtained in CA-W3. CM collected from Plants of Tasmanian Nursery contained CPs 3, 5, 6, 10 and 13, but CM collected from Bellerive only had compound 6. There were 3 CA collected from Weilangta Forest (CA-W1, W2 and W3). Both CA-W1 and CA-W2 contained the same hydroxycinnamate esters, but the content of individual compounds was different. No hydroxycinnamate ester was detected in CA-W3. The varied distribution of hydroxycinnamate esters was also observed in the two CA collected from Plants of Tasmanian Nursery (CA-TN and CA-TN1). This study

investigated the distribution of hydroxycinnamate esters in different ages of leaves at the same time. The hydroxycinnamate esters detected in five ages of CA-L leaf (CA-L-1, -2, -3, -4 and -5) were similar, but CA-L-3 and -5 did not contain compound 9.

The content of individual hydroxycinnamate ester in different *Clematis* spp. fresh leaves was investigated in this experiment. The highest content of CPs 3, 5, 6, 8, 9, 10, 11, 12 and 13 were obtained respectively in CA-L-1, CA-L-3, CA-L-1, CA-L-2, CV-RS, CA-L-2, CA-L-4, CA-L-4 and CA-L-5. As the previous discussion in Chapter 2 (2.3.1), the differences of the hydroxycinnamate esters distribution would be contributed to by several factors, such as the seasons, environmental conditions and form variation within species.

In this study, we also observed that the content of CP 6 decreased from the youngest to the oldest leaves in CA-L; but the content of CP 12 increased from the youngest to the oldest leaves in CA-L. This result is consistent with the data of the chromatographic peaks 2 and 4 presented in Figure 3.3 of Chapter 3 (3.3.1). As the description in 5.3.3 and the chemical structure shown in Figure 5.10 and 5.11, CP 6 is consistent with caffeic acid having a sugar substituent, and CP 12 is consistent with caffeic acid having a glyceric acid substituent. The phenomenon could be related to the metabolism of hydroxycinnamic esters in the growing process of *C. aristata*-L leaf. Fleuriet and Machexi[358] revealed the marked changes in the metabolism of hydroxycinnamic acid derivatives in pulp and pericarp of tomato fruit. Their study reported that the amount of these derivatives may vary greatly according its

physiological stage: it is orientated towards the formation and accumulation of quinic acid derivatives during growth and towards those of glucose derivative during maturation. The variation was contributed to by activities of enzymes. Therefore, the variation of CP 6 and CP 12 according its physiological stage could be contributed to by the enzyme activity.

Results in this experiment reveal that Tasmanian *Clematis* spp. contain novel flavonoids and hydroxycinnamic esters, which are two kinds of phenolic compounds. Phenolic compounds were reported as antioxidant compounds and their antioxidant capacities had a relationship with their structures.[359] Study from Rosch, *et al*[360] showed that the antioxidant capacity of compounds possessing an *o*-diphenolic arrangement (catechol structure) was higher than monophenols due to their ability to form *o*-quinones when reacting with free radicals.

Some phenolic compounds have benefits for human health. The French have one of the lowest incidences of coronary heart disease in the Western world despite a diet with relatively high fat content. This phenomenon has been linked to the high consumption of red wine, which is rich in complex polyphenols, in France.[361] The potent antioxidant activity of polyphenols may protect against cardiovascular disease.[362-364] Therefore, further investigation into the biological activities of these novel flavonoids and hydroxycinnamic esters in Tasmanian *Clematis* spp. are warranted.

5.4 Conclusion

The study in this chapter identified and measured the amount of nine HCA compounds in Tasmanian *Clematis* spp. To our knowledge, this is the first time HCAs in Tasmanian *Clematis* species have been obtained and the first time the isomers of (-)-4-(*E*)-caffeoyl-*D*-glyceric acid have been observed. The chemical structures of these isomers have not been determined in this study which was beyond the scope of this project.

Results of bio-active fractionation to investigate the antibacterial, antitumour and anti-inflammatory effective constituents exerted by these compounds, did not appear to show any anticancer and antibacterial activities, but these polyphenols may possess potent anti-inflammatory activity.

Chapter 6 Conclusion

This project investigated the chemical constituents, biological activities and the potential pharmaceutical compounds of leaf materials of Tasmanian native *Clematis* spp. and cultivars. This is the first time the pharmaceutical potential value of Tasmanian native *Clematis* species has been studied.

Three aspects of biological activities including antitumour, antibacterial and anti-inflammatory effects of Tasmanian native *Clematis* spp. leaf were investigated. Varied biological effects were observed in different *Clematis* spp. and cultivars. Ranunculin and its isomer were found to be the active constituents in these three aspects of biological effect. Ranunculin could be decomposed to protoanemonin in RPMI-1640, DMEM and *P. aeruginosa* bacterial culture. Ranunculin was found to be a pro-cytotoxin and protoanemonin was identified as the antitumour, antibacterial and anti-inflammatory constituent in the investgated *Clematis* spp.

Ranunculin could be hydrolysed to protoanemonin by the cell media. NCI has reported the antitumour activity of ranunculin against a tumour cell panel. The results in this current study might suggest that the antitumour activity is in fact the antitumour effect of protoanemonin.

In the antibacterial investigation, ranunculin had antibacterial activities against G- bacteria. MIC values were similar for PAO1, PAu19b and PA124 suggested that ranunculin presented the same antibactericidal effects in clinically isolated multi-drug resistant *P. aeruginosa* strains (PAu19b and PA124) as the sensitive strain (PAO1).

The toxic effects of ranunculin against multi-drug resistant *P. aeruginosa* strains involved predominantly cellular lysis, but against sensitive PAO1 involved cellular elongation. The mechanism responsible for this difference has yet to be determined.

Protoanemonin was detected in ranunculin treated *P. aeruginosa* culture. This result suggested that ranunculin penetrated bacterial membranes and moved into the bacterial cells, and hydrolysis of ranunculin occurred within the bacterial cells to produce protoanemonin. This mechanism may be useful as a model for antibacterial pro-drug to target G- bacteria. The MexXY-OrpM multidrug efflux system was detected in PAu19b and PA124. There may be a relationship between the effects of protoanemonin and this efflux pump system that contributes to the cellular lysis of both multi-drug resistant *P. aeruginosa* strains.

Tasmanian native *Clematis* species had a relatively potent effect on inhibition of NO production at levels that have low cytotoxicities. This activity was mostly due to ranunculin, but also be due to other phenolic compounds present. The positive results from the cytotokine studies provided evidence of the anti-inflammatory potential of Tasmanian native *Clematis* spp. and in vitro supported the potential therapeutic value of *Clematis* spp. in immune system diseases. The anti-inflammatory study also provided the experimental evidence for the used of *Clematis* spp. in TCM.

In addition to the biological investigation, chemical characterisation revealed some phenolic compounds in Tasmanian native *Clematis* spp. These compounds did not

contribute to the antitumour and antibacterial activities, but may have other potential biological activities, including anti-inflammatory activities.

However, there were some limitations in this study. The aim of this study was to investigate the pharmaceutical potential of compounds from the leaf of Tasmanian native *Clematis* spp. This study successfully isolated and purified the active compound, ranunculin, and also determined MICs of ranunculin against some +ve and –ve bacteria, the antitumour and anti-inflammatory IC_{50} of ranunculin, and its potential antibacterial and antitumour mechanism. However, in this research, other chemical constituents, such as novel phenolic compounds, flavonoids which were described in Chapter 5 were not isolated and their biological activities have not been investigated.

In summary, initial *in vitro* biological screening of Tasmanian native *Clematis* spp. revealed therapeutic potential in antitumour, antimicrobial and immune system diseases. Further investigations are warranted to explore the efficay of Tasmanian native *Clematis* spp. and other *Clematis* spp. used in TCM.

References

1.aWang WT, Li LQ. A new system of classification of the genus *Clematis* (Ranunculaceae). *Acta Phytotaxonomic Siinica*. 2005;43(5):431-488.

2.aGuan KL, Zhi J; Li JX; Kuang J. Preliminary study on introduction and cultivation of *Clematis*. *Acta Botanica Yunnanica*. 2002;24(3):392-396.

3.a.Xiao PG, Ding ZJ, Wan JR, Wei YF, Xun GJ, He HX, *et al*. Zhong Hua Ben Cao. Hu XM, editor. Shanghai Scientific and Technical Publisher; Shanghai. 1999.

4.aLi FL, Li F, Li YM, Wang YX, Zhu XX. Total saponins of radix clematidis, their preparation method and use in preparation of pharmaceuticals. China patent CN 1724014 A 20060125. 2006.

5.aLi JL, Jin W; Deng, XD. A chinese medicinal composition for treating gynecological diseases and dermatoses, and its preparation method. China patent CN 1772172 A 20060517. 2006.

6.aQin J. Manufacture of traditional Chinese medicines for preventing and treating cardiovascular and cerebrovascular diseases. China patent CN 1765408 A 20060503. 2006.

7.aZhang M. Chinese medicine plaster for treating rheumatosis. China patent CN 1739700 A 20060301. 2006.

8.aFu G. Traditional Chinese medicine ointment for regulating, balancing and lubricating human knee joint. China patent CN 1739661 A 20060301. 2006.

9.aLi ZZ, Jin W. "Fengshi Gubing Ke" medical composition for treating rheumatic bone diseases. China patent CN 1466980 A 20040114. 2004.

10.aLi XL, Shun L. Manufacture of effervescent granule for treating urinogenital system disease. China patent CN 1650957 A 20050810. 2005.

11.aSun J. Traditional Chinese medicine for treating ischemic necrosis of bone, delayed union and nonunion. China patent CN 1742834 A 20060308. 2006.

12.aMa JM. Chinese medicine plaster and preparation. China patent CN 1739772 A 20060301. 2006.

13.aOu BY, Zhi W. Chinese medicinal composition with litholytic, anti-inflammatory, analgesic and antibacterial effects, and its preparation method. China patent CN 1714860 A 20060104. 2006.

14.aKim MMS, Jae G, Kim SN, Kim JH, Park SG, Lee HM. Pharmaceutical composition for treatment of periodontal diseases and anti-inflammation. Korean patent KR 2000041190 A 20000715. 2000.

15.aZhang Y. A topically-applied medicinal liquor for treating traumatic injuries. China patent CN 1762463 A 20060426. 2006.

16.aWang H. A topical chinese medicinal composition for treating traumatic injuries. China patent CN 1739726 A 20060301. 2006.

17.aZhang Y. A topically-applied chinese medicinal composition comprising *Clematis lasiandra* for treating traumatic injuries. China patent CN 1762414 A 20060426. 2006.

18.aLiao Y. Chinese medicinal composition for treating traumatic injury and its preparation method. China patent CN 1723924 A 20060125. 2006.

19.aWang H. A chinese medicinal liquor for treating traumatic injury and rheumatism. China patent CN 1762472 A 20060426. 2006.

20.aMa T, Ma H. Plaster for treating fracture and hyperosteogeny. China patent CN 1759868 A 20060419. 2006.

21.aXu XX, Xu LZ, Dai M, Peng DY. The study on anti-inflammatory and analgesic effect of total saponins of *Clematis*. *Journal of Chinese Medical and Clinical Pharmacology*. 2005;21(4):34-35.

22.aYao J. Manufacture of a soft capsule for treating rhinitis. China patent CN 1730033 A 20060208. 2006.

23.aYue S. Guli thin film coated tablet for treating bone disease and fracture. China patent CN 1733285 A 20060215. 2006.

24.aZheng G. A chinese medicinal decoction for treating senile acute urine retention. China patent CN 1626172 A 20050615. 2005.

25.aPan Q. Manufacture of composite traditional Chinese medicine for treating hepatoma, hepatitis B, hepatocirrhosis, and hepatic fibrosis. China patent CN 1644213 A 20050727. 2005.

26.aLi YJ. Chinese medicine intumescent tablet for treating primary carcinoma of liver and its preparation. China patent CN 1593521 A 20050316. 2005.

27.aTian XC, Shang Q. Preparation of pharmaceutical composition for treating osteoarthritis. China patent CN 1618448 A 20050525. 2005.

28.aDou CH, Luo S, Huang F. A Chinese medicine for treating vasculitis and its preparation method. China patent CN 1589877 A 20050309. 2005.

29.aZhang J. Manufacture of traditional Chinese medicine bag for treating cholelithiasis. China patent CN 1559521 A 20050105. 2005.

30.aChen X. Medical composition for treating fungal dermatosis or bromhidrosis. China patent CN 1431008 A 20030723. 2003.

31.aSeo WS. Composition for improving erectile dysfunction and blood circulation. Korean patent KR 2003065734 A 20030809. 2003.

32.aLee JH. Composition for repressing withdrawal symptom. Korean patent KR 2001009465 A 20010205. 2001.

33.aYun YK. Plaster for treatment of nervous paralysis. Korean patent KR 2001000815 A 20010105. 2001.

34.aLassak EV, McCarthy T. Australian Medicinal Plants. Methuen, North Ryde.1983.

35.aLi RW, Myers SP, Leach DN, Lin GD, Leach G. A cross-cultural study: anti-inflammatory activity of Australian and Chinese plants. *Journal of Ethnopharmacology*. 2003;85(1):25-32.

36.aOkalebo FA, Rabah HA, Guantai AN, Kibwage IO, Mwangi JW, Masengo W. The antimalarial and antimicrobial activity and brine shrimp toxicity of *Clematis brachiata* extracts. *East and Central African Journal of Pharmaceutical Sciences*. 2002 5(1):15-18.

37.aCáceres A, Menéndez H, Méndez E, Cohobón E, Samayoa BE, Jauregui E, *et al*. Antigonorrhoeal activity of plants used in Guatemala for the treatment of sexually transmitted diseases. *Journal of Ethnopharmacology*. 1995;48(2):85-88.

38.aYeşilada E, Ustün O, Sezik E, Takaishi Y, Ono Y. Inhibitory effects of Turkish folk remedies on inflammatory cytokines: interleukin-1alpha, interleukin-1beta and tumor necrosis factor alpha. *Journal of Ethnopharmacology*. 1997;58(1):59-73.

39.aPark EK, Ryu MH, Kim YH, Lee YA, Lee SH, Woo DH, *et al*. Anti-inflammatory effects of an ethanolic extract from *Clematis mandshurica* Rupr *Journal of Ethnopharmacology*. 2006;108 (1):142-147.

40.aJung YB, Roh KJ, Jung JA, Jung K, Yoo H, Cho YB, *et al*. Effect of SKI 306X, a new herbal anti-arthritic agent, in patients with osteoarthritis of the knee: a double-blind placebo controlled study. *American Journal of Chinese Medicine*. 2001;29(3-4):485-491.

41.aLee SW, Chung WT, Choi SM, Kim KT, Yoo KS, Yoo YH. *Clematis mandshurica* protected to apoptosis of rat chondrocytes. *Journal of Ethnopharmacology* 2005;101:294-298.

42.aJung YB, Seong SC, Lee MC, Shin YU, Kim DH, Kim JM, et al. A four-week, randomized, double-blind trial of the efficacy and safety of SK1306X: A herbal anti-arthritic agent versus diclofenac in osteoarthritis of the knee. *American Journal of Chinese Medicine*. 2004;32(2):291-301.

43.aSong YW, Lee EY, Koh EM, Cha HS, Yoo B, Lee CK, *et al.* Assessment of comparative pain relief and tolerability of SK1306X compared with celecoxib in patients with rheumatoid arthritis: A 6-week, multicenter, randomized, double-blind, double-dummy, phase III, noninferiority clinical trial. *Clinical Therapeutics*. 2007;29(5):862-873.

44.aFont J, Pascual J. Ranunculin, protoanemonin, and anemonin. I. Isolation of ranunculin from *Clematis flammula*. *Anales de la Real Sociedad Espanola de Fisica y Quimica, Serie B: Quimica*. 1966;62(6):705-707.

45.aRudakov IF. The rate of anemonin accumulation in *Clematis recta*. *Uchenye Zapiski Orekhovo-Zuevsk.* 1958;11:97-99.

46.aHerz W, Pates AL, Madsen GC. The antimicrobial principle of *Clematis dioscoreifolia*. *Science*. 1951;114:206.

47.aKern JR, Cardellina JH 2nd. Native American medicinal plants. Anemonin from the horse stimulant *Clematis hirsutissima*. *Journal of Ethnopharmacology*. 1983;8(1):121-123.

48.aAl-Taweel AM, El-Deeb KS, Abdel-Kader MS. GC/MS analyses anti-inflammatory and anti-microbial activities of the volatile constituents of three *Clematis* species growing in Saudi Arabia. *Saudi Pharmaceutical Journal*. 2008;16(2):170-174.

49.aSong Z, Zhao Y, Duan J, Wang X. Review of chemical consistuents and pharmacological actions of *Clematis* species. *Natural Product Research and Development*. 1995;7(2):66-72.

50.aSouthwell IA, Tucker DJ. Protoanemonin in Australian *Clematis*. *Phytochemistry*. 1993;33(5):1099-1102.

51.aBonora A. Dall'Olio G, Donini A, Bruni A. An HPLC screening of some Italian ranunculaceae for the lactone protoanemonin. *Phytochemistry*. 1987;26(8):2277-2279.

52.aJin FM. Extraction, analysis and biological screening of *Clematis* species. MPharmSci thesis, University of Tasmania, Hobart. 2007.

53.aChirva VY, Kintya PK, Mel'nikov, VN. New data on triterpene glycosides. In: Rozinskaya VN, editor. *Ref Dokl Soobshch-Mendeleevsk S'ezd Obshch Prikl Khim, 11th*; Moscow: Nauka; 1975; 109.

54.aThapliyal RP, Bahuguna RP. An oleanolic acid based bisglycoside from *Clematis montana* roots. *Phytochemistry*. 1993;34(3):861-862.

55.aShao BQ, Guo W, Xu RS, Wu HM, Ma K. Triterpenoid saponins from *Clematis chinensis*. *Phytochemistry*. 1995;38(6):1473-1479.

56.aShao BQ, Guo W, Xu RS, Wu HM, Ma K. Saponins from *Clematis chinensis*. *Phytochemistry*. 1996;42(3):821-825.

57.aKizu H, Shimana H, Tomimori T. Studies on the constituents of *Clematis* species. VI. The constituents of *Clematis stans* Sieb. et Zucc. *Chemical & Pharmaceutical Bulletin*. 1995;43(12):2187-2194.

58.aThapliyal RP, Bahuguna RP. Clemontanoside-E, a new saponin from *Clematis montana*. *International Journal of Pharmacognosy*. 1994;32(4):373-377.

59.aThapliyal RP, Bahuguna RP. Clemontanoside B, a new saponin from *Clematis montana*. *International Journal of Crude Drug Research*. 1990;28(1):39-41.

60.aZhong HM, Chen CX, Tian X, Chui YX, Chen YZ. Triterpenoid saponins from *Clematis tangutica*. *Planta Medica*. 2001;67(5):484-488.

61.aKawata Y, Kizu H, Miyaichi Y, Tomimori T. Studies on the constituents of *Clematis* species. VIII. Triterpenoid saponins from the aerial part of *Clematis tibetana* Kuntz. *Chemical & Pharmaceutical Bulletin*. 2001;49(5):635-638.

62.aKawata Y, Kizu H, Miyaichi Y, Tomimori T. Studies on the constituents of *Clematis* species. VII. Triterpenoid saponins from the roots of *Clematis terniflora* DC. var. robusta Tamura. *Chemical & Pharmaceutical Bulletin*. 1998;46(12):1891-1900.

63.aThapliyal RP, Bahuguna RP. Clemontanoside-C, a saponin from *Clematis montana*. *Phytochemistry* 1993;33(3):671-673.

64.aKrokhmalyuk VV, Kintya PK, Chirba VY. Structure of saponin A' and B' from *Clematis songarica*. *Biologicheskiei Khimicheskie Nauki*. 1975;(6):68-70.

65.aKrokhmalyuk VV, Kintya PK, Chirba VY. In: Lazarev AM, editor. Triterpenoid glycosides from *Clematis songarica* Bge. *Tezisy Dokl Soobshch - Konf Molodykh Uch Mold, 9th*; Kishinev: Shtiintsa; 1975; 101-102.

66.aKrokhmalyuk VV, Kintya PK, Chirva VY, Boshko ZI. Structure of the principle saponin from *Clemantis songarica*. *Khimiya Prirodnykh Soedinenii*. 1975;11(4):470-474.

67.aSati OP, Uniyal SK, Bahuguna S, Kikuchi T. Clematoside-S, a triterpenoid saponin from the roots of *Clematis grata*. *Phytochemistry*. 1990;29(11):3676-3678.

68.aDong FY, Cui GH, Zhang YH, Zhu RN, Wu XJ, Sun TT, *et al*. Clematomandshurica saponin E, a new triterpenoid saponin from *Clematis mandshurica*. *Journal of Asian Natural Products Research*. 2010;12(11-12):1061-1068.

69.aJangwan JS, Dobhal M. New triterpene glycosides of *Clematis montana* and their cytotoxic activities. *Journal of Indian Chemical Society*. 2008;85(3):313-316.

70.aSun F, He Q, Xiao PG, Cheng YY. A new triterpenoid saponin from *Clematis ganpiniana*. *Chinese Chemical Letters*. 2007;18(9):1078-1080.

71.aMimaki Y, Yokosuka A, Hamanaka M, Sakuma C, Yamori T, Sashida Y. Triterpene saponins from the roots of *Clematis chinensis*. *Journal of Natural Products*. 2004;67(9):1511-1516.

72.aShi S, Jiang D, Dong C, Tu P. Triterpene Saponins from *Clematis mandshurica Journal of Natural Products*. 2006;69(11):1591-1595.

73.aFu Q, Zan K, Zhao M, Zhou S, Shi S, Jiang Y, *et al*. Triterpene saponins from *Clematis chinensis* and their potential anti-inflammatory activity. *Journal of Natural Products*. 2010;73(7):1234-1239.

74.aDai W, Fang S, Liu P. Effect of *Clematis* saponins on cell apoptosis and NF-kB expression in human gastric carcinoma cell line SGC-7901. *Nanjing Yike Daxue Xuebao*. 2010;30(8):1074-1078, 1104.

75.aHam SB, Kim YI, Kwon YS, Kim CM. Compounds of the stem of *Clematis trichotoma*. *Saengyak Hakhoechi*. 1999;30(3):301-305.

76.aShi Y, Wang H. Studies on the chemical constituents of intricate *Clematis* (*Clematis intricata*). *Chinese Traditional and Herbal Drugs*. 1997;28(6):329-330.

77.aSayed HM, El-Moghazy SA, Kamel MS. Chemical constituents of stems and leaves of *Clematis purpurea* hybrida cultivated in Egypt. *Indian Journal of Chemistry, Section B.* 1995;34B(12):1111-1113.

78.aZhang XW, Yu UT, Wen HX, Mei LJ, Shao Y, Tao YD. RP-HPLC determination of flavonoids in flowers of *Clematis tangutica* (Maxim.) Korsh. *Guoyi Guoyao*. 2010;21(12):3048-3049.

79.aUdal'tsova LA, Minina SA, Chernysheva ZI. Phytochemical study of the six-petal clematis-*Clematisahexapetala*. *TruyaLeningradskogoaKhimiko-Farmatsevtic-heskogo Instituta*. 1968;26:195-199.

80.aUlanova KP, Zaitseva NM. Comparative study of the flavnoids of far eastern species of *Clematis* and *Atragene*. *Rastitel'nye Resursy*. 1979;15(2):277-280.

81.aDu ZZ, Yang XW, Han H, Cai XH, Luo XD. A new flavone C-glycoside from *Clematis rehderiana*. *Molecules*. 2010;15:672-679.

82.aZhang L, Luo X, Tian J. Chemical constituents from *Clematis terniflora*. *Chemistry of Natural compounds*. 2007;43(2):128-131.

83.aSun F, Zhang L, Tian J, Cheng Y, Xiao P. Chemical constituents of *Clematis terniflora*. *Chinese Pharmaceutical Journal*. 2007;42(2):102-103.

84.aDong CX, Wu KS, Shi SP, Tu PF. Flavanoids from *Clematis hexapetala*. *Journal of Chinese Pharmaceutical Science*. 2006;15(1):15-20.

85.aChen YF, Jian L, Davidson, RS, Howarth OW. Isolation and structure of clematine, a new flavanone glycoside from *Clematis armandii* Franch. *Tetrahedron*. 1993;49(23):5169-5176.

86.aAritomi M, Kumamoto U. Terniflorin, a new flavonoid compound in flowers of *Clematis terniflora* var. robusta. *Chemical & Pharmaceutical Bulletin*. 1963;11 (10):1225-1228.

87.aGulibahaer A. Analysis of active ingredients and total flavonoids in *Clematis sibirica* (L.) Mill. *Shipin Kexue*. 2009;30(24):221-226.

88.aHuang WW, Kong DY, Yang PM. Studies on lignan constituents of *Clematis armandii* Franch. *Chinese Journal of Natural Medicines*. 2003;1(4):199-203.

89.aYan L, Xu L, Lin J, Zou Z, Zhao B, Yang S. Studies on lignan constituents of *Clematis parviloba*. *China Journal of Chinese Materia Medica*. 2008;33(15):1839-1843.

90.aShi SP, Jiang D, Dong CX, Tu PF. Lignans from the roots and rhizomes of *Clematis manshurica*. *Zeitschrift fur Naturforschung Section B: Chemical Sciences*. 2006; 61(10):1299-1303.

91.aYan L, Xu L, Zou Z, Yang S. Chemical constituents from stems of *Clematis armandii* (I). *Journal of Chinese Medicinal Materials*. 2007;38(3):340-342.

92.aShi SP, Dong CX, Jiang D, Tu PF. Macrocyclic glycosides from *Clematis hexapetala*. *Helvetica Chimica Acta*. 2006;89(12):3002-3006.

93.aShi SP, Dong CX, Jiang D, Tu PF. Macrocyclic glucosides from *Clematis mandshurica* and *Clematis hexapetala*. *Biochemical Systematics and Ecology.* 2007; 35 (1):57-60.

94.aYan L, Yang S, Zou Z, Luo X, Xu L. Two new macrocyclic compounds from the stems of *Clematis armandii*. *Heterocycles*. 2006;68(9):1917-1924.

95.aGulibahaer A. Optimal extraction of polysaccharides from different parts of *Clematis songarica* Bge. in Xinjiang. *Shipin Kexue*. 2010;31(22):198-202.

96.aSun Y, Chen Y. Isolation, purification, physical and chemical properties analysis of polysaccharides from root of *Clematis chinensis* Osbeck. *China Journal of Hosptial Pharmacy*. 2010;30(4):271-274.

97.aDong CX, Shi SP, Wu KS, Tu PF. Chemical constituents from the roots and rhizomes of *Clematis hexapetala* pall. *Zeitschrift fur Naturforschung Section B: Chemical Sciences*. 2007;62(6):854-858.

98.aShi S-P, Jiang D, Dong C-X, Tu P-F. New phenolic glycosides from *Clematis mandshurica*. Helvetica Chimica Acta. 2006;89(5):1023-1029.

99.aJiang B, Liao X, Jia X, Ye X, Ding J, Yu X, *et al*. Studies and comparisons on chemical components of essential oils from *Clematis hexapetala* Pall. and *Inula nervosa* Wall. *China Journal of Chinese Materia Medica*. 1990;15(8):488-490,512.

100.aZeng YX, Zhao CX, Liang YZ, Yang H, Fang HZ, Yi LZ, *et al*. Comparative analysis of volatile components from *Clematis* species growing in China. *Analytica Chemica Acta*. 2007;595 (1-2): 328-339.

101.aShi SP, Tu PF, Dong CX, Jiang D. Alkaloids from *Clematis manshurica* Rupr. *Journal of Asian Natural Products Research*. 2006;8 (1-2):73-78.

102.aChen JH, Du ZZ, Shen YM, Yang YP. Aporphine alkaloids from *Clematis parviloba* and their antifungal activity. *Archives of Pharmacal Research*. 2009;32(1):3-5.

103.aSong Z, Zhao Y, Duan J, Wang X. Chemical constituents of *Clematis intricata* Bunge. *China Journal of Chinese Materia Medica*. 1995;20(10):613-614, 40.

104.aDong CX, Shi SP, Wu KS, PF. T. Studies on chemical constituents from root of *Clematis hexapetala*. *China Journal of Chinese Materia Medica*. 2006;31(20):1696-1699.

105.aHe M, Zhang JH, CQ H. Studies on the chemical components of *Clematis chinensis*. *Acta Pharmaceutica Sinica*. 2001;36(4):278-280.

106.aYamaguchi M, Ichinohe Y, Watanabe H, Tsuda Y. Sucrose octaacetate from *Clematis*. *Phytochemistry*. 1976;15(2):326-327.

107.aHamberg M. Isolation and structures of two divinyl ether fatty acids from *Clematis vitalba*. Lipids. 2004; 39(6):565-569.

108.aSong Z, Zhao Y, Duan J, Wang X. Studies on the chemical constituents of *Clematis intricata* Bunge. *China Journal of Chinese Materia Medica*. 1995;20(10):613-614.

109.aSong Z, Zhang J, Li Y, Zhao Y, Wang X, Cai L. Studies on the chemical constituents of *Clematis intricata* Bunge (II). *Natural Product Research and Development*. 1997;9(2):11-16.

110.aYang M, Zhong C, Zhu H, Cui D, Li S. Chemical constituents of volatile oils from *Clematis manshurica* Rupr. *Chinese Traditional and Herbal Drugs*. 1997;28(4):204.

111.aLiu Z, Gao H, Zheng P, Lu R. Chemical constituents from the oil of *Clematis glauca*. *Natural Product Research and Development*. 2001;13(5):25-27.

112.aDong C, Shi S, Wu K, Tu P. Studies on chemical constituents from root of *Clematis hexapetala*. *China Journal of Chinese Materia Medica*. 2006;31(20):1696-1699.

113.aSong L, Zhang W, Wu JR, Zhou XJ. Chemical constituents study of *Clematis apiifolia* DC. volatile oil. *Shanghai Zhongyiyao Daxue Xuebao*. 2006;20(4):83-84.

114.aShi S, Jiang D, Dong C, Tu P. Chemical constituents of *Clematis mandschurica*. *Chinese Traditional and Herbal Drugs*. 2007;38(3):335-337.

115.aAl-Taweel AM, El-Deeb KS, Abdel-Kader MS, Mossa JS. GC/MS analysis of the fatty acids of three *Clematis* species growing in Saudi Arabia and their anti-inflammatory activity. *Saudi Pharmaceutical Journal*. 2007;15(3-4):224-227.

116.aYan L, Xu L, Lin J, Zou Z, Zhao B, Yang S. Chemical constituents of *Clematis parviloba*. *Chinese Traditional and Herbal Drugs*. 2008;39(11):1619-1621.

117.aXi R, Zhang H, Zhang G, Sun Z, Wang C, Zhang H. Study on volatile components in different species of Radix Clematidis. *Modern Chinese Medicine*. 2009;11(6):12-13.

118.aLi Y, Wang SF, Zhao YL, Liu KC, Wang XM, Yang YP, *et al*. Chemical constituents from *Clematis delavayi* var. spinescens. *Molecules*. 2009;14(11):4433-4439.

119.aAli-Shtayeh MS, Abu Ghdeib SI. Antifungal activity of plant extracts against dermatophytes. *Mycoses*. 1999;42(11-12):665-672.

120.aCos P, Hermans N, De Bruyne T, Apers S, Sindambiwe JB, Vanden BD, *et al*. Further evaluation of Rwandan medicinal plant extracts for their antimicrobial and antiviral activities. *Journal of Ethnopharmacology*. 2002;79(2):155-163.

121.aDu ZZ, Zhu N, Ze-Ren-Wang-Mu N, Shen YM. Two new antifungal saponins from the Tibetan herbal medicine *Clematis tangutica*. *Planta Medica*. 2003;69 (6):547-551.

122.aWang QW, Wang K, Yang X, Cui ZF. Studies on antifungal activity of ethanol extracts from 89 Traditional Chinese Medicine. *Zhejiang Gongye Daxue Xuebao*. 2009;37(3):289-294.

123.aBuzzini P, Pieroni A. Antimicrobial activity of extracts of *Clematis vitalba* towards pathogenic yeast and yeast-like microorganisms. *Fitoterapia*. 2003; 74(4):397-400.

124.aDocheva-Popova R, Popov K. Investigation of the relative antibiotic actions of ranunculaceous plants. *Biol-Geol-Geograf Fak No l-Biol*. 1955;48:41-58.

125.aKyung KH, Woo YH, Kim DS, Park HJ, Kim YS. Antimicrobial activity of an edible wild plant, apiifolia Virgin's Bower (*Clematis apiifolia* DC). *Food Science Biotechnology*. 2007;16(6):1051-1054.

126.aQiu G, Zhang M, Yang Y. The antitumour activity of total saponin of *Clematis chinensis*. *Journal of Chinese Medicinal Materials*. 1999;22(7):351-353.

127.aQiu G, Zhang M, Y. Y. The antitumour activity of total saponin of *Clematis chinensis*. *Journal of Chinese Medicinal Materials.* 1999; 22(7):351-353.

128.aDing Q, Yang LX, Yang HW, Jiang C, Wang YF, Wang S. Cytotoxic and antibacterial triterpenoids derivatives from *Clematis ganpiniana*. *Journal of Ethnopharmacology*. 2009;126(3):382-385.

129.aYan LH, Xu LZ, Lin J, Yang SL, Feng YL. Triterpenoid saponins from the stems of *Clematis parviloba*. *Journal of Asian Natural Products Research*. 2009;11(4):332-338.

130.aZhao Y, Wang CM, Wang BG, Zhang CX. Study on the anticancer activities of the *Clematis manshrica* saponins *in vivo*. *China Journal of Chinese Materia Medica*. 2005;30(18):1452-1453.

131.aLi RZ, Ji XJ. The cytotoxicity and action mechanism of ranunculin in vitro. *Acta Pharmaceutica Sinica*. 1993;28(5):326-331.

132.aChen F, Guo X, Zhong M. Effect of six petal *Clematis* root parenteral solution on interlukin-1 level in osteoarthritis joint fluid and chondrocyte culture supernatan. *Orthopedic Journal of China*. 2004;12(7):524-526.

133.aLi RW Li GD, Leach DN, Waterman PG, Myers SP. Inhibition of COXs and 5-LOX and activation of PPARs by Australian *Clematis*. *Journal of Ethnopharmacology*. 2006;104 (1/2):138-143.

134.aLiu L, Zhu Q, Wang L. Anti-inflammation and analgesia compound Weilingxian mixture. *Hei Longjiang Medicine and Pharmacy* 2004;27(1):22-23.

135.aOyang H, Chen Y. Studies on the main pharmacological effect of compound Weilingxian Zhengtong plaster. *Pharmaceutical Journal of Chinese People's Liberation Army*. 2005; 21(2):107-109.

136.aWang X, Cui J, Xiao Z. Comparative studies of Chinese drug Tougucao on antiinflammatory and analgesic effects. *Journal of Beijing Medicinal University*. 1998;30(2):145-148.

137.aYesilada E, Kupeli E. *Clematis vitalba* L. aerial part exhibits potent anti-inflammatory, antinociceptive and antipyretic effects. *Journal of Ethnopharmacology*. 2007;110(3):504-515.

138.aMostafa M, Appidi JR, Yakubu MT, Afolayan AJ. Anti-inflammatory, antinociceptive and antipyretic properties of the aqueous extract of *Clematis brachiata* leaf in male rats. *Pharmaceutical Biology*. 2010;48(6):682-689.

139.aXu X, Xia L, Dai M, Peng D. The study on anti-inflammatory and analgesic effect of total saponins of *Clematis*. *Journal of Chinese Medical and Clinical Pharmacology* 2005;21(4):34-35.

140.aXia LZ, Xu XX, Zhang R. Effect of total saponins of *Clematis* on adjuvant arthritis in rats. *Anhui Yiyao*. 2009;13(4):363-365.

141.aSun SX, Li YM, Fang WR, Cheng P, Liu L, Li F. Effect and mechanism of AR-6 in experimental rheumatoid arthritis. *Clinical and Experimental Medicine*. 2010;10(2):113-121.

142.aLiu LF, Ma XL, Wang YX, Li FW, Li YM, Wan ZQ, *et al*. Triterpenoid saponins from the roots of *Clematis chinensis* Osbeck. *Journal of Asian Natural Product Research*. 2009;11(5):389-396.

143.aWu W, Xu X, Dai Y, Xia L. Therapeutic effect of the saponin fraction from *Clematis chinensis* Osbeck roots on osteoarthritis induced by monosodium iodoacetate through protecting articular cartilage. *Phytotherapy Research*. 2010;24(4):538-546.

144.aKim JH, Ryu KH, Jung KW, Han CK, Kwak WJ, Cho YB. Effects of SKI306X on arachidonate metabolism and other inflammatory mediators. *Biological & Pharmaceutical Bulletin*. 2005;28(9):1615-1620.

145.aKim JH, Rhee HI, Jung IH, Ryu K, Jung K, Han CK, *et al*. SKI306X, an oriental herbal mixture, suppresses gastric leukotriene B4 synthesis without causing mucosal injury and the diclofenac-induced gastric lesions. *Life Science*. 2005;77(11):1181-1193.

146.aHartog A, Hougee S, Faber J, Sanders A, Zuurman C, Smit HF, *et al*. The multicomponent phytopharmaceutical SKI306X inhibits in vitro cartilage degradation and the production of inflammatory mediators. *Phytomedicine*. 2008;15(5):313-320.

147.aChoi JH, Choi JH, Kim DY, Yoon JH, Youn HY, Yi JB. Effects of SKI 306X, a new herbal agent, on proteoglycan degradation in cartilage explant culture and collagenase-induced rabbit osteoarthritis model. *Osteoarthritis and Cartilage* 2002;10(6): 471-478.

148.aLee SW, Choi SM, Chang YS, Kim KT, Kim TH, Park HT, *et al*. A purified extract from Clematis mandshurica prevents staurosporin-induced downregulation of 14-3-3 and subsequent apoptosis on rat chondrocytes. *Journal of Ethnopharmacology*. 2007;111(2):213-218.

149.aLee SW, Lee HJ, Moon JB, Choi SM, Kim DK, Kim IR, et al. A Purified Extract from *Clematis mandshurica* prevents adenoviral-TRAIL induced

apoptosis on rat articular chondrocytes. *American Journal of Chinese Medicine*. 2008;36(2):399-410.

150.aSuh SJ, Kim KS, Lee SD, Lee CH, Choi HS, JJin UH, *et al*. Effects and mechanisms of *Clematis mandshurica* Maxim. as a dual inhibitor of proinflammatory cytokines on adjuvant arthritis in rats. *Environmental Toxicology and Pharmacology*. 2006; 22(2):205-212.

151.aKarpovich VN. Preliminary investigation of plants found in Eastern recipes used in cardiovascular disease. *Leningradskogo Khimiko-Farmatsevticheskogo Instituta.* 1961;12: 195-200.

152.aHo CS, Wong YH, Chiu KW. The hypotensive action of *Desmodium styracifolium* and *Clematis chinensis*. American Journal of Chinese Medicine. 1989;17(3-4):189-202.

153.aHuang S, Jiang Z. Studies on extractive method and anti-malaria effect of Radix Clematidis. *Strait Pharmaceutical Journal*. 2001;13(4):22-24.

154.aAlvarez ME, Maria AOM, Villegas O, Saad JR. Evaluation of diuretic activity of the constituents of *Clematis montevidensis* Spreng. (Ranunculaceae) in rats. *Phytotherapy Research*. 2003;17(8):958-960.

155.aChiu HF, Lin CC, Yang CC, Yang F. The pharmacological and pathological studies on several hepatic protective crude drugs from Taiwan (I). *American Journal of Chinese Medicine*. 1988;16(3-4):127-137.

156.aMiseeva RK. Effect of Clematis fusca preparations on androgen target organs. *Bulletin of Experimental Biology and Medicine*. 1975;80(7):60-61.

157.aMin BS, Kim YH, Tomiyama M, Nakamura N, Miyashiro H, Otake T, *et al*. Inhibitory effects of Korean plants on HIV-1 activities. *Phytotherapy Research*. 2001;15(6):481-486.

158.aGulibahaer A. Antioxidant activity of total flavonoids from different organs of *Clematis glauca* willd. in Xinjiang. *Shipin Kexue*. 2010;31(23):18-21.

159.aChen Y, Sun YJ, Fang W. Study on antioxidant activity of *Clematis chinensis* Osbeck polysaccharide. *China Journal of Traditional Chinese Medicine and Pharmacy*. 2008;23(3):266-270.

160.aPawar RS, Balachandran P, Pasco DS. In: Khan I A, editor. Cytotoxicity studies of triterpenoids from Akebia trifoliata and *Clematis ligusticifolia*. *Proceedings of the fourth International Conference on Quality and Safety Issues Related to Botanicals*. Mississippi, USA. 2006.

161.aHuang YH, Lee TH, Chan KJ, Hsu FL, Wu YC, Lee MH. Anemonin is a natural bioactive compound that can regulate tyrosinase-related proteins and mRNA in human melanocytes. *Journal of Dermatological Science*. 2008; 49(2):115-123.

162.aMans DR, da Rocha AB, Schwartsmann G. Anti-cancer drug discovery and development in Brazil: targeted plant collection as a rational strategy to acquire candidate anti-cancer compounds. *Oncologist*. 2000;5(3):185-198.

163.aCorbett TH, Valeriote FA, Baker LH. Is the P388 murine tumor no longer adequate as a drug discovery model? *Investigational New Drugs*. 1987;5(1):3-20.

164.aSlater TF, Sawyer B, Straeuli U. Studies on succinate-tetrazolium reductase systems III. Points of coupling of four different tetrazolium salts. *Biochimca et Biophysica Acta*. 1963;77:383-393.

165.aArthur CL, Pawliszyn J. Solid phase microextraction with thermal desorption using fused silica optical fibers. *Analytical Chemistry*. 1990;62(19):2145-2148.

166.aChoo CY, Chan KL, Takeya K, Itokawa H. Cytotoxic activity of *Typhonium flagelliforme* (Araceae). *Phytotherapy Research*. 2001;15(3):260-262.

167.aManosroi J, Dhumtanom P, Manosroi A. Anti-proliferative activity of essential oil extracted from Thai medicinal plants on KB and P388 cell lines. *Cancer Letter*. 2006;235(1):114-120.

168.aChen YC, Ho HO, Su CH, Sheu MT. Anticancer effects of *Taiwanofungus camphoratus* extracts, isolated compounds and its combinational use. *Journal of Experimental & Clinical Medicine*. 2010;2(6):274-281.

169.aHill R, Van Heyningen R. Ranunculin: the precursor of the vesicant substance of the buttercup. *Biochemical Journal*. 1951;49:332-335.

170.aTschesche R, Welmar K, Wulff G, Snatzke G. On glycosides with lactone-forming aglycones. VI. About subsequent products of a still unknown genuine precursor of ranunculin in Ranunculaceae. *Chemische Berichte*. 1972;105(1):290-300.

171.aCancer screening data of protoanemonin and anemonin.Further information is availableaat:ahttp://dtp.nci.nih.gov/dtpstandard/servlet/MeanGraphSummary?testshortname=NCI+Cancer+Screen+Current+Data&searchtype=NSC&searchlist=94101. National Cancer Instituent, USA [cited 2010 April].

172.aCancer screening data of ranunculin.Further information is available at:

http://dtp.nci.nih.gov/dtpstandard/servlet/MeanGraphSummary?searchtype=namestarts&chemnameboolean=and&outputformat=html&searchlist=ranunculin&Submit=Submit. National Cancer Instituent, USA. [cited 2010 April].

173.aLee KH, Furukawa H, Huang ES. Antitumor agents. 3. Synthesis and cytotoxic activity of helenalin amine adducts and related derivatives. *Journal of Medicinal Chemistry*. 1972;15(6):609-611.

174.aLee KH, Kim SH, Piantadosi C, Huang ES, Geissman TA. Antitumor agents VIII: Synthesis and cytotoxic activity of o,o'-bis(acrylyl)- α , ω -alkanediols. *Journal of Pharmaceutical Sciences*. 1974;63(7):1162-1163.

175.aLee KH, Ibuka T, Kim SH, Vestal BR, Hall IH, Huang ES. Antitumor agents. 16. Steroidal α-methylene-γ-lactones. *Journal of Medicinal Chemistry*. 1975;18(8):812-817.

176.aLee KH, Huang ES, Piantadosi C, Pagano JS, Geissman TA. Cytotoxicity of Sequiterpene Lactones. *Cancer Research*. 1971;31:1649-1654.

177.aHall IH, Lee KH, Mar EC, Starnes CO, Waddell TG. Antitumor agents. 21. A proposed mechanism for inhibition of cancer growth by tenulin and helenalin and related cyclopentenones. *Journal of Medicinal Chemistry*. 1977;20(3):333-337.

178.aLoeb LA. The Enzymes, 3rd ed. Boyer PD, editor. Academic Press, New York. 1974.

179.aToohey JI. Sulfhydryl dependence in primary explant hematopoietic cells. Inhibition of growth in vitro with vitamin B12 compounds. *Proceeding of National Academy of Science of the United States of America*. 1975;72(1):73-77.

180.aAsahina Y, Fujita A. Anemonins. *Acta Phytochemistry*. 1922;1:1-42.

181.aHellstrom N. Ranunculin I. The glucosidic linkage and its stability. *Kungl Lantbrukshogskolans Annaler*. 1959;25:171-184.

182.aTechnical Resources-Media Formulations 22400-RPMI. Further information is availableaat:ahttp://www.invitrogen.com/site/us/en/home/support/Produt-Technical-Resources/media_formulation.117.html.aInvitrogen,aAustralia. [cited 2011 September].

183.aTechnical Resources-Media Formulations 21063-DMEM. Further information isaavailableaat:ahttp://www.invitrogen.com/site/us/en/home/support/Produt-Technical-Resources/media_formulation.11.html. Invitrogen, Australia. [cited 2011September].

184.aSarker SD, Nahar L, Kumarasamy Y. Microtitre plate-based antibacterial assay incorporating resazurin as an indicator of cell growth, and its application in the in vitro antibacterial screening of phytochemicals. *Methods*. 2007;42(4):321-324.

185.aMurray PR. Principle of stains and media. In: Ellen JB, editor. Manual of Clinical Microbiology 9th Edition: American Society for Microbiology Press,Washington, DC. 2007. p. 185.

186.aBassaris HP, Lianou PE, Dontas AS, Legakis NJ, Papavassiliou JT. Enhanced chemotaxis to gentamicin-resistant strains of *Pseudomonas aeruginosa*. *The Journal of Infectious Diseases*. 1980;141(4):507-509.

187.aDidry N, Dubreuil L, Pinkas M. Microbiological properties of protoanemonin isolated from *Ranunculus bulbosus*. *Phytotherapy Research*. 1993;7(1):21-24.

188.aPrior RB, Warner JF. Morphological alterations of *Pseudomonas aeruginosa* by ticarcillin: a scanning electron microscope study. *Antimicrobial Agents and Chemotherapy*. 1974;6(6):853-855.

189.aVaara M, Narra T. Outer membrane permeability barrier disruption by polymyxin in polymyxin-susceptible and -resistant *Salmonella typhimurium*. *Antimicrobial Agents and Chemotherapy*. 1981;19(4):578-583.

190.aMorita Y, Kimura N, Mima T, Mizushima T, Tsuchiya T. Roles of MexXY- and MexAB-multidrug efflux pumps in intrinsic multidrug resistance of *Pseudomonas aeruginosa* PAO1. *The Journal of General and Applied Microbiology*. 2001;47(1):27-32.

191.aMorita Y, Sobel ML, Poole K. Antibiotic inducibility of the MexXY multidrug efflux system of *Pseudomonas aeruginosa*: involvement of the antibiotic-inducible PA5471 gene product. *Journal of Bacteriology*. 2006;188(5):1847-1855.

192.aWikler MA, Cockerill FR, Bush K, Dudley MN, Eliopoulos GM, Hardy DJ, *et al*. Methods for dilution antimicrobial susceptibility tests for bacteria that grow aerobically; Approved standard-eighth edition. *Clinical and Laboratory Standards Instituent*. 2009;29(2):M07-A8.

193.aBonora A, Dall'Olio G, Bruni A. Separation and quantitation of protoanemonin in Ranunculaceae by normal- and reversed-phase HPLC. *Planta Medica*. 1985(5):364-367.

194.aMares D. Antimicrobial activity of protoanemonin, a lactone from ranunculaceous plants. *Mycopathologia*. 1987;98(3):133-140.

195.aMisra SB, Dixit SN. Antifungal principle of *Ranunculus sceleratus*. *Economic Botany*. 1980;34:362-367.

196.aNational Nosocomial Infections Surveillance (NNIS) System Report, data summary from January 1992 through June 2004, issued October 2004. *American Journal of Infection Control*. 2004;32(8):470-485.

197.aGovan JR, Deretic V. Microbial pathogenesis in cystic fibrosis: mucoid *Pseudomonas aeruginosa* and *Burkholderia cepacia*. *Microbiological Reviews*. 1996;60(3):539-574.

198.aTaneja N, Emmanuel R, Chari PS, Sharma M. A prospective study of hospital-acquired infections in burn patients at a tertiary care referral centre in North India. *Burns*. 2004;30(7):665-669.

199.aTschesche R. Chemistry of higher plant constituents with antibiotic action. *Pharma international*. 1971;2:17-23.

200.aKrogfelt KA, Utley M, Krivan HC, Laux DC, Cohen PS. Specific phospholipids enhance the activity of beta-lactam antibiotics against *Pseudomonas aeruginosa*. *Journal of Antimicrobial Chemotherapy*. 2000;46:377-384.

201.aMadigan MT. Martinko JM. Brock Biology of Microorganisms, 11th Edition. Pearson Prentice Hall, Upper Saddle River. 2006.

202.aDal Pozzo A, Dansi A, Biassoni M. Alpha, beta-unsaturated gamma-lactones correlations between lipophilicity and biological activity. *Arzneimittel-Forschung*. 1979;29(6):877-882.

203.aBradbury R, Champion A, Reid DW. Poor clinical outcomes associated with a multi-drug resistant clonal strain of *Pseudomonas aeruginosa* in the Tasmanian cystic fibrosis population. *Respirology*. 2008 Nov;13(6):886-892.

204.aBradbury RS, Champion AC, Reid DW. Epidemiology of *Pseudomonas aeruginosa* in a tertiary referral teaching hospital. *The Journal of Hosptial Infection*. 2009;73(2):151-156.

205.aCarsenti-Etesse H, Cavallo JD, Roger PM, Ziha-Zarifi I, Plesiat P, Garrabe E, *et al*. Effect of beta-lactam antibiotics on the in vitro development of resistance in *Pseudomonas aeruginosa*. *Clinical Microbiology and Infection*. 2001;7(3):144-151.

206.aKattan JN, Villegas MV, Quinn JP. New developments in carbapenems. *Clinical Microbiology and Infection*. 2008;14(12):1102-1111.

207.aHashizume T, Ishino F, Nakagawa J, Tamaki S, Matsuhashi M. Studies on the mechanism of action of imipenem (N-formimidoylthienamycin) in vitro: binding to the penicillin-binding proteins (PBPs) in *Escherichia coli* and *Pseudomonas aeruginosa*, and inhibition of enzyme activities due to the PBPs in *E. coli*. *The Journal of Antibiotics*. 1984;37(4):394-400.

208.aMares D, Bonora A, Sacchetti G, Rubini M, Romagnoli C. Protoanemonin-induced cytotoxic effects in *Euglena gracilis*. *Cell Biology International*. 1997;21(7):397-404.

209.aMares D. Electron microscopy of *Microsporum cookei* after 'in vitro' treatment with protoanemonin: a combined SEM and TEM study. *Mycopathologia*. 1989;108(1):37-46.

210.aRotter K, Gruber W. Antibiotic activity and toxicity of protoanemonin. *Mitt Versuchsantalt Gaerungsgewerbeu Inst Angew Hochschute Bodenkult*. 1949;3:56-60.

211.aDelcour AH. Outer membrane permeability and antibiotic resistance. *Biochimica et Biophysica Acta*. 2009;1794(5):808-816.

212.aNikaido H, Rosenberg EY. Porin channels in *Escherichia coli*: studies with liposomes reconstituted from purified proteins. *Journal of Bacteriology*. 1983;153(1):241-252.

213.aKobayashi Y, Takahashi I, Nakae T. Diffusion of beta-lactam antibiotics through liposome membranes containing purified porins. *Antimicrobial Agents Chemotherapy*. 1982;22(5):775-780.

214.aBradbury R. *Pseudomonas aeruginosa* in Tasmania. PhD thesis. University of Tasmanian, Hobart. 2010.

215.aMine T, Morita Y, Kataoka A, Mizushima T, Tsuchiya T. Expression in *Escherichia coli* of a new multidrug efflux pump, MexXY, from *Pseudomonas aeruginosa*. *Antimicrobial Agents Chemotherapy*. 1999;43(2):415-417.

216.aMasuda N, Sakagawa E, Ohya S, Gotoh N, Tsujimoto H, Nishino T. Substrate specificities of MexAB-OprM, MexCD-OprJ, and MexXY-oprM efflux pumps in *Pseudomonas aeruginosa*. *Antimicrobial Agents Chemotherapy*. 2000;44(12):3322-3327.

217.aAires JR, Kohler T, Nikaido H, Plesiat P. Involvement of an active efflux system in the natural resistance of *Pseudomonas aeruginosa* to aminoglycosides. *Antimicrobial Agents Chemotherapy*. 1999;43(11):2624-2628.

218.aMatsuo Y, Eda S, Gotoh N, Yoshihara E, Nakae T. MexZ-mediated regulation of mexXY multidrug efflux pump expression in *Pseudomonas aeruginosa* by binding on the mexZ-mexX intergenic DNA. *FEMS Microbiology Letter*. 2004;238(1):23-28.

219.aPirmay JP. The antibiotic resistant mechanism of *P. aeruginosa* 124. In: Bradbruy R, personal communication. Hobart. 2008.

220.aCaterson B, Flannery CR, Hughes CE, Little CB. Mechanisms involved in cartilage proteoglycan catabolism. *Matrix Biology*. 2000;19(4):333-344.

221.aMuller-Ladner U, Gay RE, Gay S. Molecular biology of cartilage and bone destruction. *Current Opinion in Rheumatology*. 1998;10(3):212-219.

222.aPoole AR. An introduction to the pathophysiology of osteoarthritis. *Frontiers in Bioscience*. 1999;4:D662-670.

223.aOkamoto H, Hoshi D, Kiire A, Yamanaka H, Kamatani N. Molecular targets of rheumatoid arthritis. *Inflammation and Allergy Drug Targets*. 2008;7(1):53-66.

224.aJiang JS, Shih CM, Wang SH, Chen TT, Lin CN, Ko WC. Mechanisms of suppression of nitric oxide production by 3-O-methylquercetin in RAW 264.7 cells. *Journal of Ethnopharmacology*. 2006;103(2):281-287.

225.aChartrain NA, Geller DA, Koty PP, Sitrin NF, Nussler AK, Hoffman EP, *et al*. Molecular cloning, structure, and chromosomal localization of the human inducible nitric oxide synthase gene. *The Journal of Biological Chemistry*. 1994;269(9):6765-6772.

226.aTsikas D. Analysis of nitrite and nitrate in biological fluids by assays based on the Griess reaction: appraisal of the Griess reaction in the L-arginine/nitric oxide area of research. *Journal of Chromatography B, Analytical Technologies in the Biomedical Life Science*. 2007;851(1-2):51-70.

227.aIgnarro LJ, Fukuto JM, Griscavage JM, Rogers NE. Oxidation of nitric oxide in aqueous solution to nitrite but not nitrate: comparison with enzymatically formed nitric oxide from L-arginine. *Proceedings of the National Academy of Sciences of the United States of America*. 1993;90(17):8103-8107.

228.aBush PA, Gonzalez NE, Griscavage JM, Ignarro LJ. Nitric oxide synthase from cerebellum catalyzes the formation of equimolar quantities of nitric oxide and citrulline from L-arginine. *Biochemical and Biophysical Research Communications*. 1992;185(3):960-966.

229.aChartrain NA, Geller DA, Koty PP, Sitrin NF, Nussler AK, Hoffman EP, *et al*. Molecular cloning, structure, and chromosomal localization of the human inducible nitric oxide synthase gene. *The Journal of Biological Chemistry*. 1994;269(9):6765-6772.

230.aZhao F, Nozawa H, Daikonnya A, Kondo K, Kitanaka S. Inhibitors of nitric oxide production from hops (*Humulus lupulus* L.). *Biological and Pharmaceutical Bulletin*. 2003;26(1):61-65.

231.aLee TH, Huang NK, Lai TC, Yang ATY, Wang GJ. Anemonin, from *Clematis crassifolia*, potent and selective inducible nitric oxide synthase inhibitor. *Journal of Ethnopharmacology*. 2008;116(3):518-527.

232.aHuang CJ, Haque IU, Slovin PN, Nielsen RB, Fang X, Skimming JW. Environmental pH regulates LPS-induced nitric oxide formation in murine macrophages. *Nitric Oxide*. 2002;6(1):73-78.

233.aPark EK, Ryu MH, Kim YH, Lee YA, Lee SH, Woo DH, *et al*. Anti-inflammatory effects of an ethanolic extract from *Clematis mandshurica* Rupr. *Journal of Ethnopharmacology*. 2006;108(1):142-147.

234.aBasu S, Hazra B. Evaluation of nitric oxide scavenging activity, *in vitro* and *ex vivo*, of selected medicinal plants traditionally used in inflammatory diseases. *Phytotherapy Research*. 2006;20(10):896-900.

235.aLim HW, Kang SJ, Park M, Yoon JH, Han BH, Choi SE, *et al*. Anti-Oxidative and Nitric Oxide Production Inhibitory Activities of Phenolic Compounds from the Fruits of *Actinidia arguta*. *Natural Product Science*. 2006;12(4):221-225.

236.aNathan C, Xie QW. Regulation of biosynthesis of nitric oxide. *The Journal of Biological Chemistry*. 1994;269(19):13725-13728.

237.aDing AH, Nathan CF, Stuehr DJ. Release of reactive nitrogen intermediates and reactive oxygen intermediates from mouse peritoneal macrophages. Comparison of activating cytokines and evidence for independent production. *Journal of Immunology*. 1988;141(7):2407-2412.

238.aStuehr DJ, Marletta MA. Mammalian nitrate biosynthesis: mouse macrophages produce nitrite and nitrate in response to *Escherichia coli* lipopolysaccharide. *Proceedings of the National Academy of Sciences of the United States of America*. 1985;82(22):7738-7742.

239.aRees DD, Monkhouse JE, Cambridge D, Moncada S. Nitric oxide and the haemodynamic profile of endotoxin shock in the conscious mouse. *British Journal of Pharmacology*. 1998;124(3):540-546.

240.aKarima R, Matsumoto S, Higashi H, Matsushima K. The molecular pathogenesis of endotoxic shock and organ failure. *Molecular Medicine Today*.1999;5(3):123-132.

241.aHarbrecht BG, Billiar TR, Stadler J, Demetris AJ, Ochoa J, Curran RD, *et al*. Inhibition of nitric oxide synthesis during endotoxemia promotes intrahepatic thrombosis and an oxygen radical-mediated hepatic injury. *Journal of Leukocyte Biology*. 1992;52(4):390-394.

242.aMoncada S, Palmer RM, Higgs EA. Nitric oxide: physiology, pathophysiology, and pharmacology. *Pharmacological Reviews*. 1991;43(2):109-142.

243.aBeckman JS, Koppenol WH. Nitric oxide, superoxide, and peroxynitrite: the good, the bad, and ugly. *The American Journal of Physiology*. 1996;271(5 Pt 1):C1424-1437.

244.aBredt DS. Endogenous nitric oxide synthesis: biological functions and pathophysiology. *Free Radical Research*. 1999;31(6):577-596.

245.aMacMicking J, Xie QW, Nathan C. Nitric oxide and macrophage function. *Annual Review of Immunology*. 1997;15:323-350.

246.aMagazine HI. Detection of endothelial cell-derived nitric oxide: current trends and future directions. *Advances of Neuroimmunology*. 1995;5(4):479-490.

247.aDimmeler S, Zeiher AM. Nitric oxide and apoptosis: another paradigm for the double-edged role of nitric oxide. *Nitric Oxide*. 1997;1(4):275-281.

248.aKrˆncke K-D, Fehsel K, Kolb-Bachofen V. Nitric Oxide: Cytotoxicity versus Cytoprotection-- How, Why, When, and Where? *Nitric Oxide*. 1997;1(2):107-120.

249.aNathan C. Inducible nitric oxide synthase: what difference does it make? The *Journal of Clinical Investigation*. 1997;100(10):2417-2423.

250.aAdams DO, Hamilton TA. The cell biology of macrophage activation. *Annual Review of Immunology*. 1984;2:283-318.

251.aKnowles RG, Moncada S. Nitric oxide synthases in mammals. *The Biochemical Journal*. 1994;298 (Pt 2):249-258.

252.aNguyen T, Brunson D, Crespi CL, Penman BW, Wishnok JS, Tannenbaum SR. DNA damage and mutation in human cells exposed to nitric oxide in vitro. *Proceedings of the National Academy of Sciences of the United States of America*. 1992;89(7):3030-3034.

253.aMiwa M, Stuehr DJ, Marletta MA, Wishnok JS, Tannenbaum SR. Nitrosation of amines by stimulated macrophages. *Carcinogenesis*. 1987;8(7):955-958.

254.aMiles AM, Bohle DS, Glassbrenner PA, Hansert B, Wink DA, Grisham MB. Modulation of superoxide-dependent oxidation and hydroxylation reactions by nitric oxide. *The Journal of Biological Chemistry*. 1996;271(1):40-47.

255.aXia Y, Zweier JL. Superoxide and peroxynitrite generation from inducible nitric oxide synthase in macrophages. *Proceedings of the National Academy of Sciences of the United States of America*. 1997;94(13):6954-6958.

256.aSalvemini D, Misko TP, Masferrer JL, Seibert K, Currie MG, Needleman P. Nitric oxide activates cyclooxygenase enzymes. *Proceedings of the National Academy of Sciences of the United States of America*. 1993;90(15):7240-7244.

257.aStadler J, Stefanovic-Racic M, Billiar TR, Curran RD, McIntyre LA, Georgescu HI, *et al*. Articular chondrocytes synthesize nitric oxide in response to cytokines and lipopolysaccharide. *The Journal of Immunology*. 1991;147(11):3915-3920.

258.aAmin AR, Di Cesare PE, Vyas P, Attur M, Tzeng E, Billiar TR, *et al*. The expression and regulation of nitric oxide synthase in human osteoarthritis-affected chondrocytes: evidence for up-regulated neuronal nitric oxide synthase. *The Journal of Experimental Medicine*. 1995;182(6):2097-2102.

259.aFarrell AJ, Blake DR, Palmer RM, Moncada S. Increased concentrations of nitrite in synovial fluid and serum samples suggest increased nitric oxide synthesis in rheumatic diseases. *Annals of Rheumatic Diseases*. 1992;51(11):1219-1222.

260.aIalenti A, Moncada S, Di Rosa M. Modulation of adjuvant arthritis by endogenous nitric oxide. *British Journal of Pharmacology*. 1993;110(2):701-706.

261.aRediske JJ, Koehne CF, Zhang B, Lotz M. The inducible production of nitric oxide by articular cell types. *Osteoarthritis Cartilage*. 1994;2(3):199-206.

262.aHauselmann HJ, Oppliger L, Michel BA, Stefanovic-Racic M, Evans CH. Nitric oxide and proteoglycan biosynthesis by human articular chondrocytes in alginate culture. *FEBS Letters*. 1994;352(3):361-364.

263.aTaskiran D, Stefanovic-Racic M, Georgescu H, Evans C. Nitric oxide mediates suppression of cartilage proteoglycan synthesis by interleukin-1. *Biochemical and Biophysical Research Communications*. 1994;200(1):142-148.

264.aDiBattista JA, Martel-Pelletier J, Fujimoto N, Obata K, Zafarullah M, Pelletier JP. Prostaglandins E2 and E1 inhibit cytokine-induced metalloprotease expression in human synovial fibroblasts. Mediation by cyclic-AMP signalling pathway. *Laboratory Investigation*. 1994;71(2):270-278.

265.aBlanco FJ, Ochs RL, Schwarz H, Lotz M. Chondrocyte apoptosis induced by nitric oxide. *The American Journal of Pathology*. 1995;146(1):75-85.

266.aDinarello CA. Interleukin-1, interleukin-1 receptors and interleukin-1 receptor antagonist. *International Review of Immunology*. 1998;16(5-6):457-499.

267.aDayer JM, Feige U, Edwards CK, 3rd, Burger D. Anti-interleukin-1 therapy in rheumatic diseases. *Current Opinion in Rheumatology*. 2001;13(3):170-176.

268.avan de Loo AA, van den Berg WB. Effects of murine recombinant interleukin 1 on synovial joints in mice: measurement of patellar cartilage metabolism and joint inflammation. *Annals of the Rheumatic Diseases*. 1990;49(4):238-345.

269.aEastgate JA, Symons JA, Wood NC, Grinlinton FM, di Giovine FS, Duff GW. Correlation of plasma interleukin 1 levels with disease activity in rheumatoid arthritis. *Lancet*. 1988;2(8613):706-709.

270.aWang J, Fathman JW, Lugo-Villarino G, Scimone L, von Andrian U, Dorfman DM, *et al*. Transcription factor T-bet regulates inflammatory arthritis through its function in dendritic cells. *The Journal of Clinical Investigation*. 2006;116(2):414-421.

271.aKeffer J, Probert L, Cazlaris H, Georgopoulos S, Kaslaris E, Kioussis D, *et al*. Transgenic mice expressing human tumour necrosis factor: a predictive genetic model of arthritis. *The EMBO Journal*. 1991;10(13):4025-4031.

272.aBrown MA, Hural J. Functions of IL-4 and control of its expression. *Critical Reviews in Immunology*. 1997;17(1):1-32.

273.aWang P, Wu P, Siegel MI, Egan RW, Billah MM. Interleukin (IL)-10 inhibits nuclear factor kappa B (NF kappa B) activation in human monocytes. IL-10 and IL-4 suppress cytokine synthesis by different mechanisms. *The Journal of Biological Chemistry*. 1995;270(16):9558-9563.

274.ate Velde AA, Huijbens RJ, Heije K, de Vries JE, Figdor CG. Interleukin-4 (IL-4) inhibits secretion of IL-1 beta, tumor necrosis factor alpha, and IL-6 by human monocytes. *Blood*. 1990;76(7):1392-1397.

275.aPaul WE. Interleukin-4: a prototypic immunoregulatory lymphokine. *Blood.* 1991;77(9):1859-1870.

276.aVannier E, Miller LC, Dinarello CA. Coordinated antiinflammatory effects of interleukin 4: interleukin 4 suppresses interleukin 1 production but up-regulates gene expression and synthesis of interleukin 1 receptor antagonist. *Proceedings of the National Academy of Sciences of the United States of America*. 1992;89(9):4076-4080.

277.aHart PH, Vitti GF, Burgess DR, Whitty GA, Piccoli DS, Hamilton JA. Potential antiinflammatory effects of interleukin 4: suppression of human monocyte tumor necrosis factor alpha, interleukin 1, and prostaglandin E2. *Proceedings of the National Academy of Sciences of the United States of America*. 1989;86(10):3803-3807.

278.aDel Prete G, De Carli M, Almerigogna F, Giudizi MG, Biagiotti R, Romagnani S. Human IL-10 is produced by both type 1 helper (Th1) and type 2 helper (Th2) T cell clones and inhibits their antigen-specific proliferation and cytokine production. *Journal of Immunology*. 1993;150(2):353-360.

279.aYssel H, De Waal Malefyt R, Roncarolo MG, Abrams JS, Lahesmaa R, Spits H, *et al*. IL-10 is produced by subsets of human CD4+ T cell clones and peripheral blood T cells. *Journal of Immunology*. 1992;149(7):2378-2384.

280.aLalani I, Bhol K, Ahmed AR. Interleukin-10: biology, role in inflammation and autoimmunity. *Annals of Allergy, Asthma & Immunology*. 1997;79(6):469-483.

281.aMoore KW, de Waal Malefyt R, Coffman RL, O'Garra A. Interleukin-10 and the interleukin-10 receptor. *Annual Review of Immunology*. 2001;19:683-765.

282.aMongan AE, Ramdahin S, Warrington RJ. Interleukin-10 response abnormalities in systemic lupus erythematosus. *Scandinavian Journal of Immunology*. 1997;46(4):406-412.

283.aHoussiau FA, Lefebvre C, Vanden Berghe M, Lambert M, Devogelaer JP, Renauld JC. Serum interleukin 10 titers in systemic lupus erythematosus reflect disease activity. *Lupus*. 1995;4(5):393-395.

284.aLlorente L, Richaud-Patin Y, Fior R, Alcocer-Varela J, Wijdenes J, Fourrier BM, *et al*. In vivo production of interleukin-10 by non-T cells in rheumatoid arthritis, Sjogren's syndrome, and systemic lupus erythematosus. A potential mechanism of B lymphocyte hyperactivity and autoimmunity. *Arthritis and Rheumatism*. 1994;37(11):1647-1655.

285.aCush JJ, Splawski JB, Thomas R, McFarlin JE, Schulze-Koops H, Davis LS, *et al*. Elevated interleukin-10 levels in patients with rheumatoid arthritis. *Arthritis Rheumatism*. 1995;38(1):96-104.

286.aMirakian R, Hammond LJ, Bottazzo GF. TH1 and TH2 cytokine control of thyrocyte survival in thyroid autoimmunity. *Nature Immunology*. 2001;2(5):371.

287.aCohen SB, Katsikis PD, Chu CQ, Thomssen H, Webb LM, Maini RN, et al. High level of interleukin-10 production by the activated T cell population within the rheumatoid synovial membrane. *Arthritis and Rheumatism*. 1995;38(7):946-952.

288.aIsomaki P, Luukkainen R, Saario R, Toivanen P, Punnonen J. Interleukin-10 functions as an antiinflammatory cytokine in rheumatoid synovium. *Arthritis and Rheumatism*. 1996;39(3):386-395.

289.aFuruzawa-Carballeda J, Alcocer-Varela J. Interleukin-8, interleukin-10, intercellular adhesion molecule-1 and vascular cell adhesion molecule-1 expression levels are higher in synovial tissue from patients with rheumatoid arthritis than in osteoarthritis. *Scandinavian Journal of Immunology*. 1999;50(2):215-222.

290.aMelgar S, Yeung MM, Bas A, Forsberg G, Suhr O, Oberg A, et al. Over-expression of interleukin 10 in mucosal T cells of patients with active ulcerative colitis. *Clinical and Experimental Immunology*. 2003;134(1):127-137.

291.aLopatin U, Yao X, Williams RK, Bleesing JJ, Dale JK, Wong D, et al. Increases in circulating and lymphoid tissue interleukin-10 in autoimmune lymphoproliferative syndrome are associated with disease expression. *Blood*. 2001;97(10):3161-3170.

292.aLoetscher P, Moser B, Baggiolini M. Chemokines and their receptors in lymphocyte traffic and HIV infection. *Advances in Immunology*. 2000;74:127-180.

293.aGerard C, Rollins BJ. Chemokines and disease. *Nature Immunology*. 2001;2(2):108-115.

294.aGay S, Gay RE, Koopman WJ. Molecular and cellular mechanisms of joint destruction in rheumatoid arthritis: two cellular mechanisms explain joint destruction? *Annals of the Rheumatic Diseases*. 1993;52 Suppl 1:S39-47.

295.aMuller-Ladner U, Gay RE, Gay S. Signaling and effector pathways. *Current Opinion in Rheumatology*. 1999;11(3):194-201.

296.aPatel DD, Zachariah JP, Whichard LP. CXCR3 and CCR5 ligands in rheumatoid arthritis synovium. *Clinical Immunology*. 2001;98(1):39-45.

297.aKoch AE, Kunkel SL, Harlow LA, Johnson B, Evanoff HL, Haines GK, *et al*. Enhanced production of monocyte chemoattractant protein-1 in rheumatoid arthritis. *The Journal of Clinical Investigation*. 1992;90(3):772-779.

298.aHarigai M, Hara M, Yoshimura T, Leonard EJ, Inoue K, Kashiwazaki S. Monocyte chemoattractant protein-1 (MCP-1) in inflammatory joint diseases and its involvement in the cytokine network of rheumatoid synovium. *Clinical Immunology and Immunopathology*. 1993;69(1):83-91.

299.aNanki T, Nagasaka K, Hayashida K, Saita Y, Miyasaka N. Chemokines regulate IL-6 and IL-8 production by fibroblast-like synoviocytes from patients with rheumatoid arthritis. *Journal of Immunology*. 2001;167(9):5381-5385.

300.aPope RM. Apoptosis as a therapeutic tool in rheumatoid arthritis. *Nature Reviews. Immunology*. 2002;2(7):527-535.

301.aCsiszar A, Nagy G, Gergely P, Pozsonyi T, Pocsik E. Increased interferon-gamma (IFN-gamma), IL-10 and decreased IL-4 mRNA expression in peripheral blood mononuclear cells (PBMC) from patients with systemic lupus erythematosus (SLE). *Clinical Experimental Immunology*. 2000;122(3):464-470.

302.aEspey MG, Miranda KM, Thomas DD, Xavier S, Citrin D, Vitek MP, *et al*. A chemical perspective on the interplay between NO, reactive oxygen species, and reactive nitrogen oxide species. *Annals of the New York Academy of Sciences*. 2002;962:195-206.

303.aMoncada S, Higgs A. The L-arginine-nitric oxide pathway. *The New England Journal of Medicine*. 1993;329(27):2002-2012.

304.aBasicsaof LC/MS. Further information is available at: http://ccc.chem.pitt.edu/wipf/Agilent%20LC-MS20primer.pdf. Agilent Technologies, UAS. [cited 2009 April].

305.aVallverdu-Queralt A, Jauregui O, Medina-Remon A, Andres-Lacueva C, Lamuela-Raventos RM. Improved characterization of tomato polyphenols usingaliquidachromatography/electrosprayaionizationalinearaionatrapaquadrupole Orbitrap mass spectrometry and liquid chromatography/electrospray ionization tandem mass spectrometry. *Rapid Communication Mass Spectromerty*. 2010;24(20):2986-2992.

306.aLukacin R, Matern U, Specker S, Vogt T. Cations modulate the substrate specificity of bifunctional class I O-methyltransferase from Ammi majus. *FEBS Letters.* 2004;577(3):367-370.

307.aBengoechea L, Hernandez T, Quesada C, Bartolome B, Estrella I, Gomez Cordoves C. Structure of hydroxycinnamic acid derivatives established by high-performance liquid chromatography with photodiode-array detection. *Chromatographia*. 1995;41(1-2):94-98.

308.aKizu H, Shimana H, Tomimori T. Studies on the constituents of Clematis species. VI. The constituents of Clematis stans Sieb. et Zucc. *Chemical & Pharmaceutical Bulletin*. 1995;43(12):2187-2194.

309.aDuthie GG, Gardner PT, Kyle JA. Plant polyphenols: are they the new magic bullet? *Proceeding of the Nutrition Society*. 2003;62(3):599-603.

310.aBoll PM. Naturally occuring lactones and lactames I. The absolute configuration of ranunculin, lichesterinic acid, and some lactone related to lichesterinic acid. *Acta Chemica Scandinavica*. 1968;22:3245-3250.

311.aBastos DH, Saldanha LA, Catharino RR, Sawaya AC, Cunha IB, Carvalho PO, *et al*. Phenolic antioxidants identified by ESI-MS from Yerba mate (*Ilex paraguariensis*) and green tea (*Camelia sinensis*) extracts. *Molecules*. 2007;12(3):423-432.

312.aParveen I, Winters A, Threadgill MD, Hauck B, Morris P. Extraction, structural characterisation and evaluation of hydroxycinnamate esters of orchard grass (*Dactylis glomerata*) as substrates for polyphenol oxidase. *Phytochemistry*. 2008;69(16):2799-2806.

313.aHahn R, Nahrstedt A. Hydroxycinnamic acid derivatives, caffeoylmalic and new caffeoylaldonic acid esters, from *Chelidonium majus*. *Planta Medica*. 1993;59(1):71-75.

314.aWang M, Shao Y, Li J, Zhu N, Rangarajan M, LaVoie EJ, et al. Antioxidative phenolic glycosides from sage (Salvia officinalis). *Journal of Natural Products*. 1999;62(3):454-456.

315.aFujise T, Terahara N, Fukui K, Sugita K, Ohta H, Matsui T, *et al*. Durable antihyperglycemic effect of 6-O-caffeoylsophorose with alpha-glucosidase inhibitory activity in rats. *Food Science and Technology Reasearch*. 2008;14(5):477.

316.aTerahara N, Matsui T, Matsumoto K, Sugita K, Matsugano K, Kichiyama K, e*t al*. Caffeoylsophorose and agents for prevention and treatment of diabetes mellitus. Japan patent JP 2003313195 A 20031106. 2003.

317.aTerahara N, Matsui T, Fukui K, Matsugano K, Sugita K, Matsumoto K. Caffeoylsophorose in a red vinegar produced through fermentation with

purple sweetpotato. *Journal of Agriculture and Food Chemistry*. 2003;51(9):2539-2543.

318.aFiorentino A, D'Abrosca B, Pacifico S, Mastellone C, Scognamiglio M, Monaco P. Identification and assessment of antioxidant capacity of phytochemicals from kiwi fruits. *Journal of Agriculture and Food Chemistry*. 2009;57(10):4148-4155.

319.aSanchez-Rabaneda F, Jauregui O, Lamuela-Raventos RM, Viladomat F, Bastida J, Codina C. Qualitative analysis of phenolic compounds in apple pomace using liquid chromatography coupled to mass spectrometry in tandem mode. *Rapid Communication in Mass Spectrometry*. 2004;18(5):553-563.

320.aIbrahim RK, Shaw M. Phenolic constituents of the oil flax (*linum usitatissimum*). 1970;9(8):1855-1858.

321.aBrighente IMC, Dias M, Verdi LG, Pizzolatti MG. Antioxidant activity and total phenolic content of some Brazilian species. *Pharmaceutical Biology*. 2007;45(2):156-161.

322.aSchwarz B, Hofmann T. Sensory-guided decomposition of red currant juice (Ribes rubrum) and structure determination of key astringent compounds. *Journal of Agriculture and Food Chemistry*. 2007;55(4):1394-1404.

323.aHamerski L, Bomm MD, Silva DH, Young MC, Furlan M, Eberlin MN, *et al*. Phenylpropanoid glucosides from leaves of *Coussarea hydrangeifolia* (Rubiaceae). *Phytochemistry*. 2005;66(16):1927-1932.

324.aBraham H, Mighri Z, Jannet HB, Matthew S, Abreu PM. Antioxidant phenolic glycosides from Moricandia arvensis. *Journal of Natural Products*. 2005;68(4):517-522.

325.aIna H, Komakid K, Iida H. Hydroxycinnamylglucoses from *Spiraea thunbergii*. Planta Medica. 1987;53(5):502.

326.aPanthamaaN,aKanokmedhakulaS,aKanokmedhakulaK.aGalloylaandahexahydroxydiphenoyl esters of phenylpropanoid glucosides, phenylpropanoids and phenylpropanoid glucosides from rhizome of Balanophora fungosa. *Chemical & Pharmaceutical Bulletin*. 2009 Dec;57(12):1352-1355.

327.aWang W, Zeng S-F, Yang C-R, Zhang Y-J. A New Hydrolyzable Tannin from Balanophora harlandii with Radical-Scavenging Activity. *Helvetica Chimica Acta*. 2009;92(9):1817-1822.

328.aIwai K, Kawamura H, Matsue H, Kitamura T, Odo A, Kawagish T. Apios flower and alfa-glucosidase inhibitor extracted therefrom as hyperglycemia-

inhibiting agent and antidiabetic food materials containing the agent. Japan patent JP 2011037800 A 20110224. 2011.

329.aShimomura H, Sashida Y, Adachi T. Phenolic glucosides from *Prunus grayana*. 1986;26(1):249-251.

330.aD'Abrosca B, Fiorentino A, Ricci A, Scognamiglio M, Pacifico S, Piccolella S, *et al*. Structural characterization and radical scavenging activity of monomeric and dimeric cinnamoyl glucose esters from Petrorhagia velutina leaves. *Phytochemistry Letters*. 2010;3(1):38-44.

331.aGao JJ, Igalashi K, Nukina M. Radical scavenging activity of phenylpropanoid glycosides in Caryopteris incana. *Bioscience Biotechnology and Biochemistry*. 1999;63(6):983-988.

332.aChiang HC, Lo YJ, Lu FJ. Xanthine oxidase inhibitors from the leaves of *Alsophila spinulosa* (Hook) Tryon. *Journal of Enzyme Inhibition*. 1994;8(1):61-71.

333.aShimomura H, Sashida Y, Adachi T. Phenylpropanoid glucose esters from *Prunus buergeriana*. *Phytochemistry*. 1988;27(2):641-644.

334.aBlanda G, Cerretani L, Cardinali A, Barbieri S, Bendini A, Lercker G. Osmotic dehydrofreezing of strawberries: Polyphenolic content, volatile profile and consumer acceptance. *LWT--Food Science and Technology*. 2009;42(1):30-36.

335.aLunkenbein S, Salentijn EMJ, Coiner HA, Boone MJ, Krens FA, Schwab W. Up- and down-regulation of *Fragaria x ananassa* O-methyltransferase: impacts on furanone and phenylpropanoid metabolism. *Journal of Experimental Botany*. 2006;57(10):2445-2453.

336.aMaeaettae-Riihinen KR, Kamal-Eldin A, Mattila PH, Gonzalez-Paramas AM, Toerroenen AR. Distribution and contents of phenolic compounds in eighteen scandinavian berry species. *Journal of Agriculture and Food Chemistry*. 2004;52(14):4477-4486.

337.aMaeaettae-Riihinen KR, Kamal-Eldin A, Toerroenen AR. Identification and auantification of phenolic compounds in berries of *Fragaria and Rubus* Species (Family Rosaceae). *Journal of Agriculture and Food Chemistry*. 2004;52(20):6178-6187.

338.aAnttonen MJ, Karjalainen RO. High-Performance Liquid Chromatography Analysis of black currant (Ribes nigrum L.) fruit phenolics grown either conventionally or organically. *Journal of Agriculture and Food Chemistry*. 2006;54(20):7530-7538.

339.aWinter M, Herrmann K. Esters and glucosides of hydroxycinnamic acids in vegetables. *Journal of Agriculture and Food Chemistry*. 1986;34(4):616-620.

340.aCamurati F, Rizzolo A, Fedeli E. Chemical components of the anatomical parts of the Olea europea fruit. II. Alcoholic extracts. Rivista *Italiana delle Sostanze Grasse*. 1981;58(11):541-547.

341.aVazquez Roncero A, Janer del Valle ML. Changes in polyphenol composition during the pickling process of green olives. I. Qualitative study. *Grasas y Aceites*. 1977;28(6):421-426.

342.aVazquez Roncero A, Graciani Constante E, Maestro Duran R. Phenolic compounds in olives. I. Polyphenols in the pulp. *Grasas y Aceites*. 1974;25(5):269-279.

343.aZane A, Steck W, Wender S. Identification of 4-0-caffeoylquinic acid and related depsides in tobacco from cigarets. *Tobacco International*. 1965;9:85-87.

344.aHarborne JB, Hall E. Plant polyphenols. XIII. Systematic distribution and origin of anthocyanins containing branched trisaccharides. *Phytochemistry*. 1964;3(3):453-463.

345.aBohm BA. Phenolic compounds in ferns. III. An examination of some ferns for caffeic acid derivatives. *Phytochemistry*. 1968;7(10):1825-1830.

346.aTanguy J, Martin C. Phenolic constituents of the cotyledonous leaves of *Phaseolus vulgaris* var Pinto plantlets. *Compues Rendus des Seances de I'Academie des Sciences, Serie D: Sciences Naturelles*. 1972;274(25):3402-3404.

347.aSimonyan AV, Litvinenko VI, Shinkarenko AL. Phenolcarboxylic acids of the *Thymus genus*. *Khimiya Prirodnykh Soedinenii*. 1972(3):383-384.

348.aPagani F. Phytoconstituents of Orchidaceae. Part 1. Components of Orchis sambucina L. and Orchis morio L. *Bollettino Chimico Farmaceutico*. 1976;115(5):407-412.

349.aSaito R, Kuchitsu K, Ozeki Y, Nakayama M. Spatiotemporal metabolic regulation of anthocyanin and related compounds during the development of marginal picotee petals in *Petunia hybrida* (Solanaceae). *Journal of Plant Research*. 2007;120(4):563-568.

350.aLi C, Chen D, Xiao P. Chemical constituents of traditional Chinese drug shengma (*Cimicifuga foetida*). *China Traditional and Herbal Drugs*. 1995;26(6):288-289, 318.

351.aBastos DHM, Saldanha LA, Catharino RR, Sawaya ACHF, Cunha IBS, Carvalho PO, *et al*. Phenolic antioxidants identified by ESI-MS from yerba mate (*Ilex paraguariensis*) and green tea (*Camellia sinensis*) extracts. *Molecules*. 2007;12(3):423-432.

352.aDu Q, Xu Y, Li L, Zhao Y, Jerz G, Winterhalter P. Antioxidant constituents in the fruits of *Luffa cylindrica* (L.) Roem. *Journal of Agriculture and Food Chemistry*. 2006;54(12):4186-4190.

353.aTominaga H, Kobayashi Y, Goto T, Kasemura K, Nomura M. DPPH radical-scavenging effect of several phenylpropanoid compounds and their glycoside derivatives. *Yakugaku Zasshi*. 2005;125(4):371-375.

354.aHelmja K, Vaher M, Pussa T, Raudsepp P, Kaljurand M. Evaluation of antioxidative capability of the tomato (*Solanum lycopersicum*) skin constituents by capillary electrophoresis and high-performance liquid chromatography. *Electrophoresis*. 2008;29(19):3980-3988.

355.aLim HW, Kang SJ, Park M, Yoon JH, Han BH, Choi SE, *et al*. Anti-oxidative and nitric oxide production inhibitory activities of phenolic compounds from the fruits of Actinidia arguta. *Nature Product Science*. 2006;12(4):221-225.

356.aHirai Y, Takase H, Kobayashi H, Yamamoto M, Fujioka N, Kohda H, *et al*. Screening test for anti-inflammatory crude drugs based on inhibition effect of histamine release from mast cell. *Shoyakugaku Zasshi*. 1983;37(4):374-380.

357.aMelzig MF, Loser B, Ciesielski S. Inhibition of neutrophil elastase activity by phenolic compounds from plants. *Pharmazie*. 2001;56(12):967-970.

358.aFleuriet A, Macheix JJ. Tissue compartmentation of phenylpropanoid metabolismainatomatoesaduringagrowthaandamaturation.a*Phytochemistry*. 1985;24(5):929-932.

359.aDu G, Li M, Ma F, Liang D. Antioxidant capacity and the relationship with polyphenol and Vitamin C in Actinidia fruits. *Food Chemsitry*. 2009;113(2):557-562.

360.aRosch D, Bergmann M, Knorr D, Kroh LW. Structure-antioxidant efficiency relationships of phenolic compounds and their contribution to the antioxidant activity of sea buckthorn juice. *Journal of Agriculture and Food Chemistry*. 2003;51(15):4233-4239.

361.aRasmussen SE, Frederiksen H, Struntze Krogholm K, Poulsen L. Dietary proanthocyanidins: occurrence, dietary intake, bioavailability, and protection against cardiovascular disease. *Molecular Nutrition and Food Research*. 2005;49(2):159-174.

362.aRasumssen SE. Functional foods, cardiovascular disease and diabetes. In: Arnoldi A, editor. Woodhead punlishing, Cambridge CBI. 2004.

363.aPervaiz S. Resveratrol: from grapevines to mammalian biology. *The FASEB Journal*. 2003;17(14):1975-1985.

364.aDell'Agli M, Busciala A, Bosisio E. Vascular effects of wine polyphenols. *Cardiovascular Research*. 2004;63(4):593-602.

Appendices

Appendix I HPLC-ELSD and HPLC-UV at 254 nm chromatograms of *C. aristata*-L, *C. microphylla*-TN and blank (Chapter 2)

Appendix II Photos from the study of antitumour activity of Tasmanian native *Clematis* spp. (Chapter 2)

Appendix III Photos of the antibacterial activities of HPLC column fractions of *C. aristata*-L against PAO1. (Chapter 3)

Appendix IV IGC-MS data of protoanemonin. (Chapter3)

Appendix V GC-MS chromatograms in the Headspace-GCMS-SPME study to determine the the decomposition of ranunculin by *P. aeruginosa* bacterial culture. (Chapter 3)

Appendix VI Photos of the Griess assay of *C. aristata*-L SPE fraction 1 to fraction 5 and the cell viabilities. (Chapter 4)

Appendix VII LC-MS chromatograms of flavonoids, ranunculin and its isomer, hydroxicinnamate easters in Table 5.1. (Chapter 5)

Appendix VIII UV spectra of hydroxicinnamate easters in Table 5.1. (Chapter 5)

Appendix I HPLC-ELSD and HPLC-UV at 254 nm chromatograms of *C. aristata*-L, *C. microphylla*-TN and blank (Chapter2)

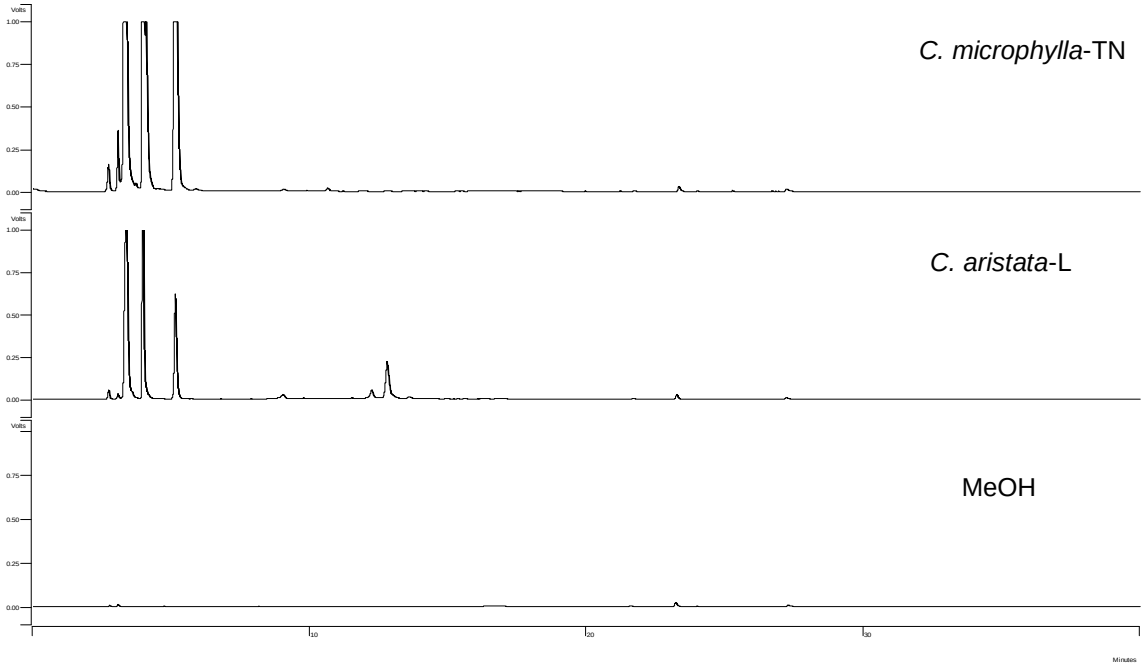

HPLC-ELSD chromatogram of *C. microphylla*-TN, *C. aristata*-L and MeOH.

Appendix II Photos from the study of antitumour activity of Tasmanian native *Clematis* spp. (Chapter 2)

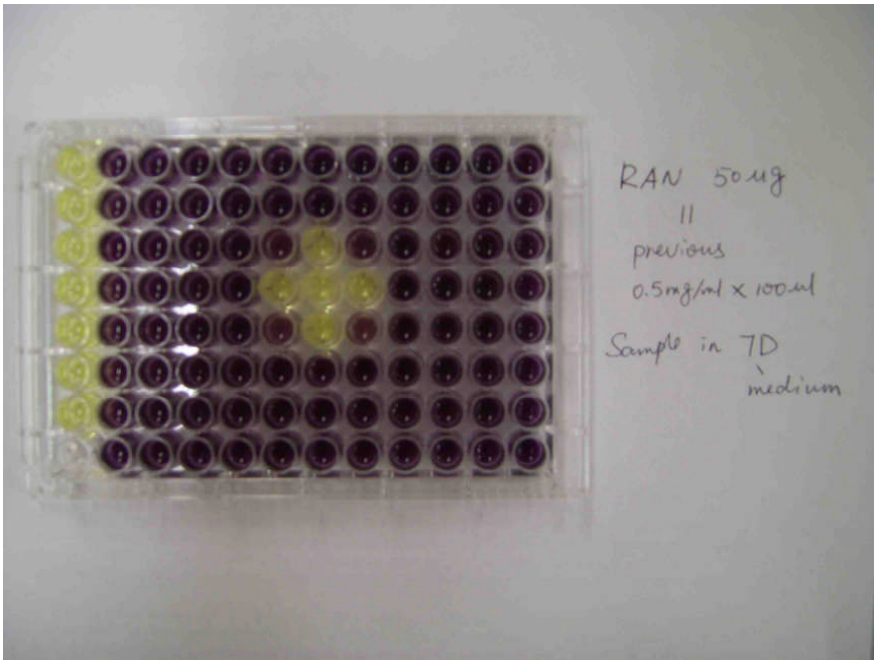

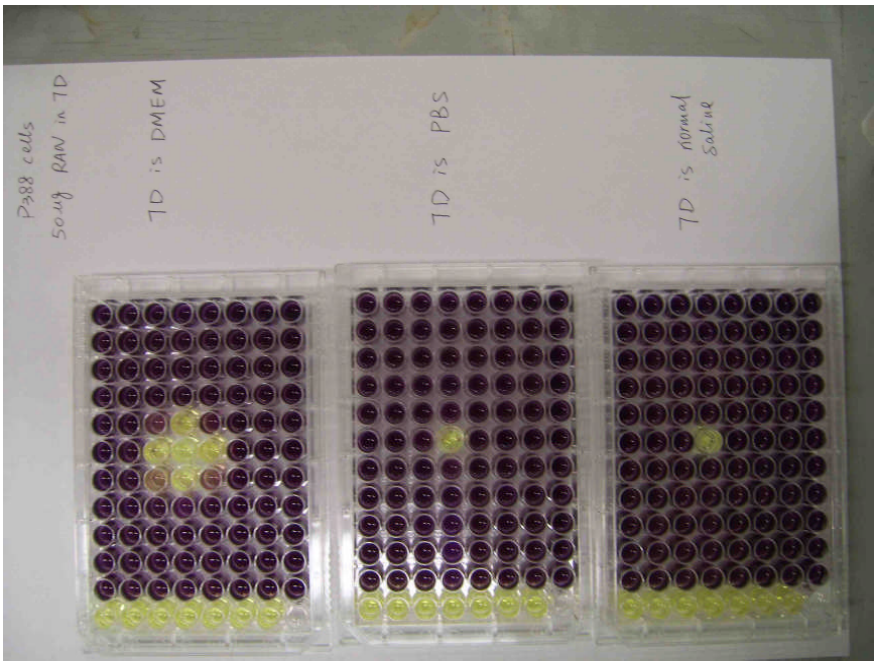

The hydrolysis property of ranunculin by cell medium (RPMI-1640 and DMEM), normal saline and PBS

Appendix III Photos of the antibacterial activities of HPLC column fractions of *C. aristata*-L against PAO1.(Chapter 3)

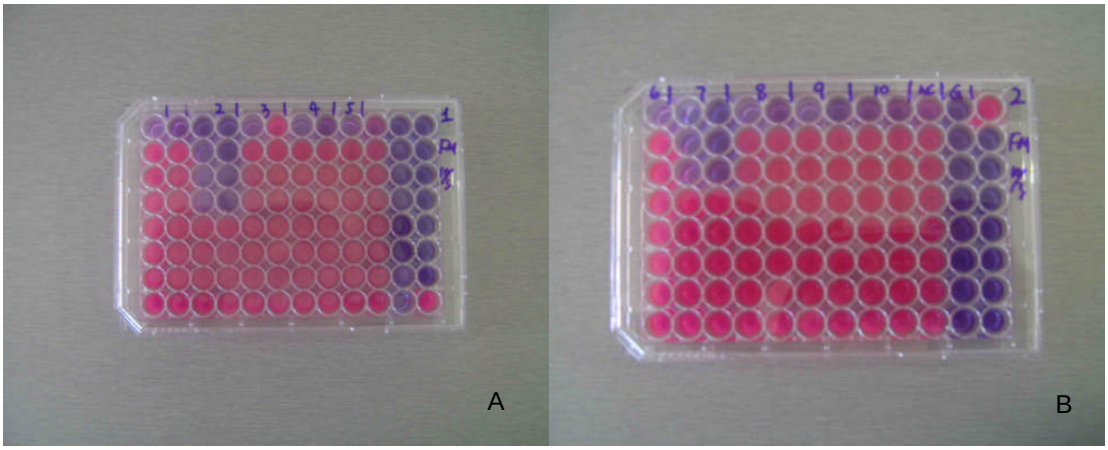

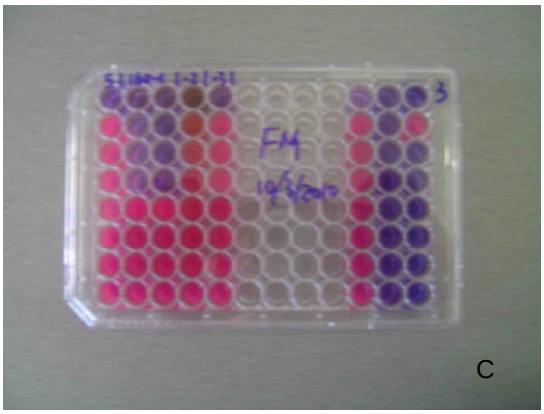

A is the HPLC carbohydrate column fractions of C18 column fraction 1. B is the HPLC carbohydrate column fractions of C18 column fraction 2. C is the HPLC C18 column fractions of C18 column fraction 2.

Appendix IV GC-MS data of protoanemonin. (Chapter 3)

Target Compound Report for #1 from 124 3hrs.xms

Sample ID:	124 3hrs	Operator:	
Instrument ID:	Varian MS #1	Last Calibration:	None
Measurement Type:	Area	Calibration Type:	External Standard
Acquisition Date:	10/11/2010 1:04 PM	Data File:	e:\gc-ms\124 3hrs.xms
Calculation Date:	16/04/2011 10:41 AM	Method:	...anemonine m_z 96.mth
Sample Type:	Analysis		
Inj. Sample Notes:	Varian 8		

Compound Information

Peak Name: protoanemonin
Result Index: 1 Compound Number: 1 CAS Number: None Identified

Identification

Parameter	Specification	Actual	Status
Search Type	Spectrum		
Retention Time	6.200 +/- 0.200	6.259 min.	Pass
Match Result	N-R >= 700	953	Pass

Integration and Quantitation

Parameter	Specification	Actual	Status
Quan Ions	96.0		
Calibration Equation	Linear, Force, 1/nX2		
Area	>=500	414417	Pass
Height		174701	
Amount	>= 0.000	414417 Counts	Pass

Match Types: N-R : Normal-Reverse

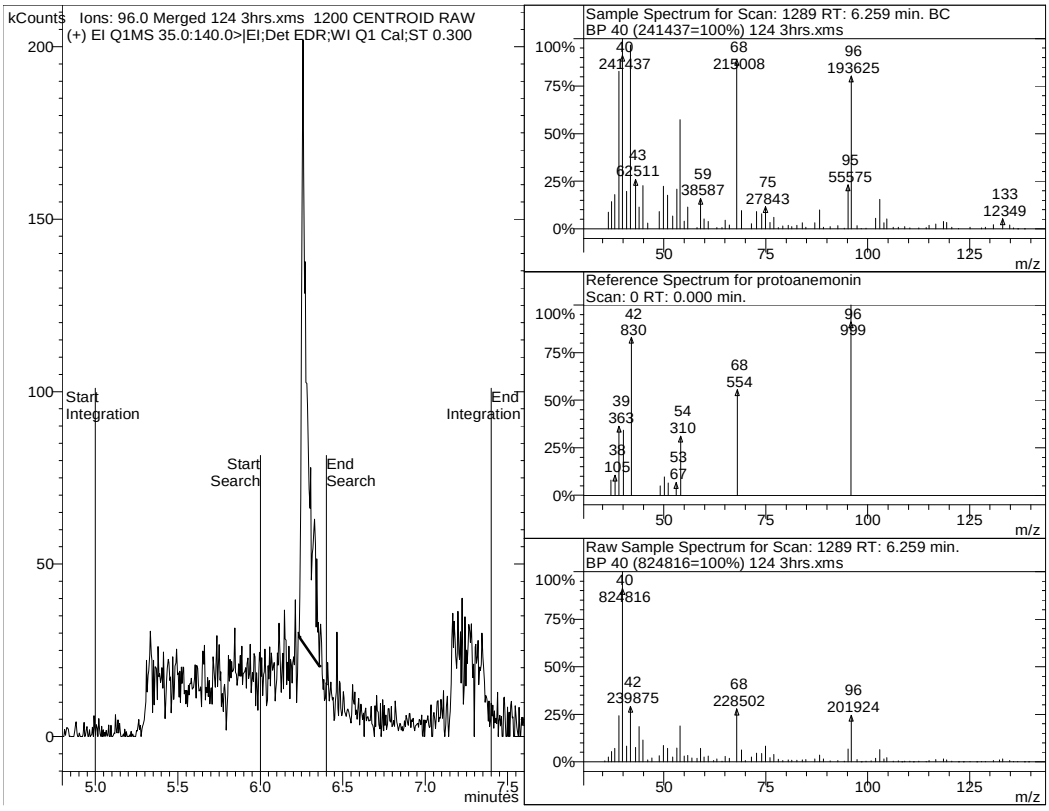

Seg 1, Time: 0.22-9.85, Channels: 1

Appendix V GC-MS chromatograms in the Headspace-GCMS-SPME study to determine the the decomposition of ranunculin by *P. aeruginosa* bacterial culture. (Chapter 3)

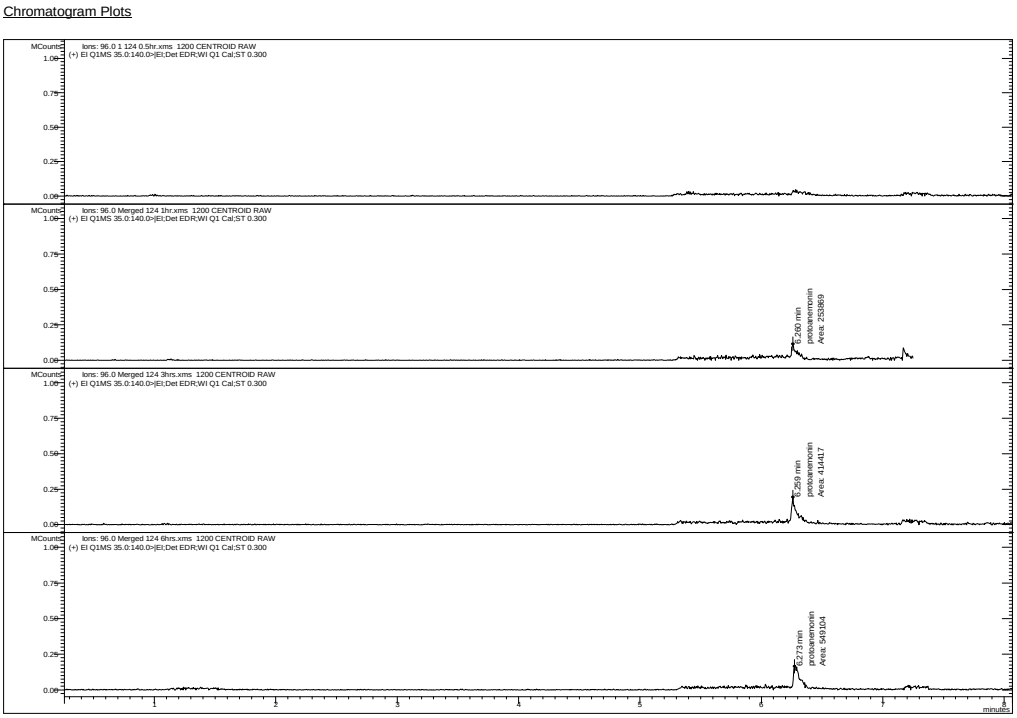

GC-MS chromatograms of PA124 incubated with ranunculin for 0.5 hr, 1hr, 3 hrs and 6hrs

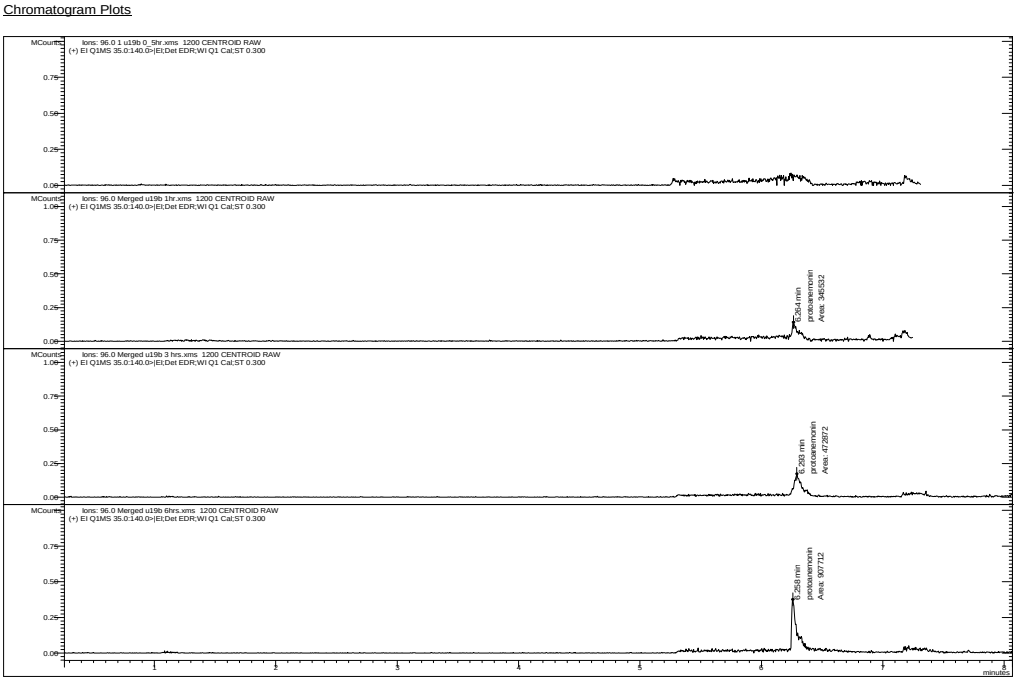

GC-MS chromatograms of PAu19b incubated with ranunculin for 0.5 hr, 1hr, 3 hrs and 6hrs

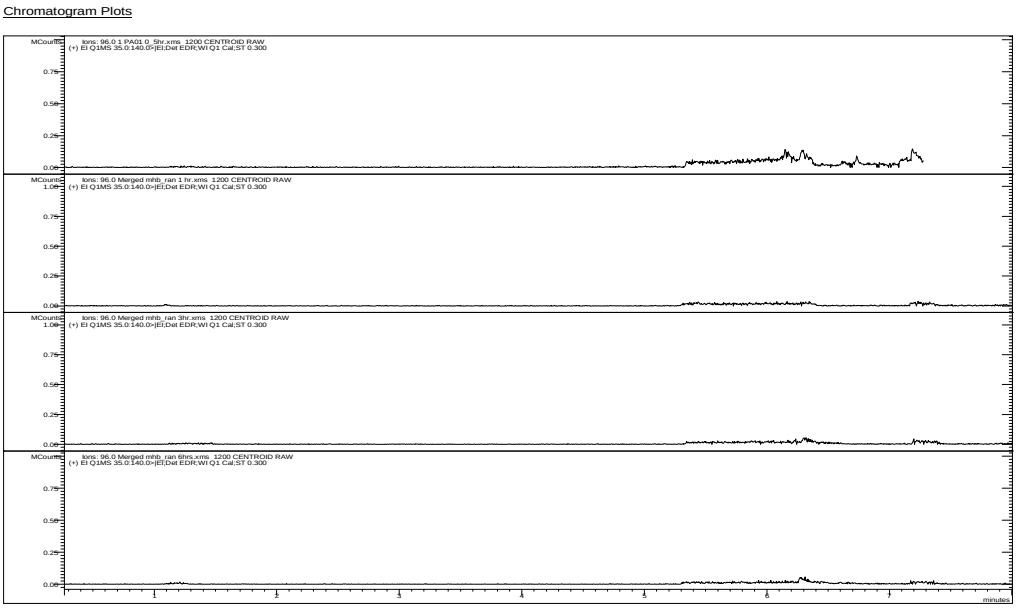

GC-MS chromatograms of PAO1 incubated with ranunculin for 0.5 hr, 1hr, 3 hrs and 6hrs

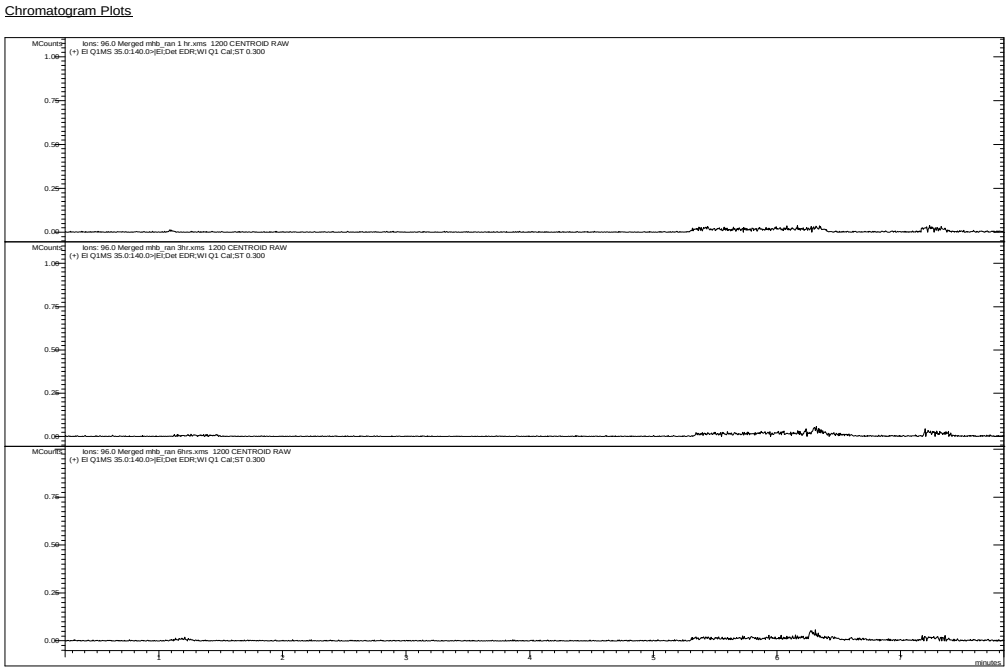

GC-MS chromatograms of MHB incubated with ranunculin for 1hr, 3 hrs and 6hrs

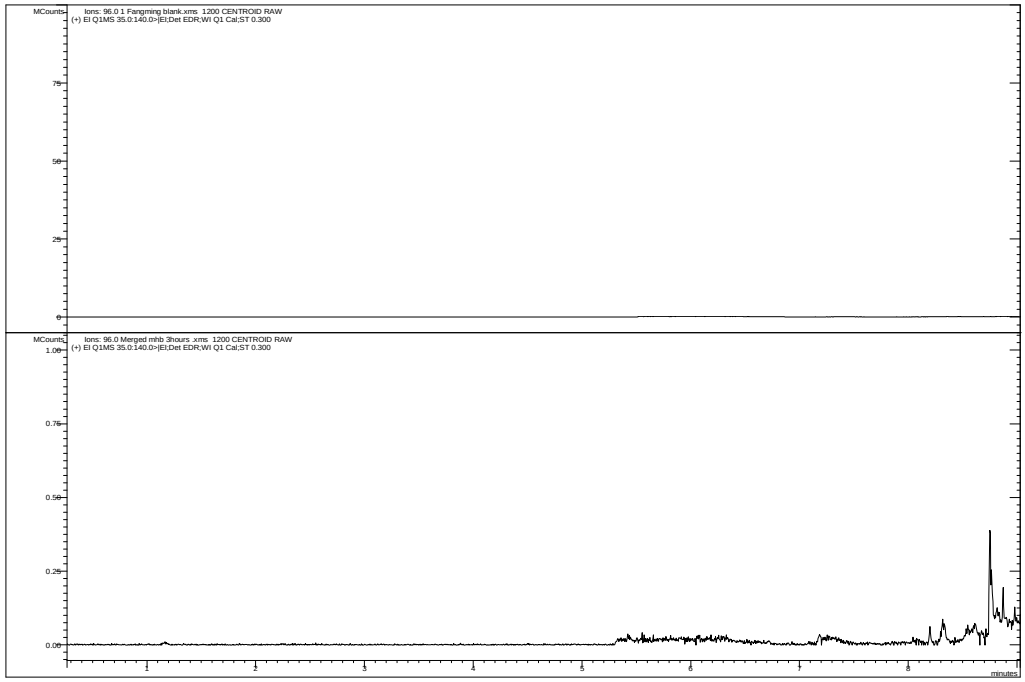

GC-MS chromatograms of blank and MHB.

Appendix VI Photos of the Griess assay of *C. aristata*-TN SPE fraction 1 to fraction 5 and the cell viabilities.

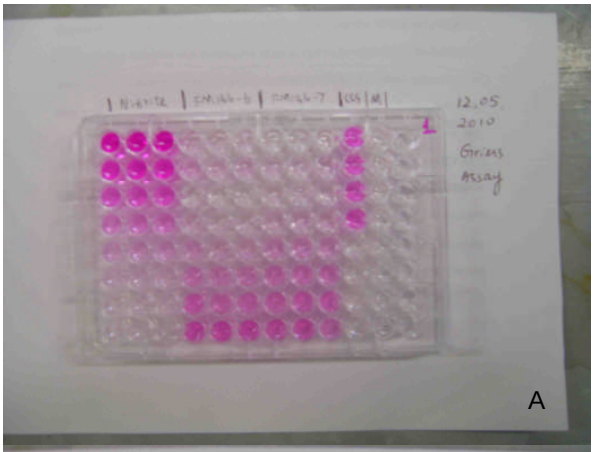

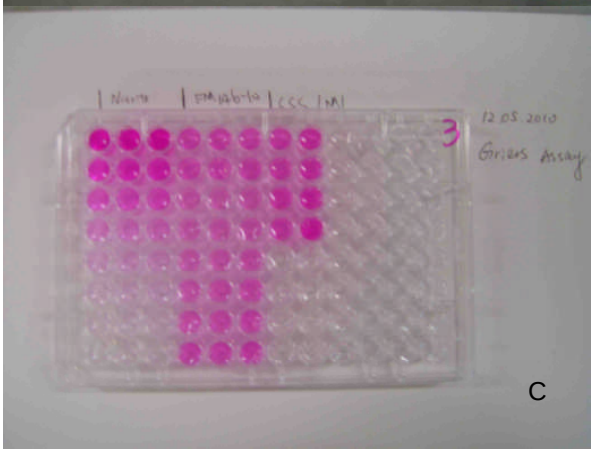

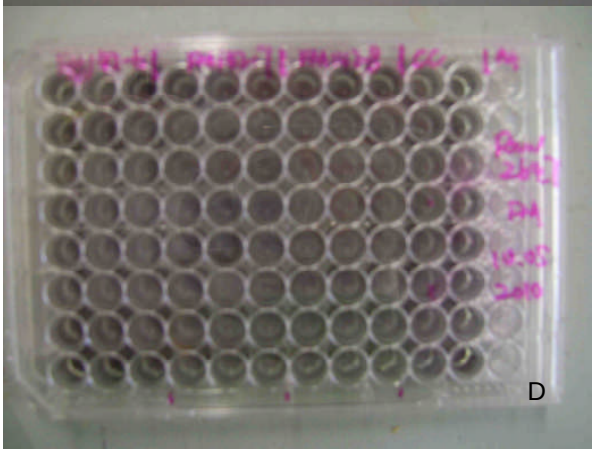

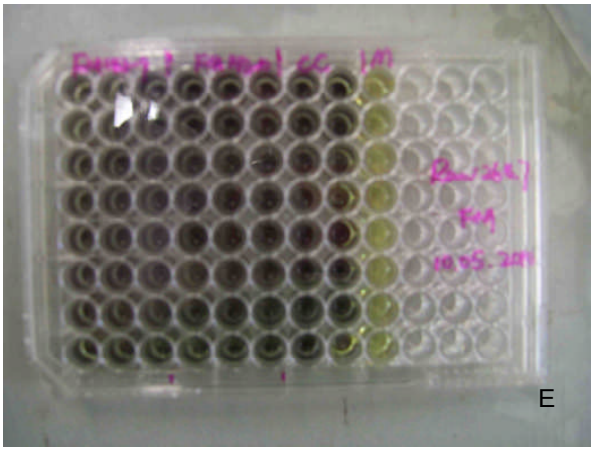

A is the Griess assay results of fraction 1 and 2. B is the Griess assay results of fraction 3 and 4. C is the Griess assay results of fraction 5. D is the MTT results of fraction 1, 2 and 3. E is the MTT results of fraction 4 and 5.

Appendix VII LC-MS chromatograms of ranunculin and its isomer, flavonoids, hydroxicinanmate easters described in Table 5.1(Chapter 5).

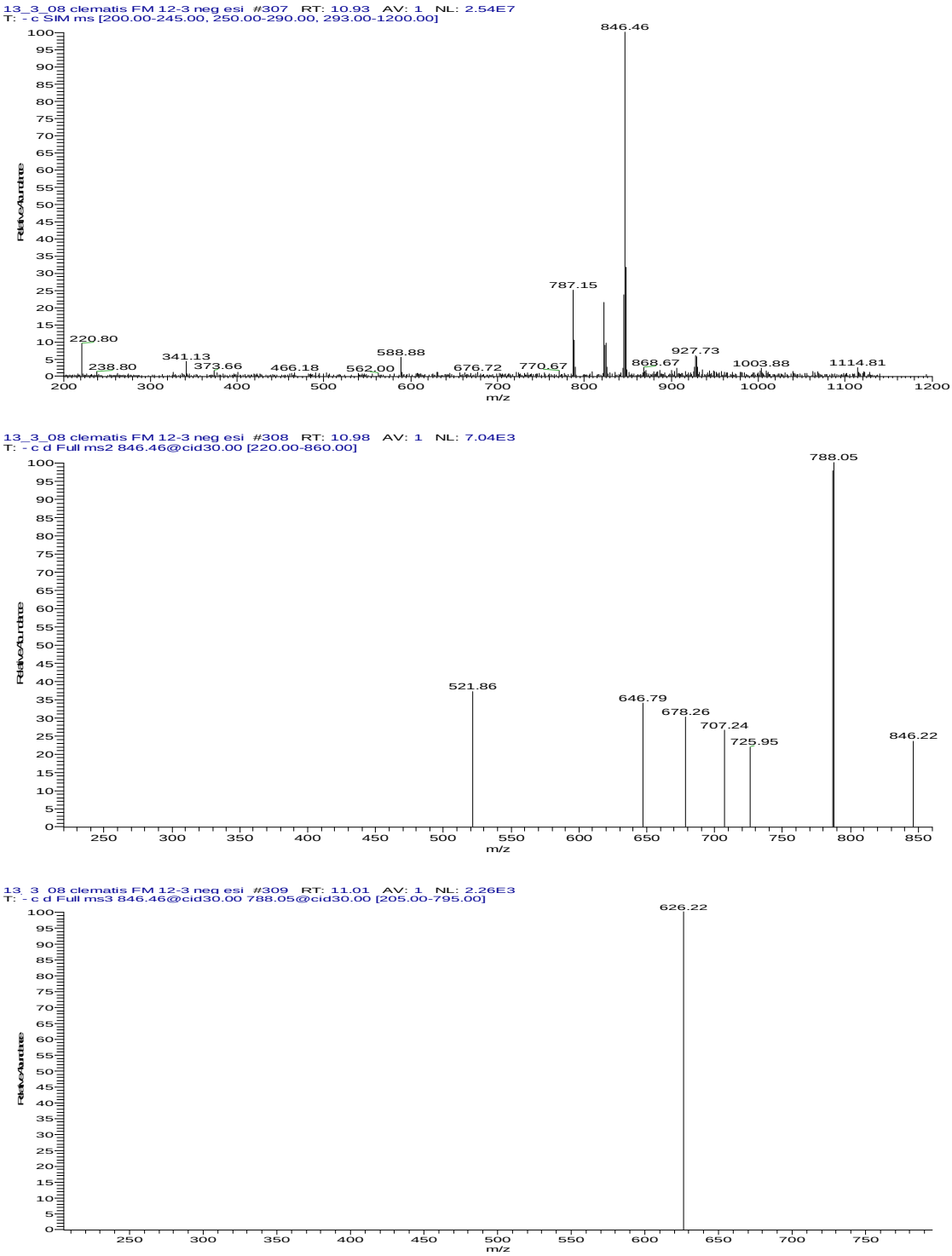

MS spectrum of MW 788 flavonoid (compound 4)

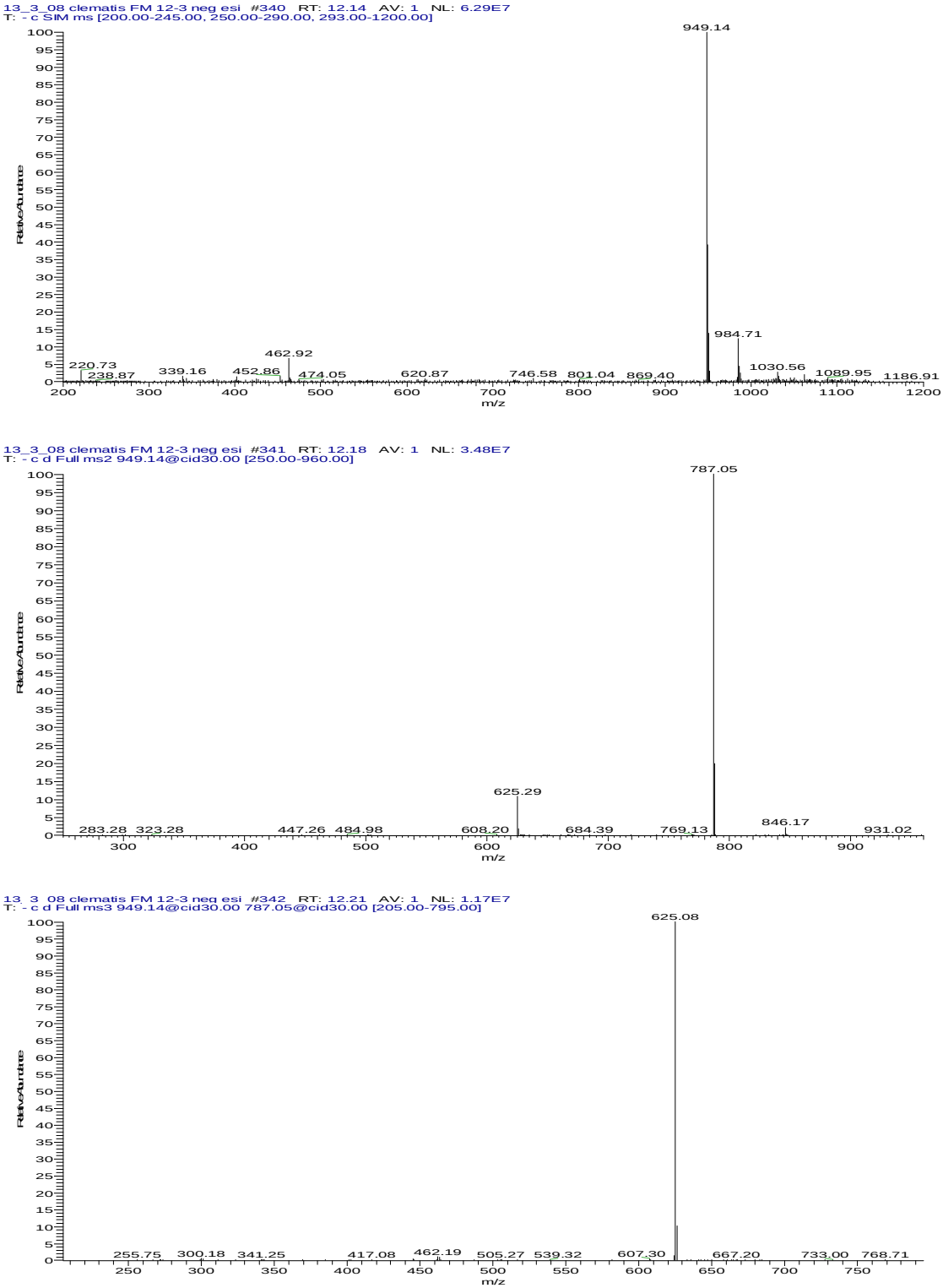

MS spectra of Mt 950 flavonoid (compound 7)

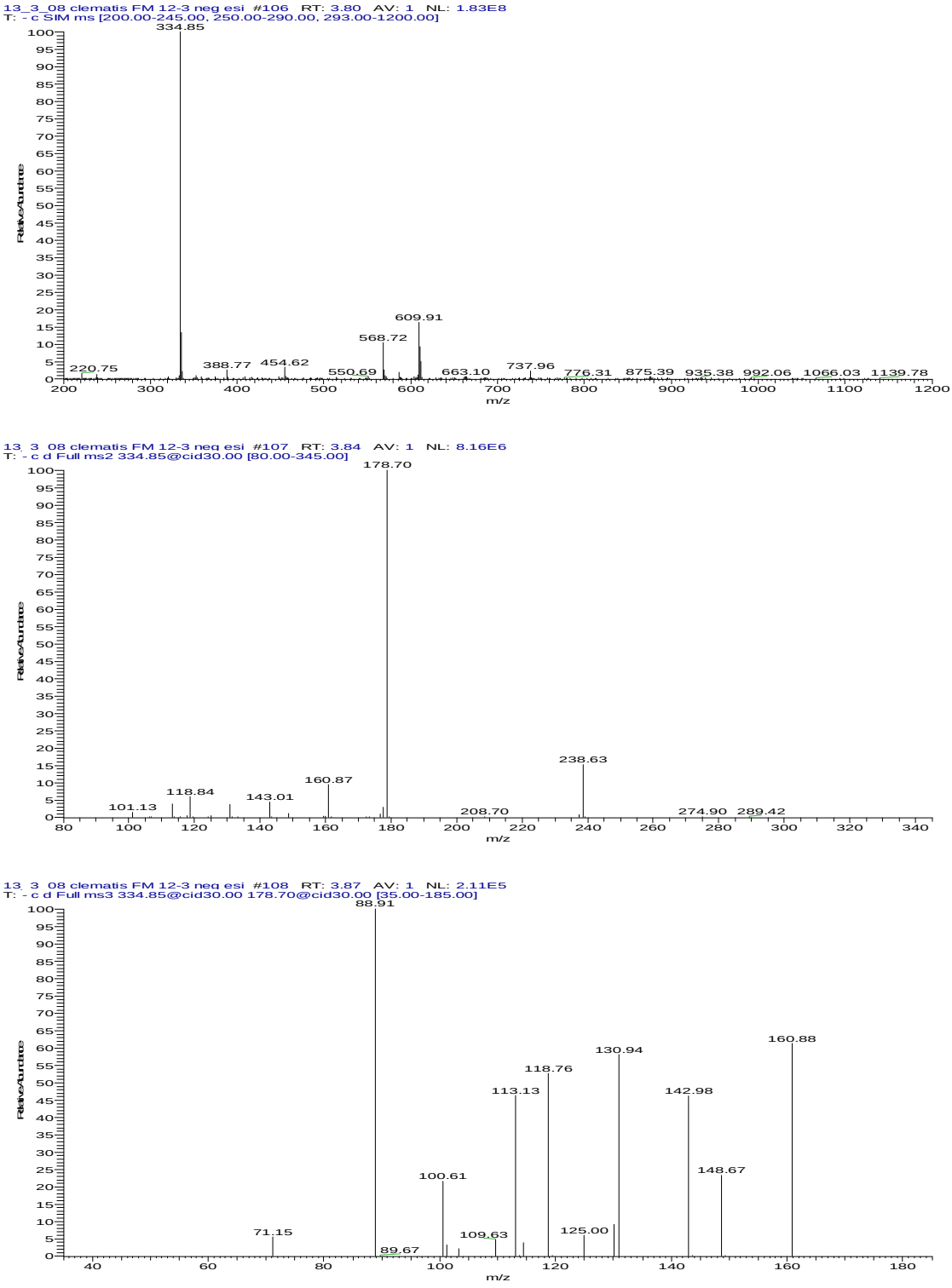

MS spectra of Compound 1

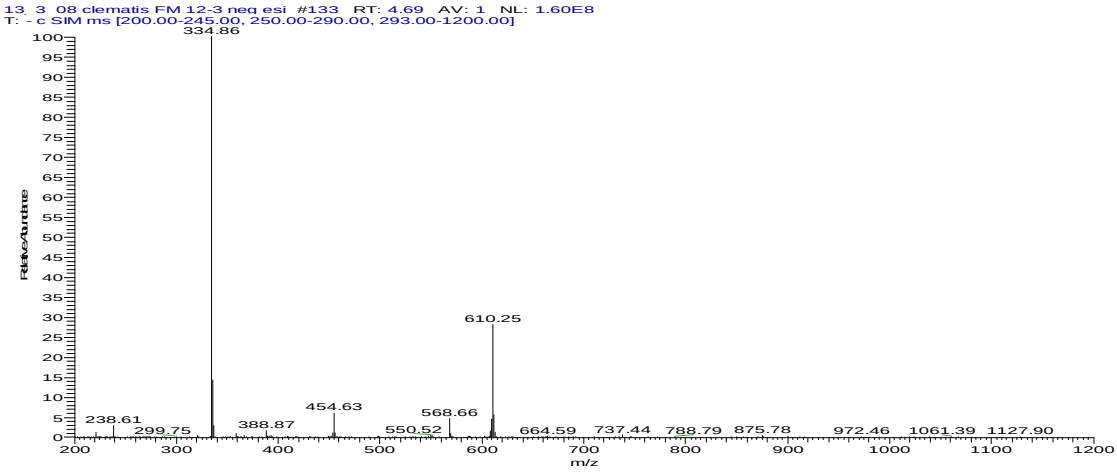

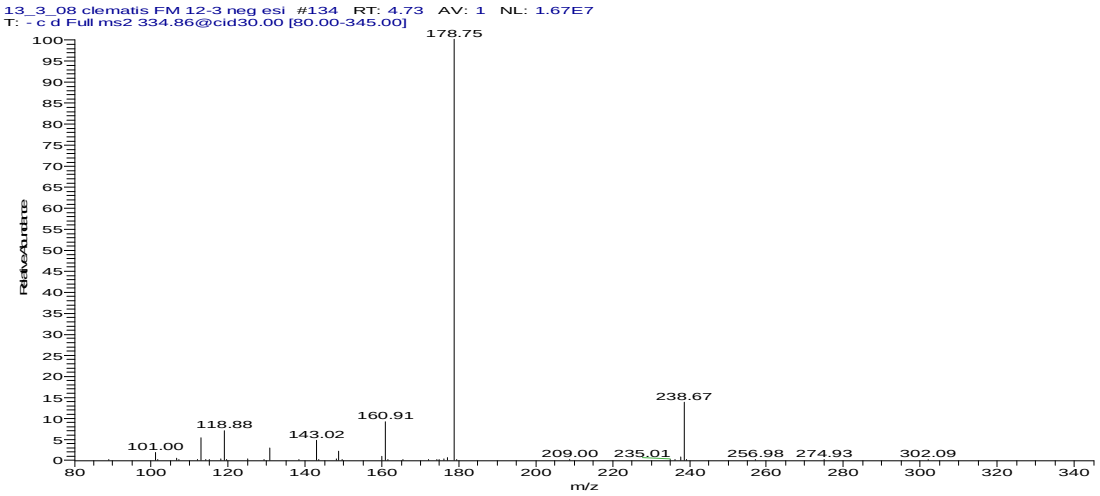

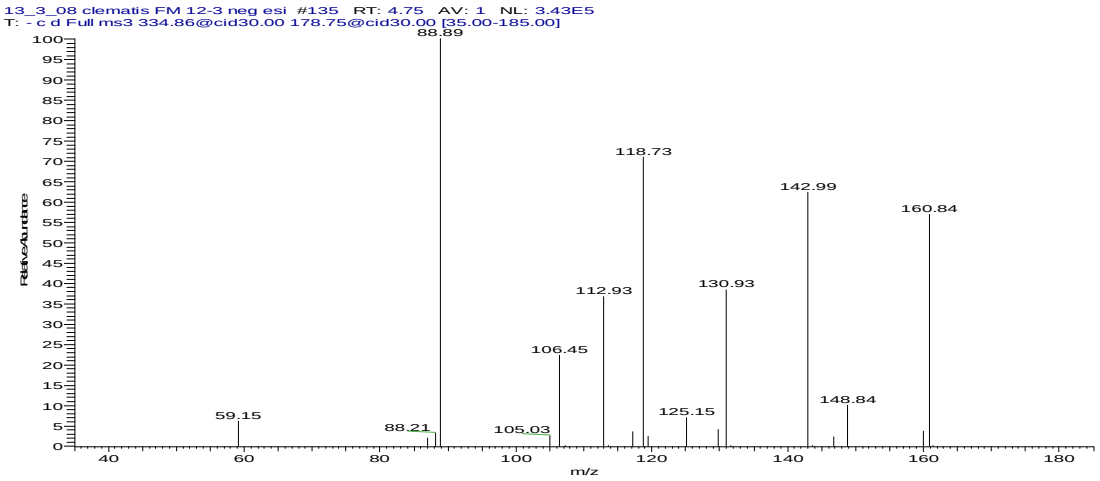

MS spectra of Compound 2

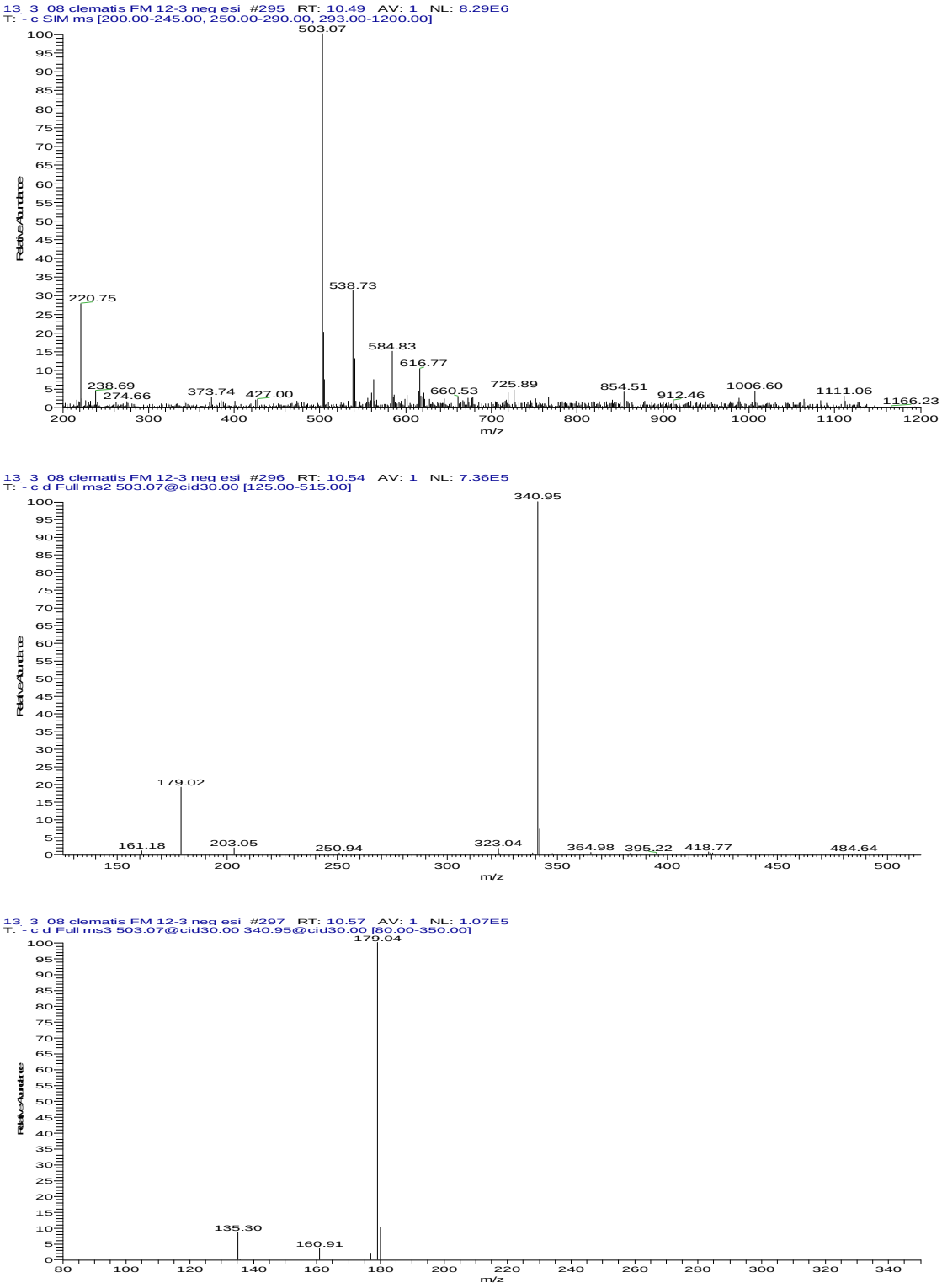

MS spectrum of Compound 3

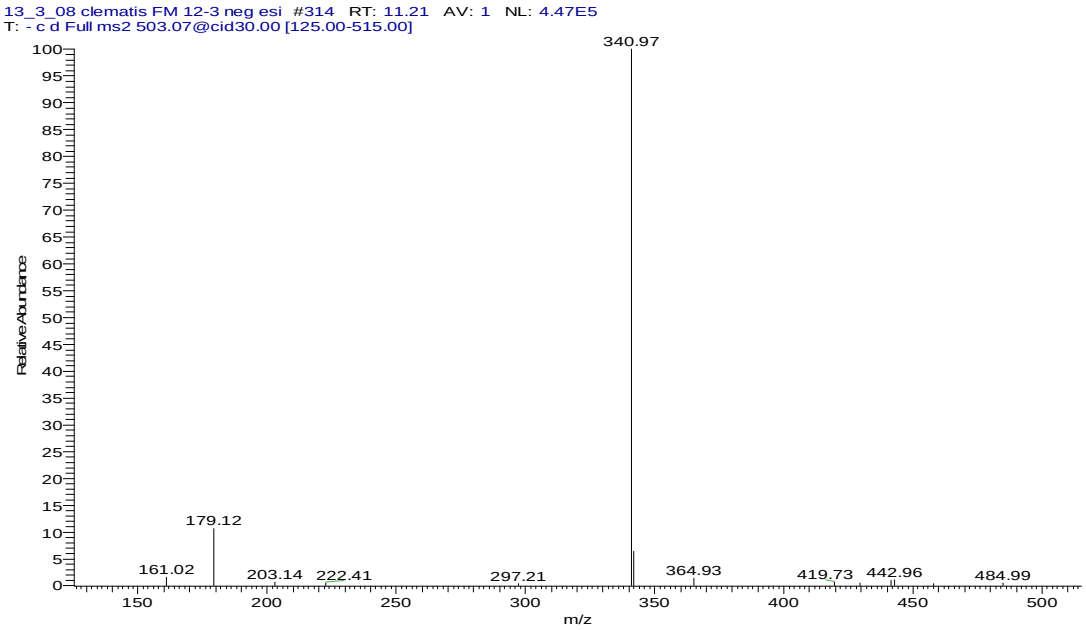

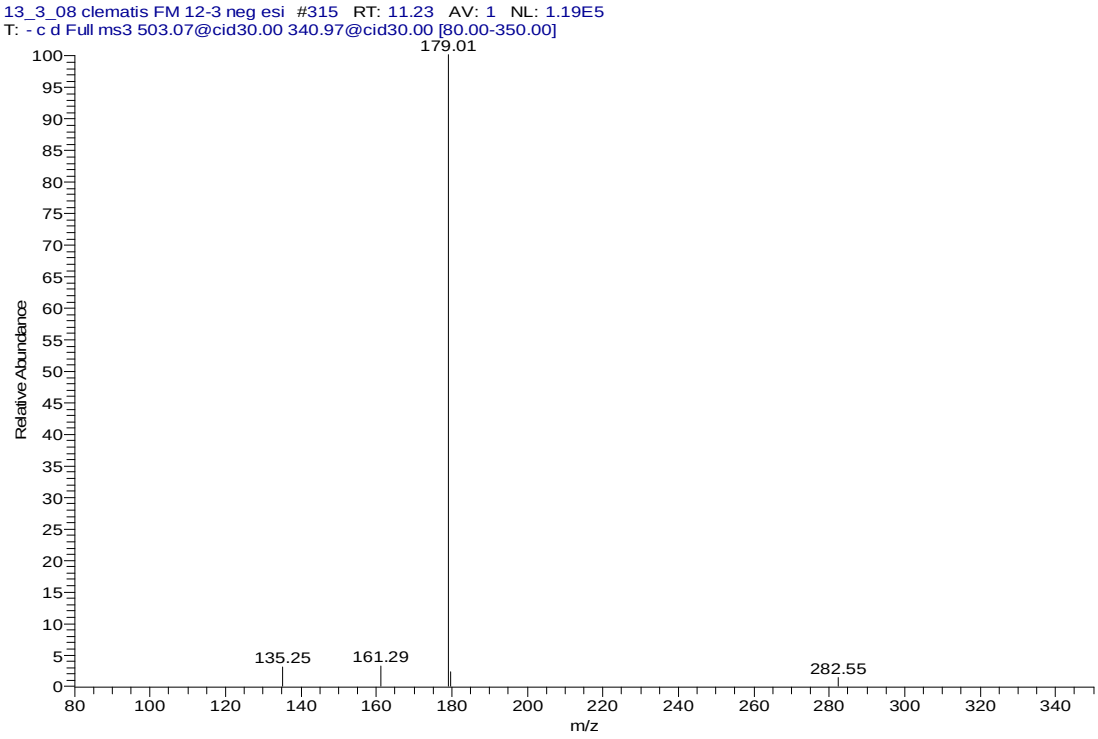

MS spectrum of Compound 5

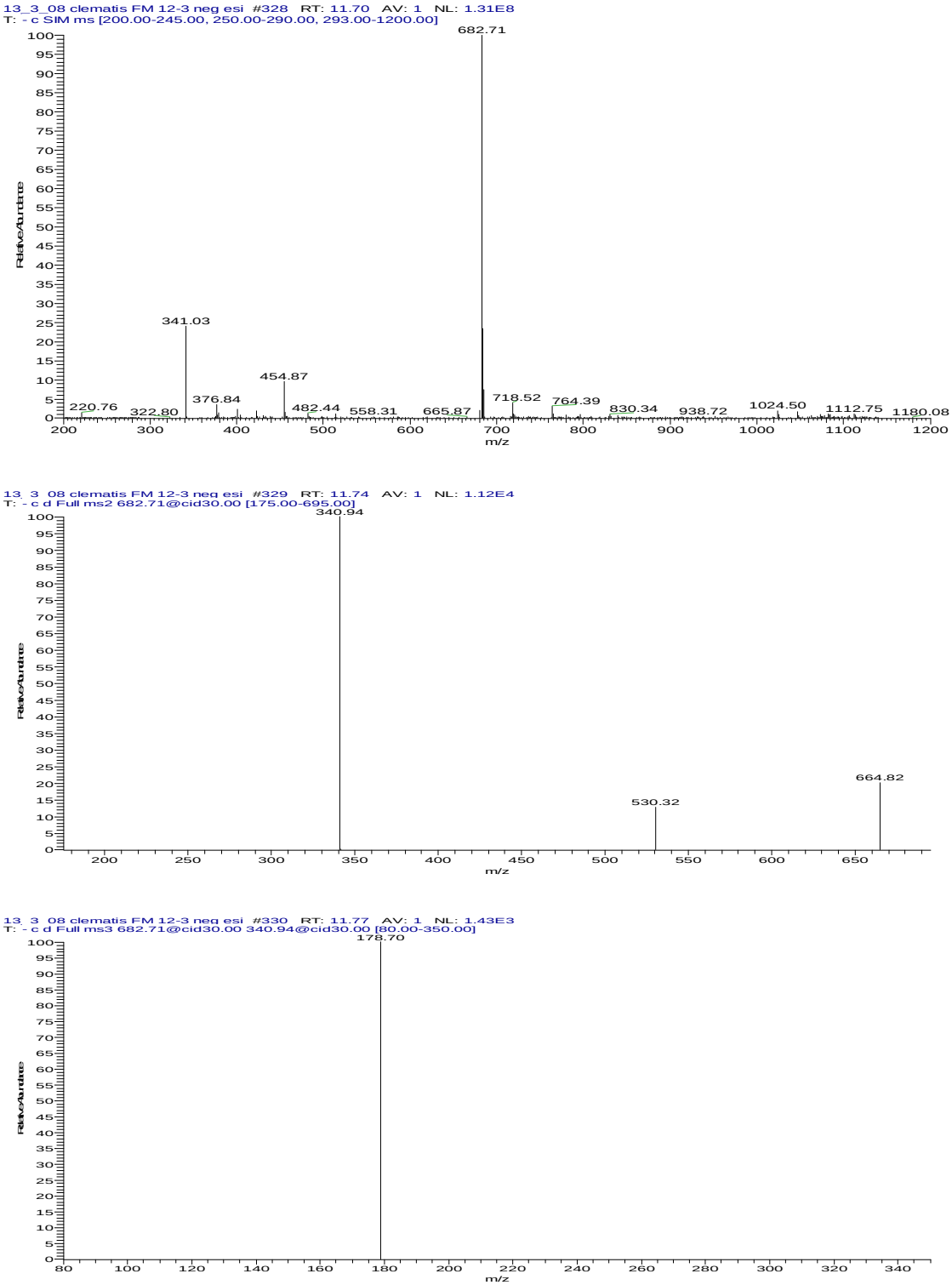

MS spectrum of Compound 6

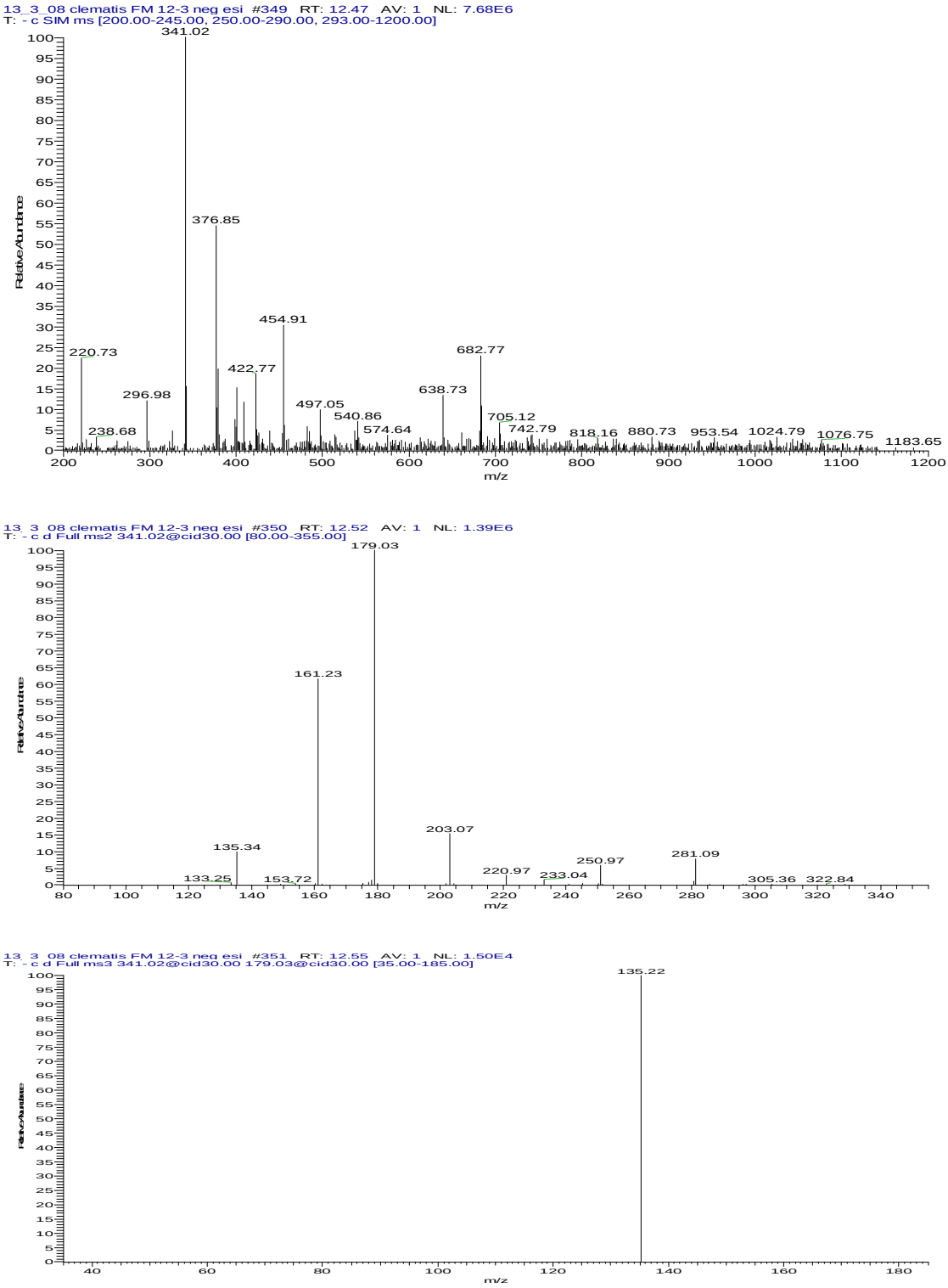

MS spectrum of Compound 8

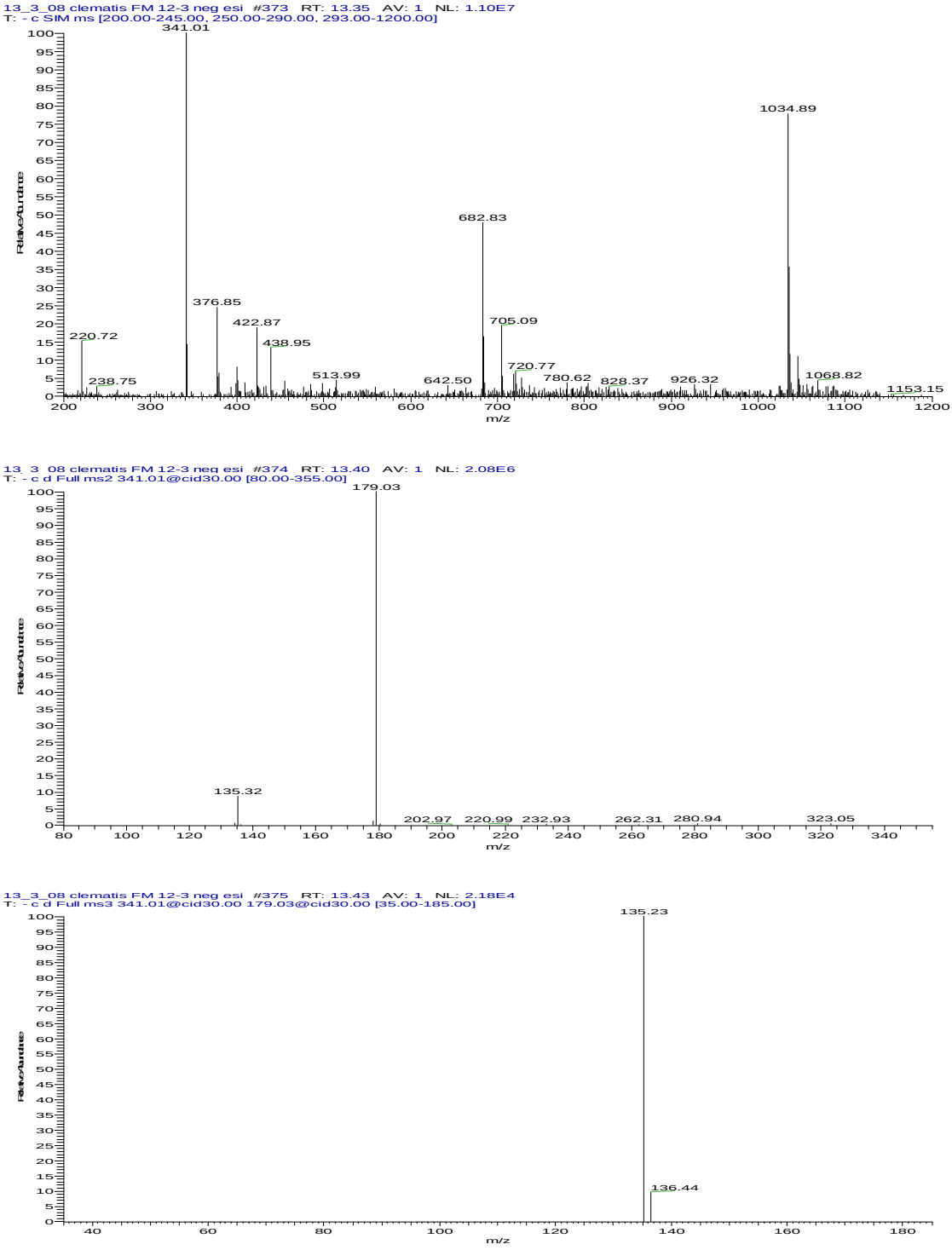

MS spectrum of Compound 10

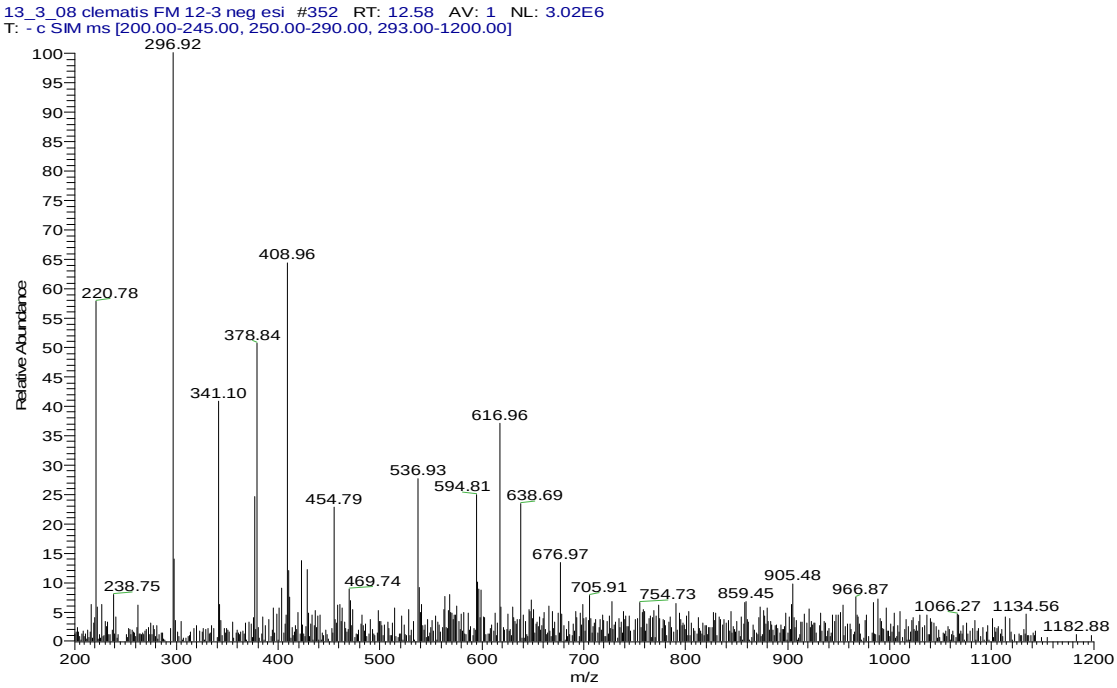

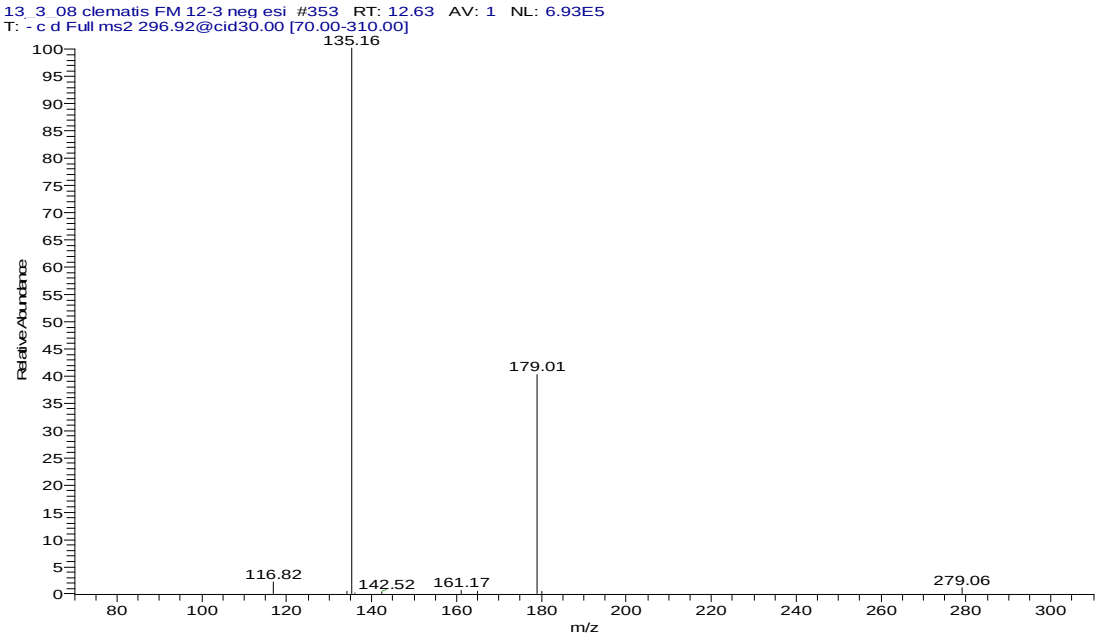

MS spectrum of Compound 9

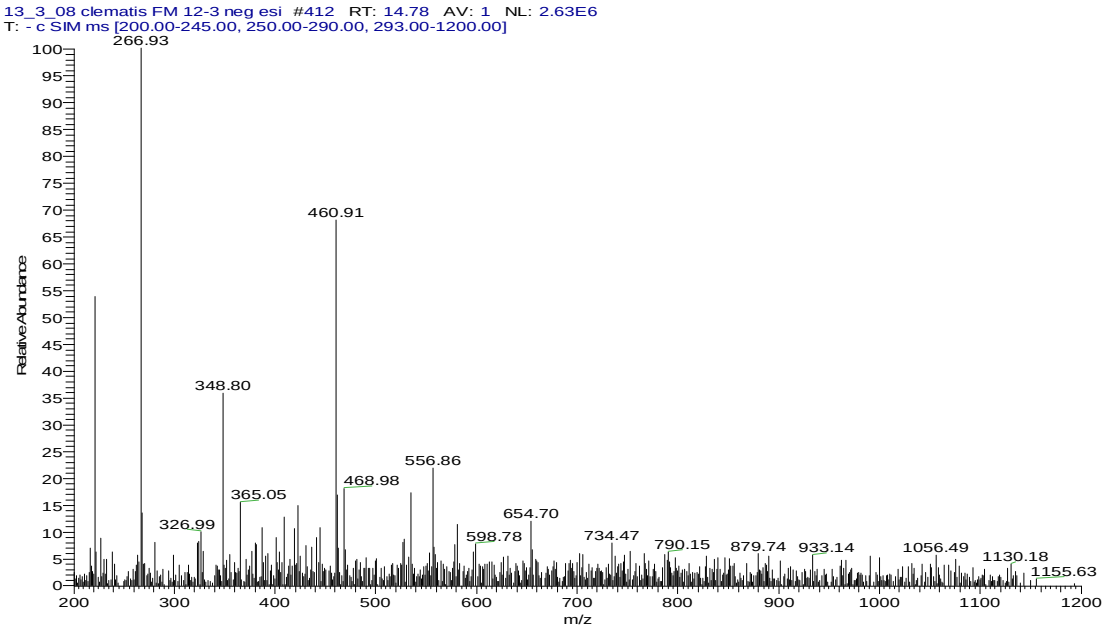

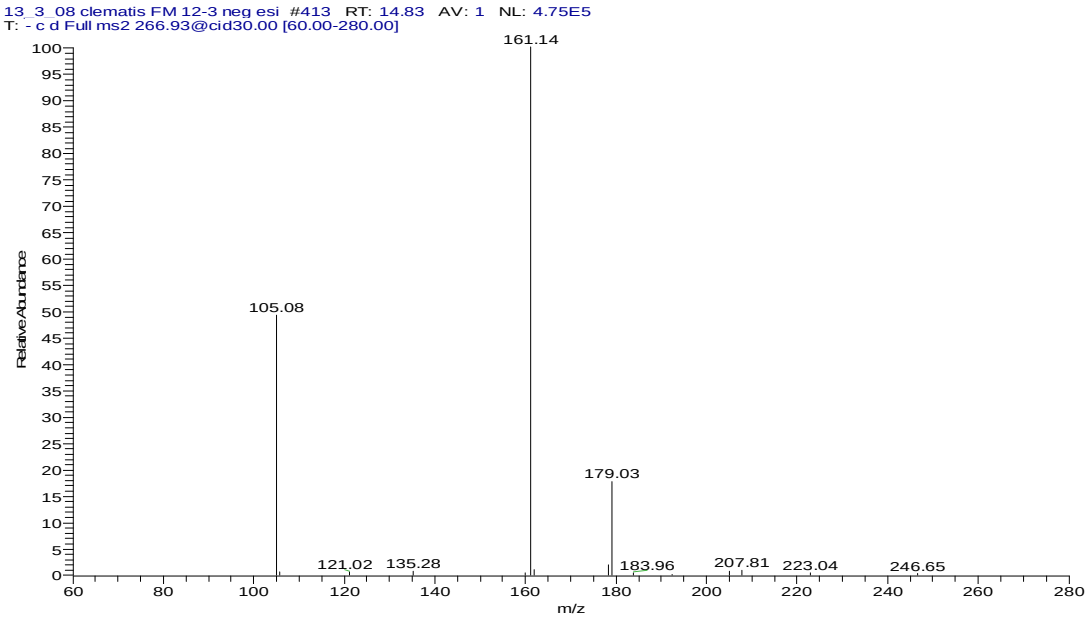

MS spectrum of Compound 11

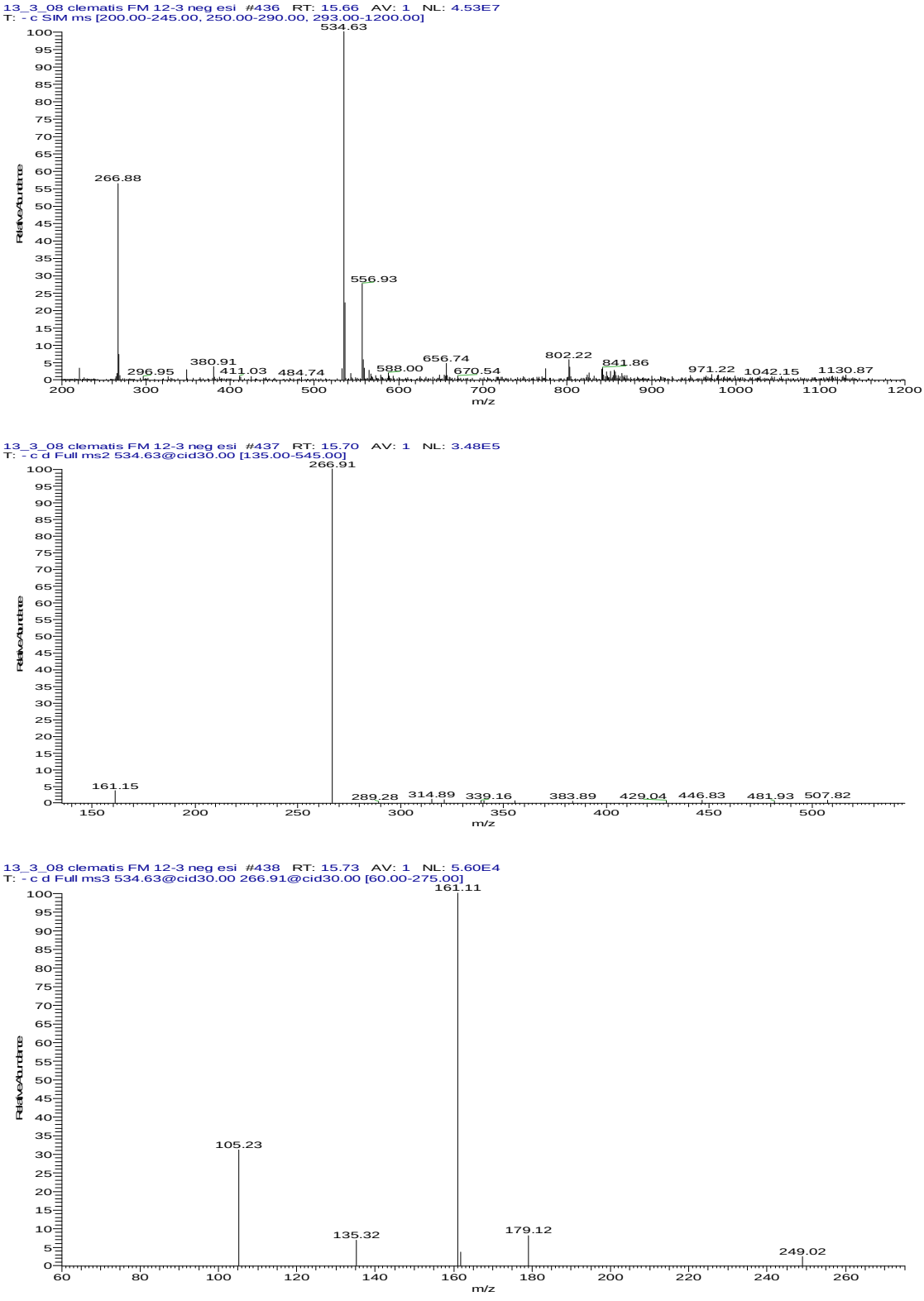

MS spectrum of compound 12

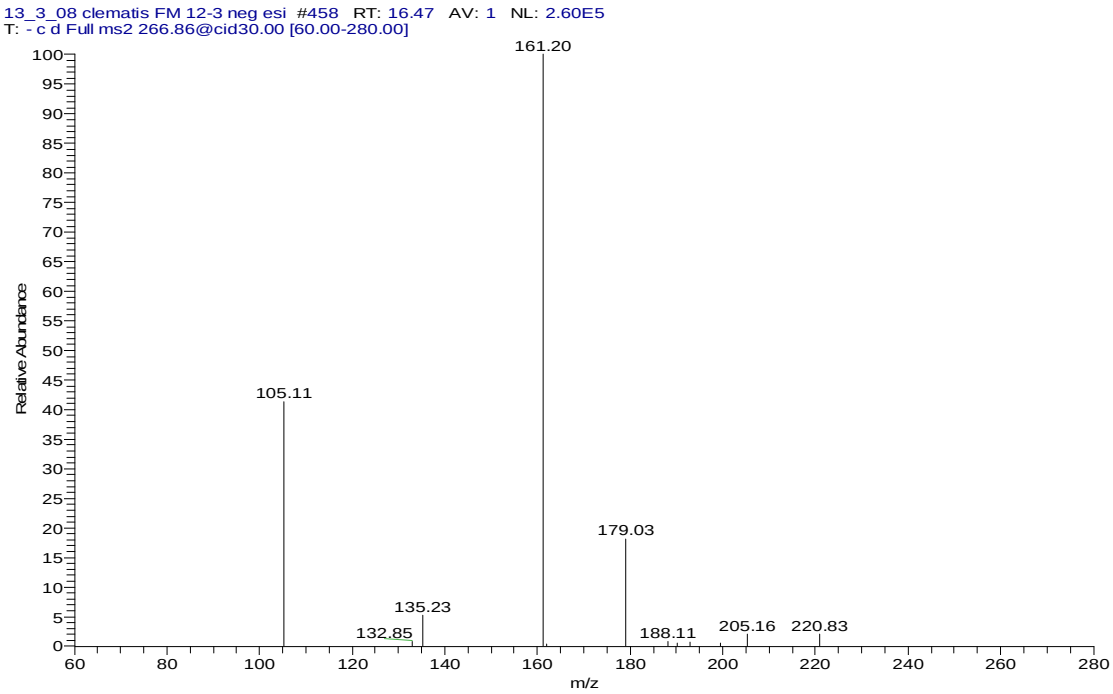

MS spectrum of compound 13

Appendix VIII UV spectra of hydroxinnamate easters in Table 5.2. (Chapter 5)

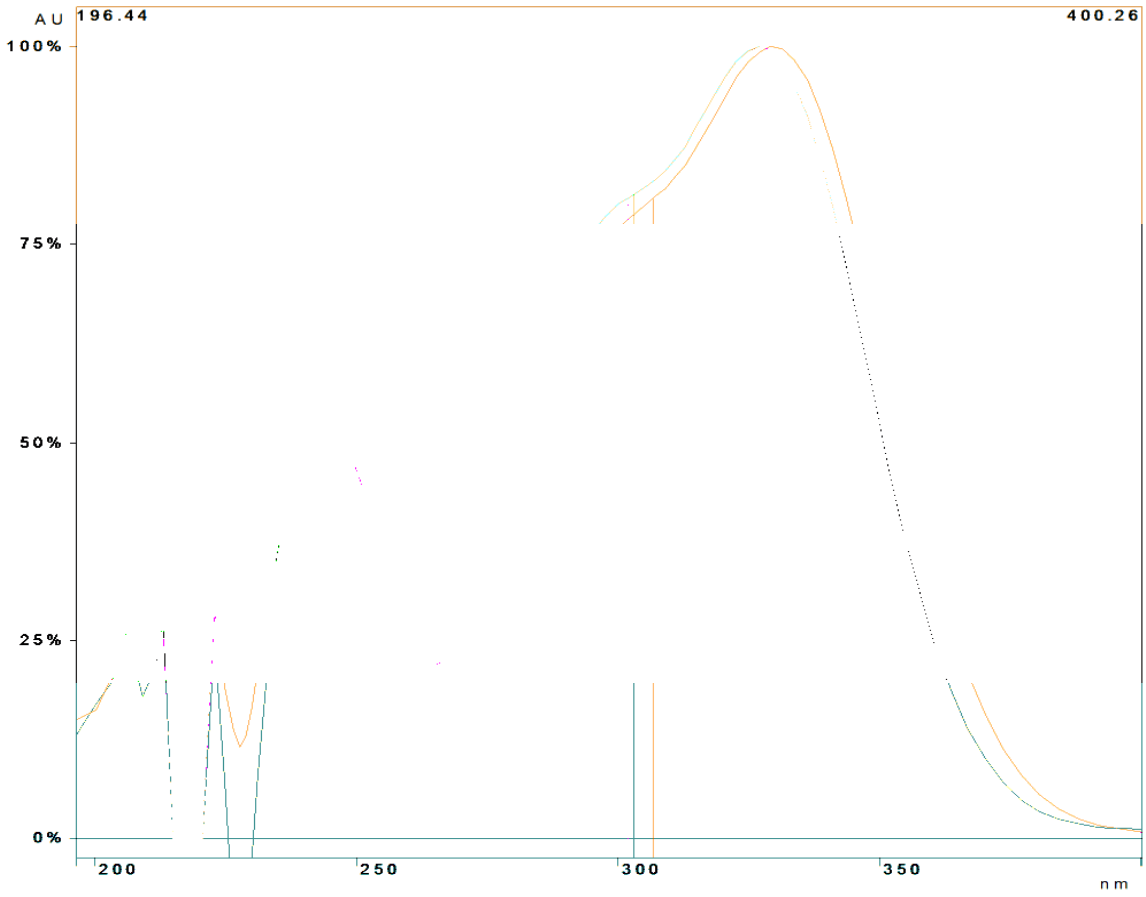

UV spectrum of compounds 3 (red), 10 (purple) and 12 (green)